STUDY OF THE THERMODYNAMIC AND STRUCTURAL BEHAVIOUR OF BINARY LIQUID ALLOYS OF TYPE $A_\mu B_\nu$

A THESIS SUBMITTED TO THE

CENTRAL DEPARTMENT OF PHYSICS

INSTITUTE OF SCIENCE AND TECHNOLOGY

TRIBHUVAN UNIVERSITY

NEPAL

FOR THE AWARD OF

DOCTOR OF PHILOSOPHY

IN PHYSICS

BY

NARAYAN PANTHI

JANUARY 2023

STUDY OF THE THERMODYNAMIC AND STRUCTURAL BEHAVIOUR OF BINARY LIQUID ALLOYS OF TYPE $A_\mu B_\nu$

A THESIS SUBMITTED TO THE

CENTRAL DEPARTMENT OF PHYSICS

INSTITUTE OF SCIENCE AND TECHNOLOGY

TRIBHUVAN UNIVERSITY

NEPAL

FOR THE AWARD OF

DOCTOR OF PHILOSOPHY

IN PHYSICS

BY

NARAYAN PANTHI

JANUARY 2023

TRIBHUVAN UNIVERSITY

Institute of Science and Technology

DEAN'S OFFICE

Kirtipur, Kathmandu, Nepal

Institute of Science & Technology
Dean's Office
Kirtipur 2045

Reference No.:

EXTERNAL EXAMINERS

The Title of Ph.D. Thesis: " Study of the Thermodynamic and Structural Behaviour of Binary Liquid Alloys of Type A_uB_v "

Name of Candidate: Mr. Narayan Panthi

External Examiners:

(1) Prof. Dr. Bhadra Pokharel
Institute of Engineering, Pulchowk Campus
Tribhuvan University, NEPAL

(2) Prof. Dr. Jagdhar Mandal
T.M. Bhagalpur University
Bhagalpur, INDIA

(3) Dr. Hari Dahal
Associate Editor of Physical Review Material and Physical Review B
American Physical Society
USA

June 16, 2023

(Dr. Surendra Kumar Gautam)
Asst. Dean

DECLARATION

Thesis entitled **" Study of the Thermodynamic and Structural Behaviour of Binary Liquid Alloys of Type** $A_\mu B_\nu$**"** which is being submitted to the Central Department of Physics, Institute of Science and Technology (IOST), Tribhuvan University, Nepal for the award of the degree of Doctor of Philosophy (Ph.D.), is a research work carried out by me under the supervision of Prof. Dr. Ishwar Koirala of Central Department of Physics, Tribhuvan University.

This research is original and has not been submitted earlier in part or full in this or any other form to any university or institute, here or elsewhere, for the award of any degree.

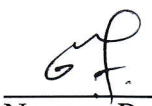

Narayan Panthi

RECOMMENDATION

This is to recommend that **Mr. Narayan Panthi** has carried out research entitled **" Study of the Thermodynamic and Structural Behaviour of Binary Liquid Alloys of Type** $A_\mu B_\nu$**"** for the award of Doctor of Philosophy (Ph.D.) in **Physics** under my supervision. To my knowledge, this work has not been submitted for any other degree.

He has fulfilled all the requirements laid down by the Institute of Science and Technology (IOST), Tribhuvan University, Kirtipur for the submission of the thesis for the award of Ph.D. degree.

.....

Dr. Ishwar Koirala
Supervisor
(Professor)
Central Department of Physics
Tribhuvan University
Kirtipur, Kathmandu, Nepal

january 2023

TRIBHUVAN UNIVERSITY
CENTRAL DEPARTMENT OF PHYSICS
Kirtipur, Kathmandu, Nepal

☎ 4331054
www.tucdp.edu.np

Tribhuvan University Central Department of Physics Kirtipur

Ref. No.: (F.No .....) CDP ..... Date: .....

LETTER OF APPROVAL

Date 04/01/2023

On the recommendation of Prof. Dr. **Ishwar Koirala**, this Ph.D. thesis submitted by **Narayan Panthi**, entitled **" Study of the Thermodynamic and Structural Behaviour of Binary Liquid Alloys of Type** $A_\mu B_\nu$**"** is forwarded by Central Department Research Committee (CDRC) to the Dean, IOST, T.U..

O.P. Niraula

Dr. Om Prakash Niraula
Professor
Head
Central Department of Physics,
Tribhuvan University
Kirtipur, Kathmandu
Nepal

ACKNOWLEDGEMENTS

Pursuing the Doctoral Degree is to set a long academic journey in the hard times of expensive market prices, financial difficulty and scarcity. This journey adds economic, physical, mental, and many other burdens to any individual involved in it from whatever background. My time spent on completing this research work was immensely important to me. I owe a lot to different people and institutions for making this task possible.

I owe an unending gratitude to my supervisor, Prof. Dr. Ishwar Koirala whose encouragement, kind mentorship, unrelenting generosity, a thorough critique of my writing and signposts suggested proceeding further making it possible to navigate on this research task.

My special thanks go to Dean of Institute of Science and Technology Prof. Dr. Binil Aryal, Head of Central Department of Physics, Prof. Dr. Om Prakash Niraula, Prof. Dr. Narayan Prasad Adhikari and Prof. Dr. Raju Khanal. Their insightful presentations, guidance and feedback on my research have always been the best tools for me to the critical understanding and interpretations in the field of scholarship.

I am grateful to Prof. George Kaptay, University of Miskolc, Hungary and Tribikram Rajaure, University of Hawaii, USA for providing many articles related to my research study. My respected teachers Assoc. Prof. Dr. Lekha Nath Mishra, Assoc. Prof. Prakash Man Shrestha, Raj Kumar Rai and friends Rajesh Kumar Bachchan, Indra Bahadur Bhandari and many others can never be forgotten for their assistance, sharing of critical and creative responses and references with me. I am grateful to University Grants Commission, Nepal for providing me grant for this research.

I am grateful to my family members: brothers and sisters, who always loved and supported me in my academic endeavors. I thank my parent-like figure, Shreedhar Adhikari, for always encouraging me in every step of my journey. I could not have even dared to join this course if my wife Kalpana Kumari Subedi had not been backing me up from where she is. She stands as the most inspiring lady for my every academic pursuit. I express my thanks to my affectionate offsprings, Bimba and Pratibimba for curiously supporting me in my academic endeavor. I thank all my relatives, friends and colleagues for their kind support, encouragement and love.

Narayan Panthi
January 2023

ABSTRACT

Due to the numerous commercial applications and anomalous concentration-dependent thermo-physical properties of binary alloys, physicists, chemists, and metallurgists have long been interested in understanding the mixing behavior of two metals that form alloys. Most alloys have different interaction energies between like and unlike atoms. Therefore, the mixing property cannot be described as the concentration average of the properties of constituent metals.

The study focuses on the thermodynamic properties of four different binary liquid alloys (Na-Hg, Pb-Mg, Bi-Tl and Cu-Al) of type $A_\mu B_\nu$ by assuming $NaHg_2$, $PbMg_2$, $BiTl_3$ and Cu_3Al_2 as their most stable intermetallic compounds respectively using the 'Quasi-Chemical Approximation' model given by Bhatia & Singh (1982). The Gibbs free energy of mixing, enthalpy of mixing, entropy of mixing, chemical activity, concentration fluctuation in long wavelength limit and chemical short range order parameter are among the properties that are the subject of study of this thesis. For this purpose, the interaction energy parameters are optimized at the melting temperatures of the aforementioned alloys. The study shows that the free energy of mixing is minimum at about compound forming concentration for all the alloys. Similarly, the theoretical analysis of structural properties indicate that all the preferred liquid alloys have ordering tendency at their melting temperature, which is found more near the vicinity of the compound forming concentration.

Next, the viscosity of preferred alloys is studied by using Kaptay model (Kaptay, 2003). The computed viscosities for Na-Hg, Pb-Mg and Bi-Tl liquid alloys are positively deviated whereas it is negatively deviated for Cu-Al liquid alloy from ideal behavior at their melting temperatures. The surface properties of the aforementioned liquid alloys have been studied by the refined Butler model (Kaptay, 2019). Surface tension and surface concentration calculations have been used to analyze the patterns of surface segregations in these liquid binary alloys. The segregation of the alloy component having a lower surface tension is confirmed by theoretical analyses.

Finally, the Quasi-Chemical Approximation model has been extended to study the thermo-physical properties of preferred liquid alloys at different temperatures. For this purpose, the interaction energy parameters for each of the alloy system have been computed at different temperatures by making the assumption that the concentrations or mole fractions and the temperature derivative interaction energy parameters are independent on temperature. The study shows that as temperature rises above melting point, the Gibbs

free energy and the enthalpy of mixing of alloys gradually become less negative. Further, the ordering tendency of these alloy systems gradually decreases. These findings are supported by increase in concentration fluctuation in long wavelength limit at higher temperatures. The viscosity and the surface tension both decrease with increase in temperature. The liquid alloys thus show the maximum tendency towards complex formation as well as maximum values of viscosity and surface tension at their respective melting temperatures.

LIST OF SYMBOLS

A, B	: Components of a Binary Liquid Alloy
$A_\mu B_\nu$	: Type of Complex
C_A, C_B	: Bulk Concentration of Constituent Elements of an Alloy
C^{S}	: Surface Segregation
G_{M}	: Gibbs Free Energy of Mixing
$G_{\mathrm{M}}^{\mathrm{Xs}}$	: Excess Gibbs Free Energy of Mixing
$\Delta G_{i,b}^{\mathrm{Xs}}$	: Partial Excess Gibbs Free Energy of i^{th} Component of an Alloy
ΔG^*	: Gibbs Activation Energy of Viscouss Flow
H_{M}	: Enthalpy of Mixing
R	: Universal Gas Constant
S_{M}	: Entropy of Mixing
$S_{\mathrm{M}}^{\mathrm{Xs}}$	: Excess Entropy of Mixing
S_i	: Partial Molar Surface Area of i^{th} Component of an Alloy
S_i^0	: Molar Surace Area of Pure Component
$S_{\mathrm{CC}}(0)$	: Concentration Fluctuation in Long Wavelength Limit
T	: Temperature of Alloy
V_i	: Molar Volume of Pure Metal at Given Temperature.
ΔV^{Xs}	: Excess Molar Volume Upon Alloy Formation
a_i	: Activity of i^{th} Component of an Alloy
α_1	: Chemical Short Range Order Parameter
η	: Viscosity of Alloy
μ, ν	: Variable Integers
σ	: Surface Tension of Alloy
$\omega, \Delta\omega_{ij}$	: Interaction Energy Parameters

LIST OF TABLES

LIST OF FIGURES

TABLE OF CONTENTS

Page No.

CHAPTER 1

1. INTRODUCTION

1.1 General Consideration

The journey of development of human beings and human society speeded up with the development of metals. As society became more advanced and civilized, more sophisticated materials were necessary to fulfil such advancement. Among these, alloying phenomena is considered as one of the important factors and hence it has drawn great attention of people especially for engineers, physicists and metallurgists. The researchers from the field of metallurgy tend to design alloy microstructure to derive the properties required for them. The microstructure of an alloy is dependent on the chemical composition, processing route and thermal processing (Yeh, 2015). The operating parameters like temperature, pressure and working atmosphere influence the microstructure of an alloy. All alloys in spite of being in the solid state later, originate from liquid state because the components of alloys must be melted before their combination obtains a concrete form and exhibits a significant variety of atomic structure. So the act of melting serves as the basic process to develop a new alloy. Furthermore, deducing the microscopic properties of binary liquid alloys from their bulk properties is often the tendency among the metallurgists (Singh & Mishra, 1988). So, the field of metallurgical synthesis is always an important area to be explored further. The field of research study needs to be concentrated towards the design, characterization, thermodynamics and structural properties of mixing of liquid alloys.

The knowledge of mixing behavior of alloys can be achieved from the experiment but the major problems are related to high reactivity after the alloys are melted at a high temperature. Similarly, the formation of alloy is not only associated with change in the structure of a given system but also in bonding among the atoms. The interaction and structural resetting of integral atoms during the formation of the alloy make the study more interesting (N. Jha & Mishra, 2001; Adhikari et al., 2010; Bhandari, Koirala, & Adhikari, 2021) . It becomes difficult to study all the properties of an alloy in solid state and analysis by X-ray diffraction method has shown that a liquid is much more like solid than gas (Guggenheim, 1952). Hence, different behavior of alloys are studied in liquid state rather than solid. Concentration, temperature and pressure affect the alloying characteristics of liquid alloys, which are considered most important for the materials' strength, stability, and electrical resistance among other things. As a result, alloy forming qualities have been regarded as the critical tools in metallurgy and the

complete study of alloy formation is a difficult task. Furthermore, there is no easy method to tell which constituent atoms in the alloy are grouped together. As a result, identifying the nearest neighboring pair of atoms is extremely challenging. To solve this challenge, thermodynamic or microscopic parameters are investigated in order to get information on closest neighbour pairings or interactions (Singh & Sommer, 1997). Components in some alloys are identical in terms of the Hume-Rothery rule (Hume-Rothery & Powell, 1935) and undergo relatively minute changes in electronic behavior on mixing. Local structure is similar to that of pure elements under these conditions, and differences in transport and thermodynamic characteristics from ideal behavior may be conveyed from the perspective of size, electrochemical effect, and electron concentration. On the other hand, a great number of alloys exist in which complicated ionic species emerge during alloying and are distinguished by remarkable atomic geometrical configurations. In these systems, there occur considerable differences in electrical behavior and large asymmetries in the concentration dependence of thermodynamic functions. The solubility of a homogeneous solid phase is influenced by the size factor, electrochemical effects and electron concentrations. As a result, from a metallurgical approach; studying the mixing behavior of liquid alloys may provide information on the energetics of the creation of binary solid alloys.

The alloys lack long-range order and therefore they are classified as disordered materials with a wide range of atomic arrangement. The interaction and bond energies between the similar and dissimilar atoms are different and the property of mixing cannot be expressed as the concentration average of constituent metals. It is therefore fascinating to investigate the different properties of alloys. The interatomic interactions between the nearest neighbours, which can occur between the atoms of same components and also distinct components are taken into account for the theoretical analysis of the various nature of liquid alloys. The atomic interactions give rise to two thermodynamic effects namely, the enthalpic and the entropic effects and the liquid alloys may exhibit a significant variety of arrangements.

Developments in statistical physics and computer approaches have made significant contributions to study liquid alloys. Statistical physics attempts to analyze binary alloys by establishing model equations that can be the simplest and the efficient means of understanding or predicting asymmetries and anomalies in mixing behavior of alloys. For many years, theoreticians (Butler, 1932; Flory, 1942; Redlich & Kister, 1948; Longuet-Higgins, 1951; Bhatia et al., 1973; Lele & Ramachandrarao, 1981; Bhatia & Singh, 1982, 1984; Kozlov et al., 1983; Singh, 1987; Prasad & Singh, 1990, 1991; Prasad et al., 1994; Liang et al., 2016; Zhang et al., 2019) have been creating various modelled equations to get various intriguing information about thermodynamic, structural, transport and surface behaviors of binary liquid alloys.

During the study, the metallurgists try to carry out the knowledge of thermodynamics, structural, transport and surface properties of the alloy. Theoretical studies of thermodynamic parameters such as free energy of mixing, chemical activities of constituent elements of alloys, enthalpy and entropy of mixing yield knowledge about interaction, phase stability, and bonding strength between constituent atoms. Similarly knowledge on the structural arrangement is gained through qualitative analysis of microscopic function; concentration fluctuation in long wavelength limit ($S_{CC}(0)$) and chemical short range order parameter (α_1). The ($S_{CC}(0)$) denotes the type of atoms' ordering, whereas α_1 denotes the degree of ordering of the atoms in the binary liquid alloys (Sharma et al., 2014; Koirala et al., 2016; Mishra et al., 2018). In equiatomic composition, curves of thermodynamic functions like Gibbs free energy of mixing and concentration fluctuation in long wavelength limit of certain alloys are symmetric, whereas the remainder have asymmetric curves. The binary liquid alloys can be categorized into symmetric and asymmetric alloys based on the symmetry of curves expressing thermodynamic functions. Asymmetric alloys are known as compound forming alloys, whereas symmetric alloys are known as regular ones. The, binary liquid alloys such as Ga-In, Mg-Zn, In-Sn, Bi-Pb etc are symmetric alloys whereas Ag-Al, Bi-Tl, Ga-Bi, Sb-Sn etc fall under the category of asymmetric alloys (Hultgren et al., 1973; Akinlade et al., 2001; Anusionwu, 2006). The deviation of thermodynamic properties from equiatomic composition is due to inter component interaction of the alloy. Figures 1 and 2 are the plots of compositional dependence of the Gibbs free energy of mixing (G_M/RT) for In-Tl liquid alloy at 723 K and Cu-Sn liquid alloy at 1400 K representing respectively symmetric and asymmetric binary liquid alloys.

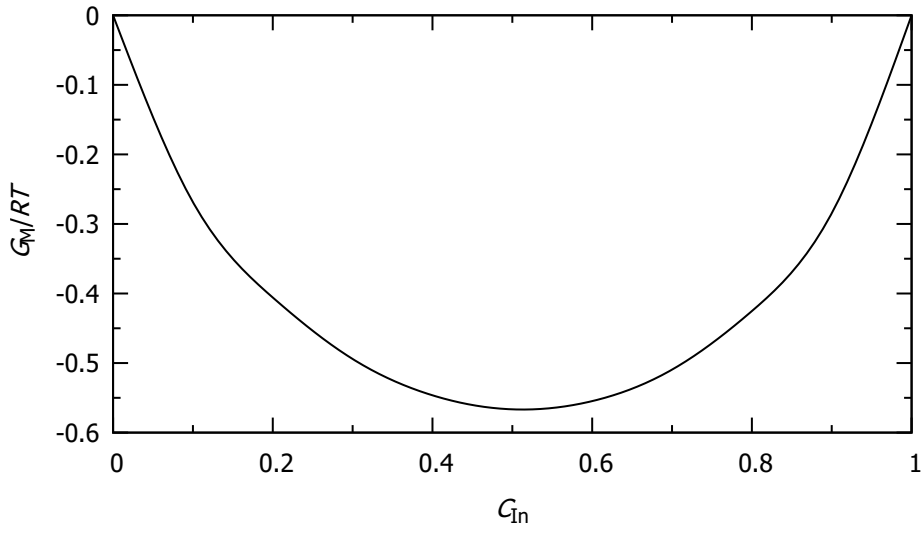

Figure 1: Gibbs free energy of mixing versus concentration of In for In-Tl liquid alloys at 723 K (Hultgren et al., 1973).

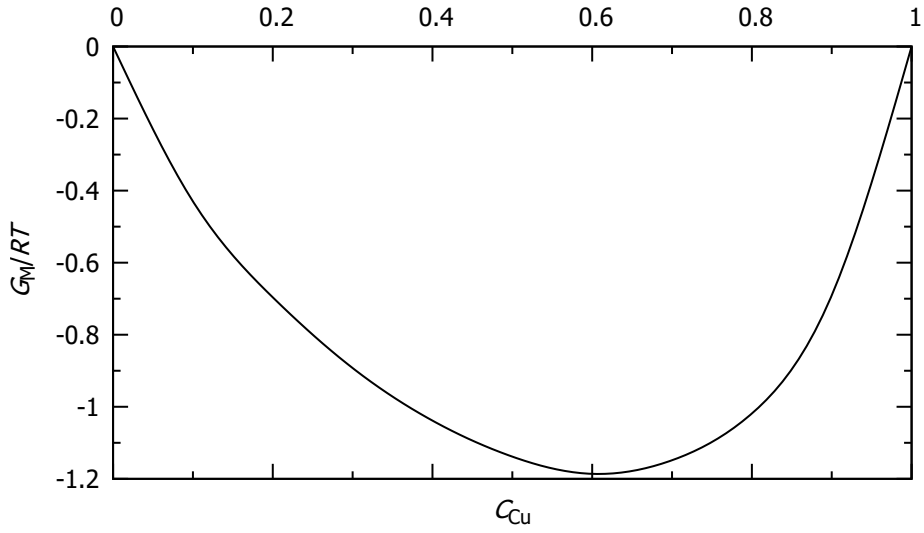

Figure 2: Gibbs free energy of mixing versus concentration of Cu for Cu-Sn liquid alloys at 1400 K (Hultgren et al., 1973).

On the other hand, the alloys can be categorized as ordering or segregating depending on the pairing of atoms of constituent elements. In segregating alloys, like atoms are grouped together but in ordering alloys, dissimilar atoms are paired together. The deviation of concentration fluctuation in long wavelength limit ($S_{\mathrm{CC}}(0)$) of binary liquid alloys with ideal concentration fluctuation in long wavelength limit ($S^{\mathrm{id}}_{\mathrm{CC}}(0)$) can be used to distinguish ordering and segregating binary liquid alloys. For the given concentration if $S_{\mathrm{CC}}(0) < S^{\mathrm{id}}_{\mathrm{CC}}(0)$, the alloy is supposed to have compound forming nature. However $S_{\mathrm{CC}}(0)$ approaches to zero if the mixture is entirely composed of complexes. Figure 3 indicates the plot of composition dependent $S_{CC}(0)$ of Na-Pb liquid alloy at 700 K representing the ordering alloy. Similarly if $S_{\mathrm{CC}}(0) > S^{\mathrm{id}}_{\mathrm{CC}}(0)$, the expected nature of the alloy is segregating. If $S_{\mathrm{CC}}(0)$ is too large in comparison to $S^{\mathrm{id}}_{\mathrm{CC}}(0)$, the segregating alloys lead to phase separation. Figure 4 shows the plot of composition dependent $S_{\mathrm{CC}}(0)$ of Ag-Pb liquid alloy at 1273 K indicating segregating alloy. Ag-Pb, Al-Ge, Co-Sn, Bi-Za etc. are segregating alloys whereas, Na-Pb, Al-Mg, Mg-Ga etc. are ordering alloys (Hultgren et al., 1973; Anusionwu et al., 2009; Yadav et al., 2016).

The following are some empirical and microscopic parameters used to identify the alloys' ordering and segregating behavior (Singh & Sommer, 1997).

1. Ordering alloys deviate from Raoult's law in a negative way, whereas segregating alloys deviate in a positive way.

2. For ordering alloys, the enthalpy of mixing and excess Gibbs free energy are negative, but for segregating alloys, these are positive.

3. The concentration fluctuation in long wavelength limit ($S_{\mathrm{CC}}(0)$) is smaller for

ordering alloys and is greater for segregating alloys than ideal value.

4. The Warren-Cowley short-range parameter (α_1) is negative for ordering alloys and is positive for segregating alloys.

However, some binary alloys exhibit unusual properties like a positive enthalpy of mixing despite a negative excess Gibbs energy of mixing (Hultgren et al., 1973). As the composition of constituent elements of the alloys changes, some liquid alloys shift from segregating to ordering and vice versa (Anusionwu, 2006; Yadav et al., 2016).

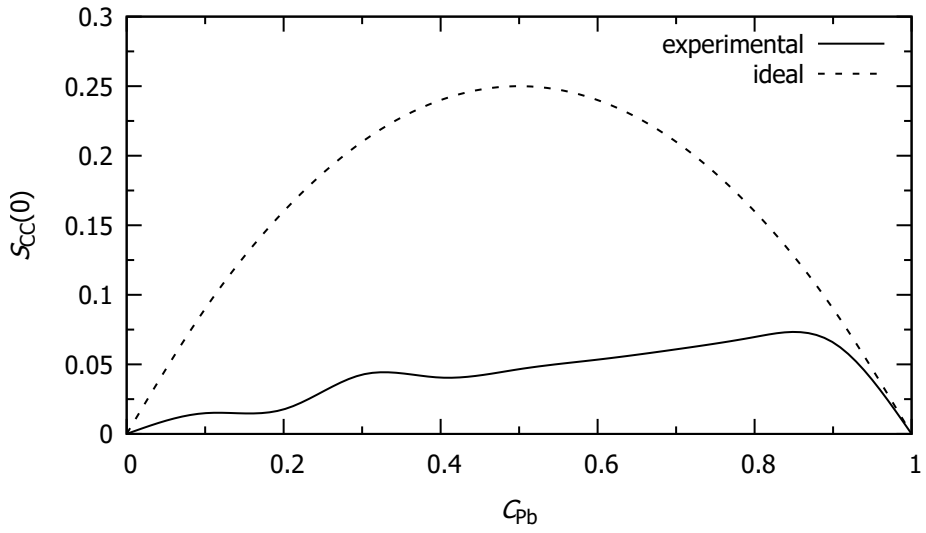

Figure 3: Concentration fluctuation in long wavelength limit versus concentration of Pb for Na-Pb liquid alloy at 700 K (Hultgren et al., 1973).

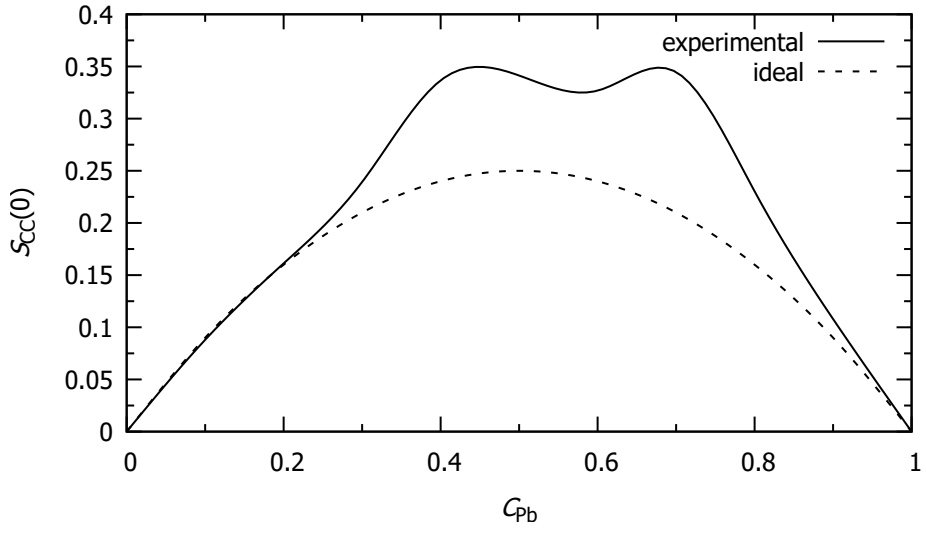

Figure 4: Concentration fluctuation in long wavelength limit versus concentration of Pb for Ag-Pb liquid alloy at 1200 K (Hultgren et al., 1973).

The surface tension and viscosity are key thermo-physical parameters examined in metallurgy to provide data of surface and transport properties of liquid alloy respectively. They are needed in casting method in order to create various devices with improved mechanical performance. Similarly, surface segregation, that primarily denotes the concentration disparity between the surfaces and bulk materials is the most essential factor to be examined in metallurgical research. The difference in surface energy between the alloy's component elements is the major cause of this disparity, in which the element with higher surface energy has tendency to segregate on the surface (Prasad et al., 1994).

The present research work deals with thermodynamic and structural properties of four different (Na-Hg, Pb-Mg, Bi-Tl and Cu-Al) binary liquid alloys of type $A_\mu B_\nu$ (where μ and ν are small integers) using Quasi-Chemical Approximation (Bhatia & Singh, 1982) as a function of concentration. The basic tenet behind this model is that a compound forming A-B alloy is understood as an alloy of pseudo-ternary mixture of A atoms, B atoms and $A_\mu B_\nu$ complexes. The thermodynamic and structural properties under the study include Gibbs free energy of mixing, chemical activity, enthalpy of mixing, entropy of mixing, concentration fluctuation in long wavelength limit and Warren-Cowley short range order parameter. Similarly viscosity and surface tension of the alloys are studied by Kaptay's equation (Kaptay, 2003) and improved derivation of Butler equation (Kaptay, 2019).

The numbers denoted by the indices μ and ν ($A_\mu B_\nu \rightarrow \mu A + \nu B$) correspond to the number of A and B atoms in the alloy respectively. It is therefore instructive to study the effect of different pairs of μ and ν values on thermodynamic properties of binary liquid alloys. In the present research, we consider three types of complexes or three pairs of μ and ν values as mentioned below:

values of μ and ν	Types of Complex
$\mu = 1$ and $\nu = 2$	AB_2
$\mu = 1$ and $\nu = 3$	AB_3
$\mu = 3$ and $\nu = 2$	A_3B_2

1.2 Overview of Preferred Binary Liquid Alloys

When small composition differences in the alloy (made up of two components A and B) cause a large change in thermodynamic properties, the phase of the alloy is termed as an intermetallic compound and is often stoichiometric. Such alloy is expressed in the form of $A_\mu B_\nu$. Thus among various binary liquid alloys, the alloys of type $A_\mu B_\nu$ are referred to as compound forming alloys as they form compound in solid state at one or more stoichiometric composition. The intermetallic compounds are known to possess extraordinary functions and characteristics that are not present in common alloys.

Intermetallic alloys have a variety of special characteristics that make them interesting for high-temperature structural applications, including high melting and disordering temperatures, high stiffness, low diffusivity, etc. (Porter & Easterling, 2009).

This section provides an overview of following four compound-forming binary liquid alloys which are the research interest in the present thesis.

1.2.1 Na-Hg System

Sodium is one of the most reactive metals. As a liquid, it is substantially more reactive in air than as a solid. Likewise Mercury is a chemical element and only common metal that is liquid at room temperature. When mercury alloys with sodium, copper, zinc and tin, the term amalgam is used. Hence sodium amalgam (Na-Hg) is an alloy of mercury and sodium.

The high pressure sodium lamp contains Na-Hg alloy, where sodium is used to generate the right color and mercury to exhibit electrical properties. It is also used as a strong reducing agent in chemical reactions. Another most significant use of sodium amalgam is the electrolysis process, which produces alkali and chlorine using liquid mercury as a cathode.

The phase diagram of Na-Hg (Hultgren et al., 1973; Balej, 1979) indicates that there are various intermetallic compounds and hence it shows anomalous mixing behavior as a function of concentration. Morachevskii (2014) also suggested that sodium and mercury form a congruently melting compound $NaHg_2$ (mp. 626 K). The atomic volume ratio ($V_{Na}/V_{Hg} = 1.6$), electronegativity difference ($E_{Na} - E_{Hg} = -1.07$) and ionic character ($IC = 0.2489$) are insufficient to explain the anomalous behavior of the alloy.

1.2.2 Pb-Mg System

Lead is a soft and ductile metal. It is commercially used as an alloy with different metals like magnesium, tin, antimony, calcium, arsenic etc. Similarly magnesium is a chemically active element that replaces hydrogen in boiling water and can be used in the thermic reduction of its salts and oxidized forms to produce a wide variety of metals. Alloys made of magnesium are the lightest structural metals. The primary benefit of magnesium is its lightness, which makes it appealing for use in a variety of commercial and medical settings where the demand for lightweight structures is great (Loukil, 2021).

The lead magnesium alloy has a eutectic temperature 248.7 °C at 83% of Pb (Nayeb-Hashemi & Clark, 1985). It shows an asymmetric nature of many thermodynamic properties. Thus, different experimentalists tried to investigate the different thermodynamic behavior of the alloys at about melting temperature of the alloy (Okajima & Sakao, 1968; Hultgren et al., 1973).

The atomic volume ratio (V_{Pb}/V_{Mg}), electronegativity difference ($E_{Pb} - E_{Mg}$) and ionic character of the alloy are 1.3, 1.02 and 0.2290 respectively. The phase diagram of Pb-Mg alloy shows the existence of $PbMg_2$ as one of the most stable intermetallic complex in solid state (Hultgren et al., 1973).

1.2.3 Bi-Tl System

Bismuth has a low melting point and is durable and malleable when mixed with other metals. This property makes the bismuth alloy acceptable for its use as solders as it is considered a safer alternative to lead solders. Furthermore bismuth is replacing lead in its alloys in a variety of uses, including pigments for paints, low melting solders, fusible alloys, fishing sinkers, brass for plumbing, and as constituents in grease for lubrications (Suganuma, 2001; Plevachuk et al., 2011). On the other hand thallium also instantly forms alloys with many other metals. It has the most consistent atomic vibration to date. The use of thallium in atomic clocks was preceded by this feature of the metal. It is also mostly used in semiconductor industry as well as producing electronic devices and switches (Bhandari et al., 2021).

The atomic volume ratio (V_{Bi}/V_{Tl}), electronegativity difference ($d = E_{Bi} - E_{Tl}$) and ionic character of the alloy are 1.23, 0.4 and 0.0392 respectively. The phase diagram of Bi-Tl (Okamoto et al., 1990) indicates that Bi and Tl atoms are energetically favoured to form intermetallic compound $BiTl_3$.

1.2.4 Cu-Al System

Pure copper being extremely good conductor of heat and electricity, is frequently used for cables and wires, electrical contacts as well as a number of other items that must carry electrical currents. Likewise because of their superior mechanical properties, the copper alloys are used in communication and electronic industries, auto mobile industries, high thermal and electrical performance, fine bending proof performance and very large corrosion resistance. Pure aluminum is easy to cast, machine and mold and has excellent corrosion resistance, a low density and strong thermal conductivity. It has wide application in preparing foil and conductor cables. The aluminium metal is one of the lightest engineering materials. It is alloyed with other elements to attain the larger strengths necessary for industrial uses (Verma & Lila, 2021).

Numerous researchers (Kanibolotsky et al., 2002; Curioni et al., 2010; Altıntas et al., 2015; Rasch et al., 2019) have been interested in the copper-aluminum alloys for some years as these alloys provide a combination of different properties such as high strength, hardness, corrosion resistance etc. The atomic volume ratio (V_{Al}/V_{Cu}), electronegativity difference ($d = E_{Al} - E_{Cu}$) and ionic character of the alloy are 1.41, −0.29 and 0.0208

respectively. The alloy shows a number of intermetallic phases viz. $CuAl_2$, Cu_3Al_2, Cu_9Al_4 (Hultgren et al., 1973). The present reserach thesis focuses on the study of Cu_3Al_2 as energetically favoured intermetallic compound in the molten state.

1.3 Rationale of the Study

There are countless uses of the alloys, including those in the medical, industrial, military, and commercial fields. Data regarding various properties of liquid alloy at various temperatures are not accessible and it is not feasible to do such experimental tests at any desired temperature because it would be costly and time-consuming. In this situation, the required data should be predicted or estimated by developing theoretical model that provides beneficial to comprehend alloying behaviour of liquid alloys.

The study focuses on the completely new type of alloys. From the study of different properties of alloys, we are able to confirm, whether the alloy is suitable or not for commercial and engineering use. The uses of the alloys vary depending on the various properties and can be employed in the appropriate sector.

1.4 Objectives of the Study

In the present work four liquid alloys (Na-Hg, Pb-Mg, Bi-Tl and Cu-Al) of type $A_\mu B_\nu$ are selected for the study. The Quasi Chemical Approximation method is applied to study thermodynamic and structural properties. The transport and surface properties of these alloys have been investigated in the frame work of Kaptay Model and Modified form of Butler equation respectively to predict transport and surface properties of the alloys. The interaction energy parameters required to investigate different properties are optimized by successive approximation method with the help of experimental values. The model is further extended to predict these properties of concerned liquid alloys at different temperatures. In summary, the objectives of this research are pointed as follows:

1.5 General Objective

The general objective of the proposed research work is to study the mixing behavior of binary liquid alloys of type $A_\mu B_\nu$.

1.6 Specific Objectives

To fulfill the general objective of our study, we aim to study

1. the thermodynamic properties of binary liquid alloys,
2. the structural properties of binary liquid alloys,

3. the transport properties of binary liquid alloys and
4. the surface properties of binary liquid alloys.

1.7 Organization of the Thesis

The thesis has been organized as follows:

CHAPTER 1: INTRODUCTION

This chapter presents introduction to binary liquid alloys and general overview of Na-Hg, Pb-Mg, Bi-Tl and Cu-Al binary alloys studied in this work. Additionally, it includes rationale of the study and research objectives.

CHAPTER 2: LITERATURE REVIEW

In this chapter, we have reviewed some previous literatures related to the electronic and statistical theories of mixing as well as theoretical models of viscosity and surface tension of liquid alloys.

CHAPTER 3: MATERIALS AND METHODS

In this chapter, a brief formulation of various thermo-physical properties of binary liquid alloy have been presented.

CHAPTER 4: RESULTS AND DISCUSSION

In this chapter, the results and discussion of thermodynamic, structural, transport and surface properties of Na-Hg, Pb-Mg, Bi-Tl and Cu-Al binary liquid alloys at their respective melting temperatures are included. Further, the above mentioned properties of three liquid alloys Pb-Mg, Bi-Tl and Cu-Al are studied at higher temperatures by extending Quasi-Chemical Approximation method.

CHAPTER 5: CONCLUSION AND RECOMMENDATIONS

In this chapter, we present conclusions of the present work and its possible extension for further study.

CHAPTER 6: SUMMARY

Here, a brief overview of the whole studies have been presented.

Finally, the references are listed and appendices are given before closing this document.

CHAPTER 2

2. LITERATURE REVIEW

A detailed grasp of the alloy's energetics and kinetics is required in order to create specific alloys with predetermined qualities. As a result, several attempts to promote the theoretical approach have been launched. The two basic theoretical methodologies that have been established in this discipline are electronic and statistical theory of mixing. This part provides a review of the literature on these theoretical methodologies which sparked our interest in doing this study.

2.1 Review of Electronic Theory of Mixing

Drude-Lorentz (Drude, 1900; Ramaswamy, 1971) offered the first hypothesis to describe the process of electrical conduction in metals in the beginning of the twentieth century. According to their hypothesis, a metal is made up of positive metal ions that are fixed in the lattice whose valence electrons roam around aimlessly in the positive sea, like that of the gas molecules in a vessel. Electrostatic forces between positively charged ions and free electrons are supposed to hold the metal together. Based on this theory Hume-Rothery et al. (1934) presented principles of metal alloying based on size and electronegativity. The electronic theory of Hard Sphere Model (Percus & Yevick, 1958; Rushbrooke, 1963; Thiele, 1963) makes a significant contribution to the theoretical study of binary alloys. Lebowitz (1964) further generalized the Percus-Yevick equation for radial distribution function to an m-component mixture. According to Faber (1972) , the Hard Sphere Model can be used to describe the entropies in metals and alloys. Similarly, Hoshino & Young (1980) obtained the general expression for the partial and total structure factor of an m-component hard sphere mixture on basis of solution of Percus-Yevick equation and applied to the Li-Pb alloy. By correlating the electronic theory of Hard Sphere Model to thermodynamics, many researchers such as Singh & Choudhary (1981) calculated the heat and entropies of mixing of equiatomic AI-Mg, Cd-In, Cd-TI, In-Zn, Cd-Zn and Mg-Zn liquid alloys, Schwitzgebel & Langen (1981) calculated mutual diffusion coefficient of Bi-Sn and Sn-Zn binary alloys, Khanna (1984) calculated the entropy of mixing of Na-Hg and Sb-Zn alloys, Matsunaga et al. (1999) made structural study of Na-Pb liquid alloys, Arzpeyma et al. (2013) calculated the entropy of mixing of Ag-Cu,Ag-Ga, Ag-Pb,Bi-Cd, Bi-In,Bi-Na,.Bi-Zn, Cd-Hg, Cd-Pb, Cd-Zn, Cu-Fe, Hg-In, Hg-Na, Hg-Zn ,In-Na,In-Sn, In-Sn and K-Pb binary alloys.

The Pseudopotential theory is another significant electronic theory for calculating many

properties of metals, semiconductors, alloys and other materials. The nucleus as well as other electrons in the atom exert a force on an electron inside the atom. The major difficulty in the study of condensed matter and its behavior is determining the forces experienced by an electron rotating around the nucleus in specific orbits. Bardeen (1937) was the first to explain the average interaction experienced by an electron using the concept of self-consistent screening in this competition. Later on, this concept was used to investigate a variety of solid property (Harrison, 1966; Heine & Weaire, 1966), which is also known as Pseudopotential theory. It was an important development for the study of solid state physics.

Based on the pseudopotential theory, Hasegawa & Young (1977) investigated the solid-liquid co-existence in the Cd-Mg and Na- K System, Dubinin et al. (2007) calculated few thermodynamic properties of Fe-Co liquid alloy, Vora (2010) calculated the electrical properties of liquid binary alloys Cu_{1-X} Ga_X, Malan & Vora (2021) studied the thermodynamic properties of binary Na-K liquid alloy. Despite the fact that electronic theories are devoid of prior assumptions, they have certain limitations. The structural features of binary alloys such as segregation and phase separation are not determined using the Hard Sphere model. Osman & Singh (1993, 1995) solved this problem in the hard sphere model by incorporating attractive interaction. Furthermore, Pseudo potential theory are not used with confidence to alloys whose mixing properties exhibit aberrant behavior due to intense interplay between dissimilar atoms heading to compound formation (Hoshino & Young, 1980; Lai et al., 1983; Young, 1992). Because of this constraint, electrical theories must be improved in order to study different properties of binary liquid alloys.

2.2 Review of Statistical Approach of Mixing

2.2.1 Review of Thermodynamic and Structural Properties

To get over the difficulties of electronic theory, some theoreticians (Meyer, 1939; Flory, 1942; Hildebrand & Scott, 1950; Guggenheim, 1952; Bhatia & Singh, 1982; Prigogine & Defay, 1958; Bhatia & Thornton, 1970; Singh & Mishra, 1988; Adhikari et al., 2010; Koirala et al., 2014; Yadav et al., 2018) shifted their attention and devised statistical theory based on various assumptions in order to access the energetics of liquid mixtures and examine the local arrangement of atoms in alloys. Calculating the thermodynamic properties of a mixture from the forces between the atoms or molecules is the basic problem in statistical theory of solution. Likewise, getting the microscopic properties of binary molten alloys from bulk properties is a key emphasis of that theory's research.

Meyer (1939) found the entropy of mixing of long chain chemical compounds dissolved in simple solvents, providing a more convincing explanation for the anomalies of long chain

or polymeric molecules. He then proposed an idealized model for such a solution. Based on this model, Flory-Huggins (Flory, 1942; Huggins, 1942) carried out a derivation of the partial molal entropies of dilution in idealized solutions of chain compounds and for the activities of a high polymer solutions by considering a lattice model for polymers. This model is applicable to find the thermodynamics of liquid alloys when the constituent atoms of mixture differ strongly in volume. Similarly, the concept of an ideally associated solution was developed to characterize the properties of liquid alloys by the researchers (Hildebrand & Scott, 1950; Guggenheim, 1952; Prigogine & Defay, 1958; Bhatia & Hargrove, 1974). Though there is no enthalpy change during mixing in the ideal solution model, the Gibbs free energy of mixing has an entropic contribution since the mixture has become disordered.

Longuet-Higgins (1951) introduced the Conformal Solution Model, which takes the energetic effect into account. The molecules in a liquid mixture are supposed to be organized in a regular lattice, according to this idea. Bhatia & Thornton (1970) defined partial structure factor in relation to concentration fluctuation in long wavelength limit which became powerful tool for the qualitative analysis of the local arrangement of atoms in binary liquid alloys (Prasad & Singh, 1991; Singh et al., 1991; N. Jha & Mishra, 2001; Anusionwu, 2003; Costa et al., 2014; Koirala et al., 2015; Panthi et al., 2020; Bhandari, Panthi, Koirala, & Adhikari, 2021). Theoreticians (Bhatia et al., 1973; Alonso & March, 1982) used Conformal Solution Model to analyze and explain concentration fluctuations in the long wave length limit, where a liquid mixture with particles of nearly equal size is expected to interact. Parrinello et al. (1974) on the other hand, used this model to obtain the mathematical expressions for partial structural factors of a binary liquid alloy. Similarly, Guggenheim's quasi-chemical theory (Guggenheim, 1952) has been found to be effective in the investigation of concentration fluctuation in the long wavelength limit as well as the chemical short range order parameter for binary liquid alloys.

The comprehensive analysis of heat of mixing for certain binary liquid alloys as done by Kleppa (1958) revealed that valence difference causes the heat of mixing curve to become more asymmetric. The Zn-Cd curve, he claimed, is essentially symmetric, whereas the Cd-Bi curve has a lot of asymmetry. Similarly the study of the liquid alloy using neutron diffraction (Ruppersberg & Egger, 1975; Alblas, 1983; Takeda et al., 1987; Harada et al., 1988; Reijers et al., 1989) revealed anomalous behavior in short range order, with intensities exhibiting a distinct peak before the principal peak of diffraction pattern. The foregoing explanation, based on experimental evidence, demonstrated that anomalous features of compound forming liquid alloys occur at or near stoichiometric compositions in which stable intermetallic compounds exist in solid phase. Thus many theoreticians added the concept that some of the alloy system has clusters of atoms (complex) in equilibrium with a 'matrix' of more randomly arranged constituent atoms (Wilson, 1965;

Jordan, 1970; Prasad & Singh, 1990). Moreover the thermodynamic data compiled by Hultgren et al., as well as a number of experimental reports (Predel & Oehme, 1974; Matsunaga et al., 1983; Yakymovych et al., 2008) show that the properties of mixing of a large number of liquid binary alloys are asymmetric with concentration, despite the constituent atoms' size differences. The enthalpy and the free energy of mixing are usually large negative values at a concentration or another. Thus, based on the grouping of constituent element atoms, alloys can be divided into two categories: compound forming alloys (ordering), in which like atoms tend to be nearest neighbor over unlike atoms, and segregating alloys, in which unlike atoms tend to be nearest neighbor over like atoms (Novakovic et al., 2004).

To acquire a better grasp of the degree of ordering in binary liquid alloys, the chemical short range order parameter (Cowley, 1950; Warren, 1969) was devised that delivers information of the local arrangement of atoms in the liquid mixture. Bhatia & Singh (1982) created a model that establishes a quantitative relationship between thermodynamic parameters and the short range order parameter.

The asymmetry in mixing properties of binary liquid alloys as a function of concentration cannot be explained by the theories outlined above. Hence the different complex formation models of binary liquid alloys have been proposed. Jordan (1970) presented the Regular Associated Solution Model for studying the thermodynamics of melting AB compounds. He assumed association in the liquid phase with species A, B, and AB present and took into consideration their interactions. He derived the equations for the thermodynamic and the liquidus curve in the Zn-Te and Cd-Te binary alloys. Lele & Ramachandrarao (1981) provided a comprehensive analytical procedure for the treatment of regular associated solutions. He demonstrated how the interaction energies and equilibrium constant for the formation of complexes in liquid alloys can be obtained. Using this model, they were also able to accurately characterize the thermodynamic characteristics of Mg-Sn and In-Sb liquid alloys. Adhikari et al. (2014) extended this model by presenting the formulae for concentration fluctuation in long wavelength limit and chemical short range order parameter and investigated thermodynamic and structural properties of Cd-Na, Ag-Sb, Cu-Sn, Mg-Tl binary liquid alloys. Similarly Yadav and his coworkers (Yadav et al., 2015) studied the thermodynamic and structural properties of In-Bi and Tl-Bi binary liquid alloys by using the Regular Associated Solution model.

Bhatia et al. (1974) derived analytical expressions for the concentration dependence of free energy of mixing and concentration fluctuation in the long wavelength limit by assuming the chemical complex ($A_\mu B_\nu$) in the liquid state using another model called 'Compound Formation Model'. Bhatia & Hargrove (1974) explained the complex nature of Mg-Bi, Ag-Al and Cu-Sn liquid alloys having small volume difference at about their melting temperatures in order to understand the mixing nature of binary liquid

alloys. However the short range order parameter was not taken into account in Bhatia and Hargrove's attempt. Bhatia & March (1975) developed a theory of concentration fluctuation in long wavelength limit for the Na-Cs binary alloy of large volume ratio.

Bhatia & Singh (1984) recast Bhatia and Hargrove's Compound Formation Model into quasi-lattice theory utilizing a quasi-lattice picture. The reformulation is based on the assumption that all atoms in a binary solution are located at lattice sites, each of which has Z nearest neighbors. It presents an expression for the short range order parameter, unlike the Bhatia and Hagrove technique. However, this model presupposes that the sizes of the two types of atoms in the mixture differ by 50 % which is not always the case. Novakovic et al. (2005) investigated the surface and transport properties of an Au-Sn liquid alloy using this model. Surface, kinetic, and structural aspects of liquid Al–Ti alloys were investigated by Novakovic et al. (2012).

Singh & Mishra (1988) proposed another model: the Simple Statistical Model. The model uses pairwise interaction energies to calculate conditional probabilities for neighboring atoms' occupation in binary liquid alloys. This model has been extended to derive equations for activity, free energy of mixing, concentration fluctuation in the long wavelength limit, and chemical short range parameters. The concentration dependent thermodynamic properties for Cu Pb, Na-K, Li-Mg, and Cd-Mg were explained in this statistical framework by evaluating ordering energy. Singh et al. (1990) extended this approach to describe the level of hetero-coordination in Cd-based regular binary liquid alloys such as Cd-Bi, Cd-Mg, and Cd-Ga. Koirala (2016) studied the thermodynamic and structural properties of four segregating In-Tl, Ag-Cu, Cd-Pd, In-Pb and four ordering ,Bi-In, Cd-Bi, and Ag-Cu, Al-Mg liquid alloys. The model has the drawback of only being able to study regular alloy.

Bhatia & Singh (1982) enhanced the model called ' Quasi- Chemical Approximation' by incorporating the idea of grand partition function and taking into account the interaction energy of AA,AB, and BB pairs depending on whether the bond is part of complex AB or not. The model also assumes that atoms of alloys are located on lattice sites, each of which has Z nearest neighbors. Their interaction is short range and effective between nearest neighbors. The atomic partition function of an A atom associated with the translational degrees of freedom is the same wherever A is located, and that the partition function for B is the same wherever B is located. Based on this assumption, they formulated the mathematical expressions for various thermodynamic functions. This model is preferable to the complex formation model in the sense that it may be utilized to obtain short range order for compound forming binary liquid alloys.

Based on this model, Singh (1987) studied the concentration fluctuation in long wavelength limit and short range parameter for Mg-Bi and Ag-Al liquid alloys. Prasad & Singh

(1990) explained the thermodynamic and structural properties of Au-Zn liquid alloy. Anusionwu et al. (2009) explained thermodynamics of Al-Ge and Al-Ga liquid alloys. I. Jha et al. (2016) studied the thermodynamic and structural properties of Tl-Na liquid alloy. But still there remains lack of thermodynamic study of some compound forming binary liquid alloys.

2.2.2 Review of Theoretical Model of Viscosity

The Knowledge of atomic transport properties such as viscosity may be utilized to acquire a better understanding of the structure and binding of binary liquid alloys at the microscopic level. Temperature and composition dependent viscosity values are very desirable, however the data for viscosity is confined to a few systems and is still insufficient to meet the technological needs.

Although various theoreticians (Born & Green, 1947; Rice & Kirkwood, 1959; Rice & Allnatt, 1961) produced various hypotheses to describe the viscosity of liquid metals, the theoretical study of viscosity of alloys was discovered later. The first theoretical model for determining the viscosity of binary liquid alloys using enthalpy of mixing was created by E.A. Moelwyn-Hughes in 1961 (Hughes, 1961). T. Iida et al. (1976) developed an equation that connected the viscosity of a binary system to the diameters and masses of various atoms, as well as the integral molar enthalpy of mixing. Singh & Sommer (1998) found that positive deviations are expected in compound forming systems and negative deviations in segregating systems. Seetharaman & Sichen (1994) proposed a relationship for the viscosity of binary substitutional liquid alloys based on the energy of mixing in binary metallic melts and the viscosities of the corresponding unary systems. They determined the viscosities of In-Sn, Ag-Au, Ag-Sn, Ag-Sb, Ag-ln, Bi-Sn, Co-Fe, and Bi-Cu binary alloys. Kaptay (2003) modified Seetharaman and Sichen's viscosity relation in relation to the theoretical link between the alloy's cohesion energy and the activation energy of viscous flow.

On the other hand, Hirai (1993) formulated a theoretical model to predict the viscosity of alloys by examining the impact of composition and temperature on the viscosities of liquid metals, extending Arrhenius' formula. Singh & Sommer (2012) reformulated and extended the Andrade relation for liquid metal viscosity to obtain a relationship for alloy viscosity in terms of atomic mass, atomic volume, Debye temperature, and activation energy of liquid metals, as well as heat of mixing and excess volume of mixing of the liquid alloy. The diffusion coefficient and shear viscosity of Ag-In liquid alloy are examined using the distribution function approach developed by Bhuiyan et al. (2003) in which the interionic interaction is modeled using a local pseudopotential.

2.2.3 Review of Theoretical Model of Surface Properties

In metallurgy and industry, the surface properties (surface tension and surface concentration) of liquid alloy or liquid metal is considered a prime factor for both processing and production of new materials because it is associated with surface as well as interface in the molten metal process. Similarly it helps in monitoring several features of liquid alloys including mechanical behavior, kinetics of phase transformation and catalytic activity. Surface tension measurement, like thermodynamic and transport characteristics, is a critical job in the study of surfaces and interfaces, as well as an essential quantity from both a physical and technological standpoint. In industrial operations like casting, welding and solidification, a deeper understanding of the behaviors of surface tension is crucial for liquid metals with high melting temperatures. As a result, it can be claimed that surface properties and phenomena are quite important in material design and characterization (Prasad & Singh, 2000; Anusionwu, 2003; Prasad & Jha, 2005; Novakovic et al., 2008; Mukai et al., 2008; Koirala, 2018; Mehta et al., 2020; Panthi et al., 2021).

Butler (1932) proposed a model for surface tension based on the idea of a monolayer at the liquid's surface existing in equilibrium with the bulk phase. He made the assumption that the surface of a solution should be treated as a distinct phase from the bulk phase. Hoar & Melford (1957) modified Butler's model for non-ideal binary mixture with components having unequal molar surface areas considering the case of zero surface area of mixing.

Similarly, Guggenheim (1952) proposed a novel Statistical Model on the assumption of a layered structure near the interface based on the simple zeroth approximation applied to the Quasi-Lattice Model. The grand partition function of the surface has been solved in this model (Guggenheim, 1952; Prasad & Singh, 1991).

Speiser et al. (1987) and Yeum et al. (1989) later proposed a model for estimating the surface tension of binary alloys based on the assumption that the chemical potential in the bulk phase and the surface phase can be described in the same form. They demonstrated that their model can provide reasonable estimates without the use of any adjustable parameters. Mukai and his co-authors (Mukai et al., 2008) proposed another model to explain surface tension of binary and multicomponent alloys using chemical thermodynamics, which represents surface tension as a function of thermodynamic parameters without making any assumptions. For the validity of model, they compared the surface tension of Fe-Cu and Fe-Si binary alloys with experimental results and found the good agreement between experimental and theoretical model.

Kaptay (2019) updated Butler's surface tension equation for binary alloys. According to him, Butler's equation has an incorrect definition of partial surface tension of components. Thus he gave a definition of surface tension as well as information regarding the significant knowledge gap that is missing in Butler's expression (Kaptay, 2015, 2019).

2.2.4 Research Gap

The review of the literature survey reveals that there has been significant interest in the study of the various thermo-physical properties of compound forming binary liquid alloys for many years. Hence several theoretical efforts so far have been put forward by many researchers in the field of metallurgical science to comprehend the energetic of liquid alloys. One important effort is the development of Quasi-Chemical Approximation model (Bhatia & Singh, 1982) because the model incorporates the idea of grand partition function to deal the properties of complex binary liquid alloys and paves way in the desired direction by making the link between microscopic and macroscopic properties. However, study of some compound forming binary liquid alloys by Quasi-Chemical Approximation is still lacking. On the other hand, most of the theoretical models have been used to study different properties at about melting temperatures of the binary alloys. The alloys have wide application at higher temperature than their melting temperatures such as in casting of the alloys. But the focus of alloy research has not exceeded the melting temperature of the alloy.

In this thesis, the thermodynamic and microscopic structural characteristics of compound forming binary liquid alloys are explored theoretically by using Quasi-Chemical Approximation. The importance of interaction energy parameters is given more attention during the research. For the detailed thermophysical research of binary liquid alloys, the Kaptay equation (Kaptay, 2003) and new improved derivation of Butler equation (Kaptay, 2019) are used for evaluating viscosity and surface properties. Similarly, the Quasi-Chemical Approximation model has been extended to predict the thermo-physical properties of some compound forming liquid alloys at higher temperatures.

CHAPTER 3

3. MATERIALS AND METHODS

The research is based on theoretical work and hence the study is carried out using theoretical model. In this chapter we shall discuss theoretical backgrounds of models used for the study of binary liquid alloys.

When two metals A and B are combined to form alloys, some of the alloys exhibit rapid changes in free energy of mixing for minor compositional variations and form intermetallic compounds at one or more stoichiometric compositions. Hence, phases of the alloys in this case is referred to as an intermetallic compound and generally expressed as $A_\mu B_\nu$. In this regard, four types of alloys viz. Na-Hg, Pb-Mg, Bi-Tl and Cu-Al have been selected as study materials by assuming $NaHg_2$, $PbMg_2$, $BiTl_3$ and Cu_3Al_2 as their most stable intermetallic compounds respectively. Similarly, the software 'Microsoft Office Excel 2013' and 'Octave' have been used for handling the problems easily.

3.1 Quasi - Chemical Approximation for Thermodynamic Functions

In order to investigate thermodynamic properties by Quasi-Chemical Approximation, it is essential to optimize interaction energy parameters as well as temperature derivative interaction energy parameters of the concerned alloys. The interaction energy parameters of each of the alloys are optimized by the method successive approximation with the help of corresponding experimental values of free energy of mixing of the alloys and then used in the mathematical formulation of Gibbs free energy of mixing as derived in Subsection 3.1.1 to deal the property. Similarly, the temperature derivative interaction energy parameters are also optimized with the help of experimental enthalpy of mixing of the alloys and used in the equation of enthalpy of mixing as derived in Subsection 3.1.2.

3.1.1 Excess Gibbs Free Energy and Gibbs Free Energy of Mixing

Let us consider a bulk of binary alloy of N_A and N_B atoms of elements A and B respectively. Let total number of atoms be N. Then,

$$N_A + N_B = N \tag{3.1}$$

The grand partition function of bulk material is

$$\Xi^b = q_A^{N_A}(T) q_B^{N_B}(T) \exp[(\mu_A N_A + \mu_B N_B - E)]/k_B T \tag{3.2}$$

where $q_i^{N_i}(T)$ and μ_i be partition functions of atoms ($i = A$ or B) with inner and translational degrees of freedom and chemical potential of atoms respectively. E is cofigurational energy of the atoms.

Now, to define the configurational energy 'E' explicitly we assume that the entire set of lattice sites is present in a tiny cluster of a few lattice sites, say in domain 1 and remaining lattice sites in domain 2. Using prefixes 1 and 2 to distinguish the quantities corresponding to the tiny cluster and the reminder, we get:

$$N_A = N_{1A} + N_{2A} \tag{3.3}$$

$$N_B = N_{1B} + N_{2B} \tag{3.4}$$

$$E = E_1 + E_2 + E_{12} \tag{3.5}$$

where E_i ($i = 1, 2$) are the configurational energies of domain i and E_{12} takes into account the interaction between the atoms of domain 1 and 2. Thus the grand partition function can be written as the product of the partition functions of first and second domains i.e.

$$\Xi = \Xi_1^{'}\Xi_2 \tag{3.6}$$

where a prime on Ξ_1 denotes that the interaction of domain 1 with domain 2 is incorporated in it.

The partition function $\Xi_1^{'}$ can be written as:

$$\Xi_1^{'} = \sum_{E_1} \zeta_A^{N_{1A}} \zeta_B^{N_{1B}} \exp[-(E_1 + E_{12})/k_{\mathrm{B}}T] \tag{3.7}$$

where

$$\zeta_A = q_A(T) \exp(\mu_A/k_{\mathrm{B}}T), \quad \zeta_B = q_B(T) \exp(\mu_B/k_{\mathrm{B}}T) \tag{3.8}$$

and similar expression exits for Ξ_2.

Here, $E_{12}/k_{\mathrm{B}}T$ is the average energy of interaction through which atoms of domain 1 interact with the rest of domain 2. By the simple approximation (Fowler & Guggenheim, 1939),

$$\exp\left(\frac{-E_{12}}{k_{\mathrm{B}}T}\right) \approx \phi_A^{\nu_A} \phi_B^{\nu_B} \tag{3.9}$$

where ϕ_A and ϕ_B are constants. ν_A denotes the number of lattice sites in domain 2 that are closest neighbor of the A atoms in the cluster and similarly for ν_B. Now, Equation

(3.7) becomes

$$\Xi_1^{'} = \sum_{E_1} \zeta_A^{N_{1A}} \zeta_B^{N_{1B}} \phi_A^{\nu_A} \phi_B^{\nu_B} \exp[-(E_1)/k_{\mathrm{B}}T] \tag{3.10}$$

The average values of A and B atoms in the cluster are given as:

$$\langle N_{1A} \rangle = \zeta_A \frac{\partial \ln \Xi_1^{'}}{\partial \zeta_A}, \qquad \langle N_{1B} \rangle = \zeta_B \frac{\partial \ln \Xi_1^{'}}{\partial \zeta_B} \tag{3.11}$$

Dividing second by first, we get,

$$\frac{\langle N_{1B} \rangle}{\langle N_{1A} \rangle} = \frac{1-C}{C} = \frac{C_B}{C_A} = \frac{\zeta_B}{\zeta_A} \frac{\frac{\partial \ln \Xi_1^{'}}{\partial \zeta_B}}{\frac{\partial \ln \Xi_1^{'}}{\partial \zeta_A}} \tag{3.12}$$

where C and $(1-C)$ represent the average concentrations of A and B atoms in the cluster respectively and are assumed to be equivalent to the concentrations of A and B atoms in the alloys. As a result, $(1-C)/C$ (or $(C_B)/C_A)$) is independent of the size of cluster. Hence, cluster of different sites may be utilized to assess Equation (3.12).

First we consider one lattice site which can be occupied by either an A atom or a B atom. In this case there are no AA, AB or BB bonds and hence $E_1 = 0$. Similarly, ν_A and ν_B in Equation (3.9) is coordination number (Z) of the lattice site. Now, Equation (3.10) reduces to

$$\Xi_1^{'(1)} = \zeta_A \phi_A^Z + \zeta_B \phi_B^Z \tag{3.13}$$

Here, superscript (1) is added to indicate that this is the expression for $\Xi_1^{'}$ for the cluster of one atom.

For a cluster of two lattice sites, the cluster can have either two A atoms or two B atoms or an A and a B atom. The table below shows all conceivable atom configurations on sites inside a cluster (Singh, 1987) .

Table 1: Possible configurations of A and B atoms in the cluster with two lattice sites

Site 1	Site 2	ν_A	ν_B	E_1
A	A	$2(Z-1)$	0	ϵ_{AA}
B	B	0	$2(Z-1)$	ϵ_{BB}
A	B	$Z-1$	$Z-1$	ϵ_{AB}
B	A	$Z-1$	$Z-1$	ϵ_{AB}

Now, for the cluster of two lattice sites, Equation (3.10) becomes

$$\Xi_1^{'(2)} = \zeta_A^2 \phi_A^{2(Z-1)} e^{-\epsilon_{AA}/k_B T} + \zeta_B^2 \phi_B^{2(Z-1)} e^{-\epsilon_{BB}/k_B T} + 2\zeta_A \zeta_B (\phi_A \phi_B)^{Z-1} e^{-\epsilon_{AB}/k_B T} \quad (3.14)$$

While deriving Equation (3.14), we didn't consider the probability of formation of complex or compound alloys of type $A_\mu B_\nu$. Actually a binary alloy is a mixture of three types of constituents; A atoms, B atoms and complexes of type $A_\mu B_\nu$. Let ϵ_{ij} $(i, j = A, B)$ denotes the energy of ij bond if the ij bond is free bond and let $\epsilon_{ij} + \Delta\epsilon_{ij}$ denote its energy if the ij bond is one of the bonds in the complex. Further, let p_{ij} signify the probability that an ij bond is a member of the complex. If the cluster contains two A atoms, the energy is given by

$$E_1 = (1 - p_{AA})\epsilon_{AA} + p_{AA}(\epsilon_{AA} + \Delta\epsilon_{AA}) = \epsilon_{AA} + p_{AA}\Delta\epsilon_{AA} \quad (3.15)$$

If the cluster contains two B atoms, the energy is given by

$$E_1 = \epsilon_{BB} + p_{BB}\Delta\epsilon_{BB} \quad (3.16)$$

and if the cluster contains two A and B atoms, the energy is

$$E_1 = p_{AB}(\epsilon_{AB} + \Delta\epsilon_{AB}) \quad (3.17)$$

Now, Equation (3.14) can be rewritten as:

$$\Xi_1^{'(2)} = \zeta_A^2 \phi_A^{2(Z-1)} \varrho_{AA} + \zeta_B^2 \phi_B^{2(Z-1)} \varrho_{BB} + 2\zeta_A \zeta_B (\phi_A \phi_B)^{Z-1} \varrho_{AB} \quad (3.18)$$

where

$$\varrho_{ij} = \exp\left(-\frac{\epsilon_{ij} + p_{ij}\Delta\epsilon_{ij}}{k_B T}\right) \quad (3.19)$$

The bond in the cluster being a part of complex $A_\mu B_\nu$ allows p_{ij} to take following relation (Bhatia & Singh, 1982).

$$p_{AB} = C^{\mu-1}(1 - C)^{\nu-1}[2 - C^{\mu-1}(1 - C)^{\nu-1}] \quad (3.20)$$

By the same method, it is possible to obtain

$$p_{AA} = C^{\mu-2}(1 - C)^{\nu}[2 - C^{\mu-2}(1 - C)^{\nu}], \quad \mu \geq 2 \quad (3.21)$$

$$p_{BB} = C^{\mu}(1 - C)^{\nu-2}[2 - C^{\mu}(1 - C)^{\nu-2}], \quad \nu \geq 2 \quad (3.22)$$

For $\mu = 1$, $p_{AA} = 0$ and for $\nu = 1$, $p_{BB} = 0$, since Equations (3.21) and (3.22) are used

only for $\mu \geq 2$ and $\nu \geq 2$ respectively.

Now, from Equations (3.12) and (3.18), we get

$$\frac{1-C}{C} = \frac{\zeta_B}{\zeta_A} \frac{\zeta_B \phi_B^{2(Z-1)} \varrho_{BB} + \zeta_A (\phi_A \phi_B)^{Z-1} \varrho_{AB}}{\zeta_A \phi_A^{2(Z-1)} \varrho_{AA} + \zeta_B (\phi_A \phi_B)^{Z-1} \varrho_{AB}} \tag{3.23}$$

From the Equations (3.12) and (3.13), we get

$$\frac{1-C}{C} = \frac{\zeta_B}{\zeta_A} \left[\frac{\phi_B}{\phi_A}\right]^Z \tag{3.24}$$

From Equations (3.23) and (3.14), we get

$$\tau^2 + \left(\frac{1-2C}{\lambda C}\right) - \frac{1-C}{C} = 0 \tag{3.25}$$

where

$$\tau = \left(\frac{\phi_B}{\phi_A}\right) \left(\frac{\varrho_{AA}}{\varrho_{BB}}\right)^{1/2} \tag{3.26}$$

$$\lambda = \frac{(\varrho_{AA} \varrho_{BB})^{1/2}}{\varrho_{AB}} \tag{3.27}$$

By solving Equation (3.25), we get

$$\tau = \frac{\beta - 1 + 2C}{2\lambda C} \tag{3.28}$$

with

$$\beta = [1 + 4C(1-C)(\lambda^2 - 1)]^{1/2} \tag{3.29}$$

Following Equations (3.27) and (3.28), we get

$$\tau = \left[\frac{1-C}{C} \frac{\beta - 1 + 2C}{\beta + 1 - 2C}\right]^{1/2} \tag{3.30}$$

From Equations (3.24) and (3.26),

$$\frac{\zeta_A}{\zeta_B} = \frac{C}{1-C} \tau^Z \left(\frac{\varrho_{BB}}{\varrho_{AA}}\right)^{Z/2} \tag{3.31}$$

From Equations (3.19) and (3.27),

$$\lambda^2 = \exp\left(\frac{2\omega}{Z k_B T}\right) \exp \frac{2 p_{AB} \Delta\epsilon_{AB} - p_{AA} \Delta\epsilon_{AA} - p_{BB} \Delta\epsilon_{BB}}{k_B T} \tag{3.32}$$

where

$$\omega = Z\left(\epsilon_{AB} - \frac{\epsilon_{AA} + \epsilon_{BB}}{2}\right) \tag{3.33}$$

is known as interchange energy that is needed to convert an AA pair and a BB pair into two AB pairs.

The activity coefficients γ_A and γ_B of two species are given as:

$$\mu_A - \mu_A^0 = k_\mathrm{B}T\ln(C\gamma_A) \tag{3.34}$$

$$\mu_B - \mu_B^0 = k_\mathrm{B}T\ln[(1-C)\gamma_B] \tag{3.35}$$

where μ_i^0 is the chemical potential of pure component.

Solving Equations (3.19), (3.26), (3.31), (3.34) and (3.35), we get

$$\ln\gamma = Z\ln\tau + \frac{Z}{2k_\mathrm{B}T}(p_{AA}\Delta\epsilon_{AA} - p_{BB}\Delta\epsilon_{BB}) + \varphi \tag{3.36}$$

where γ is ratio of activity coefficients of two components A and B. φ is constant and independent on concentration.

Here, ω and $\Delta\epsilon_{ij}$ are sufficiently smaller and hence λ^2 in Equation (3.32) can be expressed in the linear terms of these parameters as:

$$\lambda^2 = 1 + \frac{1}{Zk_\mathrm{B}T}\left(2\omega + 2p_{AB}\Delta\omega_{AB} - p_{AA}\Delta\omega_{AA} - p_{AB}\Delta\omega_{BB}\right) \tag{3.37}$$

where $\Delta\omega_{ij} = Z\Delta\epsilon_{ij}$ and is called interaction energy parameter. Let us write above Equation (3.37) as:

$$\lambda^2 = 1 + Y \tag{3.38}$$

where

$$Y = \left(\frac{1}{Zk_\mathrm{B}T}\right)\left[2\omega + 2p_{AB}\Delta\omega_{AB} - p_{AA}\Delta\omega_{AA} - p_{BB}\Delta\omega_{BB}\right]$$

Using Equation (3.38), Equation (3.29) can be written as:

$$\beta = \left[1 + 4C(1-C)Y\right]^{1/2} \approx 1 + 2C(1-C)Y \tag{3.39}$$

$$\beta = 1 + \frac{2C(1-C)}{Zk_BT}(2\omega + 2p_{AB}\Delta\omega_{AB} - p_{AA}\Delta\omega_{AA} - p_{BB}\Delta\omega_{BB}) \tag{3.40}$$

Now, Equation(3.30) becomes

$$\ln \tau = \frac{1}{2} \ln[Y - 2CY - CY^2 + C^2Y^2 + 1] \tag{3.41}$$

As the values of $\omega/(k_{\mathrm{B}}T)$ and $\Delta\omega_{ij}/(k_{\mathrm{B}}T)$ are smaller than unity (Guggenheim, 1952; Bhatia & Singh, 1982) , we can easily conclude that $Y \leq 1$. As a result, the power of Y can be neglected. Thus,

$$\ln \tau = \ln \left[1 + \frac{1}{2} Y(1 - 2C) \right] \tag{3.42}$$

Using the relation $\ln(1 + x) = x - \frac{x^2}{2} + \frac{x^3}{3} \ldots$ and neglecting the higher order terms, we get

$$\ln \tau = \left[\frac{1}{2} Y(1 - 2C) \right]$$

Using Equation (3.42), Equation (3.36) can be written as:

$$\ln \gamma = Z \frac{1}{2} Y(1 - 2C) + \frac{Z}{2k_{\mathrm{B}}T} (p_{AA}\Delta\epsilon_{AA} - p_{BB}\Delta\epsilon_{BB}) + \varphi \tag{3.43}$$

Substituting the value of Y and simplifying, we get

$$\ln \gamma = \frac{1}{k_{\mathrm{B}}T} \left[(1 - 2C)(\omega + p_{AB}\Delta\omega_{AB}) + C p_{AA}\Delta\omega_{AA} - (1 - C) p_{BB}\Delta\omega_{BB} \right] + \varphi \tag{3.44}$$

The excess free energy of mixing (Bhatia & Singh, 1982) can be written as:

$$\frac{G_{\mathrm{M}}^{\mathrm{Xs}}}{N k_{\mathrm{B}}T} = \int_0^C \ln \gamma \, dC \tag{3.45}$$

Since $G_{\mathrm{M}}^{\mathrm{Xs}}$ is zero at $C = 0$ and 1. Thus the value of φ can be obtained by setting $\int_0^1 \ln \gamma dC = 0$. Hence,

$$\int_0^1 \frac{1}{k_{\mathrm{B}}T} \left[(1 - 2C)(\omega + p_{AB}\Delta\omega_{AB}) + C p_{AA}\Delta\omega_{AA} - (1 - C) p_{BB}\Delta\omega_{BB} + \varphi \right] \, dC = 0 \tag{3.46}$$

Now, simplying Equation (3.46) after substituting the values of p_{ij} from Equations (3.20)

to (3.22), the value of φ can be obtained as:

$$\begin{aligned}\varphi =&\frac{\Delta\omega_{AB}}{k_{\mathrm{B}}T}\left[2\beta(\mu+1,\nu)\right]-2\beta(\mu,\nu+1)+\beta(2\mu-1,2\nu)-\beta(2\mu,2\nu-1)\right]\\&+\frac{\Delta\omega_{AA}}{k_{\mathrm{B}}T}\left[\beta(2\mu-2,2\nu+1)-2\beta(\mu,\nu+1)\right]\\&+\frac{\Delta\omega_{BB}}{k_{\mathrm{B}}T}\left[2\beta(\mu+1,\nu))-\beta(2\mu+1,2\nu-2)\right]\end{aligned}\tag{3.47}$$

where $\beta(m,n)$ is the beta function related to the gamma function as usual. Now, for one mole of substance the $G_{\mathrm{M}}^{\mathrm{Xs}}$ can be written in simplified form as:

$$G_{\mathrm{M}}^{\mathrm{Xs}}=RT\left[\Psi\frac{\omega}{k_{\mathrm{B}}T}+\Psi_{AB}\frac{\Delta\omega_{AB}}{k_{\mathrm{B}}T}+\Psi_{AA}\frac{\Delta\omega_{AA}}{k_{\mathrm{B}}T}+\Psi_{BB}\frac{\Delta\omega_{BB}}{k_{\mathrm{B}}T}\right]\tag{3.48}$$

where $\Psi=C(1-C)$ and Ψ_{ij} are simple polynomial in C which can be written explicitly for given value of μ and ν.

For $\mu=1$ and $\nu=2$,

$$\begin{aligned}\Psi_{AB}&=\frac{1}{6}C+C^2-\frac{5}{3}C^3+\frac{1}{2}C^4\\\Psi_{AA}&=0\\\Psi_{BB}&=-\frac{1}{4}C+\frac{1}{2}C^2-\frac{1}{4}C^4\end{aligned}\tag{3.49}$$

For $\mu=1$ and $\nu=3$,

$$\begin{aligned}\Psi_{AB}&=\frac{1}{5}C+\frac{2}{3}C^2-C^4-\frac{1}{5}C^5+\frac{1}{3}C^6\\\Psi_{AA}&=0\\\Psi_{BB}&=-\frac{3}{20}C+\frac{2}{3}C^3-\frac{3}{4}C^4+\frac{2}{5}C^5-\frac{1}{6}C^6\end{aligned}\tag{3.50}$$

For $\mu=3$ and $\nu=2$,

$$\begin{aligned}\Psi_{AB}&=\frac{13}{420}C+\frac{2}{3}C^3-\frac{3}{2}C^4+\frac{3}{5}C^5+\frac{2}{3}C^6-\frac{5}{7}C^7+\frac{1}{4}C^8\\\Psi_{AA}&=-\frac{53}{840}C+\frac{2}{3}C^3-\frac{5}{4}C^4+\frac{6}{5}C^5-C^6+\frac{4}{7}C^7-\frac{1}{8}C^8\\\Psi_{BB}&=\frac{23}{280}C-\frac{1}{2}C^4+\frac{2}{5}C^5+\frac{1}{7}C^7-\frac{1}{8}C^8\end{aligned}\tag{3.51}$$

The Gibbs free energy of mixing can be obtained as:

$$G_{\mathrm{M}}=G_{\mathrm{M}}^{\mathrm{Xs}}+G_{\mathrm{M}}^{\mathrm{id}}\tag{3.52}$$

where

$$G_{\mathrm{M}}^{\mathrm{id}} = RT\left[C\ln C + (1-C)\ln(1-C)\right] \tag{3.53}$$

is ideal Gibbs free enery of mixing.

Using Equations (3.48) and (3.53), one can readily obtain

$$G_{\mathrm{M}} = RT\left[\Psi\frac{\omega}{k_{\mathrm{B}}T} + \Psi_{AB}\frac{\Delta\omega_{AB}}{k_{\mathrm{B}}T} + \Psi_{AA}\frac{\Delta\omega_{AA}}{k_{\mathrm{B}}T} + \Psi_{BB}\frac{\Delta\omega_{BB}}{k_{\mathrm{B}}T} + C\ln C + (1-C)\ln(1-C)\right] \tag{3.54}$$

The Equation (3.54) is used to compute the free energy of mixing of compound forming binary liquid alloys. Before using that the interaction energy parameters ($\omega, \Delta\omega_{i,j}$) are optimized with the help of experimental free energy of mixing.

If there are no complexes in the alloy, the expression for G_{M} can be expressed as:

$$G_{\mathrm{M}} = RT\left[\Psi\frac{\omega}{k_{\mathrm{B}}T} + C\ln C + (1-C)\ln(1-C)\right] \tag{3.55}$$

3.1.2 Enthalpy of Mixing

As two or more substances are mixed to form a solution, there is breaking of the atomic bonds in the reactants and rearrangement and formation of new bonds to make the products. Energy is involved in the breaking or forming of chemical bonds in a system, which can be either absorbed or evolved from the system. Thus, the generation or absorption of heat occurs when two substances are mixed to produce a solution. The total amount of heat evolved or absorbed during mixing process at constant pressure is known as heat of mixing or enthalpy of mixing. In the case of ideal mixing, the heat of mixing is zero where as it is positive or negative in non-ideal solution depending upon the interaction of constituent particles. The magnitude of enthalpy of mixing of a system is therefore a measure of its deviation from ideal behavior; the closer the enthalpy of mixing to zero, the more ideal the mixture's behavior becomes. Mixing is endothermic when the heat of mixing is positive, and exothermic when the heat of mixing is negative. Thus the heat of mixing of binary liquid alloy is a significant thermodynamic function that reveals the nature and strength of bonding of the liquid alloy (Pelton & Blander, 1986; Yang et al., 2009; Dębski et al., 2014).

The enthalpy of mixing of binary liquid alloys can be expressed in terms of free energy

of mixing by standard thermodynamic relation as

$$H_{\mathrm{M}} = G_{\mathrm{M}} - T\left(\frac{\partial G_{\mathrm{M}}}{\partial T}\right)_P$$

or,

$$\frac{H_{\mathrm{M}}}{RT} = \frac{G_{\mathrm{M}}}{RT} - \frac{1}{R}\left(\frac{\partial G_{\mathrm{M}}}{\partial T}\right)_P \tag{3.56}$$

Substituting the value of G_{M} from Equation (3.54) to Equation (3.56), we get

$$\begin{aligned}\frac{H_{\mathrm{M}}}{RT} =& \Psi\left[\frac{\omega}{k_{\mathrm{B}}T} - \frac{1}{k_{\mathrm{B}}}\frac{\partial\omega}{\partial T}\right] + \Psi_{AB}\left[\frac{\Delta\omega_{AB}}{k_{\mathrm{B}}T} - \frac{1}{k_{\mathrm{B}}}\frac{\partial(\Delta\omega_{AB})}{\partial T}\right] \\ &+ \Psi_{AA}\left[\frac{\Delta\omega_{AA}}{k_{\mathrm{B}}T} - \frac{1}{k_{\mathrm{B}}}\frac{\partial(\Delta\omega_{AA})}{\partial T}\right] + \Psi_{BB}\left[\frac{\Delta\omega_{BB}}{k_{\mathrm{B}}T} - \frac{1}{k_{\mathrm{B}}}\frac{\partial(\Delta\omega_{BB})}{\partial T}\right]\end{aligned} \tag{3.57}$$

3.1.3 Activity

The deviation of an alloy from ideal behavior in terms of constituent atoms can be explained by activity. The varied thermodynamic and structural features may also be represented and discussed using activity as a foundation. It is the fundamental thermodynamic function that may be acquired from experiments such as electromotive force, vapour pressure, chemical equilibria etc. (Okajima & Sakao, 1968; Tripathi & Chandrasekharaiah, 1983; Zajaczkowski & Botor, 1995).

Since the integral value can be divided in to partial values, the Gibbs free energy of mixing of an alloy can be expressed in terms of partial Gibbs energies G_A and G_B of components as:

$$G_{\mathrm{M}} = C_A G_A + C_B G_B = (1 - C_B)G_A + C_B G_B \tag{3.58}$$

where $C_A = C$ is concentration of first element A and $C_B = 1 - C$ is concentration of second element B of binary liquid alloy. Differentiating with respect to C_B

$$\frac{\partial G_{\mathrm{M}}}{\partial C_B} = G_B - G_A + C_A\frac{\partial G_A}{\partial C_B} + C_B\frac{\partial G_B}{\partial C_B} \tag{3.59}$$

From Gibbs-Duhem relation, (Darken, 1950), $C_A\partial G_A + C_B\partial G_B = 0$. Therefore,

$$G_B = G_{\mathrm{M}} + \frac{\partial G_{\mathrm{M}}}{\partial C_B}(1 - C_B) \tag{3.60}$$

In general,

$$G_i = G_{\mathrm{M}} + \frac{\partial G_{\mathrm{M}}}{\partial C_i}(1 - C_i) \tag{3.61}$$

The partial free energy is related to the activity of component of a binary liquid alloy as (Singh & Sommer, 1997):

$$G_i = RT \ln a_i \tag{3.62}$$

where a_i is activity of i^{th} component of the alloy. From Equations (3.61) and (3.62), we get

$$RT \ln a_i = G_{\mathrm{M}} + \frac{\partial G_{\mathrm{M}}}{\partial C_i}(1 - C_i) \tag{3.63}$$

Substituting the values of G_{M} from Equation (3.54) in Equation (3.61), the activities of components A and B of the alloy are found as:

$$\ln a_A = \frac{G_{\mathrm{M}}}{RT} + \frac{1 - C_A}{k_{\mathrm{B}}T}\left[(1 - 2C_A)\omega + \Delta\omega_{AB}\Psi'_{AB} + \Delta\omega_{AA}\Psi'_{AA} + \Delta\omega_{BB}\Psi'_{BB} + \ln\frac{C_A}{C_B}\right] \tag{3.64}$$

$$\ln a_A = \frac{G_{\mathrm{M}}}{RT} - \frac{C_A}{k_{\mathrm{B}}T}\left[(1 - 2C_A)\omega + \Delta\omega_{AB}\Psi'_{AB} + \Delta\omega_{AA}\Psi'_{AA} + \Delta\omega_{BB}\Psi'_{BB} + \ln\frac{C_A}{C_B}\right] \tag{3.65}$$

where Ψ'_{ij} is first concentration derivative of Ψ_{ij}.

3.1.4 Entropy of Mixing

The knowledge of entropy of mixing of liquid alloy is considered a major factor required to specify the equilibrium state of system. The entropy of mixing or the increase in uncertainty about the positions of molecules when they are intermingled, is valuable because it offers information about structural changes that occur as a result of mixing. Basically, it reflects the energy transfer between the atoms in the melt. The value of entropy of mixing of an alloy at given temperature can be used to examine the deviation in the nature of mixing of an alloy from regular behavior (Tanaka et al., 1990; Bhuiyan et al., 2009). Thus, measuring the entropy of mixing quantitatively is crucial for a comprehensive understanding of mixing of metals in binary liquid alloys.

In order to derive the relation of entropy of mixing S_{M}, let us start from following standard

thermodynamic relation.

$$S_{\mathrm{M}} = -\left(\frac{\partial G_{\mathrm{M}}}{\partial T}\right)_P \tag{3.66}$$

Substituting the value of G_{M} from Equation (3.54) to Equation (3.66), we get

$$\begin{aligned} S_{\mathrm{M}} = -R\Bigg[&\Psi\frac{1}{k_{\mathrm{B}}}\frac{\partial\omega}{\partial T} + \Psi_{AB}\frac{1}{k_{\mathrm{B}}}\frac{\partial\Delta\omega_{AB}}{\partial T} + \Psi_{AA}\frac{1}{k_{\mathrm{B}}}\frac{\partial\Delta\omega_{AA}}{\partial T} \\ &+\Psi_{BB}\frac{1}{k_{\mathrm{B}}}\frac{\partial\Delta\omega_{BB}}{\partial T} - C\ln C - (1-C)\ln(1-C)\Bigg] \end{aligned} \tag{3.67}$$

3.1.5 Concentration Fluctuation in Long Wavelength Limit

The structure factor is critical in studying the structure of a crystal since it is the sole factor that provides information about atomic locations. The structure factor of a basis is given as: (Kittel, 1966),

$$S = \sum_j f_j \exp(-i\vec{G}.\vec{r_j}) \tag{3.68}$$

where f_j is atomic scattering factor of j^{th} atom, G is reciprocal lattice vector and r_j is position of the j^{th} atom.

Bhatia & Thornton (1970) showed that the structure factor for a binary alloy may be represented in q space in terms of three partial structure factors $S_{NN}(q)$, $S_{\mathrm{CC}}(q)$ and $S_{NC}(q)$ using the weak scattering approximation and the Van Hove (1954)) correlation-function approach.

$$S_{NN}(q) = 1 + \rho_0 \int (g_{NN}(r) - 1)\exp(-i\vec{q}.\vec{r})\vec{dr} \tag{3.69}$$

$$S_{\mathrm{CC}}(q) = C_A C_B + \rho_0 \int g_{\mathrm{CC}}(r)\exp(-i\vec{q}.\vec{r})\vec{dr} \tag{3.70}$$

$$S_{NC}(q) = 1 + \rho_0 \int g_{NC}(r)\exp(-i\vec{q}.\vec{r})\vec{dr} \tag{3.71}$$

where $g_{NN}(r)$, $g_{\mathrm{CC}}(r)$ and $g_{NC}(r)$ are radial distribution function and ρ_0 is number density of particles.

At $q \to 0$, the structure factor $S_{NN}(0)$ represents the mean square fluctuation in the particle number where as, $S_{\mathrm{CC}}(0)$ represents the mean square fluctuation in the concentration. Similarly, $S_{NC}(0)$ stands for the correlation between these two fluctuations. The partial

structure factors at this condition can be expressed as:

$$S_{NN}(0) = \quad \langle(\Delta N)^2\rangle/N \tag{3.72}$$

$$S_{\mathrm{CC}}(0) = \quad N\langle(\Delta C_A)^2\rangle \tag{3.73}$$

$$S_{NC}(0) = \quad N\langle(\Delta N\Delta C_A)^2\rangle \tag{3.74}$$

where $(\Delta N)^2$ is the mean square fluctuation in the number of particles in the given element of volume V, $(\Delta C_A)^2$ is the mean square fluctuation in the concentration and $< \Delta N\Delta C_A >$ is correlation between the two fluctuations. ΔN and ΔC_A are expressed as (Bhatia & Thornton, 1970):

$$\Delta N = \Delta N_A + \Delta N_B \tag{3.75}$$

$$N\Delta C_A = C_B\Delta N_A - C_A\Delta N_B \tag{3.76}$$

Here, ΔN_A and ΔN_B represent the instantaneous deviation from mean number of atoms N_A and N_B respectively. The mean square fluctuation in the concentration $(\Delta C_A)^2$ in binary mixture can be expressed as the second concentration derivative of Gibbs free energy (Bhatia & Thornton, 1970; March & Tosi, 1976) as:

$$\langle(\Delta C_A)^2\rangle = \frac{1}{N}\left[\frac{Nk_{\mathrm{B}}T}{\partial^2 G_{\mathrm{M}}/\partial C_A^2}\right]_{T,P,N} \tag{3.77}$$

From Equations (3.73) and (3.78), the concentration fluctuation in long wavelength limit $(S_{\mathrm{CC}}(0))$ is expressed by following expression

$$S_{\mathrm{CC}}(0) = \left[\frac{Nk_{\mathrm{B}}T}{\partial^2 G_{\mathrm{M}}/\partial C_A^2}\right]_{T,P,N} \tag{3.78}$$

The concentration fluctuation in long wavelength limit is also related to the observed activities of components of binary alloys (Singh & Mishra, 1988) as given below.

$$S_{\mathrm{CC}}(0) = C_B a_A\left[\left(\frac{\partial a_A}{\partial C_A}\right)_{T,P,N}\right]^{-1} = C_A a_B\left[\left(\frac{\partial a_B}{\partial C_B}\right)_{T,P,N}\right]^{-1} \tag{3.79}$$

Substituting the value of G_{M} from Equation (3.54) to Equation (3.78), the expression for the concentration fluctuation in long wavelength limit can be expressed as below,

$$S_{\mathrm{CC}}(0) = \frac{C(1-C)}{1 + C(1-C)\left(-2\frac{\omega}{k_{\mathrm{B}}T} + \Psi''_{AB}\frac{\Delta\omega_{AB}}{k_{\mathrm{B}}T} + \Psi''_{AA}\frac{\Delta\omega_{AA}}{k_{\mathrm{B}}T} + \Psi''_{BB}\frac{\Delta\omega_{BB}}{k_{\mathrm{B}}T}\right)} \tag{3.80}$$

where Ψ''_{ij} are second concentration derivatives of Ψ_{ij}.

If there is no interaction between the constituent particles or for the ideal case, Equation (3.80) can be written as:

$$S_{CC}^{id}(0) = C(1 - C) \tag{3.81}$$

For the theoretical study of local arrangement of constituent particles in the binary liquid alloy, the $S_{CC}^{id}(0)$ is considered as reference value. For given temperature and pressure, if the value of $S_{CC}(0)$ is less than $S_{CC}^{id}(0)$, there is pairing of unlike atoms (heterocoordinating) in the alloys and if the value of $S_{CC}^{id}(0)$ is greater than $S_{CC}(0)$, there is pairing of like atoms together (homocoordinating). The heterocoordinating condition of the alloy is called ordering whereas the homocoordinating condition of the alloy is called segregating.

3.1.6 Chemical Short Range Order Parameter

Chemical Short range order parameter or the Warren-Cowley short range order parameter (Cowley, 1950; Warren, 1969) is important for gaining a better understanding of the degree of ordering in binary liquid alloys as it quantifies the degree of chemical ordering of binary liquid alloy and refers to the regular and predictable arrangement of atoms over a short distance, often on the order of few nearest neighbor spacing.

The conditional probability of finding A atoms as nearest neighbour of a B atom is given as (Cowley, 1950; Warren, 1969):

$$p_{A/B} = C_A(1 - \alpha_1) \quad \text{or} \quad \alpha_1 = 1 - \frac{p_{A/B}}{C_A} \tag{3.82}$$

When $p_{A/B} = 1$, $\alpha_1 = \frac{-(1-C_A)}{C_A} = -\frac{C_B}{C_A}$ and when $p_{A/B} = 0$, $\alpha_1 = 1$.

Maximum probability occurs at equiatomic composition where the value of α_1 is -1. Thus the minimum and maximum values of α_1 are respectively -1 and $+1$. Hence it can be concluded that the negative value of α_1 gives the information of ordering nature of an alloy and it is complete for $\alpha_1 = -1$. Similarly, the positive value of α_1 indicates segregating nature which is complete for $\alpha_1 = -1$. If $\alpha_1 = 0$, then there is complete randomness of arrangement of the atoms in the alloy.

By taking probabilistic approach, the values of α_1 are found to be in the range

$$-\frac{C_A}{1 - C_A} \leq \alpha_1 \leq 1 \qquad C_A \leq \frac{1}{2} \tag{3.83}$$

$$-\frac{1 - C_A}{C_A} \leq \alpha_1 \leq 1 \qquad C_A \geq \frac{1}{2} \tag{3.84}$$

If X_{ij} is the generalized probability that one lattice site of nearest neighbour pair is

occupied by an i atom and other by a j atom, then from Equation (3.18) (Bhatia & Singh, 1982; Singh, 1987),

$$X_{AB} = \frac{2\zeta_A\zeta_B(\phi_A\phi_B)^{(Z-1)}\varrho_{AB}}{\Xi_1'^2} \tag{3.85}$$

$$X_{AA} = \frac{2\zeta_A^2\phi_A^{2(Z-1)}\varrho_{AA}}{\Xi_1'^2} \tag{3.86}$$

$$X_{BB} = \frac{\zeta_B^2\phi_A^{2(Z-1)}\varrho_{BB}}{\Xi_1'^2} \tag{3.87}$$

From Equations (3.27), (3.85), (3.86) and (3.87),

$$\lambda^2 = \frac{X_{AA}X_{BB}}{X_{AB}^2} \tag{3.88}$$

From the normalization condition,

$$X_{AA} + X_{BB} + X_{AB} + X_{BA} = 1 \tag{3.89}$$

Solving Equations (3.23), (3.85),(3.86) and (3.87) we get

$$X_{AB} = C - X_{AA} = (1 - C) - X_{BB} \tag{3.90}$$

Similarly, by solving Equations (3.88) and (3.90), we get

$$X_{AB} = \frac{2C(1-C)}{\beta + 1} \tag{3.91}$$

The relation between generalized probability and conditional probability is given as (Bhatia & Singh, 1982):

$$X_{AB} = (1 - C)p_{A/B} \quad \text{or} \quad X_{AB} = C(1 - C)(1 - \alpha_1) \tag{3.92}$$

From the Equations (3.91) and (3.92),

$$\alpha_1 = \frac{\beta - 1}{\beta + 1} \tag{3.93}$$

The relation between $S_{CC}(0)$ and α_1 is obtained by taking the second derivative of Gibbs free energy with respect to concentration using Equation (3.78) and then using Equations

(3.40) and (3.93) as given below (Singh, 1987):

$$\begin{aligned} S_{CC}(0) = &\quad C(1-C)(1+\alpha_1)[1-(Z-1)\alpha_1]^{-1} \\ \alpha_1 = &\quad \frac{S-1}{S(Z-1)+1} \end{aligned} \tag{3.94}$$

where

$$S = \frac{S_{CC}(0)}{S^{id}_{CC}(0)} \tag{3.95}$$

3.2 Transport Property

According to Seetharaman & Sichen (1994), viscous flow in liquids may be thought of as a thermally activated process in which an atom in metallic melts must overcome an energy barrier in order to migrate to a nearby unoccupied site. Based on this assumption they developed an equation of viscosity of alloy as:

$$\eta = \frac{hN_A D}{M} \exp \frac{\Delta G^*}{RT} \tag{3.96}$$

where

h = Plancks constant
N_A = Avogadro number
D = density of the alloy
M = molecular weight of the alloy
ΔG^* = Gibbs activation energy of viscous flow

In the case of binary liquid alloys the molecular weight and density of the alloy can be expressed as:

$$M = C_A M_A + C_B M_B \tag{3.97}$$

$$D = C_A D_A + C_B D_B \tag{3.98}$$

where M_i and D_i are the molecular weight and the density of components of the alloy respectively. Similarly, Gibbs activation energy of viscous flow (ΔG^*) due to mutual

interaction between different components is expressed as:

$$\begin{aligned}\Delta G^* &= C_A \Delta G_A^* + C_B \Delta G_B^* + G_{\mathrm{M}} + 3RTC_AC_B \\ &= C_A \Delta G_A^* + C_B \Delta G_B^* + H_{\mathrm{M}} - TS_{\mathrm{M}}^{\mathrm{Xs}} \\ &\qquad + RT(C_A \ln C_A + C_B \ln C_B) + 3RTC_AC_B \end{aligned} \tag{3.99}$$

where $S_{\mathrm{M}}^{\mathrm{Xs}}$ is excess entropy of mixing.

Kaptay (2003) pointed certain limitations and hence suggested to improve following points.

1. The ratio M/D should be replaced by molar volume V, as this quantity varies linearly with mole fractions. The molar volume of the binary liquid alloys can be expressed as below:

$$V = C_A V_A + C_B V_B + \Delta V^{\mathrm{Xs}} \tag{3.100}$$

   where V_i is the molar volume of pure metal at given temperature and ΔV^{Xs} is the excess molar volume upon alloy formation.

2. The major thermodynamic property that determines the activation of energy of the alloy is enthalpy of mixing. Thus third, fourth and fifth terms in Equation (3.99) can be excluded.

3. The enthalpy of mixing expresses the change in the cohesion energy upon alloying and when it is negative, the atoms in the alloy are bonded to each other and hence viscous flow is expected to be higher than in an ideal solution and vice versa. Thus this term should be written with a negative sign. In such situation, Equation (3.99) can be written as:

$$\eta = \frac{hN_{\mathrm{A}}}{C_A V_A + C_B V_B + \Delta V^{\mathrm{Xs}}} \exp\left(\frac{C_A \Delta G_A^* + C_B \Delta G_B^* - H_{\mathrm{M}}}{RT}\right) \tag{3.101}$$

   But during the viscous flow, only tiny part of cohesive energy (α) is broken at each step. It is computed by taking the average ratio of activation energy of viscous flow to the cohesion energy and hence the value of α is 0.155 ± 0.015 (Kaptay, 2003; Kaptay et al., 2003). Now, the equation of viscosity of binary alloy takes the following form:

$$\eta = \frac{hN_{\mathrm{A}}}{C_A V_A + C_B V_B + \Delta V^{\mathrm{Xs}}} \exp\left(\frac{C_A \Delta G_A^* + C_B \Delta G_B^* - \alpha H_{\mathrm{M}}}{RT}\right) \tag{3.102}$$

The Gibbs activation energy of viscous flow of i^{th} component can be expressed as:

$$\Delta G_i{}^* = RT \ln\left(\frac{\eta_i V_i}{hN_{\text{A}}}\right) \tag{3.103}$$

where η_i is the viscosity of i^{th} component of the alloy and the variation of viscosity with temperature for metals is given as (Brandes & Brook, 2013):

$$\eta_i = \eta_0 \exp \frac{\ni}{RT} \tag{3.104}$$

where η_0 and $\ni$ are constants with units of viscosity and energy per mole respectively.

3.3 Surface Properties

The surface properties of binary liquid alloys, such as surface tension and surface concentration insight the information on several important properties such as mechanical behavior, kinetics of phase transformation and so on. Butler's equation, as improved by Kaptay (2019), has been used to calculate the surface tension and surface concentration of binary liquid alloys.

In the Butler's equation of surface tension (Butler, 1932), the partial surface tension of components is added without being clearly specified (Kaptay, 2015; Korozs & Kaptay, 2017; Kaptay, 2019). As a result, it necessitates the refinement of Butler's surface tension equation in order to illustrate the formal thermodynamic relationship between the partial surface tension of different components of solution and the surface tension of the same solution. The mathematical working expression for improved Butler's equation is shown below.

Consider a system with two bulk phases: a liquid phase (L) and an equilibrium vapour phase (V), separated by a planar surface (S). The system contains various parts that are collectively referred to as 'i' throughout both phases. The three terms given below define the chemical potential of the bulk liquid phase.

$$\mu_{i,\text{b}} = \mu^0_{i,\text{b}} + RT \ln C_{i,\text{b}} + \Delta G^{\text{Xs}}_{i,\text{b}} \tag{3.105}$$

where, $\mu^0_{i,\text{b}}$ is the bulk chemical potential of pure liquid, $\Delta G^{\text{Xs}}_{i,\text{b}}$ is the excess partial molar Gibbs energy of component i in the bulk liquid phase.

The following fundamental Gibbs equation is valid for planar surfaces (Gibbs, 1928).

$$dG_{\text{s}} = \sum \mu_{i,\text{s}} dn_{i,\text{s}} + \sigma dA \tag{3.106}$$

where G_{s} is the Gibbs energy of the surface region. $\mu_{i,\text{s}}$ and $n_{i,\text{s}}$ are the chemical potential

and amount of i^{th} component in the surface region, A is the surface area between the two bulk phases. For the surface region , the Gibbs energy is

$$G_{\text{s}} = G - G_{\text{b}} \tag{3.107}$$

where G and G_{b} are Gibbs energies of the system and bulk phases respectively. Similarly total amount of matter in the surface region is

$$n_{i,\text{s}} = n_i - n_{i,\text{b}} \tag{3.108}$$

According to Gibbs (1928), the surface tension of solution is

$$\sigma = \left(\frac{\partial G_{\text{s}}}{\partial A}\right)_{T,P,n_{i.\text{s}}} \tag{3.109}$$

The chemical potential of the i^{th} component in the surface region can be defined from Equation (3.106) as follows.

$$\mu_{i,\text{s}} = \left(\frac{\partial G_{\text{s}}}{\partial n_{i,\text{s}}}\right)_{T,P,n_{j\neq i,s}} - S_i\sigma \tag{3.110}$$

where S_i is partial molar surface area of i^{th} component in the liquid mixture. It is expressed as:

$$S_i = \left(\frac{\partial A}{\partial n_{i,\text{s}}}\right)_{T,P,n_{j\neq i,s}} \tag{3.111}$$

In the Equation (3.110), the term $\frac{\partial G_{\text{s}}}{\partial n_{i,\text{s}}}$ is reduced chemical potential of i^{th} component in the surface means chemical potential without the term $S_i\sigma$. Let us represent it by $\mu^*_{i,\text{s}}$. Thus, Equation (3.110) can be rewritten as:

$$\mu_{i,\text{s}} = \mu^*_{i,\text{s}} - S_i\sigma \quad \text{or} \quad \sigma = \frac{\mu^*_{i,\text{s}} - \mu_{i,\text{s}}}{S_i} \tag{3.112}$$

The reduced chemical potential $\mu^*_{i,\text{s}}$ can be expressed similar to Equation (3.105) as:

$$\mu^*_{i,\text{s}} = \mu^{0*}_{i,\text{s}} + RT\ln C_{i,\text{s}} + \Delta G^{\text{Xs}}_{i,\text{s}} \tag{3.113}$$

At equilibrium condition, the chemical potential of same component is same in all phases. Thus,

$$\mu_i = \mu_{i,\text{b}} = \mu_{i,\text{s}} \tag{3.114}$$

Solving Equations (3.105), (3.112), (3.113) and (3.114), the surface tension can be expressed as:

$$\sigma = \frac{\mu_{i,\mathrm{s}}^{0*} - \mu_{i,\mathrm{s}}^{0}}{S_i} + \frac{RT}{S_i} \ln \frac{C_{i,\mathrm{s}}}{C_{i,\mathrm{b}}} + \frac{G_{i,\mathrm{s}}^{\mathrm{Xs}} - \Delta G_{i,\mathrm{b}}^{\mathrm{Xs}}}{S_i} \tag{3.115}$$

If we substitute $C_{i,\mathrm{b}} = C_{i,\mathrm{s}} = 1$ in Equation (3.115) then the surface tension of pure i^{th} component (σ_i^0) becomes:

$$\sigma_i^0 = \frac{\mu_{i,\mathrm{s}}^{0*} - \mu_{i,\mathrm{s}}^{0}}{S_i^0} \tag{3.116}$$

where S_i^0 is the molar surface area of pure i^{th} component when the whole system is made up of only one component. Now, from Equations (3.115) and (3.116) we get

$$\sigma = \sigma_i^0 \frac{S_i^0}{S_i} + \frac{RT}{S_i} \ln \frac{C_{i,\mathrm{s}}}{C_{i,\mathrm{b}}} + \frac{\Delta G_{i,\mathrm{s}}^{\mathrm{Xs}} - \Delta G_{i,\mathrm{b}}^{\mathrm{Xs}}}{S_i} \tag{3.117}$$

For a liquid metal, the molar surface area can be expressed as (Kaptay, 2008, 2015, 2018):

$$S_i^0 = f (V_i^0)^{2/3} (N_{\mathrm{av}})^{2/3} \tag{3.118}$$

where, V_i^0 is the molar volume of pure component and f is geometrical constant. The geometrical constant is given as:

$$f = \left(\frac{3 f_{\mathrm{V}}}{4} \right)^{2/3} \frac{\pi^{1/3}}{f_{\mathrm{S}}} \tag{3.119}$$

where f_{V} and f_{S} respectively are volume and surface packing fraction. For liquid metal, the values of f_{V} and f_{S} are 0.66 and 0.906 respectively (Kaptay, 2008). In the case of binary liquid alloys, Equation (3.117) can be rewritten as:

$$\begin{aligned} \sigma &= \sigma_A^0 \frac{S_A^0}{S_A} + \frac{RT}{S_A} \ln \frac{C_{A,\mathrm{s}}}{C_{A,\mathrm{b}}} + \frac{\Delta G_{A,\mathrm{s}}^{\mathrm{Xs}} - \Delta G_{A,\mathrm{b}}^{\mathrm{Xs}}}{S_A} \\ &= \sigma_B^0 \frac{S_B^0}{S_B} + \frac{RT}{S_B} \ln \frac{C_{B,\mathrm{s}}}{C_{B,\mathrm{b}}} + \frac{\Delta G_{B,\mathrm{s}}^{\mathrm{Xs}} - \Delta G_{B,\mathrm{b}}^{\mathrm{Xs}}}{S_B} \end{aligned} \tag{3.120}$$

The bulk partial excess free energy of components ($\Delta G_{i,\mathrm{b}}^{\mathrm{Xs}}$) of the liquid alloy required to compute surface properties of the alloy at different temperatures can be determined by using activity of each component by following relation.

$$\Delta G_{i,\mathrm{b}}^{\mathrm{Xs}} = RT \ln \left(\frac{a_i}{C_i} \right) \tag{3.121}$$

CHAPTER 4

4. RESULTS AND DISCUSSION

4.1 Introduction

In this chapter, we describe our study and offer the key findings. As we are dealing with properties of four different types of binary alloys of type $A_\mu B_\nu$, the results and discussion of each problem are separately presented sectionally for simplicity as follows:

4.2 Free Energy of Mixing of Binary Liquid Alloys

We have derived the mathematical framework for the Quasi-Chemical Approximation in the previous chapter to analyze the thermodynamic characteristics of binary liquid alloys. We also came up with an equation for the free energy of mixing. Before employing the expression to compute free energy of mixing as a function of concentration for preferred binary liquid alloys, we explain the impact of interaction energy parameters on the free energy of mixing.

4.2.1 Significance of Energy Parameters on the Free Energy of Mixing

The compound forming tendency in the binary liquid alloys is caused by the existence of chemical short range order where unlike atom interaction between the components of alloys is preferred than that of like atoms. In such circumstances, the interaction energies between such atomic pairs are lower than the others and hence these atomic pair configurations are more energetically favorable. The expression for free energy of mixing given in the Equation (3.54) demonstrates that it is also a function of both temperature and interaction energy parameters. If temperature is kept constant, the interaction energy parameters (ω and $\Delta\omega_{ij}$) are taken to be the fundamental inputs for the estimation of various thermodynamic properties of the alloys under the Quasi-Chemical Approximation. The interpretation about the impact of these parameters on the free energy of mixing is associated with initial process of assessing them using modelling equations as mentioned in the previous chapter. It is found that if a complex is to be formed, ω has negative value. The parameters ω and $\Delta\omega_{ij}$ have been calculated by the successive approximation and using the experimental values as free parameters. In the course of our calculation, it is found that $\Delta\omega_{ij}$ have minor influence in most of the cases as compared to the parameter ω.

In the case of compound forming binary liquid alloys, the value of free energy (G_{M}) is

positive with positive value of ω and negative with negative value of ω when $\Delta\omega_{ij}$ are kept zero. As we increase the negative value of ω, the negative value of G_{M} also increases. Similarly negative value of $\Delta\omega_{ij}$ gives negative value of G_M and vice versa.The values $\Delta\omega_{ij}$ may vary the magnitude and sign of ω (Prasad et al., 1998). However, during fitting such interaction parameters in the the preferred compound forming binary liquid alloys, the value of ω is always negative but $\Delta\omega_{ij}$ may take any value indicating that it has less significant effect than that of ω. If ω is more negative then $\Delta\omega_{ij}$ may take the positive value for negative value of G_{M} . Thus, the sign and magnitude of ω may be used to understand the fundamental idea of attractive or repulsive interactions between the atoms of the components of the alloy in the melt. Its negative value indicates that the respective species are attracted to one another, whilst its positive value indicates that they are repelled by each other.

4.2.2 Results for Na-Hg, Pb-Mg, Bi-Tl and Cu-Al Liquid Alloys

In this section, we evaluate the interaction energy parameters and present the findings of the free energy of mixing as a function of concentration for Na-Hg, Pb-Mg, Bi-Tl and Cu-Al binary liquid alloys. Similarly for the validity of modelled equation we compare computed results with experimental results (Hultgren et al.,1973) at about melting temperatures of the alloys.

4.2.2.1 Gibbs Free Energy of Mixing of Na-Hg Liquid Alloy at 673 K

The phase diagram of Na-Hg liquid alloy (Hultgren et al., 1973; Morachevskii,2014) indicates that the $NaHg_2$ is one of the stable intermetallic complex in the solid state. Hence by assuming $NaHg_2$ complex, the values of interaction energy parameters are evaluated by successive approximation method with the help of experimental values of Gibbs free energy of mixing (Hultgren et al., 1973) at 673 K in the concentration range $C_{\mathrm{Na}} = 0.1$ to $C_{\mathrm{Na}} = 0.9$. The results of the calculation show that the interaction energy parameters of Na-Hg liquid alloy at aforementioned temperature are (Panthi, Bhandari, & Koirala, 2021)

$$\frac{\omega}{k_{\mathrm{B}}T} = -10.524\,, \quad \frac{\Delta\omega_{AB}}{k_{\mathrm{B}}T} = 2.714 \quad \text{and} \quad \frac{\Delta\omega_{BB}}{k_{\mathrm{B}}T} = 9.987$$

Now using such interaction energy parameters and values of Ψ_{ij} for $\mu = 1$ and $\nu = 2$ from Equation (3.49) to Equation (3.54), the free energy of mixing ($G_{\mathrm{M}}/(RT)$) of the alloy is computed. The free energy of mixing thus computed and experimental values are listed in Table 2 and plotted against concentration of sodium (C_{Na}) as shown in the Figure 5 . The minimal value of the free energy of mixing (= −3.102) found at $C_{\mathrm{Na}} = 0.4$ (at the vicinity of compound forming concentration $C_C = \mu/(\mu + \nu) = 1/(1 + 2) = 0.33$ of Na) shows

that the alloy is asymmetric about the equi-atomic composition $C_{Na} = 0.5$. The computed values and experimental values exhibit good agreement between them. The negative value of $\omega/(k_B T)$ reveals that Na and Hg are attracted to each other and hence form complex in the liquid mixture. Thus it can be understood from the theoretical calculations of the free energy of mixing that the alloy Na-Hg in the liquid state is interacting and hence shows tendency of compound formation.

Table 2: Free energy of mixing for liquid Na-Hg alloy at 673 K for different concentrations of sodium.

Concentration of Na	Free energy of mixing (G_M/RT)	
C_{Na}	Theoretical	Experimental*
0.1	−1.404	−1.354
0.2	−2.323	−2.292
0.3	−2.872	−2.872
0.4	−3.102	−3.126
0.5	−3.056	−3.084
0.6	−2.775	−2.776
0.7	−2.300	−2.275
0.8	−1.670	−1.650
0.9	−0.914	−0.914

*Hultgren et al. (1973)

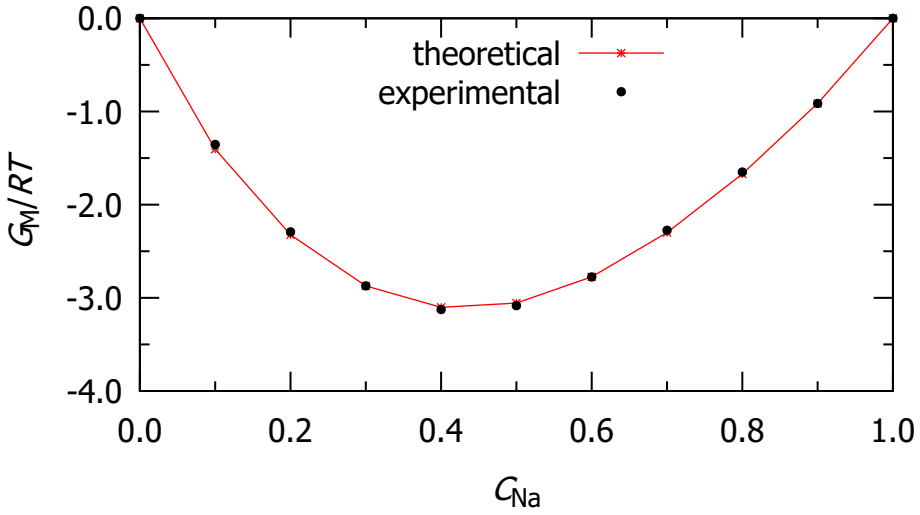

Figure 5: Free energy of mixing versus concentration of Na for Na-Hg liquid alloy at 673 K.

4.2.2.2 Gibbs Free Energy of Mixing of Pb-Mg Liquid Alloy at 973 K

The phase diagram (Hultgren et al., 1973) shows that $PbMg_2$ is one of the most stable intermetallic complexes in solid state. As a result, using this complex as a foundation,

we estimated the interaction parameters and were able to compute the composition dependent free energy of mixing based on the Quasi-Chemical Approximation. By using experimental values of the Gibbs free energy of mixing (Hultgren et al., 1973) at 973 K in the concentration range $C_{\mathrm{Pb}} = 0.1$ to $C_{\mathrm{Pb}} = 0.9$, the values of the interaction parameters are assessed. The approximate values of the energy parameters are

$$\frac{\omega}{k_{\mathrm{B}}T} = -5.779\,, \quad \frac{\Delta\omega_{AB}}{k_{\mathrm{B}}T} = 2.808 \quad \text{and} \quad \frac{\Delta\omega_{BB}}{k_{\mathrm{B}}T} = 4.984$$

Table 3: Free energy of mixing for liquid Pb-Mg alloy at 973 K for different concentrations of lead.

Concentration of Pb	Free energy of mixing (G_{M}/RT)	
C_{Pb}	Theoretical	Experimental*
0.1	−0.875	−0.882
0.2	−1.406	−1.419
0.3	−1.706	−1.723
0.4	−1.819	−1.830
0.5	−1.777	−1.784
0.6	−1.609	−1.610
0.7	−1.339	−1.344
0.8	−0.987	−0.986
0.9	−0.560	−0.558

*Hultgren et al. (1973)

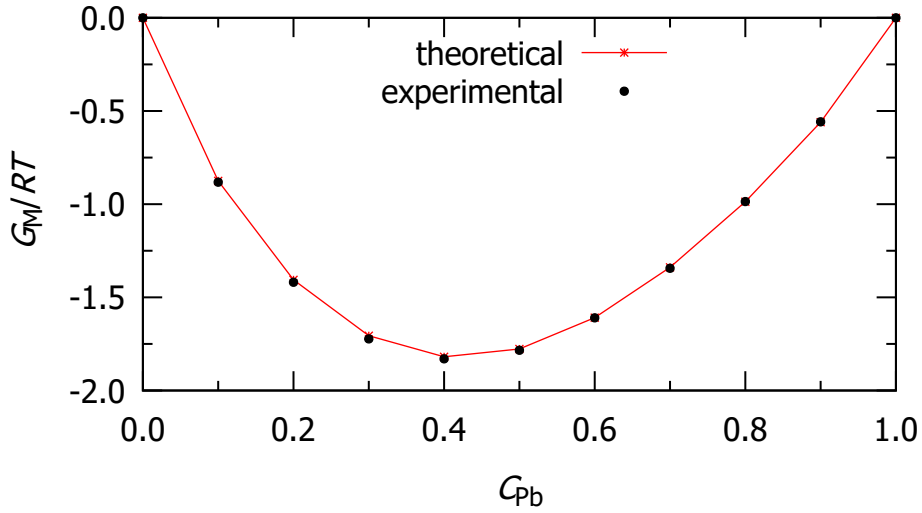

Figure 6: Free energy of mixing versus concentration of Pb for Pb-Mg liquid alloy at 973 K.

After finding such interaction parameters and following same procedure as mentioned in Subsection 4.2.2.1,the free energy of mixing G_{M}/RT of Pb-Mg liquid alloy at 973 K is

computed. The computed and experimental values of free energy of mixing are shown in Table 3. The plots of the theoretical and experimental values of G_M/RT versus concentration of lead (C_{Pb}) are shown in Figure 6. Both the computed and experimental values of free energy of mixing are in good agreement.The theoretical value of free energy of mixing is minimum -1.819 at $C_{Pb} = 0.4$ which is nearly same with experimental value -1.830. From these negative values of free energy of mixing, it can be said that the alloy system is weakly interacting.

4.2.2.3 Gibbs Free Energy of Mixing of Bi-Tl Liquid Alloy at 750 K

The phase diagram of Bi-Tl alloy (Okamoto and Massalski ,1990) indicates that the $BiTl_3$ is one of the stable intermetallic complex in the solid state. Hence by assuming this complex, the values of interaction parameters are evaluated by successive approximation method with the help of experimental values of Gibbs free energy of mixing (Hultgren et al., 1973) at 750 K in the concentration range $C_{Tl} = 0.1$ to $C_{Tl} = 0.9$. The results of the calculation show that the interaction energy parameters of Bi-Tl liquid alloy at aforementioned temperature are

$$\frac{\omega}{k_B T} = -1.084\,, \quad \frac{\Delta\omega_{AB}}{k_B T} = -3.660 \quad \text{and} \quad \frac{\Delta\omega_{BB}}{k_B T} = 1.493$$

The value of G_M/RT for the Bi-Tl liquid alloy at 750 K is now calculated from Equation (3.54) using these interaction energy parameters and the values of Ψ_{ij} for $\mu = 1$ and $\nu = 3$ as determined by Equation (3.50). The theoretically computed and experimental values of G_M/RT are shown in Table 4 and the plots of the theoretical and experimental values of G_M/RT versus concentration of Tl are shown in Figure 7.

Table 4: Free energy of mixing for liquid Bi-Tl alloy at 750 K for different concentrations of thallium.

Concentration of Tl	Free energy of mixing (G_M/RT)	
C_{Tl}	Theoretical	Experimental*
0.1	−0.519	−0.486
0.2	−0.872	−0.844
0.3	−1.141	−1.126
0.4	−1.335	−1.331
0.5	−1.445	−1.445
0.6	−1.455	−1.455
0.7	−1.343	−1.343
0.8	−1.087	−1.086
0.9	−0.665	−0.657

*Hultgren et al. (1973)

The theoretical values of G_M/RT are in good agreement with experimental values (Hultgren et al., 1973) within whole range of concentration of Tl. The minimum value

of G_M/RT for Bi-Tl is -1.445 at $C_{Tl} = 0.6$ which is exactly same with experimental value. The less negative value of G_M/RT suggests that the alloy is weakly interacting, nevertheless it shows complex nature. As the alloy exhibits asymmetry at an equiatomic concentration of $C_{Tl} = 0.5$, it is categorized as an irregular alloy.

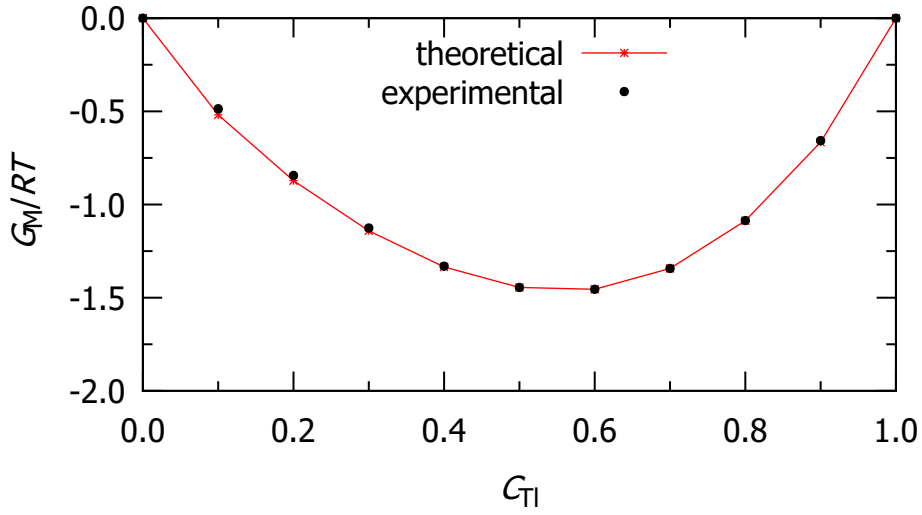

Figure 7: Free energy of mixing versus concentration of Tl for Bi-Tl liquid alloy at 750 K.

4.2.2.4 Gibbs Free Energy of Mixing of Cu-Al Liquid Alloy at 1373 K

According to the phase diagram Hultgren et al. (1973), Cu_3Al_2 is one of the most stable intermetallic complexes in the solid state. As a result, using this complex as a foundation, the interaction parameters are estimated in order to compute the composition dependent free energy of mixing based on the Quasi-Chemical Approximation. For this the values of the interaction energy parameters are so evaluated at 1373 K that they offer reasonable agreement with experimental results. The estimated values of interaction energy parameters are given below:

$$\frac{\omega}{k_B T} = -4.710\,, \quad \frac{\Delta\omega_{AB}}{k_B T} = 26.942, \quad \frac{\Delta\omega_{AA}}{k_B T} = -61.061 \quad \text{and} \quad \frac{\Delta\omega_{BB}}{k_B T} = -37.995$$

For the phase Cu_3Al_2, $\mu = 3$ and $\nu = 2$. So values of Ψ_{ij} are taken from Equation (3.51) and the values of G_M/RT are computed using Equation (3.54) with the help of above mentioned interaction energy parameters.

The computed and experimental values of G_M/RT are shown in Table 5. The plots of the theoretical and experimental values versus concentration of Cu are shown in Figure 8.

From the figure, it is observed that the computed and experimental values of G_M/RT are in good agreement. The theoretical value of free energy G_M/RT of mixing is minimum

i.e. -1.943 at 0.6 concentration of Cu. The negative value of $\omega/k_{\mathrm{B}}T$ and the theoretical free energy of mixing indicate that at liquid state the alloy Cu-Al shows the compound forming tendency but moderately interacting i.e. the tendency of compound formation is not so strong. The alloy is classified as an irregular alloy since it shows asymmetry at $C_{\mathrm{Cu}} = 0.5$ equiatomic concentration.

Table 5: Free energy of mixing for liquid Cu-Al alloy at 1373 K for different concentrations of copper.

Concentration of Cu	Free energy of mixing (G_{M}/RT)	
C_{Cu}	Theoretical	Experimental*
0.1	−0.610	−0.632
0.2	−1.054	−1.088
0.3	−1.430	−1.450
0.4	−1.729	−1.723
0.5	−1.915	−1.895
0.6	−1.943	−1.939
0.7	−1.781	−1.798
0.8	−1.418	−1.439
0.9	−0.855	−0.865

*Hultgren et al. (1973)

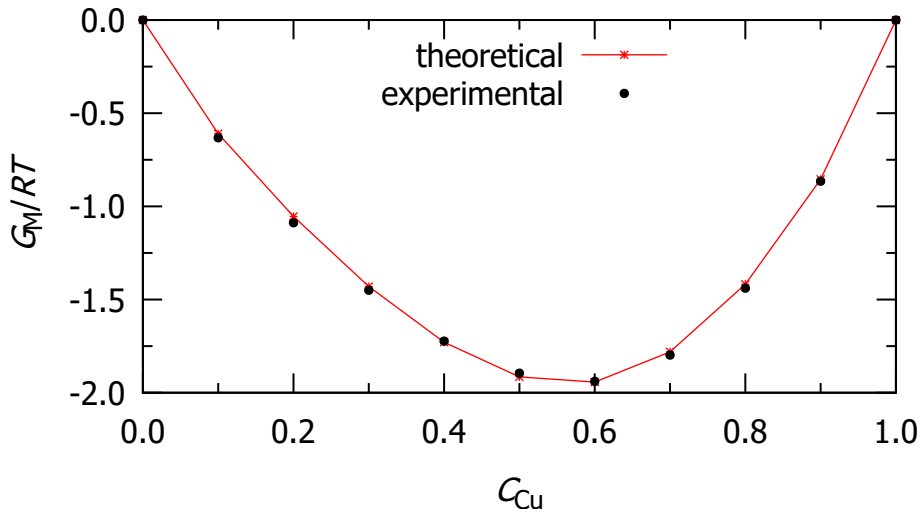

Figure 8: Free energy of mixing versus concentration of Cu for Cu-Al liquid alloy at 1373 K.

4.3 Enthalpy of Mixing of Binary Liquid Alloys

Enthalpy of mixing, which provides information on the kind and extent of bonding between the constituent atoms of liquid alloys, has been identified as one of the important thermodynamic features. Breaking of chemical bonds often occurs when two substances are mixed to produce a solution. Heat can either be absorbed by or evolved from a system

while breaking or forming chemical bonds. Thus the evolution or absorption of heat typically occurs when two substances are mixed to form a solution which is known as enthalpy of mixing or heat of formation. The interatomic attractions between the atoms of constituent elements are generally considered as the main contributors to the enthalpy of mixing. The enthalpy of mixing directly leads to the nature of binding in liquid solutions. In an ideal solution, where atoms are randomly mixed at all temperatures, the enthalpy of mixing is zero; however, in a non-ideal solution, it is an extra molar amount that may be either positive or negative depending on how the atoms of the elements of mixture interact. As a result, the magnitude of a system's enthalpy of mixing serves as a measure of how far away from ideal behavior it deviates; the closer to zero the enthalpy of solution is, the more ideal the behavior of the solution is. Mixing is endothermic when the enthalpy of mixing is positive and it is exothermic when the enthalpy of mixing is negative.

The type of interaction among the constituent species of the alloys may be incorporated into the theoretical knowledge of the enthalpy of mixing as a function of concentration. Hence as discussed in Chapter 2, large number of theoreticians have long been interested in the study of the enthalpy of mixing metal alloys and considerable effort has gone into developing a theoretical approach to calculate the enthalpy of mixing of binary liquid alloys. In the present work, we have used Quasi-Chemical Approximation (Bhatia & Singh, 1982) to compute the concentration dependent enthalpy of mixing of four different binary liquid alloys.

4.3.1 Results for Na-Hg, Pb-Mg, Bi-Tl and Cu-Al Liquid Alloys

In Chapter 3, the formula for the enthalpy of mixing binary liquid alloys has been developed. It is obvious from Equation (3.57) that the interaction energy parameters and temperature derivative interaction energy parameters are the fundamental inputs for the computation of the enthalpy of mixing in Quasi-Chemical Approximation. In order to preserve consistency, the interaction energy parameter values have been kept the same as before but the approach of successive approximation on the basis of experimental values of enthalpy of mixing (Hultgren et al., 1973) has been used to estimate the temperature derivative interaction energy parameters until the best fit values are found. The computed values of enthalpy of mixing are compared with experimental results in order to find the level of consistency.

4.3.1.1 Enthalpy of Mixing of Na-Hg Liquid Alloy at 673 K

For Na-Hg liquid alloy, the best fit values of temperature derivative interaction energy parameters for computing enthalpy of mixing at 673 K as determined by successive

approximation method are found as follows (Panthi, Bhandari, & Koirala, 2021):

$$\frac{1}{k_B}\frac{\partial \omega}{\partial T} = -2.097, \quad \frac{1}{k_B}\frac{\partial \Delta\omega_{AB}}{\partial T} = 8.971 \quad \text{and} \quad \frac{1}{k_B}\frac{\partial \Delta\omega_{BB}}{\partial T} = -19.105$$

Now using such parameters, the theoretically computed values of enthalpy of mixing and experimental values (Hultgren et al., 1973) are given in Table 6 and the plot of computed along with observed enthalpy of mixing of the alloy as a function of concentration is shown in Figure 9.

Table 6: Enthalpy of mixing for liquid Na-Hg alloy at 673 K for different concentrations of sodium.

Concentration of Na	Enthalpy of mixing(H_M/RT)	
C_{Na}	Theoretical	Experimental*
0.1	−1.498	−1.361
0.2	−2.613	−2.571
0.3	−3.321	−3.372
0.4	−3.621	−3.674
0.5	−3.539	−3.544
0.6	−3.123	−3.064
0.8	−1.617	−1.610
0.9	−0.751	−0.829

*Hultgren et al. (1973)

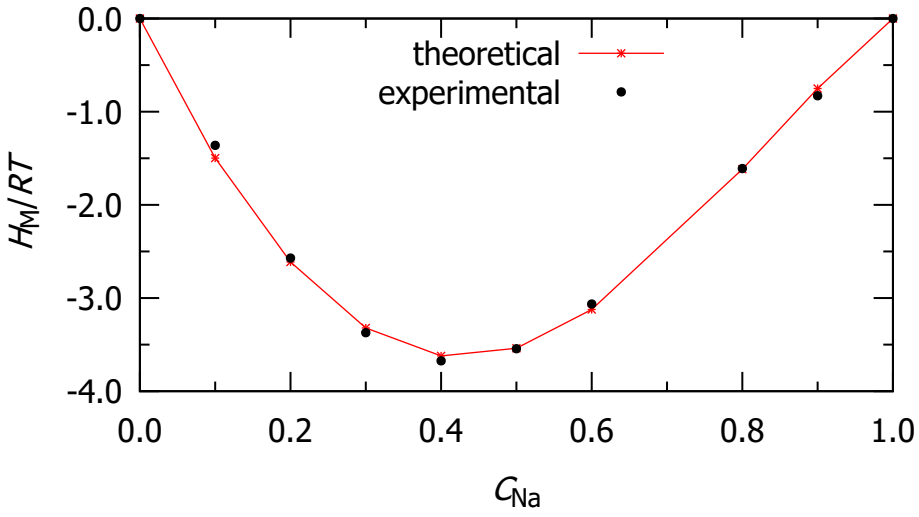

Figure 9: Enthalpy of mixing versus concentration of Na for Na-Hg liquid alloy at 673 K.

Theoretical and experimental calculations of the enthalpy of mixing of the liquid Na-Hg alloy are reasonably consistent. The values are lowest at $C_{Na} = 0.4$ for both theoretical and experimental data. The theoretical value of H_M at this concentration is $-3.621RT$, while the corresponding experimental value is $-3.674RT$. According to the low negative

value −3.674, the alloy system is interacting. Thus, the proposed theoretical model has provided a good explanation for the enthalpy of mixing of the concerned alloy.

4.3.1.2 Enthalpy of Mixing of Pb-Mg Liquid Alloy at 973 K

The quasi-chemical temperature derivative interaction parameters for the Pb-Mg alloy in the molten state at temperature 973 K have been found to be

$$\frac{1}{k_B}\frac{\partial\omega}{\partial T} = -2.345\,, \quad \frac{1}{k_B}\frac{\partial\Delta\omega_{AB}}{\partial T} = 3.819 \quad \text{and} \quad \frac{1}{k_B}\frac{\partial\Delta\omega_{BB}}{\partial T} = -4.691$$

The Table 7 provides the calculated and actual values of the enthalpy of mixing for molten Pb-Mg alloy at 973 K. As shown in Figure 10, we have plotted the computed values of enthalpy of mixing as a function of concentration of lead along with the experimental values.

Table 7: Enthalpy of mixing for liquid Pb-Mg alloy at 973 K for different concentrations of lead.

Concentration of Pb	Enthalpy of mixing(H_M/RT)	
C_{Pb}	Theoretical	Experimental*
0.1	−0.528	−0.489
0.2	−0.905	−0.912
0.3	−1.131	−1.184
0.4	−1.214	−1.241
0.5	−1.168	−1.161
0.6	−1.014	−0.987
0.7	−0.781	−0.760
0.8	−0.505	−0.513
0.9	−0.228	−0.256

*Hultgren et al. (1973)

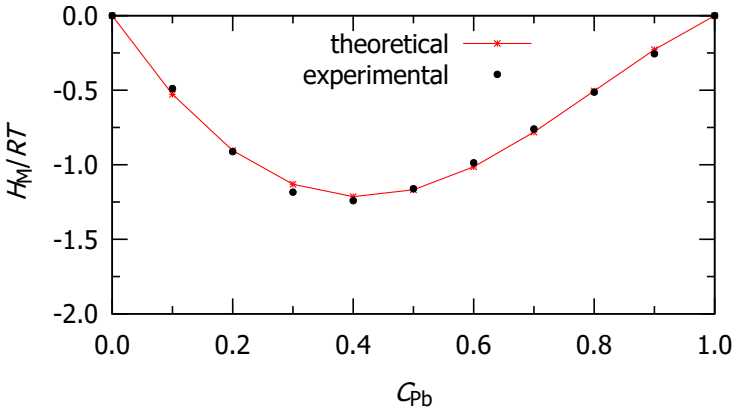

Figure 10: Enthalpy of mixing versus concentration of Pb for Pb-Mg liquid alloy at 973 K.

For Pb-Mg alloys, the theoretically calculated enthalpy of mixing are nearly in agreement

with the observed values (Hultgren et al., 1973). According to the results of the current investigation, the alloy's estimated values for enthalpy of mixing are negative within entire concentration range of lead. Our theoretical calculation shows that the minimum value of H_M is $-1.214RT$ at $C_{Pb} = 0.4$ while the equivalent experimental value is $-1.241RT$. The Pb-Mg alloy appears to be weakly interacting based on the minimum value of enthalpy of mixing.

4.3.1.3 Enthalpy of Mixing of Bi-Tl Liquid Alloy at 750 K

The best fit values of temperature derivative interaction energy parameters for computing enthalpy of mixing of Bi-Tl liquid alloy at 750 K as determined by successive approximation method are found as follows;

$$\frac{1}{k_B}\frac{\partial\omega}{k_B T} = 0.489\,, \quad \frac{1}{k_B}\frac{\partial\Delta\omega_{AB}}{\partial T} = -0.985 \quad \text{and} \quad \frac{1}{k_B}\frac{\partial\Delta\omega_{BB}}{\partial T} = 2.488$$

The computed and experimental values of H_M/RT at 750 K are listed in Table 8. Similarly, the plot of theoretical along with experimental values of H_M/RT as a function of concentration of Tl in the concentration range $C_{Tl} = 0.1$ to 0.9 is shown in the Figure 11.

From the figure it is observed that the theoretical results are in reasonable agreement with experimental values. It is also found that the enthalpy of mixing of Bi-Tl liquid alloy at temperature 750 K is negative or exothermic in the whole concentration range of thallium .The negative value of enthalpy of mixing indicates that there is release of energy during mixing and the alloy shows ordering or compound forming nature.

Table 8: Enthalpy of mixing for liquid Bi-Tl alloy at 750 K for different concentrations of thallium.

Concentration of Tl	Enthalpy of mixing(H_M/RT)	
C_{Tl}	Theoretical	Experimental*
0.1	−0.182	−0.183
0.2	−0.343	−0.343
0.3	−0.485	−0.470
0.4	−0.602	−0.576
0.5	−0.685	−0.685
0.6	−0.717	−0.733
0.7	−0.680	−0.693
0.8	−0.557	−0.557
0.9	−0.332	−0.321

*Hultgren et al. (1973)

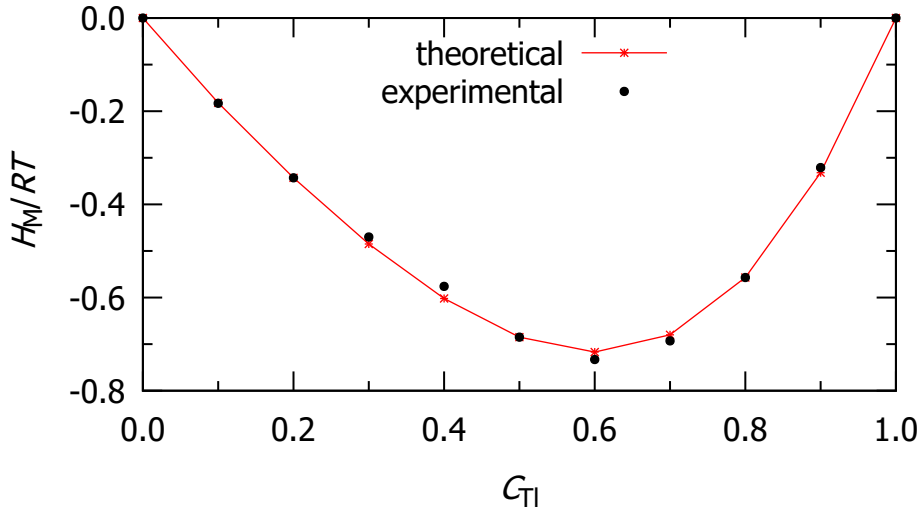

Figure 11: Enthalpy of mixing versus concentration of Tl for Bi-Tl liquid alloy at 750 K.

4.3.1.4 Enthalpy of Mixing of Cu-Al Liquid Alloy at 1373 K

For the Cu-Al liquid alloy, the best fit values of temperature derivative interaction energy parameters at 973 K are found to be

$$\frac{1}{k_B}\frac{\partial\omega}{\partial T} = -3.221\,, \quad \frac{1}{k_B}\frac{\partial\omega_{AB}}{\partial T} = 26.850$$
$$\frac{1}{k_B}\frac{\partial\Delta\omega_{AA}}{\partial T} = -53.466 \quad \text{and} \quad \frac{1}{k_B}\frac{\partial\Delta\omega_{BB}}{\partial T} = -37.402$$

Table 9: Enthalpy of mixing for liquid Cu-Al alloy at 1350 K for different concentrations of copper.

Concentration of Cu	Enthalpy of mixing(H_M/RT)	
C_{Cu}	Theoretical	Experimental*
0.1	−0.095	−0.100
0.2	−0.179	−0.187
0.3	−0.257	−0.257
0.4	−0.328	−0.315
0.5	−0.379	−0.374
0.6	−0.401	−0.401
0.7	−0.379	−0.379
0.8	−0.304	−0.304
0.9	−0.175	−0.175

*Hultgren et al. (1973)

Using these parameters in Equation (3.57), the computed and experimental values of enthalpy of mixing of the alloy at all concentration of Cu are displayed in the Table 9. The plot of theoretical along with experimental values of H_M/RT as a function of concentration is shown in the Figure 12. The calculated and the observed results

for the enthalpy of mixing of the alloy are in agreement. It is observed that both the theoretical and experimental values of enthalpy of mixing are negative within entire concentration of Cu. The theoretical and experimental values both reach their minimum at $C_{Cu} = 0.6$ indicating weakly interacting system. It is also noted that the Quasi-Chemical Approximation model accurately reproduces the concentration-dependent asymmetry found in the experiment.

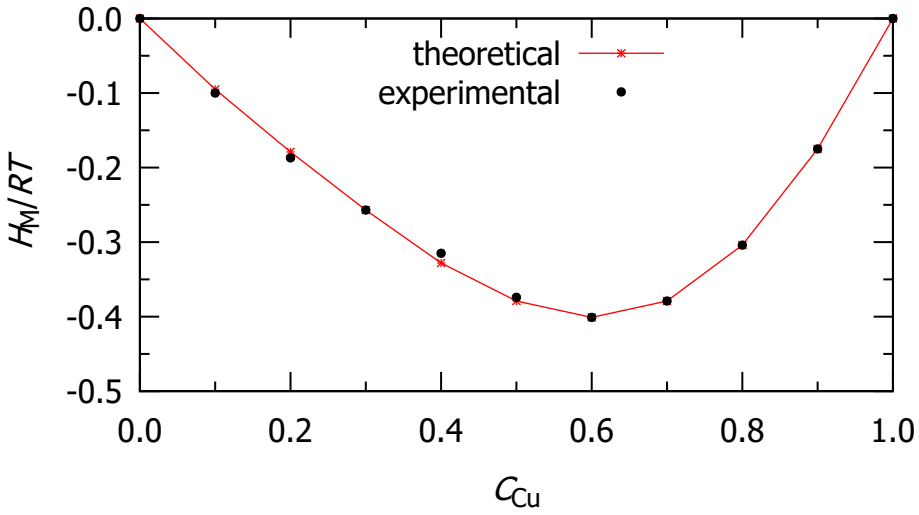

Figure 12: Enthalpy of mixing versus concentration of Cu for Cu-Al liquid alloy at 1373 K.

4.4 Activity of Binary Liquid Alloys

The concentration of a substance in a solution or mixture may not be an accurate indicator of its chemical effectiveness. Hence the concept of activity is established and used instead of the concentration in calculations. The activity is a measure of effective concentration or the measure of how much a solution deviates from the ideal solution. A more precise way to describe how all of the particles behave in mixture is through activity. Therefore the activity is regarded as another crucial thermodynamic property of the alloy. The use of activity allows scientists to explain various discrepancies between ideal solutions and real solutions. According to Porter & Easterling (2009), it informs the tendency of constituents of the mixture whether they are willing to leave the mixture or not. The atoms have a high tendency to leave the mixture when activity is high, and the opposite is also true. The attractive or repulsive nature of components of the alloys can be linked with activity of each component of an ideal solution. The activity of each component of ideal solution is equal to its mole fraction (or concentration). When activity is less than ideal, the attracting force predominates. Similarly, when activity is greater than ideal, the repulsive force predominates.

Although the activities are thermodynamic functions of state, it is believed that their

magnitudes are influenced by interactions between the system's constituent particles, which in turn affect bond energies and the spatial configurations that the particles assume (Azakami & Yazawa, 1976).

4.4.1 Results for Na-Hg, Pb-Mg,Bi-Tl and Cu-Al Binary Liquid Alloys

In this section, we present the methods to estimate the activities and results so obtained together with a discussion for four distinct liquid alloys: Na-Hg, Pb-Mg,Bi-Tl and Cu-Al on the basis of Quasi-Chemical Approximation.

4.4.1.1 Activities of Na (a_{Na}) and Hg (a_{Hg}) for Na-Hg Liquid Alloy at 673 K

Following the Equations (3.64) and (3.65), we have calculated the activities of Na and Hg in Na-Hg liquid alloy. We have used same values of interaction energy parameters as mentioned in Subsection 4.2.2.1 to calculate the activities of both the components. The calculated values of activities of Na and Hg are furnished in Table 10 along with experimental values (Hultgren et al., 1973). The calculated activities of Na and Hg along with their experimental values are plotted against concentration of Na as depicted in Figure 13.

Table 10: Activities of Na (a_{Na}) and Hg (a_{Hg}) for liquid Na-Hg alloy at 673 K for different concentrations of sodium.

Concentration of Na	Activity of Na (a_{Na})		Activity of Hg (a_{Hg})	
C_{Na}	Theoretical	Experimental*	Theoretical	Experimental*
0.1	0.000	0.000	0.757	0.791
0.2	0.000	0.000	0.417	0.458
0.3	0.004	0.003	0.178	0.195
0.4	0.027	0.024	0.063	0.066
0.5	0.110	0.112	0.020	0.019
0.6	0.290	0.335	0.006	0.005
0.7	0.536	0.565	0.002	0.002
0.8	0.759	0.749	0.001	0.001
0.9	0.904	0.888	0.000	0.000

*Hultgren et al. (1973)

From the figure, it is observed that there is good agreement between the computed and observed values of activities of both species Na and Hg of the concerned system at 673 K. The interaction of two lines doesn't have any physical significance. It just informs that the two components of the alloy have same value of activity at certain concentration. The activities of both components are quite small in comparision to their respective concentrations. This result is the indication of metallurgical stability of the alloy.

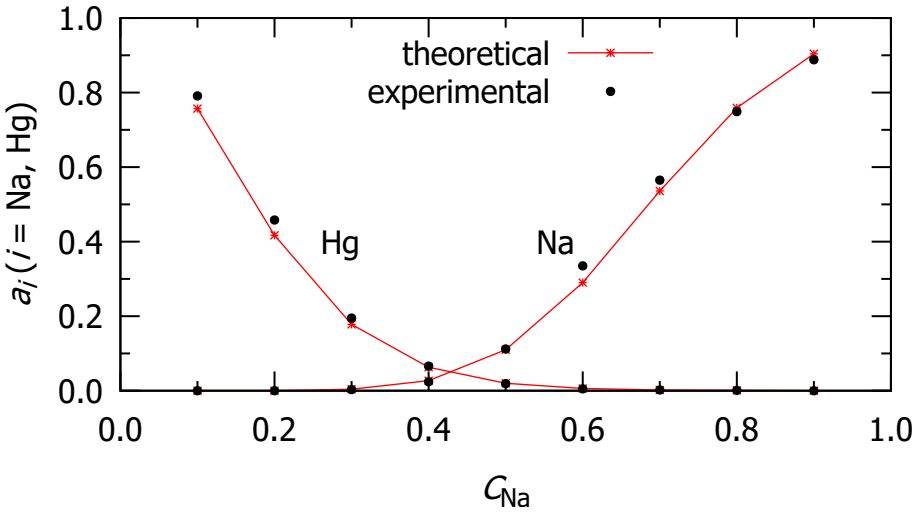

Figure 13: Activities of Na (a_{Na}) and Hg (a_{Hg}) for Na-Hg liquid alloy at 673 K.

4.4.1.2 Activities of Pb (a_{Pb}) and Mg (a_{Mg}) for Pb-Mg Liquid Alloy at 973 K

We have computed the activities of Pb and Mg for Pb-Mg liquid alloy using Equations (3.64) and (3.65). The interaction energy parameters are the primary component used for the computation of activity. We have used same values of interaction energy parameters for the evaluation of activity as given in Subsection 4.2.2.2. The calculated along with experimental (Hultgren et al., 1973) values of activities of each components of the alloy at 973 K are shown in Table 11. Similarly, the plot of computed and experimental activities Pb (a_{Pb}) and Ag (a_{Mg}) against concentration of Pb is shown in the Figure 14.

The Figure 14 shows that theoretical and experimental values of activity of Pb and Mg in liquid Pb-Mg alloy are in excellent agreement to each other. The activities of both components have smaller value at their lower concentration and both increase with increase in their concentration. This result gives the idea that the $PbMg_2$ is one of the stable intermetallic phases of the alloy.

Table 11: Activities of Pb (a_{Pb}) and Mg (a_{Mg}) for liquid Pb-Mg alloy at 973 K for different concentrations of lead.

Concentration of Pb	Activity of Pb (a_{Pb})		Activity of Mg (a_{Mg})	
C_{Pb}	Theoretical	Experimental*	Theoretical	Experimental*
0.1	0.001	0.001	0.813	0.812
0.2	0.009	0.009	0.553	0.550
0.3	0.045	0.044	0.331	0.326
0.4	0.135	0.137	0.183	0.179
0.5	0.292	0.299	0.098	0.094
0.6	0.487	0.501	0.053	0.050
0.7	0.672	0.680	0.029	0.028
0.8	0.812	0.819	0.017	0.016
0.9	0.911	0.913	0.009	0.009

*Hultgren et al. (1973)

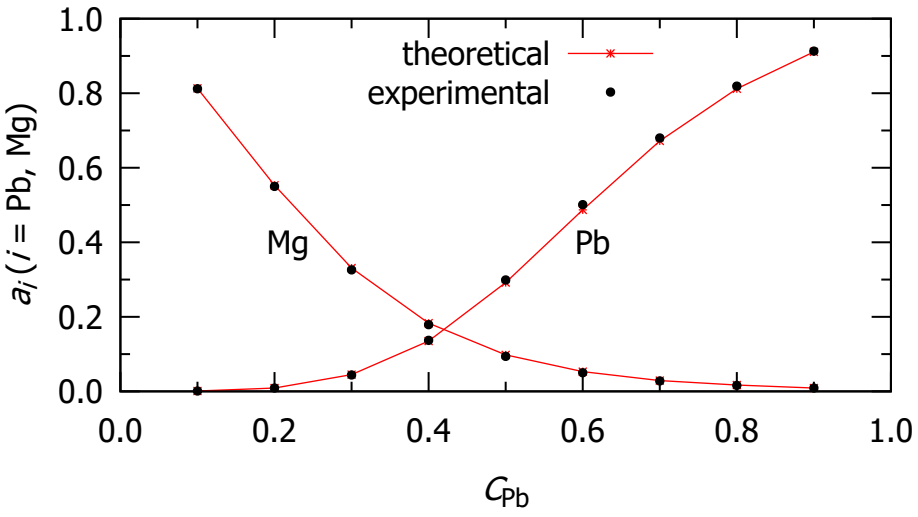

Figure 14: Activities of Pb (a_{Pb}) and Mg (a_{Mg}) for Pb-Mg liquid alloy at 973 K.

4.4.1.3 Activities of Bi (a_{Bi}) and Tl (a_{Tl}) for Bi-Tl Liquid Alloy at 750 K

We have determined the activities of Bi and Tl for a Bi-Tl liquid alloy using Equations (3.64) and (3.65). The interaction energy parameters are the primary components used for the computation of activity. We have used same values of interaction energy parameters for the evaluation of activity as given in Subsection 4.2.2.3 The calculated along with experimental (Hultgren et al., 1973) values of activities of each components of the alloy at 750 K are listed in Table 12. Similarly, the plot of computed and experimental activities Bi (a_{Bi}) and Tl (a_{Tl}) against concentration of Tl is shown in the Figure 15.

From the Figure 15, it is observed that the theoretical and experimental values of activities of Bi and Tl agree throughout the entire concentration of Tl. The activities

Table 12: Activities of Bi (a_{Bi}) and Tl (a_{Tl}) for liquid Bi-Tl alloy at 750 K for different concentrations of thallium.

Concentration of Tl	Activity of Tl (a_{Tl})		Activity of Bi (a_{Bi})	
C_{Tl}	Theoretical	Experimental*	Theoretical	Experimental*
0.1	0.016	0.018	0.892	0.911
0.2	0.036	0.034	0.774	0.811
0.3	0.063	0.058	0.641	0.677
0.4	0.104	0.100	0.487	0.505
0.5	0.172	0.170	0.323	0.326
0.6	0.283	0.283	0.175	0.175
0.7	0.448	0.447	0.074	0.075
0.8	0.658	0.669	0.023	0.022
0.9	0.862	0.870	0.005	0.005

*Hultgren et al. (1973)

of both components have smaller value at their lower concentration and both increase with increase in their concentration. This result depicts that $BiTl_3$ is one of the stable intermetallic phases of the alloy.

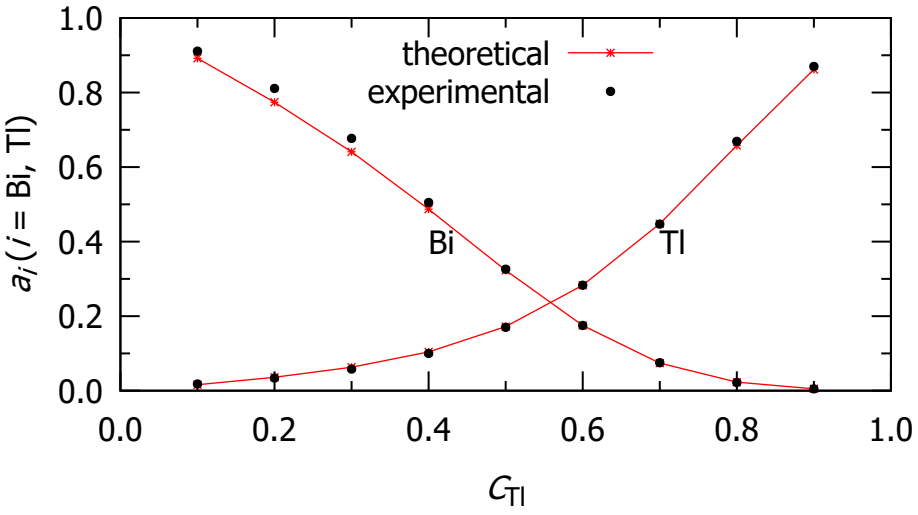

Figure 15: Activities of Bi (a_{Bi}) and Tl (a_{Tl}) for Bi-Tl liquid alloy at 750 K.

4.4.1.4 Activities of Cu (a_{Cu}) and Al (a_{Al}) for Cu-Al Liquid Alloy at 1373 K

The activities of Cu and Al for Cu-Al liquid alloy are determined using Equations (3.64) and (3.65). The same values of interaction energy parameters as mentioned in Subsection 4.2.2.4 are used for the evaluation of activity. The calculated along with experimental (Hultgren et al., 1973) values of activities of each components of the alloy at 1373 K are listed in Table 13 and the plot of computed and experimental activities Cu (a_{Cu}) and Al (a_{Al}) against concentration of Cu is shown in the Figure 16.

Table 13: Activities of Cu (a_{Cu}) and Al (a_{Al}) for liquid Cu-Al alloy at 1373 K for different concentrations of copper.

Concentration of Tl	Activity of Cu (a_{Cu})		Activity of Al (a_{Al})	
C_{Cu}	Theoretical	Experimental*	Theoretical	Experimental*
0.1	0.007	0.005	0.886	0.889
0.2	0.013	0.013	0.787	0.759
0.3	0.022	0.025	0.669	0.609
0.4	0.040	0.046	0.482	0.441
0.5	0.083	0.085	0.260	0.266
0.6	0.185	0.166	0.098	0.116
0.7	0.370	0.352	0.027	0.028
0.8	0.610	0.600	0.006	0.006
0.9	0.832	0.839	0.001	0.001

*Hultgren et al. (1973)

From the figure it is observed that the computed and experimental results somehow agree to each other except slight discrepancy of activity of Al at 0.1 to 0.3 concentration of Cu. The activities of both components have very small value at their lower concentrations indicating stability of liquid alloy.

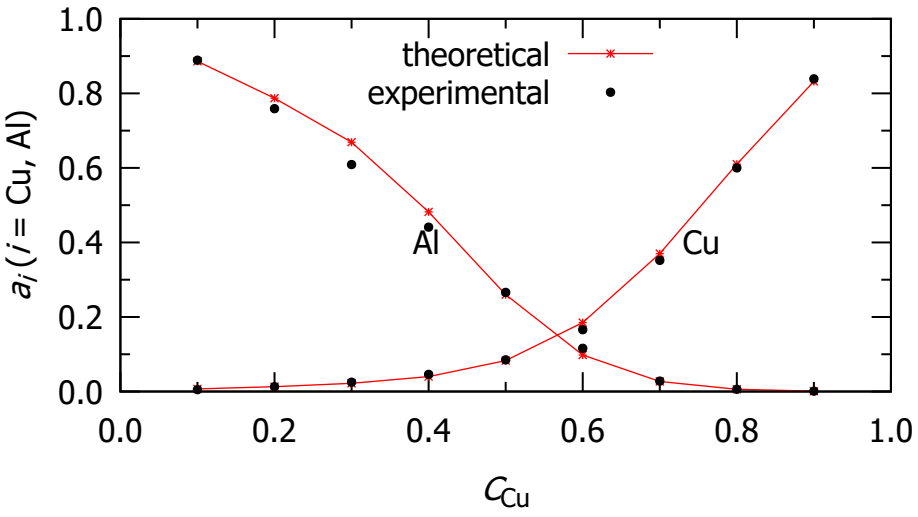

Figure 16: Activities of Cu (a_{Cu}) and Al (a_{Al}) for Cu-Al liquid alloy at 1373 K.

4.5 Entropy of Binary Liquid Alloys

Understanding the mixing behavior of binary liquid alloys requires an understanding of an essential thermodynamic function called entropy of mixing. It offers deep understanding of the direction of spontaneous change for many common processes and also defines the equilibrium state of a system. When the energy is at its lowest and the entropy is at its highest, a system is said to have reached equilibrium state. It is thought that

information regarding the structural arrangement of the atoms in binary liquid alloys can be found in the entropy of mixing. The value of the entropy of mixing of an alloy at a given temperature can be used to examine the deviation in the nature of mixing of the alloy from the regular behavior (Sommer et al., 2001). In this work we have employed Quasi-Chemical Approximation for the theoretical study of entropy of mixing of some binary liquid alloys.

4.5.1 Results for Na-Hg, Pb-Mg, Bi-Tl and Cu-Al Binary Liquid Alloys

In this section, we present the methods to calculate the entropy of mixing for four distinct liquid alloys; Na-Hg, Pb-Mg, Bi-Tl and Cu-Al on the basis of Quasi-Chemical Approximation. The results so obtained together with a discussion and the calculated results are compared with experimental results.

4.5.1.1 Entropy of Mixing of Na-Hg Binary Liquid Alloy at 673 K

We have employed Equation (3.67) to compute the entropy of mixing of Na-Hg binary liquid alloy at 673 K as a function of concentration. $NaHg_2$ is most stable intermetallic compound of sodium mercury alloy. Hence the values of Ψ_{ij} are used from Equation (3.49). We used the same interaction parameter values from Subsections 4.2.2.2 and 4.3.1.2 as primary input parameters.

Table 14: Entropy of mixing for liquid Na-Hg alloy at 673 K for different concentrations of sodium.

Concentration of Na	Entropy of mixing(S_M/R)	
C_{Na}	Theoretical	Experimental*
0.1	−0.093	−0.007
0.2	−0.290	−0.279
0.3	−0.449	−0.500
0.4	−0.519	−0.548
0.5	−0.483	−0.459
0.6	−0.348	−0.289
0.7	−0.149	−0.098
0.8	0.053	0.040
0.9	0.164	0.086

*Hultgren et al. (1973)

Table 14 displays the calculated and actual values of entropy of mixing for liquid Na-Hg alloy at 673 K. Figure 17 displays the plot of the calculated values of mixing entropy as a function of concentration in the concentration range C_{Na} = 0.1 to 0.9 together with the experimental values. There is a slight departure of computed result than that of experimental result as shown in the Figure 17. In the both experimental and theoretical results, the entropy of mixing (S_M/R) are negative at $C_{Na} < 0.8$ concentration of Na

but behind this concentration, it is positive. The decrease in microstate promoting the formation of complex is indicated by the negative entropy.

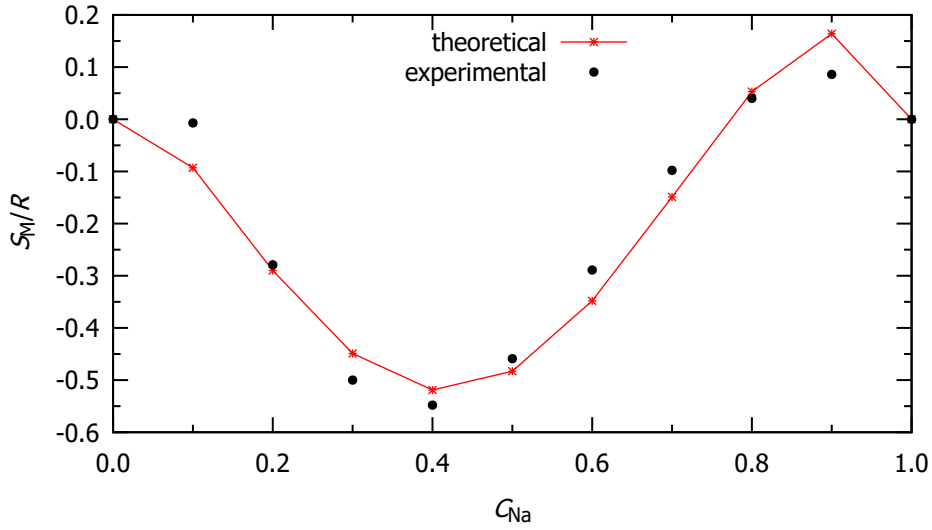

Figure 17: Entropy of mixing versus concentration of Na for Na-Hg liquid alloy at 673 K.

4.5.1.2 Entropy of Mixing of Pb-Mg Binary Liquid Alloy at 973 K

Table 15: Entropy of mixing for liquid Pb-Mg alloy at 973 K for different concentrations of lead.

Concentration of Pb	Entropy of mixing(S_M/R)	
C_{Pb}	Theoretical	Experimental*
0.1	0.325	0.394
0.2	0.472	0.506
0.3	0.548	0.539
0.4	0.583	0.589
0.5	0.595	0.624
0.6	0.586	0.623
0.7	0.553	0.583
0.8	0.479	0.473
0.9	0.330	0.302

*Hultgren et al. (1973)

To determine the entropy mixing of a binary Pb-Mg liquid alloy as a function of concentration at 973 K, the Equation (3.67) is employed. Since $PbMg_2$ is most stable intermetallic compound of lead magnesium alloy, the values of Ψ_{ij} are used from Equation (3.49). We used the same interaction parameter values from Subsection 4.2.2.2 and 4.3.1.2 as basic input parameters.

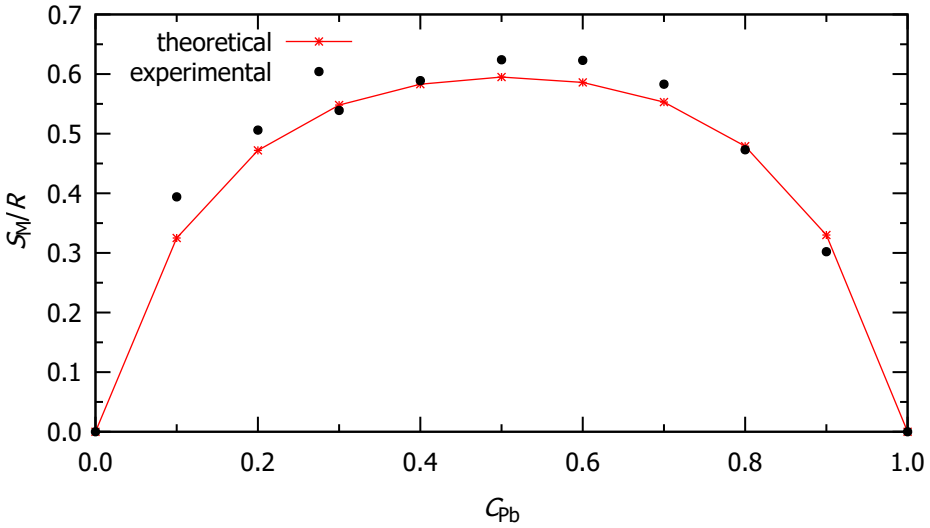

Figure 18: Entropy of mixing versus concentration of Pb for Pb-Mg liquid alloy at 973 K.

Table 15 depicts the calculated and actual values of entropy of mixing for liquid Pb-Mg alloy at 973 K. Figure 18 displays the plot of the calculated values of mixing entropy as a function of concentration in the concentration range C_{Pb} = 0.1 to 0.9 together with the experimental values (Hultgren et al., 1973). There is small departure in the theoretical results from the corresponding experimental results . Both experimental and theoretical values are positive throughout the entire concentration of Pb.

4.5.1.3 Entropy of Mixing of Bi-Tl Binary Liquid Alloy at 750 K

As we have already discussed in Subsection 4.2.2.3 that the complex $BiTl_3$ is one of the most stable state of Bi-Tl alloy. So the values of Ψ_{ij} has been used as mentioned in Equation (3.50) and the entropy of mixing of Bi-Tl binary liquid alloy as a function of concentration has been computed using Equation (3.67). The fundamental input parameters for the computation of entropy of mixing are temperature derivative interaction energy parameters. We utilized the same interaction parameter values that were used in Subsection 4.3.1.3 for the calculation of entropy of mixing. The computed and experimental values of entropy of mixing for Bi-Tl alloy in liquid state at 750 K are presented in Table 16. The plot of computed values of entropy of mixing as a function of concentration in the concentration range C_{Tl} = 0.1 to 0.9 along with the experimental values is shown in Figure 19.

The computed values of entropy of mixing (S_{M}/R) as a function of concentration are good agreement with the experimental results. Thus we can conclude that the alloy is disorder at all composition however degree of disorder is more at $\mathrm{C_{Tl}}$ = 0.5. Similarly the entropy of mixing (S_{M}/R) for Bi-Tl alloy in liquid state is symmetric around equi-atomic

Table 16: Entropy of mixing for liquid Bi-Tl alloy at 750 K for different concentrations of thallium.

Concentration of Tl	Entropy of mixing(S_M/R)	
C_{Tl}	Theoretical	Experimental*
0.1	0.337	0.304
0.2	0.529	0.501
0.3	0.657	0.656
0.4	0.733	0.754
0.5	0.760	0.760
0.6	0.738	0.721
0.7	0.662	0.649
0.8	0.530	0.529
0.9	0.333	0.336

*Hultgren et al. (1973)

composition which has been successfully explained on the basis of Quasi-chemical Approximation.

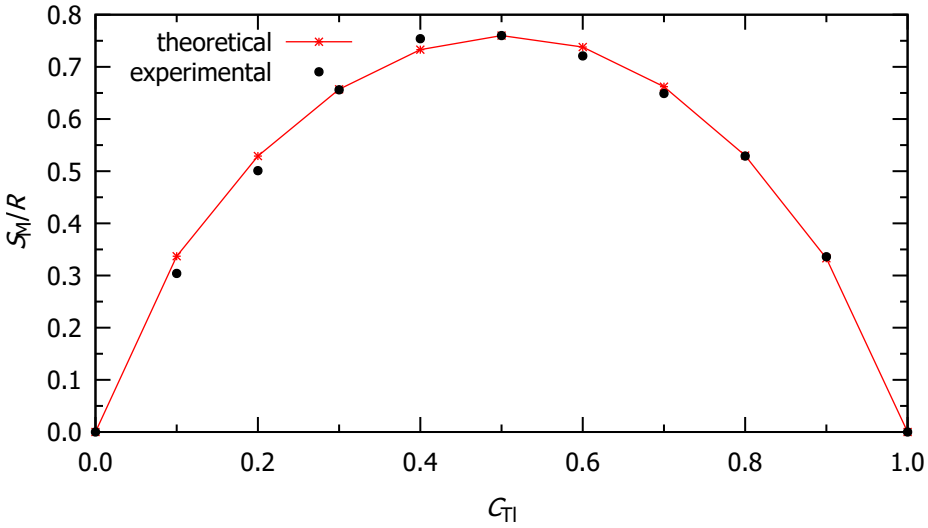

Figure 19: Entropy of mixing versus concentration of Tl for Bi-Tl liquid alloy at 750 K.

4.5.1.4 Entropy of Mixing of Cu-Al Binary Liquid Alloy at 1373 K

$CuAl_3$ is one of the stable intermetallic compounds of Cu-Al binary alloy. Thus the values of Ψ_{ij} have been used from Equation (3.51) in order to determine the entropy of mixing of Cu-Al binary liquid alloy at 1373 K as a function of concentration by using Equation (3.67). As basic input parameters, we utilized the same interaction parameter values that were used in Subsection 4.3.1.4.

The computed and experimental values of entropy of mixing for Cu-Al alloy in liquid state at 1373 K are presented in Table 17. The plot of computed values of entropy of

Table 17: Entropy of mixing for liquid Cu-Al alloy at 1373 K for different concentrations of copper.

Concentration of Cu	Entropy of mixing(S_M/R)	
C_{Cu}	Theoretical	Experimental*
0.1	0.516	0.532
0.2	0.875	0.901
0.3	1.172	1.193
0.4	1.402	1.408
0.5	1.535	1.521
0.6	1.542	1.538
0.7	1.402	1.420
0.8	1.114	1.135
0.9	0.680	0.690

*Hultgren et al. (1973)

mixing as a function of concentration in the concentration range C_{Cu} = 0.1 to 0.9 along with the experimental values is shown in Figure 20.

From the Figure 20, it can be observed that both experimental and theoretical results are agree and positive in the whole concentration range of copper. The rise in disorder or randomness of mixing event is indicated by the positive entropy of mixing.

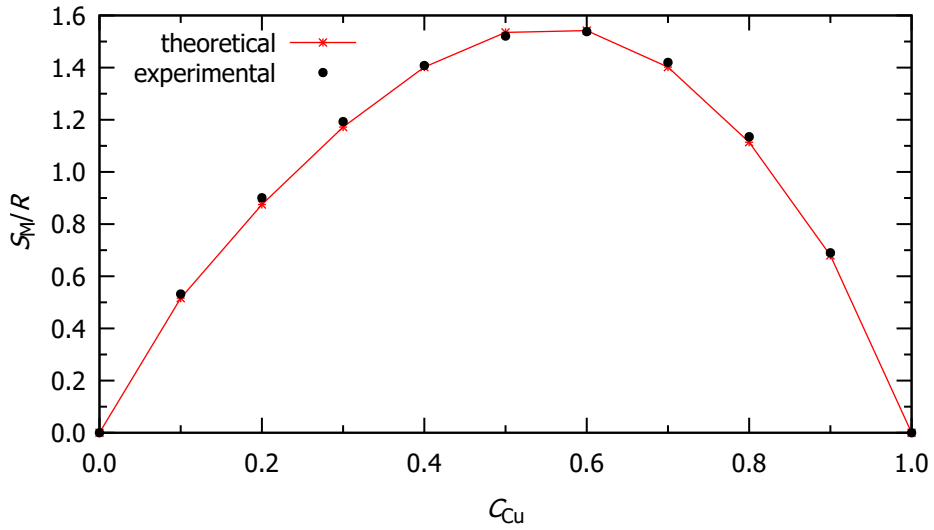

Figure 20: Entropy of mixing versus concentration of Cu for Cu-Al liquid alloy at 1373 K.

4.6 Concentration Fluctuation in Long Wavelength Limit and Chemical Short Range Order Parameter

The liquid states are known as disordered states and hence the basic feature of liquid is that it exhibits short range order in contrast to the long-range periodicity of solid crystals. From the understanding of the bulk characteristics, a great deal of interest has been

exhibited in determining the microscopic properties of binary molten alloys. The work of Bhatia and Thornton (Bhatia & Thornton, 1970) of compound forming molten alloys has shown the path in the desired direction. The key microscopic function developed by Bhatia and Thornton to visualize and understand the nature of microscopic structure in molten binary alloys are the concentration fluctuation in long wave length limit ($S_{CC}(0)$) and chemical short range order parameter (α_1).

4.6.1 Results for Na-Hg, Pb-Mg, Bi-Tl and Cu-Al Binary Liquid Alloys

In the present section, we intend to apply the Quasi-Chemical Approximation for the study of Na-Hg, Pb-Mg, Bi-Tl and Cu-Al binary alloys and analyze their microscopic ordering. For this we compare theoretical as well as experimental concentration fluctuation in long wavelength limit $S_{CC}(0)$ with ideal concentration fluctuation in long wavelength limit (S^{id}_{CC} (0)) since visualizing the type of atomic interactions in the mixture depends on the departure of $S_{CC}(0)$ from the ideal value (Singh & Sommer, 1998). The ideal concentration fluctuation in long wavelength limit is obtained using Equation (3.81) for all the alloys. Similarly, the degree of ordering or segregating of the alloys is quantified by chemical short range order parameter (α_1) with the help of Equation (3.94).

4.6.1.1 $S_{CC}(0)$ and α_1 for Na-Hg Liquid Alloy at 673 K

Equation (3.80) has been used to calculate theoretical values of $S_{CC}(0)$ for Na-Hg liquid alloy at 673 K as a function of concentration . Interaction energy parameters, which have previously been computed in Subsection 4.2.2.1, make up the fundamental input parameters. Equation (3.49) is used to get the values of second derivative terms with respect to concentration. The experimental values of $S_{CC}(0)$ have been obtained by applying Equation (3.79), which uses the observed activities of sodium and mercury (Hultgren et al., 1973). The values of the chemical short range order parameter (α_1) have been calculated using the theoretical values of $S_{CC}(0)$) in Equation (3.94). During the calculation, the value of coordination number (Z) is taken as 10 . Table 18 lists the calculated values for $S_{CC}(0)$ together with the corresponding experimental and ideal values and chemical short range order parameter (α_1) . Similar to this, Figures 21 and 22 respectively illustrate the plots of $S_{CC}(0)$ and α_1 as a function of concentration. From the Figure 21, It is clear that both theoretical and experimental values of $S_{CC}(0)$ are smaller than ideal values and there is agreement between the two sets of the values at all concentrations. The figure depicts that the concerned Na-Hg liquid alloy shows ordering nature at its melting temperature. Figure 22 suggests that the theoretical values of α_1 are negative at all concentrations, supporting the notion of the liquid alloy as described by $S_{CC}(0)$. We may also infer that the alloy is compound forming with preferable alliance between Na and Hg in the liquid state at 673 K.

Table 18: Concentration fluctuation in long wavelength limit and Chemical short range parameter for liquid Na-Hg alloy at 673 K for different concentrations of sodium.

Concentration of Na	$S_{CC}(0)$			α_1
C_{Na}	Theoretical	Experimental*	Ideal	
0.1	0.022	0.013	0.090	-0.233
0.2	0.027	0.018	0.160	−0.331
0.3	0.031	0.037	0.210	−0.370
0.4	0.036	0.033	0.240	−0.375
0.5	0.043	0.037	0.250	−0.355
0.6	0.051	0.053	0.240	−0.311
0.7	0.064	0.083	0.210	−0.247
0.8	0.082	0.072	0.160	−0.165
0.9	0.083	0.073	0.090	−0.075

*Hultgren et al. (1973)

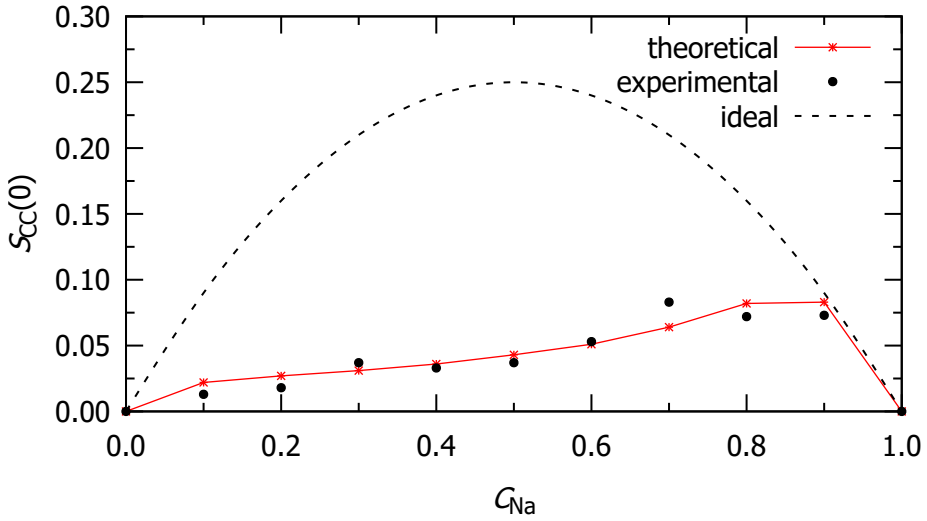

Figure 21: Concentration fluctuation in long wavelength limit versus concentration of Na for Na-Hg liquid alloy at 673 K.

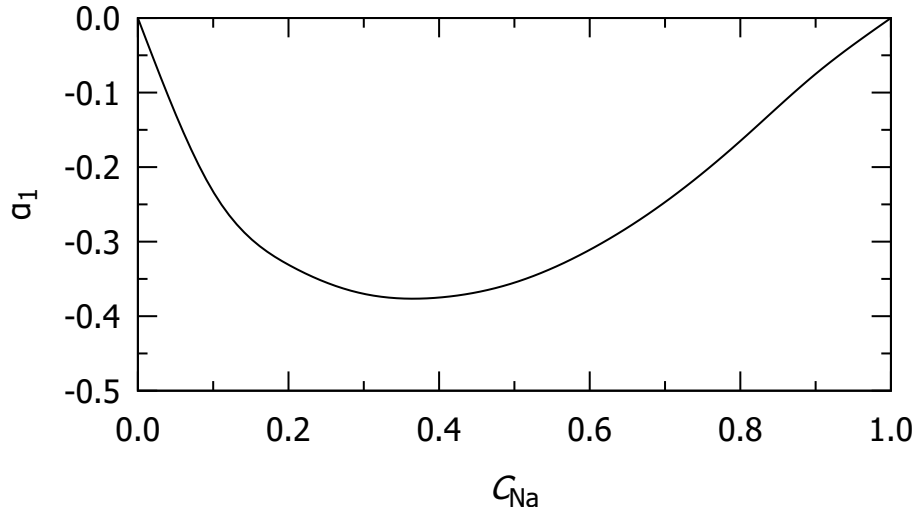

Figure 22: Chemical short range order parameter versus concentration of versus concentration of Na for Na-Hg liquid alloy at 673 K.

4.6.1.2 $S_{CC}(0)$ and α_1 for Pb-Mg Liquid Alloy at 973 K

For the theoretical calculation of the concentration fluctuation in long wavelength limit ($S_{CC}(0)$) for the Pb-Mg binary liquid alloy at 973 K, Equation (3.80) has been utilized. We have used the same interaction energy parameter values that were used to get the free energy of mixing in Subsection 4.2.2.2 in order to preserve consistency. Equation (3.79) is used to calculate the experimental $S_{CC}(0)$ from the experimental activities of components Pb (a_{Pb}) and Mg (a_{Mg}). Equation (3.49) provides the values of second derivative terms with regard to concentration. The value of the chemical short range order parameter (α_1) as a function of concentration is determined by Equation (3.94).

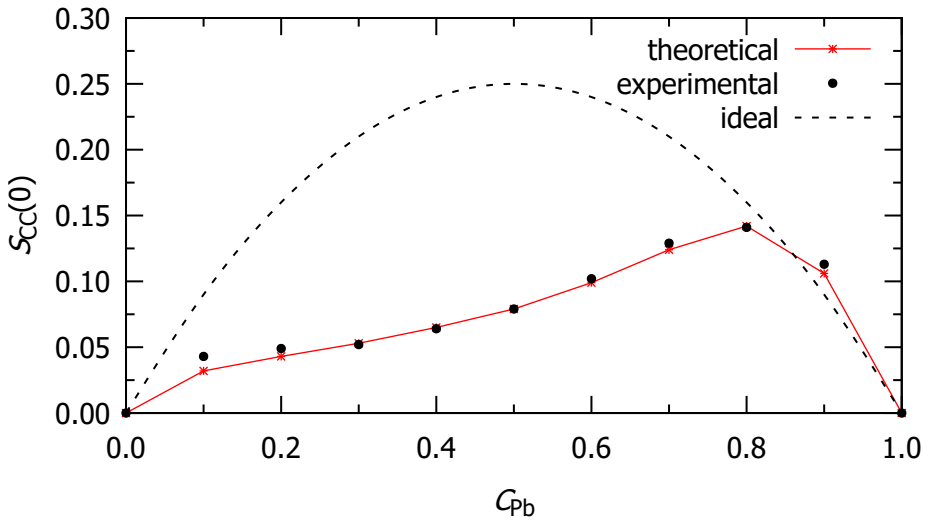

Figure 23: Concentration fluctuation in long wavelength limit versus concentration of Pb for Pb-Mg liquid alloy at 973 K.

Table 19: Concentration fluctuation in long wavelength limit and Chemical short range parameter for liquid Pb-Mg alloy at 973 K for different concentrations of lead.

Concentration of Pb	$S_{CC}(0)$			α_1
C_{Pb}	Theoretical	Experimental*	Ideal	
0.1	0.032	0.043	0.090	−0.152
0.2	0.043	0.049	0.160	−0.214
0.3	0.053	0.052	0.210	−0.229
0.4	0.065	0.064	0.240	−0.214
0.5	0.079	0.079	0.250	−0.177
0.6	0.099	0.102	0.240	−0.125
0.7	0.124	0.129	0.210	−0.065
0.8	0.142	0.141	0.160	−0.012
0.9	0.106	0.113	0.090	0.016

*Hultgren et al. (1973)

The calculated values for $S_{CC}(0)$ together with the corresponding experimental and ideal values as well as values of chemical short range order parameter (α_1) are shown in the Table 19. Figures 23 and 24 respectively illustrate the plots of $S_{CC}(0)$ and (α_1) against concentration of Pb for Pb-Mg liquid alloy at 973 K.

The Figure 23 demonstrates that the calculated values of $S_{CC}(0)$ are less than ideal at about 0.8 concentration of Pb and are higher beyond 0.8 concentration, indicating that the alloy is ordering in nature up to about 0.8 concentration of Pb and segregating above this concentration at its melting temperature. The computed values of $S_{CC}(0)$ are in good agreement with the experimental and theoretical values of $S_{CC}(0)$ within entire concentration. The theoretical value of α_1 shown in Figure 24 is negative at around 0.8 concentrations of Pb and then positive above that level, validating the idea of the liquid alloy as stated by $S_{CC}(0)$.

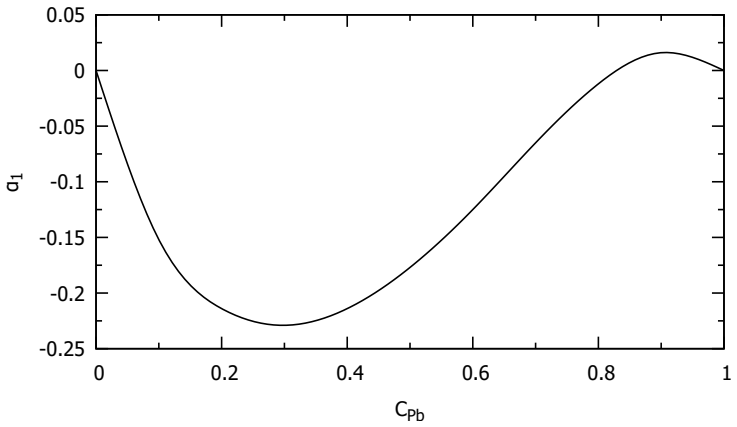

Figure 24: Chemical short range order parameter versus concentration of Pb for Pb-Mg liquid alloy at 973 K.

4.6.1.3 $S_{CC}(0)$ and α_1 for Bi-Tl Liquid Alloy at 750 K

We have used Equation (3.80) for the theoretical calculation of concentration fluctuation in long wavelength limit ($S_{CC}(0)$) for Bi-Tl binary liquid alloy at 750 K. In order to maintain consistency, we have utilized the same interaction energy parameters as used to calculate the free energy of mixing in Subsection 4.2.2.3. As mentioned above, the experimental $S_{CC}(0)$ is derived from the experimental activities of components Bi(a_{Bi}) and Tl(a_{Tl}) (Hultgren et al., 1973) throughout the entire concentration using Equation (3.79). The values of second derivative terms with respect to concentration are obtained from Equation (3.50). Equation (3.94) is used to calculate the value of the chemical short range order parameter α_1 as a function of concentration.

Table 20: Concentration fluctuation in long wavelength limit and Chemical short range parameter for liquid Bi-Tl alloy at 750 K for different concentrations of thallium.

Concentration of Tl	$S_{CC}(0)$			α_1
C_{Tl}	Theoretical	Experimental*	Ideal	
0.1	0.079	0.085	0.090	−0.014
0.2	0.124	0.144	0.160	−0.028
0.3	0.135	0.128	0.210	−0.053
0.4	0.120	0.111	0.240	−0.091
0.5	0.100	0.095	0.250	−0.131
0.6	0.082	0.082	0.240	−0.161
0.7	0.070	0.070	0.210	−0.167
0.8	0.060	0.058	0.160	−0.142
0.9	0.048	0.051	0.090	−0.079

*Hultgren et al. (1973)

The theoretically computed values of $S_{CC}(0)$ along with the corresponding experimental and ideal values and α_1 are given in Table 20. The plots of $S_{CC}(0)$ and α_1 against concentration of Tl are shown in the Figures 25 and 26 respectively.

From the Figure 25, it is observed that there is departure of theoretical values of $S_{CC}(0)$ from experimental values. However, both theoretical and computed values of $S_{CC}(0)$ lie below ideal value. Since compound forming tendency appears at about 0.75 concentration of Tl or 0.25 concentration of Bi, the $S_{CC}(0)$ is markedly depressed near that concentration of Tl.

Similarly, more negative value of α_1 at about 0.75 concentration of Tl insights that the ordering nature of the alloy is maximum near the stoichiometric concentration.

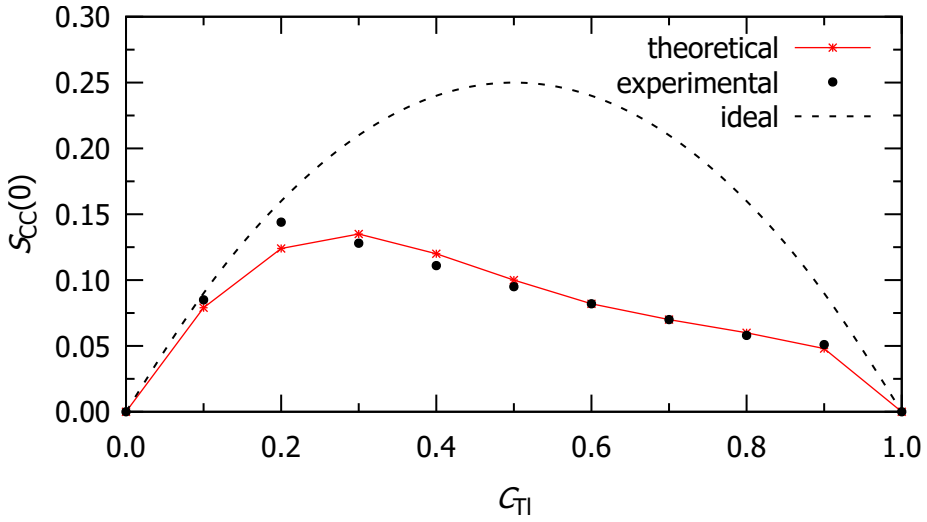

Figure 25: Concentration fluctuation in long wavelength limit versus concentration of Bi for Bi-Tl liquid alloy at 750 K.

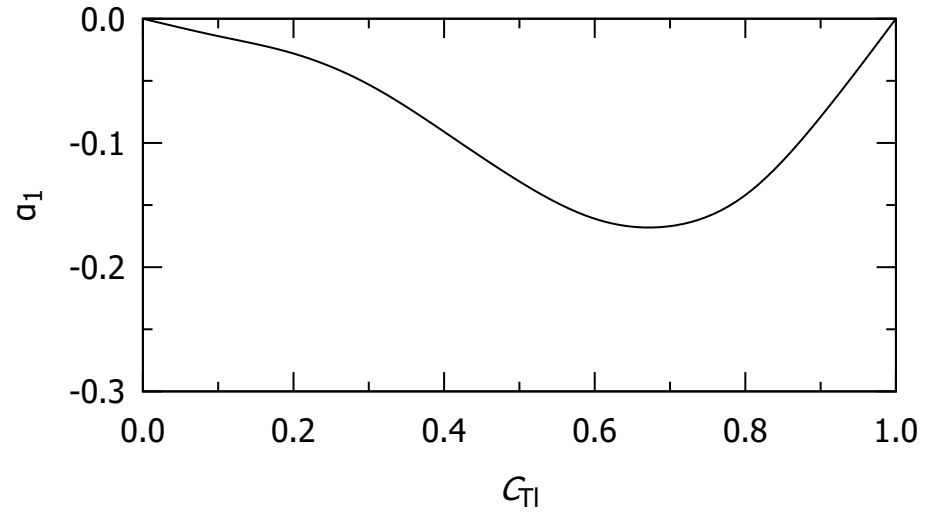

Figure 26: Chemical short range order parameter versus concentration of Bi for Bi-Tl liquid alloy at 750 K.

4.6.1.4 $S_{CC}(0)$ and α_1 for Cu-Al Liquid Alloy at 1373 K

Theoretical values of $S_{CC}(0)$ for Cu-Al liquid alloy at 1373 K have been computed as a function of concentration from Equation (3.80). The basic input parameters are interaction energy parameters which have already been estimated in Subsection 4.2.2.4. The values of second derivative terms with respect to concentration are obtained following similar procedure from Equation (3.51) as mentioned above . Utilizing the measured activities of copper and aluminum (Hultgren et al., 1973) in Equation (3.79), the experimental values of $S_{CC}(0)$ have been derived. With the help of the theoretical values of $S_{CC}(0)$ in

Equation (3.94), the values of the chemical short range order parameter (α_1) have been computed.

The computed values of $S_{CC}(0)$ along with the corresponding experimental and ideal values and α_1 are given in Table 21. Similarly, the plots of $S_{CC}(0)$ and α_1 against concentration of Cu are shown in the Figures 27 and 26 respectively.

Table 21: Concentration fluctuation in long wavelength limit and Chemical short range parameter for liquid Cu-Al alloy at 1373 K for different concentrations of copper.

Concentration of Cu	$S_{CC}(0)$			α_1
C_{Cu}	Theoretical	Experimental*	Ideal	
0.1	0.082	0.068	0.090	−0.010
0.2	0.159	0.109	0.160	−0.001
0.3	0.135	0.108	0.210	−0.053
0.4	0.088	0.101	0.240	−0.147
0.5	0.063	0.081	0.250	−0.229
0.6	0.052	0.050	0.240	−0.265
0.7	0.050	0.045	0.210	−0.245
0.8	0.051	0.047	0.160	−0.177
0.9	0.041	0.040	0.090	−0.106

*Hultgren et al. (1973)

Figure 27 shows that the theoretical and experimental values of $S_{CC}(0)$ go below the ideal value of $S_{CC}(0)$ throughout the concentration of the alloy as well as displays shallow minimum in the concentration range at which intermetallic phases occur. This result depicts that the alloy is completely ordering in nature at 1373 K and the mixing of the dissimilar atoms of the preferred alloy takes place in the initial melt.

Similarly, Figure 28 indicates that the computed values of chemical short range order parameter (α_1) are negative within entire concentrations. The value being more negative at about compound forming concentration, allows us to claim that the degree of ordering is maximum at that concentration.

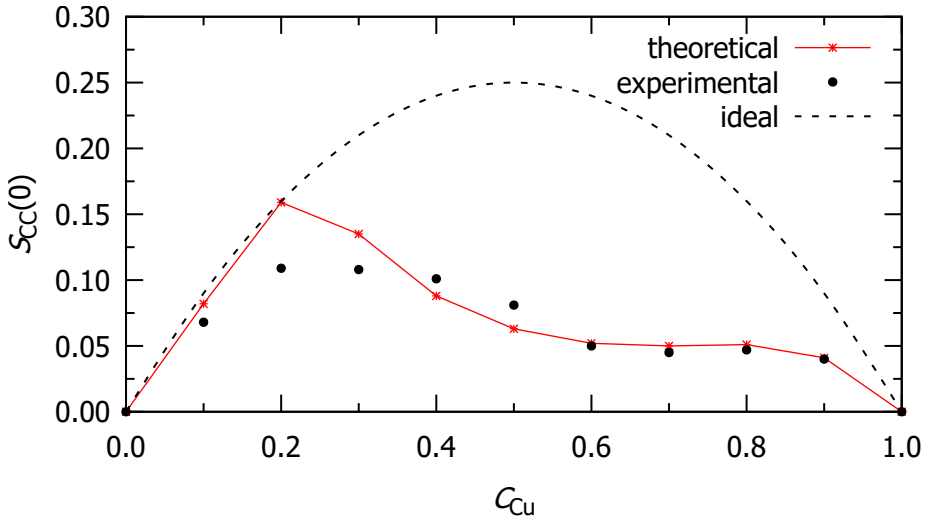

Figure 27: Concentration fluctuation in long wavelength limit versus concentration of Cu for Cu-Al liquid alloy at 1373 K.

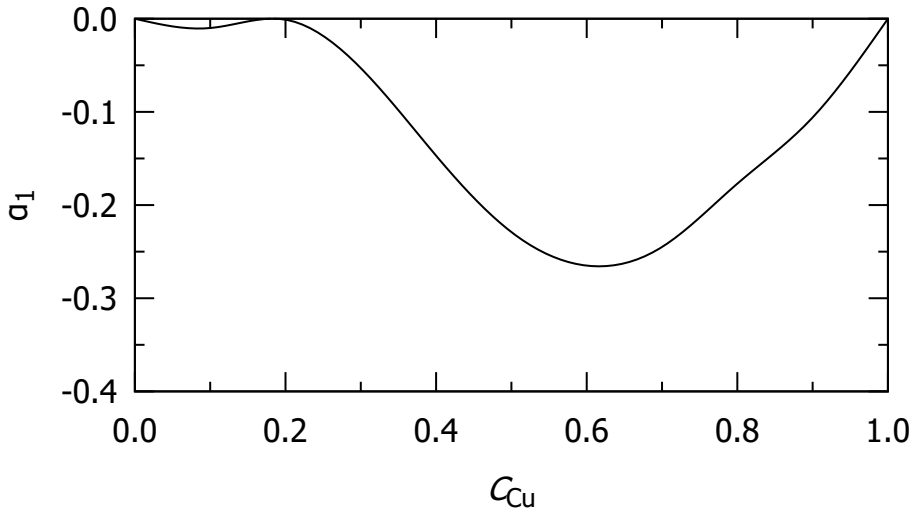

Figure 28: Chemical short range order parameter versus concentration of Cu for Cu-Al liquid alloy at 1373 K.

4.7 Transport Property

Although there are theoretically quite a few different transport properties, three are by far the most significant from a practical and scientific standpoint which correspond to the transfer of momentum, energy, and matter respectively from one region of a material to another under the influence of composition, temperature or velocity gradients. These are important for the most efficient engineering design of many processes in the chemical, oil and biotechnological industries.

Among the three, the transport of the momentum of the fluid is incorporated by the property called viscosity. It is characterized as a form of internal friction brought on by the layers of the liquid and is mainly related to fluids in metallurgy. Every ordinary fluid has viscosity. It displays the microscopic interactions between the molecules of the material. It is a significant factor in deciding the forces that must be overcome when fluids are utilized in lubrication and transported in pipelines. Thus it is a measure of the amount of energy that is irreversibly lost when a fluid is forced to flow through a physical configuration that involves boundaries that are not moving at the same velocity (Hendriks et al., 2010; Gąsior, 2014; Delsante et al., 2019) . In the present work, we have used Kaptay's model (Kaptay, 2003) to compute the concentration dependent viscosity of four different binary liquid alloys.

4.7.1 Results for Na-Hg , Pb-Mg. Bi-Tl and Cu-Al Binary Liquid Alloys

In this section, we present the methods to estimate the viscosity and results so obtained together with a discussion for four distinct liquid alloys: Na-Hg, Pb-Mg, Bi-Tl and Cu-Al on the basis of Kaptay's model. The ratio of atomic mass to density is used to calculate the molar volume of the pure component. The densities and the viscosities required for each component are taken from Table 22.

Table 22: Densities and Viscosities of pure metals of the alloys (Brandes & Brook, 2013).

Metals	Melting temperature T_0 (K)	Density (kg m^{-3})	Viscosity (N s m^{-2})
Aluminum (Al)	933	$2385 - 0.28 \times (T - T_0)$	1.49×10^{-4} exp$(16.50 \times 10^3/RT)$
Bismuth (Bi)	544	$10068 - 1.33 \times (T - T_0)$	4.46×10^{-4} exp $(6.45 \times 10^3/RT)$
Copper (Cu)	1356	$8000 - 0.80 \times (T - T_0)$	3.01×10^{-4}exp$(30.50 \times 10^3/RT)$
Lead (Pb)	600	$10678 - 1.32 \times (T - T_0)$	4.64×10^{-4} exp$(8.61 \times 10^3/RT)$
Magnesium (Mg)	924	$1590 - 0.27 \times (T - T_0)$	2.45×10^{-5}exp $(30.50 \times 10^3/RT)$
Mercury (Hg)	234.1	$13691 - 2.44 \times (T - T_0)$	5.57×10^{-4}exp$(2.51 \times 10^3/RT)$
Sodium (Na)	369.5	$927 - 0.24 \times (T - T_0)$	1.53×10^{-4} exp$(5.24 \times 10^3/RT)$
Thallium (Tl)	575	$11280 - 1.43 \times (T - T_0)$	2.98×10^{-4}exp$(10.50 \times 10^3/RT)$

Now, Equation (3.102) is used to calculate the viscosities of liquid alloys using the aforementioned input parameters at their corresponding melting temperatures. The computed viscosities of Na-Hg, Pb-Mg, Bi-Tl and Cu-Al binary liquid alloys are respectively given in Tables 23, 24, 25 and 26. Similarly, the corresponding natures of the viscosities are shown in Figures 29, 30, 31 and 32 respectively. Due to scarcity of experimental data of the alloys, the computed values are not compared with experimental results. However in order to gain the knowledge of interacting tendency of the components of the alloys, the computed viscosities are compared with ideal viscosity (i.e. $\eta_{\text{ideal}} = \eta_A C_A + \eta_B C_B$).

Figure 29 gives the information that the viscosity of Na-Hg varies nonlinearly with

Table 23: Viscosity for liquid Na-Hg alloy at 673 K for different concentrations of sodium.

Concentration of Na	Viscosity(η) (mN s m^{-2})	
C_{Na}	Theoretical	Ideal
0.1	1.000	0.823
0.2	1.085	0.775
0.3	1.110	0.727
0.4	1.070	0.679
0.5	0.974	0.630
0.6	0.844	0.582
0.7	0.705	0.534
0.8	0.576	0.486
0.9	0.469	0.437

increase in the concentration of Na and shows maximum positive deviation from the ideal viscosity at about compound forming concentration of the alloy. As expected, with addition of Na component having smaller value of viscosity at 673 K (Brandes & Brook, 2013), the viscosity of the alloy is observed finally to decrease towards Na rich end. Similarly, the viscosities of other three liquid alloys, Pb-Mg, Bi-Tl and Cu-Al vary nonlinearly with increase in the concentration of Pb, Tl and Cu respectively as shown in the Figures 30, 31 and 32.

Table 24: Viscosity for liquid Pb-Mg alloy at 973 K for different concentrations of lead.

Concentration of Pb	Viscosity(η) (mN s m^{-2})	
C_{Pb}	Theoretical	Ideal
0.1	1.248	1.091
0.2	1.319	1.119
0.3	1.365	1.147
0.4	1.386	1.175
0.5	1.385	1.204
0.6	1.369	1.232
0.7	1.344	1.260
0.8	1.321	1.288
0.9	1.309	1.316

Figure 31 shows that the viscosity of Bi-Tl increases with increase in the concentration of Tl and looks deviated more at its compound forming concentration. Similarly, Figure 32 indicates the increasing tendency of viscosity with increase in concentration of Cu in the case of Cu-Al liquid alloy but it is negatively deviated than that of ideal viscosity. The trend of this curve resembles similarity to the experimentally determined viscosity at 1345 K by Trybula et al. (2018) to 0.5 concentration of Cu. The viscosities of

Na-Hg,Pb-Mg and Bi-Tl alloys show maxima on the viscosity plots in the region close to the stoichiometric compositions of intermetallic compounds. Such anomalies give the information of strong interaction between unlike atoms of these alloys. Thus we conclude that for compound forming liquid alloys, non linear behaviour of viscosity has been noted and usually maxima on the viscosity curves of the compound forming systems frequently lie close to the stoichiometric compositions of their intermetallic compounds.

Table 25: Viscosity for liquid Bi-Tl alloy at 750 K for different concentrations of thallium.

Concentration of Tl	Viscosity(η) (mN s m^{-2})	
C_{Tl}	Theoretical	Ideal
0.1	1.319	1.287
0.2	1.386	1.323
0.3	1.452	1.358
0.4	1.515	1.394
0.5	1.573	1.429
0.6	1.621	1.465
0.7	1.653	1.500
0.8	1.664	1.536
0.9	1.649	1.571

Table 26: Viscosity for liquid Cu-Al alloy at 1373 K for different concentrations of copper.

Concentration of Cu	Viscosity(η) (mN s m^{-2})	
C_{Cu}	Theoretical	Ideal
0.1	0.775	1.005
0.2	0.947	1.377
0.3	1.156	1.749
0.4	1.410	2.121
0.5	1.724	2.493
0.6	2.099	2.865
0.7	2.542	3.237
0.8	3.059	3.609
0.9	3.658	3.981

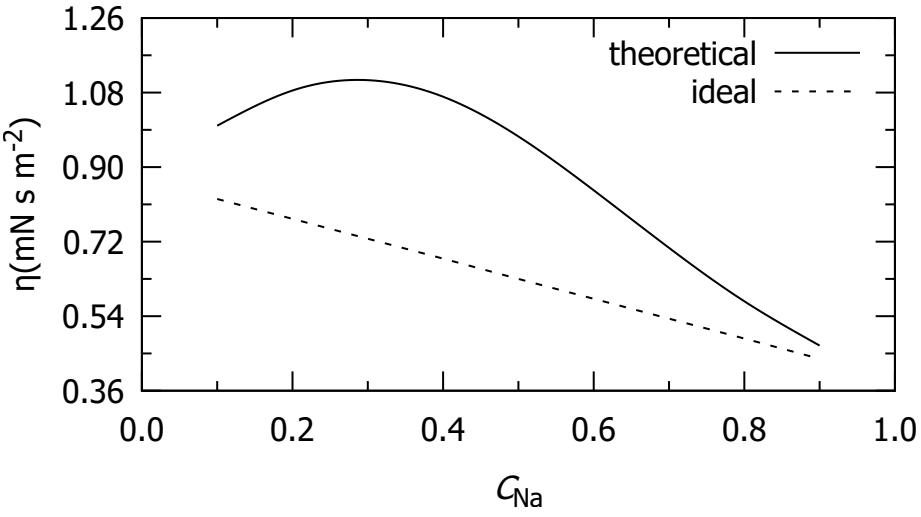

Figure 29: Viscosity versus concentration of Na for Na-Hg liquid alloy at 673 K.

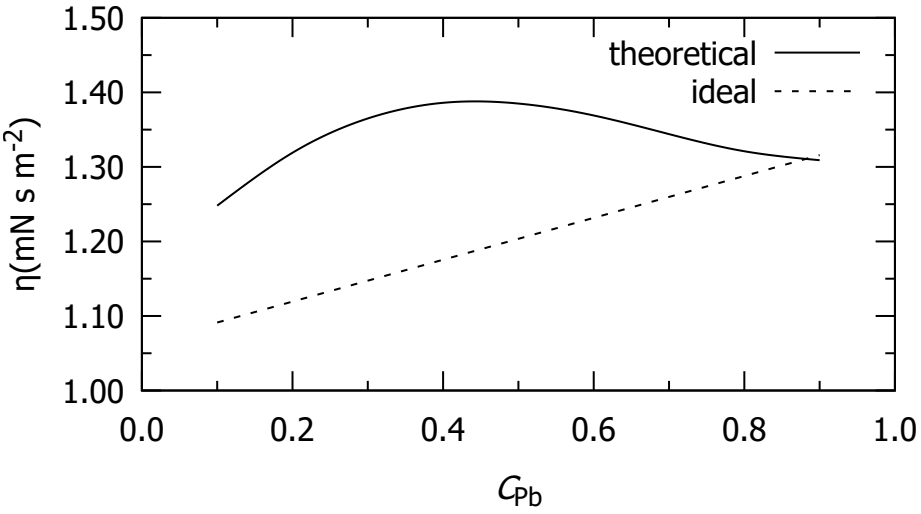

Figure 30: Viscosity versus concentration of Pb for Pb-Mg liquid alloy at 973 K.

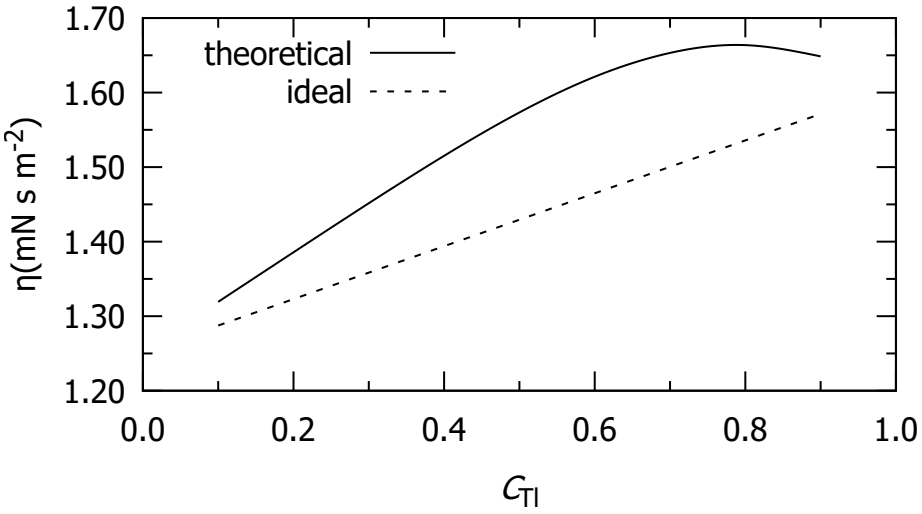

Figure 31: Viscosity versus concentration of Bi for Bi-Tl liquid alloy at 750 K.

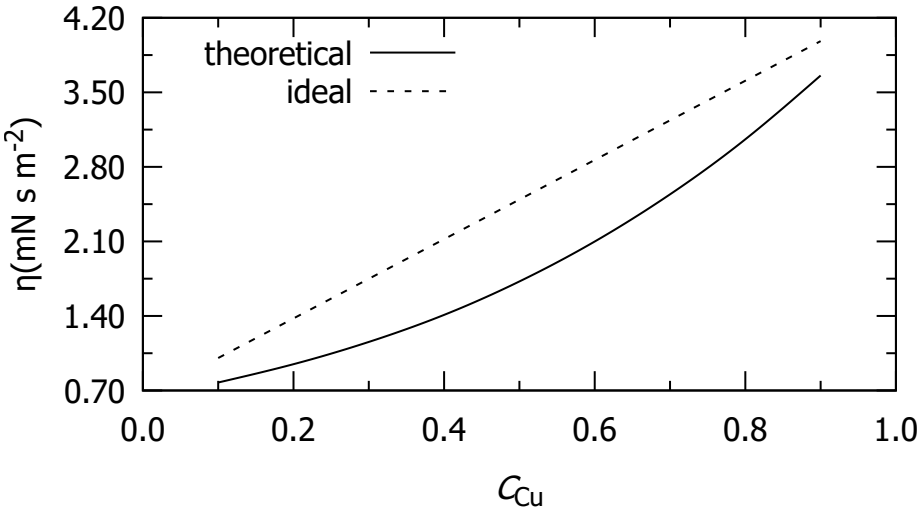

Figure 32: Viscosity versus concentration of Cu for Cu-Al liquid alloy at 1373 K.

4.8 Surface Property

The liquid phase is characterized by free deformable surfaces. The surface atoms of liquids are loosely bonded and hence have a higher energy in comparison to the corresponding bulk atoms. This is the physical cause of surface tension. The concept of surface tension is derived from the tendency of system to reduce its free energy. The fundamental factors affecting surface tension are the forces of attraction between the particles and also upon the gas, solid, or liquid in contact with it.

In the present work, we have used Butler equation as improved by Kaptay (2019) to compute the concentration dependent surface segregation and surface tension of four

different binary liquid alloys.

4.8.1 Results for Na-Hg, Pb-Mg, Bi-Tl and Cu-Al Binary Liquid Alloys

In this section, we present the methods to estimate the surface tension and surface concentration and results so obtained together with a discussion for four distinct liquid alloys: Na-Hg, Pb-Mg, Bi-Tl and Cu-Al on the basis of improved Butler's equation. It is important to have accurate reference data on the surface tension of pure metals of the alloys in order to determine the surface tension of molten metallic alloys. At any temperature (T), they can be taken as given in the Table 27.

Table 27: Surface tensions of pure metals of the alloys (Brandes & Brook, 2013)

Metals	Melting temperature T_0 (K)	Surface tension (Nm^{-1})
Aluminum(Al)	933	$0.914 - 0.35 \times 10^{-3}$ (T-T0)
Bismuth(Bi)	544	$0.361 - 0.10 \times 10^{-3}$ (T-T0)
Copper (Cu)	1356	$1.285 - 0.13 \times 10^{-3}$ (T-T0)
Lead(Pb)	600	$0.468 - 0.13 \times 10^{-3}$ (T-T0)
Magnesium(Mg)	924	$0.559 - 0.35 \times 10^{-3}$ (T-T0)
Mercury(Hg)	234.1	$0.498 - 0.20 \times 10^{-3}$ (T-T0)
Sodium(Na)	369.5	$0.195 - 0.09 \times 10^{-3}$ (T-T0)
Thallium(Tl)	575	$0.464 - 0.08 \times 10^{-3}$ (T-T0)

The partial molar surface area of each component is calculated using Equation (3.118) and surface molar excess partial energy($\Delta G^{\mathrm{Xs}}_{i,\mathrm{b}}$) of i^{th} component required for the calculation is obtained from observed bulk excess bulk molar partial energy ($\Delta G^{\mathrm{Xs}}_{i,\mathrm{b}}$) using following relation:

$$\Delta G^{\mathrm{Xs}}_{i,\mathrm{s}} = \beta \Delta G^{\mathrm{Xs}}_{i,\mathrm{b}} \tag{4.1}$$

where β is the ratio of surface molar excess partial energy to the bulk molar excess partial energy is also termed as adjustable parameter. Its value is taken to be 0.83 (Tanaka et al., 1996). Due to a lower value of the coordination number in the surface layer compared to the bulk phase, it is believed that the partial excess free energy of the i^{th} component in the surface layer is lower than that in the bulk phase (Trybula et al., 2014).

The bulk composition is typically known. However, it is uncertain what makes up the surface. Therefore, it is necessary to find the surface concentration with the help of bulk concentrations. Here, it could be appropriate to point out that $C^{\mathrm{s}}_A + C^{\mathrm{s}}_B = 1$ and $C^{\mathrm{b}}_A + C^{\mathrm{b}}_B = 1$.

For the calculation of surface properties,densities and partial excess free energies of the component of pure metals at the temperature of investigations are also required.The

density which is used to calculate molar volume of metals are obtained as given by Brandes & Brook (2013).

The middle and right sides of Equation (3.120) are solved with the aid of the aforementioned estimated input parameters to obtain the surface concentration of the components of the alloys at working temperature for whole bulk concentration range. Following the finding of such surface concentrations as well as bulk concentrations of components of the alloys, the composition dependent surface tension of the corresponding alloy is estimated. However, the computed values cannot be compared with experimental results due to the dearth of experimental data for the alloys.

The computed surface concentrations of components and surface tensions of Na-Hg, Pb-Mg, Bi-Tl and Cu-Al binary liquid alloys along with their ideal mixing are displayed in the following Tables 28,29, 30 and 31 respectively. Accordingly, the corresponding plots are shown in the figures as given below.

Table 28: Surface concentrations of Na and Hg and surface tension for liquid Na-Hg alloy at 673 K for different concentrations of sodium.

Concentration of Na (C_{Na})	Surface concentration of Na (C^S_{Na})	Surface concentration of Hg (C^S_{Hg})	Surface tension $\sigma(\mathrm{Nm}^{-1})$
0.1	0.376	0.624	0.377
0.2	0.669	0.331	0.334
0.3	0.832	0.169	0.294
0.4	0.913	0.087	0.259
0.5	0.954	0.046	0.232
0.6	0.975	0.025	0.211
0.7	0.986	0.014	0.195
0.8	0.993	0.007	0.184
0.9	0.997	0.003	0.175

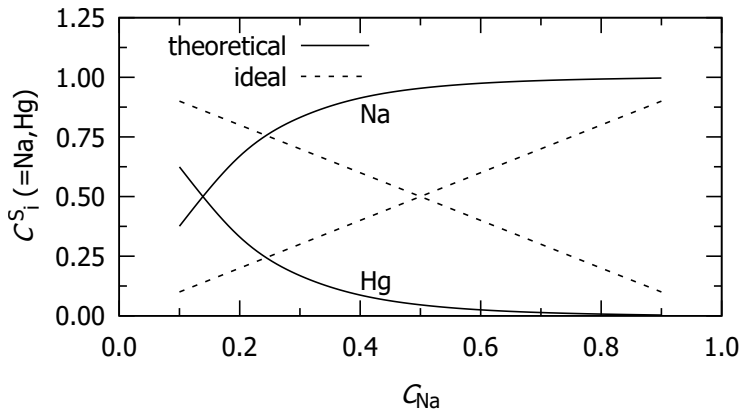

Figure 33: Surface segregation of Na and Hg versus concentration of Na For Na-Hg liquid alloy at 673 K.

Figure 33 is the plot of surface segregation (or concentration) of Na and Hg with respect to the bulk concentration of Na for Na-Hg liquid alloy at 673 K. The figure elucidates that the surface concentration of Hg is lower than the corresponding ideal value, that of Na is higher than the ideal value. The intersecting point of two curves at certain bulk concentration of Na indicates the equal amount of surface segregation of both the components. The figure also depicts that mostly the Hg atoms remain in the bulk of the liquid mixture and Na atoms segregate to the surface. Since the size of Na atom is more than Hg atom, the Na atom has more surface energy. This causes the Na atoms to remain on the surface. Similarly, as shown in Figure 34, the surface tension of the alloy decreases with increase in concentration of Na.

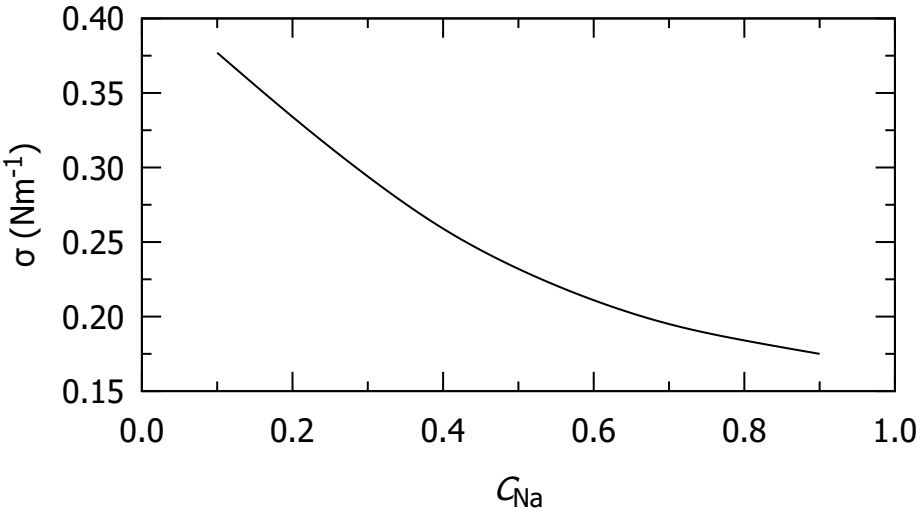

Figure 34: surface tension versus concentration of Na For Na-Hg liquid alloy at 673 K.

Table 29: Surface concentrations of Pb and Mg and surface tension for liquid Pb-Mg alloy at 973 K for different concentrations of lead.

Concentration of Pb (C_{Pb})	Surface concentration of Pb (C^S_{Pb})	Surface concentration of Mg (C^S_{Mg})	Surface tension $\sigma(\mathrm{Nm}^{-1})$
0.1	0.119	0.881	0.541
0.2	0.294	0.706	0.533
0.3	0.479	0.521	0.518
0.4	0.637	0.363	0.500
0.5	0.754	0.246	0.481
0.6	0.837	0.163	0.464
0.7	0.895	0.105	0.450
0.8	0.937	0.063	0.438
0.9	0.971	0.029	0.428

Figure 35 shows that above 0.3 bulk concentration of Pb, the surface concentration of Pb exceeds that of Mg. Accordingly the Mg atoms segregate on the surface of liquid

mixture below 0.3 bulk concentration of Pb at 973 K. Pb and Mg have higher and lower surface concentrations respectively than their corresponding ideal values. The surface tension of the Pb-Mg alloy gradually reduces with increase in the bulk concentration of Pb as shown in Figure 36.

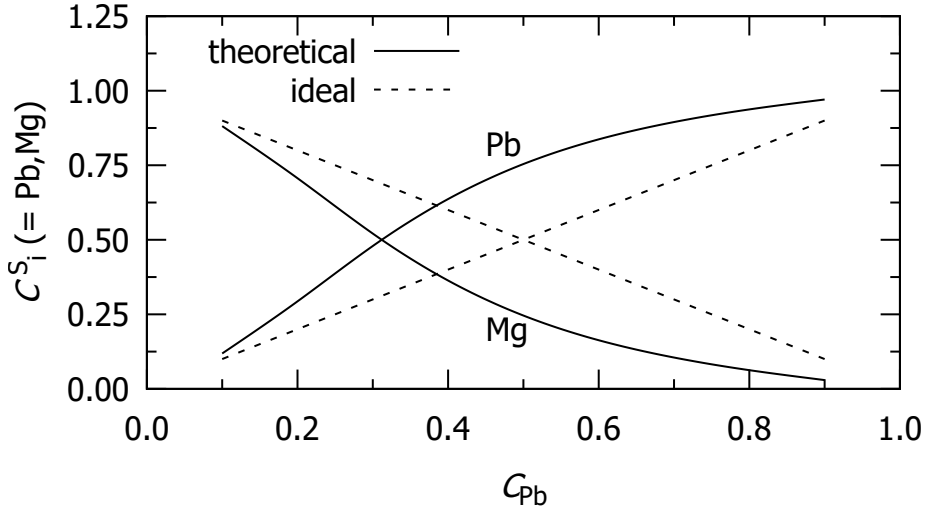

Figure 35: Surface segregation of Pb and Mg versus concentration of Pb For Pb-Mg liquid alloy at 973 K.

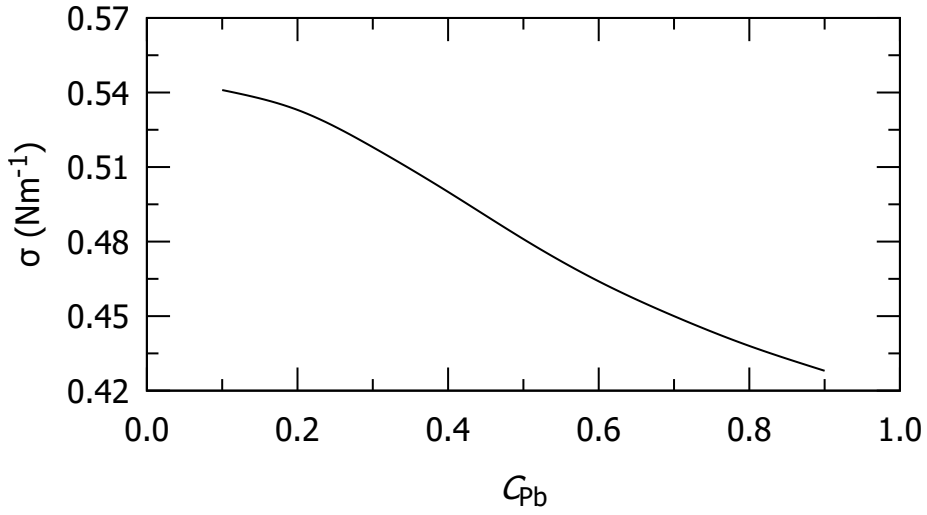

Figure 36: Surface tension versus concentration of Pb For Pb-Mg liquid alloy at 973 K.

Figure 37 shows that the surface segregation of Tl is less than ideal value but that of Bi is more than the ideal value within entire concentration of Tl. Thus, theoretically it is observed that the Bi atoms have tendency to remain on the surface of the alloy. Similarly, it is observed from the Figure 38 that the surface tension of the system increases with increase in the bulk concentration of Tl.

Table 30: Surface concentrations of Bi and Tl and surface tension for liquid Bi-Tl alloy at 750 K for different concentrations of thallium.

Concentration of Tl (C_{Tl})	Surface concentration of Tl (C^S_{Tl})	Surface concentration of Bi (C^S_{Bi})	Surface tension $\sigma(\mathrm{Nm}^{-1})$
0.1	0.032	0.968	0.370
0.2	0.071	0.929	0.378
0.3	0.119	0.881	0.386
0.4	0.181	0.819	0.395
0.5	0.264	0.736	0.406
0.6	0.377	0.623	0.417
0.7	0.522	0.478	0.429
0.8	0.690	0.310	0.439
0.9	0.856	0.144	0.446

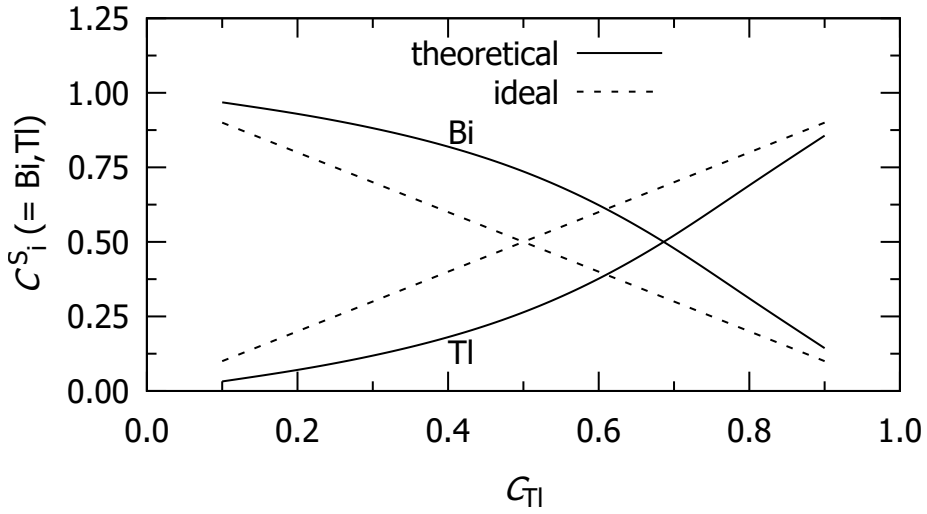

Figure 37: Surface segregation of Bi and Tl versus concentration of Bi For Bi-Tl liquid alloy at 750 K.

Figure 39 shows the variation of surface segregation of Cu and Al with respect to the bulk concentration of Cu for Cu-Al liquid alloy at 1373 K. It shows that the aluminum atoms have high tendency to remain on the surface where as copper atoms remain on the bulk at almost all concentration of Cu. Figure 40 is the plot of surface tension of Cu-Al against the concentration of Cu. It indicates that the surface tension of the alloy increases with increase in bulk concentration of Cu.

From all of the four alloys , it is observed that the components having lower surface tension segregate on the surface of their corresponding alloys.

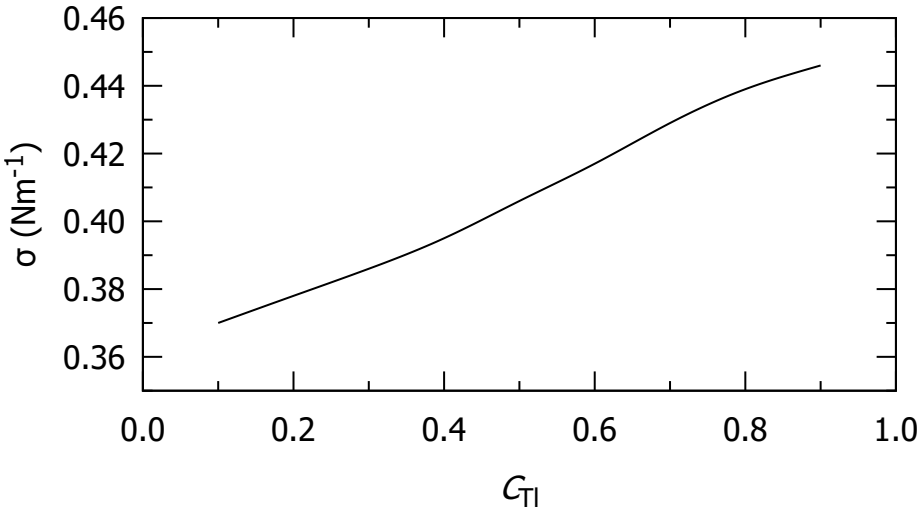

Figure 38: Surface tension versus concentration of Tl For Bi-Tl liquid alloy at 750 K.

Table 31: Surface concentrations of Cu and Al and surface tension for liquid Cu-Al alloy at 1373 K for different concentrations of copper.

Concentration of Cu (C_{Cu})	Surface concentration of Cu (C^S_{Cu})	Surface concentration of Al (C^S_{Al})	Surface tension $\sigma(\mathrm{Nm}^{-1})$
0.1	0.013	0.987	0.783
0.2	0.028	0.972	0.808
0.3	0.046	0.954	0.838
0.4	0.074	0.926	0.876
0.5	0.119	0.881	0.927
0.6	0.196	0.804	0.993
0.7	0.318	0.682	1.067
0.8	0.492	0.508	1.143
0.9	0.719	0.281	1.216

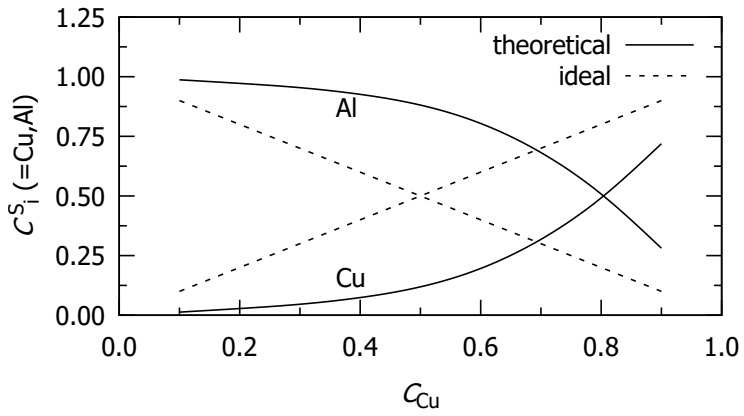

Figure 39: Surface segregation of Cu and al versus concentration of Cu For Cu-Al liquid alloy at 1373 K.

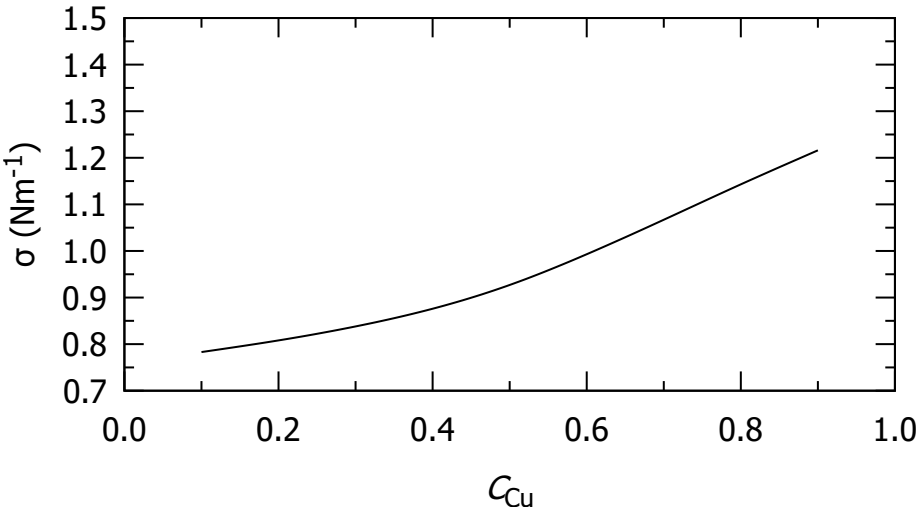

Figure 40: Surface tension versus concentration of Cu For Cu-Al liquid alloy at 1373 K.

4.9 Examination of Behavior of Binary Liquid Alloys at Various Temperatures

Understanding the nature of thermophysical functions above and below the melting point is crucial to comprehend the energetics of liquid alloys. The phase separation or complex formation of the alloy is particularly important when extrapolating thermodynamic data from one given region of temperature to another as these are important parameters for anomalies behavior. In many situations, it becomes challenging to make very accurate experimental observations over a broad temperature range. Therefore, conducting such research inside a theoretical framework is extremely interesting.

This section deals with the extension made in the Quasi-Chemical Approximation to predict the thermodynamic, structural, transport and surface properties of preferred binary liquid alloys at temperatures above their melting points. Such predictions have been made by developing theoretical modelling equation in the frame work of the Quasi-Chemical Approximation. We have also presented the findings and discussions related to the properties of liquid alloys at various temperatures.

4.9.1 Theoretical Modelling Equation

The main assumption for the theoretical modeling equation is that the mole fraction and the temperature derivative interaction energy parameters remain constant with change in temperature of the liquid alloys. The equation has been used to compute the interaction energy parameters of the alloys at various temperatures, which have then been used to compute various properties. The interaction energy parameters can be linked to the temperature derivative terms of the interaction energy parameters using the formula

below:

$$
\begin{aligned}
d[\omega_{ij}(T)] &= \frac{\partial \omega_{ij}(T)}{\partial T} dT, \qquad i \neq j \\
\omega_{ij}(T_K) &= \omega_{ij}(T_0) + \frac{\partial \omega_{ij}}{\partial T}(T_K - T_0)
\end{aligned}
\tag{4.2}
$$

Here, T_0 denotes the melting point of the concerned liquid alloy under and T_K denotes the temperature of interest for determining the various properties of the liquid alloy.

Thus, by using Equation (4.2), the interaction energy parameters of the alloys for different temperatures are determined but the temperature derivative terms of interaction energy parameters are kept constant.

4.9.2 Free Energy of Mixing at Different Temperatures

This section covers the study of composition dependent free energy of mixing of Pb-Mg, Bi-Tl and Cu-Al liquid alloys at different temperatures. In order to calculate and predict the free energy of mixing of the alloys under the Quasi-Chemical treatment at different temperatures, it is necessary to determine the interaction energy parameters and their temperature derivatives at the concerned temperatures of the alloys. For small change in temperature the temperature derivatives of interaction energy parameters are considered constant. The interaction parameters at high temperatures are obtained under the assumption that the parameters are linearly dependent on temperature and independent on the concentration of each component of the alloy with the help of Equation 4.2. The temperature of study for Pb-Mg liquid alloy are 973 K, 1073 K, 1173 K and 1273K, for Bi-Tl liquid alloys are 750 K, 850 K, 950 K, and 1050 K and for Cu-Al liquid alloy are 137 3K, 1573 K, 1773 K and 1973 K. The temperatures 973 K, 750 K and 1373 K are assumed as melting temperatures of the Pb-Mg, Bi-Tl and Cu-Al liquid alloys respectively.

The interaction energy parameters for different alloys at concerned temperatures thus found are shown respectively in the Tables 32, 33 and 34 for Pb-Mg, Bi-Tl and Cu-Al binary liquid alloys respectively.

Table 32: Interaction energy parameters for Pb-Mg liquid alloy at different temperatures.

Temperature (K)	$\omega/k_{\mathrm{B}}T$	$\Delta\omega_{AB}/k_{\mathrm{B}}T$	$\Delta\omega_{BB}/k_{\mathrm{B}}T$
973	-5.779	2.808	4.984
1073	-5.459	2.902	4.082
1173	-5.194	2.980	3.334
1273	-4.970	3.046	2.704

Using such parameters of different alloys at concerned temperatures in the Equation

Table 33: Interaction energy parameters for Bi-Tl liquid alloy at different temperatures.

Temperature (K)	$\omega/k_{\mathrm{B}}T$	$\Delta\omega_{AB}/k_{\mathrm{B}}T$	$\Delta\omega_{BB}/k_{\mathrm{B}}T$
750	-1.084	-3.660	1.493
850	-0.899	3.345	1.493
950	-0.753	-3.097	1.703
1050	-0.634	-2.896	1.777

Table 34: : Interaction energy parameters for Cu-Al liquid alloy at different temperatures.

Temperature(K)	$\omega/k_{\mathrm{B}}T$	$\Delta\omega_{AB}/k_{\mathrm{B}}T$	$\Delta\omega_{AA}/k_{\mathrm{B}}T$	$\Delta\omega_{AA}/k_{\mathrm{B}}T$
1373	-4.710	26.942	-61.061	-37.995
1573	-4.521	26.931	-60.095	-37.919
1773	-4.374	26.922	-59.347	-37.861
1973	-4.257	26.914	-58.751	-37.836

(3.54), the free energy of mixings (G_{M}/RT) of the liquid alloys are computed as shown in the Tables 35, 36 and 37. The plots of the free energy of mixing for the Pb-Mg, Bi-Tl and Cu-Al liquid alloys as a function of concentration at elevated temperatures are shown respectively in the Figures 41, 42 and 43.

Table 35: Free energy of mixing for liquid Pb-Mg alloy at different temperatures for different concentrations of lead.

Concentration of Pb	Free energy of Mixing(G_{M}/RT)			
C_{Pb}	973 K	1073 K	1173 K	1273 K
0.1	−0.875	−0.825	−0.785	−0.750
0.2	−1.406	−1.321	−1.252	−1.193
0.3	−1.706	−1.601	−1.513	−1.439
0.4	−1.819	−1.706	−1.612	−1.533
0.5	−1.777	−1.668	−1.578	−1.502
0.6	−1.609	−1.515	−1.436	−1.370
0.7	−1.339	−1.267	−1.206	−1.155
0.8	−0.987	−0.940	−0.901	−0.868
0.9	−0.560	−0.539	−0.522	−0.507

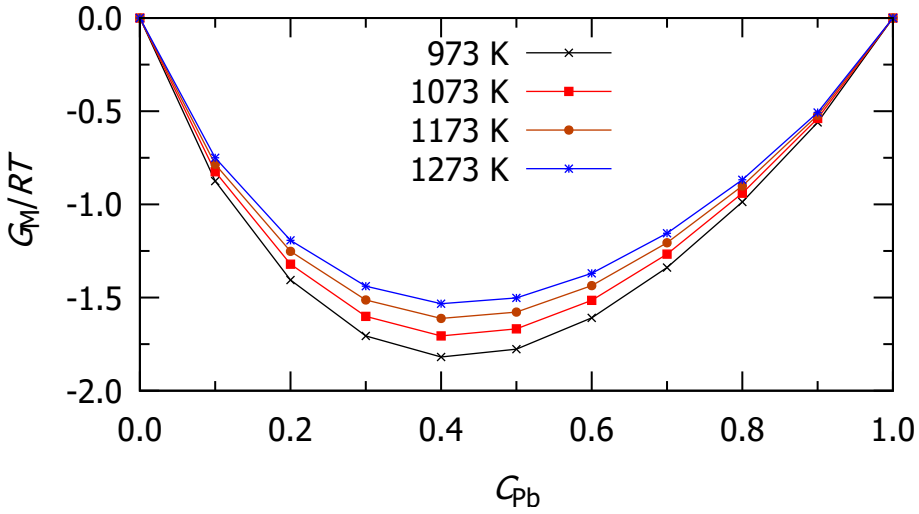

Figure 41: Free energy of mixing for Pb-Mg liquid alloy at different temperatures.

Table 36: Free energy of mixing for liquid Bi-Tl alloy at different temperatures for different concentrations of thallium.

Concentration of Tl	Free energy of mixing(G_M/RT)			
C_{Tl}	750 K	850 K	950 K	1050 K
0.1	−0.519	−0.498	−0.481	−0.467
0.2	−0.872	−0.832	−0.800	−0.774
0.3	−1.141	−1.084	−1.039	−1.003
0.4	−1.335	−1.264	−1.209	−1.163
0.5	−1.445	−1.365	−1.301	−1.250
0.6	−1.455	−1.370	−1.304	−1.250
0.7	−1.343	−1.263	−1.199	−1.148
0.8	−1.087	−1.022	−0.970	−0.928
0.9	−0.665	−0.626	−0.595	−0.570

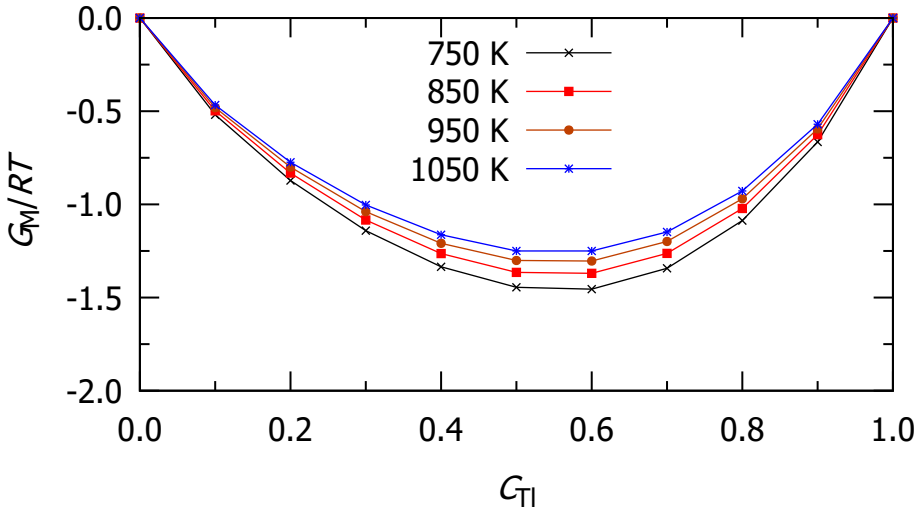

Figure 42: Free energy of mixing for Bi-Tl liquid alloy at different temperatures.

Table 37: Free energy of mixing for liquid Cu-Al alloy at different temperatures for different concentrations of copper.

Concentration of Cu	Free energy of mixing (G_M/RT)			
C_{Cu}	1373 K	1573 K	1773 K	1973 K
0.1	−0.610	−0.598	−0.589	−0.582
0.2	−1.054	−1.031	−1.014	−1.000
0.3	−1.430	−1.397	−1.371	−1.352
0.4	−1.729	−1.687	−1.655	−1.630
0.5	−1.915	−1.866	−1.829	−1.800
0.6	−1.943	−1.892	−1.852	−1.821
0.7	−1.781	−1.733	−1.695	−1.666
0.8	−1.418	−1.380	−1.350	−1.326
0.9	−0.855	−0.833	−0.816	−0.802

Theoretical research demonstrates that as temperature increases above the melting point of the liquid alloys, the values of free energy of mixing G_M/RT for the alloy become less negative. The rate of decrease in the free energy of mixing is small in Cu-Al alloy in comparison to other two liquid alloys. However the results of free energies of mixing of the alloys suggest that when temperatures rise, the bonding strength between the atoms of the alloy systems weakens. As a result, the alloys are less interacting and the tendencies towards the complex formation decrease.

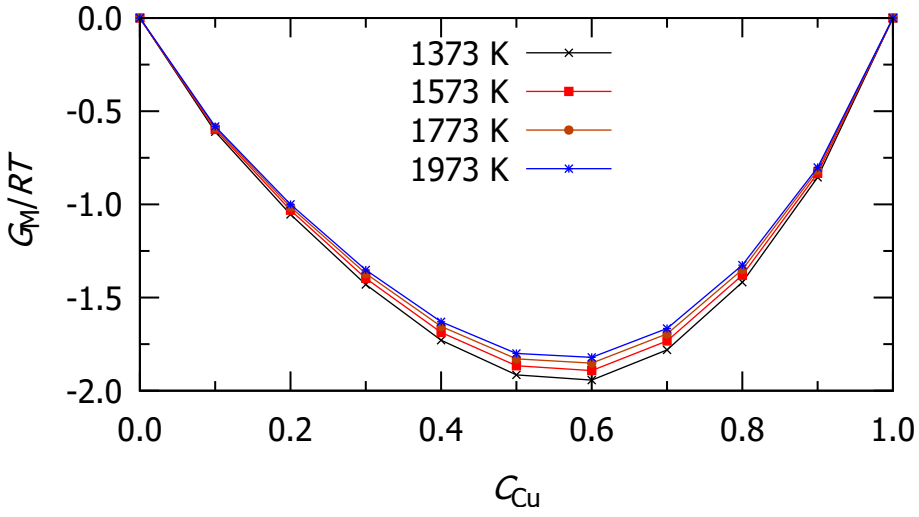

Figure 43: Free energy of mixing for Cu-Al liquid alloy at different temperatures.

4.9.3 Enthalpy of Mixing at Different Temperatures

In this section, we study and predict the enthalpy of mixing of liquid alloys of Pb-Mg, Bi-Tl, and Cu-Al at various temperatures. On the floor of present theoretical modelling, the values of the interaction energy parameters and their temperature derivatives are necessary for the study of the alloys at different temperatures. The interaction energy parameters are used as obtained in the Section 4.9.2. However, the temperature derivatives of such parameters are employed as determined at their melting temperatures because they are considered to be constant for small changes in temperature.

Now, the enthalpy of mixing (H_M/RT) of liquid alloys at various temperatures are determined using such parameters as illustrated in Tables 38, 39 and 40. Similarly, the plots of enthalpy of mixing for the Pb-Mg, Bi-Tl and Cu-Al liquid alloys as a function of concentration at elevated temperatures are shown respectively in the Figures 44, 45 and 46.

Table 38: Enthalpy of mixing for liquid Pb-Mg alloy at different temperatures for different concentrations of lead.

Concentration of Pb	Enthalpy of mixing(H_M/RT)			
C_{Pb}	973 K	1073 K	1173 K	1273 K
0.1	−0.528	−0.479	−0.438	−0.404
0.2	−0.905	−0.821	−0.751	−0.692
0.3	−1.131	−1.026	−0.938	−0.865
0.4	−1.214	−1.101	−1.007	−0.928
0.5	−1.168	−1.059	−0.969	−0.892
0.6	−1.014	−0.920	−0.841	−0.775
0.7	−0.781	−0.709	−0.648	−0.597
0.8	−0.505	−0.458	−0.419	−0.386
0.9	−0.228	−0.207	−0.189	−0.175

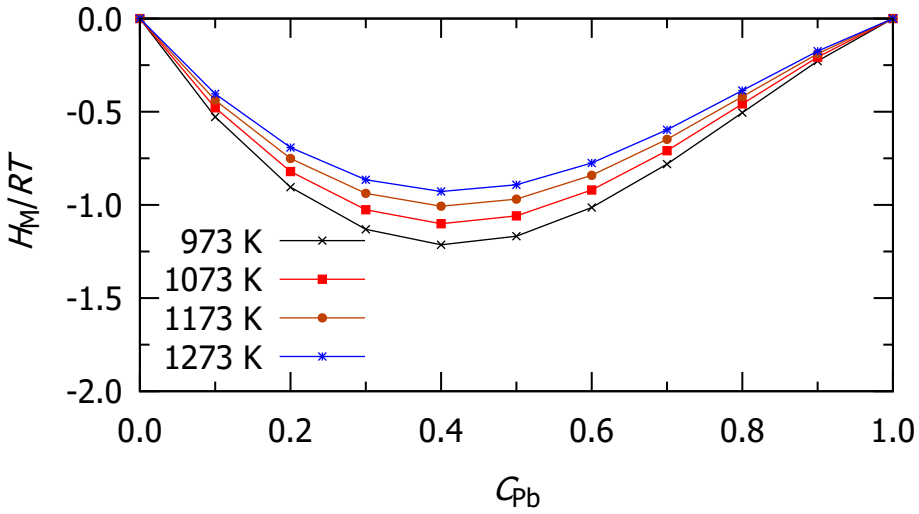

Figure 44: Enthalpy of mixing for Pb-Mg liquid alloy at different temperatures.

Table 39: Enthalpy of mixing for liquid Bi-Tl alloy at different temperatures for different concentrations of thallium.

Concentration of Tl	Enthalpy of mixing(H_M/RT)			
C_{Tl}	750 K	850 K	950 K	1050 K
0.1	−0.182	−0.161	−0.144	−0.130
0.2	−0.343	−0.303	−0.271	−0.245
0.3	−0.485	−0.428	−0.383	−0.346
0.4	−0.602	−0.531	−0.475	−0.430
0.5	−0.685	−0.604	−0.541	−0.489
0.6	−0.717	−0.633	−0.566	−0.512
0.7	−0.680	−0.600	−0.537	−0.486
0.8	−0.557	−0.491	−0.440	−0.398
0.9	−0.332	−0.293	−0.262	−0.237

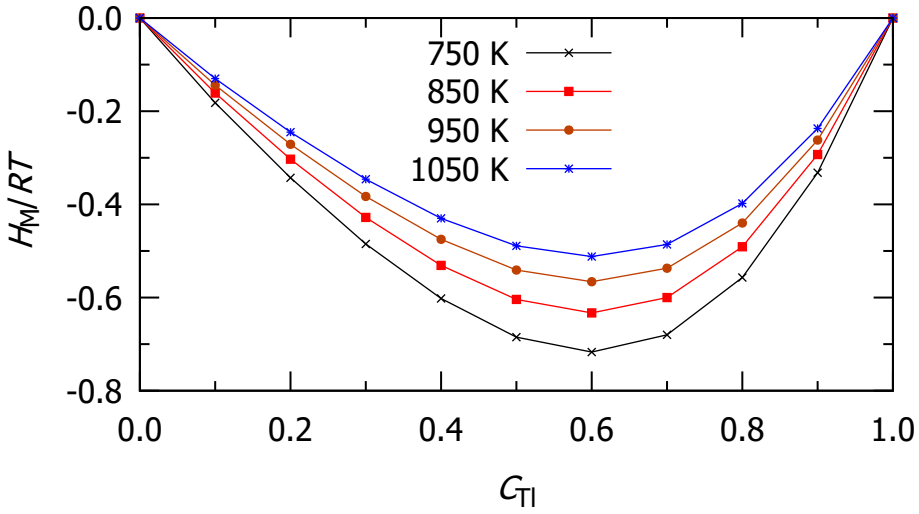

Figure 45: Enthalpy of mixing for Bi-Tl liquid alloy at different temperatures.

Table 40: Enthalpy of mixing for liquid Cu-Al alloy at different temperatures for different concentrations of copper.

Concentration of Cu	Enthalpy of mixing(H_M/RT)			
C_{Cu}	1373 K	1573 K	1773 K	1973 K
0.1	−0.095	−0.083	−0.073	−0.066
0.2	−0.179	−0.156	−0.138	−0.125
0.3	−0.257	−0.225	−0.199	−0.180
0.4	−0.328	−0.286	−0.254	−0.228
0.5	−0.379	−0.331	−0.294	−0.265
0.6	−0.401	−0.350	−0.310	−0.279
0.7	−0.379	−0.330	−0.293	−0.264
0.9	−0.175	−0.153	−0.136	−0.122

The study of enthalpy of mixing of the preferred alloys are negative at their elevated temperatures. This demonstrates that mixing of the alloys are exothermic. The values of enthalpy of mixing (H_M/RT) for all the alloys are found to decrease when temperature rises above the melting point of the liquid alloys. These findings imply that, as predicted by the results of free energy mixing, the bonding strength between the atoms of the complex atoms reduces with increase in temperature causing the declination of complex formation of the alloys.

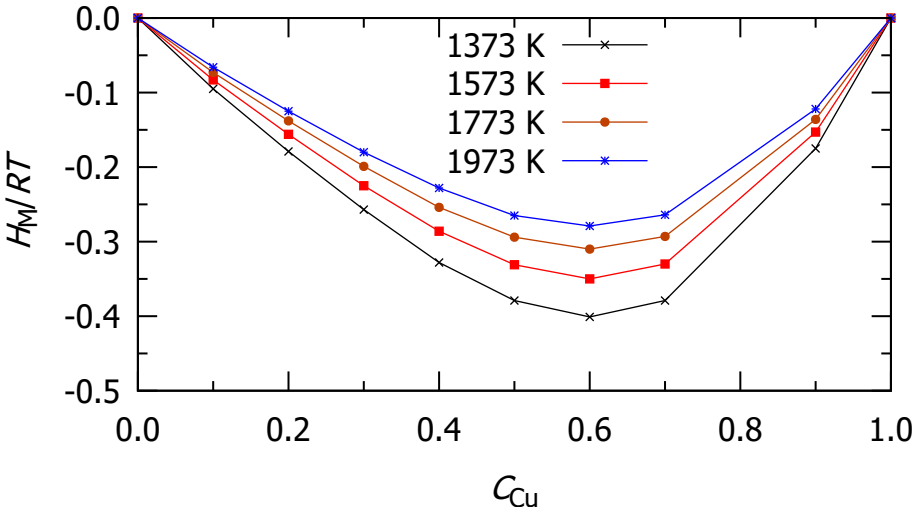

Figure 46: Enthalpy of mixing for Cu-Al liquid alloy at different temperatures.

4.9.4 Activities of the Components of the Alloys at Different Temperatures

This section deals with the theoretical study of composition dependent activities of the constituents of each Pb-Mg, Bi-Tl and Cu-Al liquid alloys at various temperatures. The basic inputs for theoretical calculation of activity of the component atoms of the alloys are interaction energy parameters. The values of such parameters required for the study at various temperatures on the ground of the current theoretical modeling are taken from Section 4.9.2 that were used for the computation of free energy of mixing. Using such parameters in the Equations (3.64) and (3.65), the activities of each components of the liquid alloys at different temperatures are computed as shown in the Tables 41, 42 and 43 and their plots at elevated temperatures are shown respectively in the Figures 47, 48 and 49.

Table 41: Activities of Pb (a_{Pb}) and Mg (a_{Mg}) for liquid Pb-Mg alloy at different temperatures for different concentrations of lead.

Con. of	Activity of Pb (a_{Pb})				Activity of Mg (a_{Mg})			
Pb(C_{Pb})	973 K	1073 K	1173 K	1273 K	973 K	1073 K	1173 K	1273 K
0.1	0.001	0.002	0.002	0.003	0.813	0.819	0.824	0.828
0.2	0.009	0.013	0.017	0.021	0.553	0.569	0.582	0.594
0.3	0.045	0.055	0.065	0.075	0.331	0.353	0.372	0.388
0.4	0.135	0.153	0.169	0.184	0.183	0.204	0.223	0.241
0.5	0.292	0.310	0.326	0.340	0.098	0.115	0.131	0.146
0.6	0.487	0.497	0.506	0.513	0.053	0.065	0.077	0.088
0.7	0.672	0.672	0.672	0.672	0.029	0.037	0.045	0.054
0.8	0.812	0.812	0.813	0.815	0.017	0.021	0.027	0.032
0.9	0.911	0.908	0.906	0.904	0.009	0.011	0.013	0.016

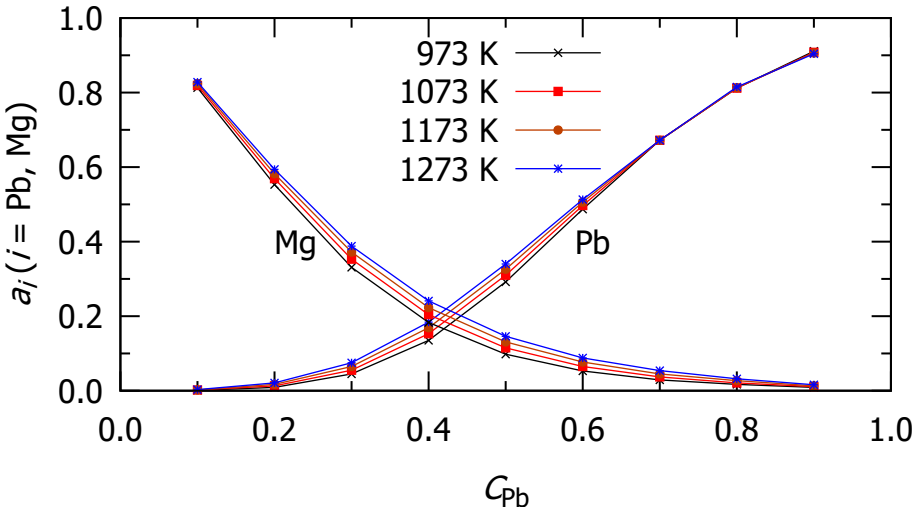

Figure 47: Activities of Pb (a_{Pb}) and Mg(a_{Mg}) for Pb-Mg liquid alloy at different temperatures.

Table 42: Activities of Bi (a_{Bi}) and Tl (a_{Tl}) for liquid Bi-Tl alloy at different temperatures for different concentrations of thallium.

Conc. of	Activity of Tl (a_{Tl})				Activity of Bi (a_{Bi})			
Tl(C_{Tl})	750 K	850 K	950 K	1053 K	750 K	850 K	950 K	1050 K
0.1	0.016	0.019	0.022	0.025	0.892	0.893	0.894	0.895
0.2	0.036	0.043	0.049	0.056	0.774	0.777	0.780	0.782
0.3	0.063	0.074	0.085	0.094	0.641	0.647	0.653	0.657
0.4	0.104	0.120	0.135	0.148	0.487	0.498	0.507	0.515
0.5	0.172	0.193	0.212	0.228	0.323	0.338	0.350	0.360
0.6	0.283	0.308	0.329	0.347	0.175	0.191	0.204	0.215
0.7	0.448	0.473	0.493	0.510	0.074	0.085	0.096	0.105
0.8	0.658	0.675	0.688	0.699	0.023	0.029	0.035	0.040
0.9	0.862	0.867	0.871	0.875	0.005	0.007	0.009	0.011

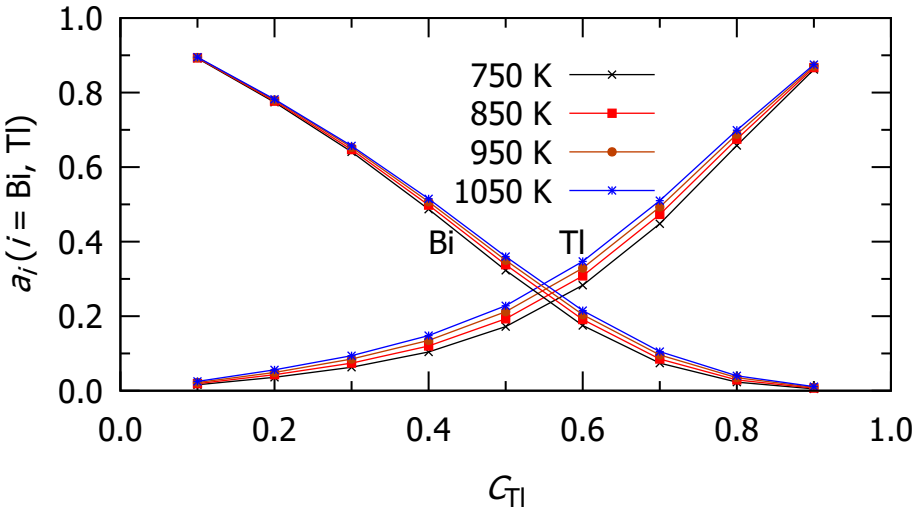

Figure 48: Activities of Bi(a_{Bi}) and Tl(a_{Tl}) for Bi-Tl liquid alloy at different temperatures.

From above theoretical study, we have observed that in the strongly interacting system, the absolute values of activities of the components remain small for considerable range of concentration and hence magnitude of activities in interacting systems are smaller than that in the less interacting systems. As the components of the alloys interact less with increasing temperature, the activities of components gradually rise for the alloy system. The rise in activities of Cu and Al seems to be very small than the activities of the components of other two liquid alloys. Thus from the point of view of activity, we can predict that the alloys are shifted from more interacting to less interacting with rise in their temperatures and the tendency of complex formation is maximum for all the alloys at their respective melting temperatures.

Table 43: Activities of Cu (a_{Cu}) and Al (a_{Al}) for liquid Cu-Al alloy at different temperatures for different concentrations of copper.

Conc.of	Activity of Cu (a_{Cu})				Activity of Al (a_{Al})			
Cu(C_{Cu})	1373 K	1573 K	1773 K	1973 K	1373 K	1573 K	1773 K	1973 K
0.1	0.007	0.007	0.008	0.009	0.886	0.887	0.888	0.888
0.2	0.013	0.015	0.016	0.017	0.787	0.788	0.790	0.791
0.3	0.022	0.024	0.026	0.028	0.669	0.671	0.673	0.675
0.4	0.040	0.043	0.046	0.049	0.482	0.487	0.491	0.493
0.5	0.083	0.090	0.095	0.099	0.260	0.267	0.271	0.275
0.6	0.185	0.194	0.202	0.209	0.098	0.103	0.107	0.110
0.7	0.370	0.382	0.391	0.398	0.027	0.029	0.032	0.033
0.8	0.610	0.618	0.624	0.629	0.006	0.007	0.008	0.008
0.9	0.832	0.835	0.836	0.838	0.001	0.001	0.001	0.002

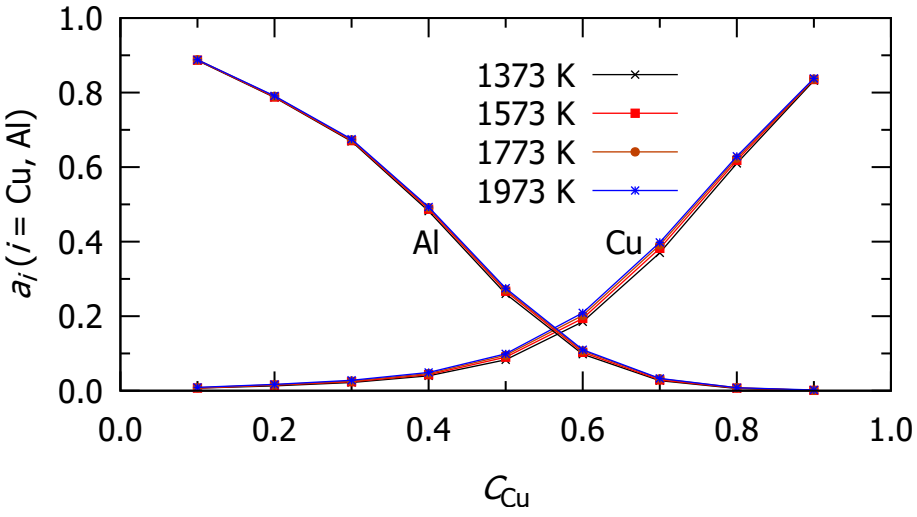

Figure 49: Activities of Cu (a_{Cu}) and Al (a_{Al}) for Cu-Al liquid alloy at different temperatures.

4.9.5 Structural Properties of the Alloys at Different Temperatures

The importance of microscopic functions, concentration fluctuation in the long wavelength limit $S_{CC}(0)$ and chemical short range order parameter (α_1) for the structural study of binary liquid alloys has already been discussed in previous chapters. This section focuses on the theoretical analysis and prediction of the structural properties $S_{CC}(0)$ and α_1 for Pb-Mg, Bi-Tl, and Cu–Al liquid alloys at various concerned temperatures. Interaction energy parameters are also the fundamental inputs for theoretical calculations of concentration fluctuation in the long wavelength limit and chemical short range order parameter of the alloys. The values of these parameters, which were used to calculate the free energy of mixing, were obtained from Section 4.9.2 in order to conduct the investigation at various temperatures. The concentration fluctuation in long wavelength limit at various temperatures thus determined using such parameters are illustrated in Tables 41, 42 and 43 for Pb-Mg, Bi-Tl and Cu-Al liquid alloys . Similarly, the computed values of chemical short range order parameter for these alloys are respectively given in tables 44, 45 and 46. The Figures 50, 51 and 52 illustrate the plots of concentration fluctuation in long wavelength limit for preferred alloys at different temperatures .

Table 44: Concentration fluctuation in long wavelength limit for liquid Pb-Mg alloy at different temperatures for different concentrations of lead.

Concentration of Pb C_{Pb}	Concentration fluctuation in long wavelength limit($S_{\mathrm{CC}}(0)$)			
	973 K	1073 K	1173 K	1273 K
0.1	0.032	0.034	0.036	0.037
0.2	0.043	0.047	0.049	0.052
0.3	0.053	0.058	0.062	0.065
0.4	0.065	0.070	0.076	0.081
0.5	0.079	0.086	0.093	0.100
0.6	0.099	0.106	0.114	0.121
0.7	0.124	0.128	0.134	0.140
0.8	0.142	0.143	0.144	0.145
0.9	0.106	0.100	0.097	0.094

Table 45: Concentration fluctuation in long wavelength limit for liquid Bi-Tl alloy at different temperatures for different concentrations of thallium.

Concentration of Tl C_{Tl}	Concentration fluctuation in long wavelength limit ($S_{\mathrm{CC}}(0)$)			
	750 K	850 K	950 K	1050 K
0.1	0.079	0.080	0.081	0.082
0.2	0.124	0.128	0.131	0.133
0.3	0.135	0.140	0.144	0.148
0.4	0.120	0.126	0.132	0.136
0.5	0.100	0.106	0.112	0.117
0.6	0.082	0.088	0.094	0.098
0.7	0.070	0.075	0.080	0.084
0.8	0.060	0.065	0.069	0.073
0.9	0.048	0.051	0.055	0.057

Table 46: Concentration fluctuation in long wavelength limit for liquid Cu-Al alloy at different temperatures for different concentrations of copper.

Concentration of Cu C_{Cu}	Concentration fluctuation in long wavelength limit ($S_{\mathrm{CC}}(0)$)			
	1373 K	1573 K	1773 K	1973 K
0.1	0.082	0.083	0.083	0.084
0.2	0.159	0.162	0.163	0.164
0.3	0.135	0.137	0.139	0.140
0.4	0.088	0.090	0.092	0.093
0.5	0.063	0.065	0.066	0.067
0.6	0.052	0.054	0.055	0.056
0.7	0.050	0.051	0.053	0.054
0.8	0.051	0.053	0.054	0.056
0.9	0.041	0.042	0.043	0.044

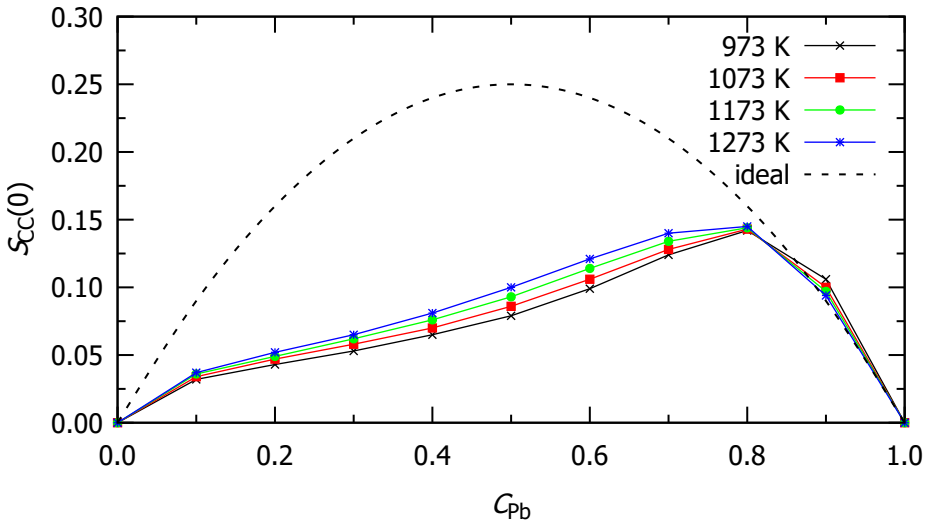

Figure 50: Concentration fluctuation in long wavelength limit for Pb-Mg liquid alloy at different temperatures.

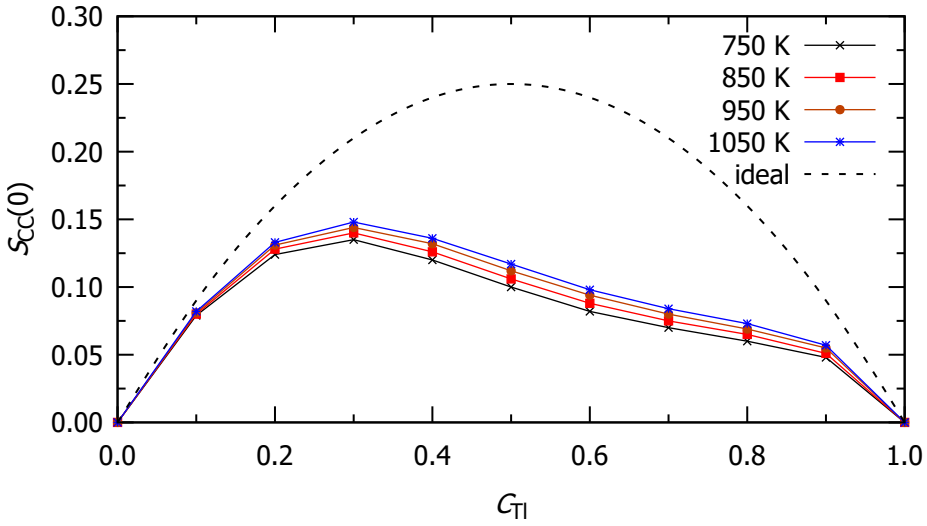

Figure 51: Concentration fluctuation in long wavelength limit for Bi-Tl liquid alloy at different temperatures.

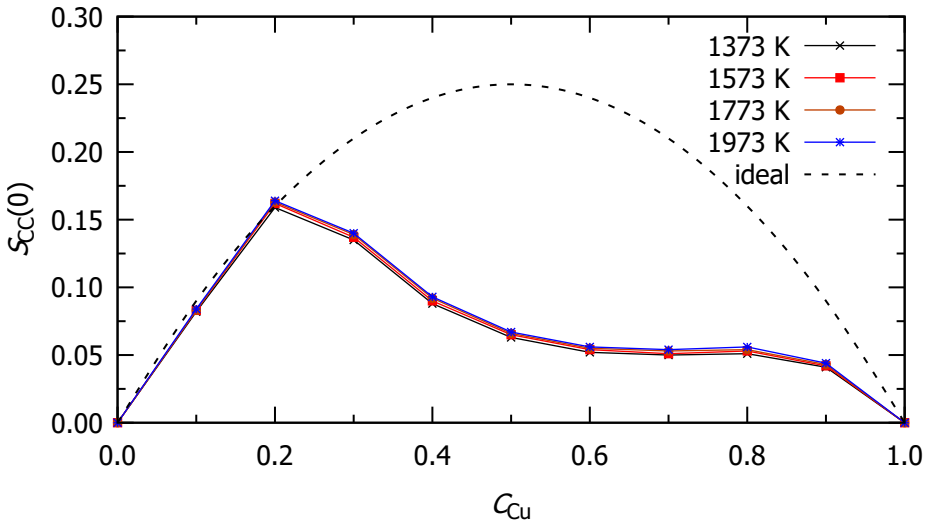

Figure 52: Concentration fluctuation in long wavelength limit for Cu-Al liquid alloy at different temperatures.

From the computed results, we have observed that $S_{CC}(0)$ mainly depends on the interaction energy parameter(ω). But as value of interaction energy parameters vary, the values of $S_{CC}(0)$ obviously vary. It is observed that as (ω) becomes less negative, the values of $S_{CC}(0)$ increase showing the decreasing tendency of ordering nature of the alloys. Thus all the preferred liquid alloys show the decreasing tendency of the ordering nature with increase in temperatures. However behind 0.8 concentration of Pb , the segregating tendency of the alloy of Pb-Mg has decreased with increase in temperatures.

The values of chemical short range order parameter for these alloys computed at concerned temperatures of the alloys are given in Tables 47, 48 and 49 and their respective plots are given in Figures 53, 54 and 55.

It is observed that the α_1 is sensitive to $S_{CC}(0)$ and coordination number (Z). The value of α_1 goes towards less negative with increase in temperature which is the indication of decreasing tendency of ordering nature of the alloys as predicted by $S_{CC}(0)$. But behind 0.8 concentration of lead for Pb-Mg liquid alloy,the value of α_1 goes towards less positive predicting the trend of segregating to ordering transformation.

Table 47: Chemical short range parameter for Pb-Mg liquid alloy at different temperatures for different concentrations of lead.

Concentration of Pb	Chemical short range order parameter(α_1)			
C_{Pb}	973 K	1073 K	1173 K	1273 K
0.1	−0.152	−0.139	−0.131	−0.124
0.2	−0.214	−0.196	−0.183	−0.173
0.3	−0.229	−0.209	−0.194	−0.181
0.4	−0.214	−0.194	−0.178	−0.164
0.5	−0.177	−0.159	−0.144	−0.131
0.6	−0.125	−0.112	−0.100	−0.090
0.7	−0.065	−0.060	−0.053	−0.048
0.8	−0.012	−0.014	−0.014	−0.014
0.9	0.016	0.010	0.007	0.004

Table 48: Chemical short range parameter for Bi-Tl liquid alloy at different temperatures for different concentrations of thallium.

Concentration of Tl	Chemical short range order parameter(α_1)			
C_{Tl}	750 K	850 K	950 K	1050 K
0.1	−0.014	−0.012	−0.011	−0.009
0.2	−0.028	−0.025	−0.022	−0.020
0.3	−0.053	−0.048	−0.044	−0.040
0.4	−0.091	−0.082	−0.076	−0.071
0.5	−0.131	−0.120	−0.110	−0.103
0.6	−0.161	−0.147	−0.135	−0.126
0.7	−0.167	−0.152	−0.140	−0.130
0.8	−0.142	−0.127	−0.116	−0.106
0.9	−0.079	−0.072	−0.061	−0.055

Table 49: Chemical short range parameter for Cu-Al liquid alloy at different temperatures for different concentrations of copper.

Concentration of Cu	Chemical short range order parameter(α_1)			
C_{Cu}	1373 K	1573 K	1773 K	1973 K
0.1	−0.010	−0.009	−0.008	−0.007
0.2	−0.001	0.001	0.002	0.002
0.3	−0.053	−0.051	−0.049	−0.048
0.4	−0.147	−0.143	−0.140	−0.137
0.5	−0.229	−0.223	−0.218	−0.215
0.6	−0.265	−0.258	−0.252	−0.248
0.7	−0.245	−0.237	−0.230	−0.225
0.8	−0.177	−0.169	−0.163	−0.158
0.9	−0.106	−0.102	−0.099	−0.096

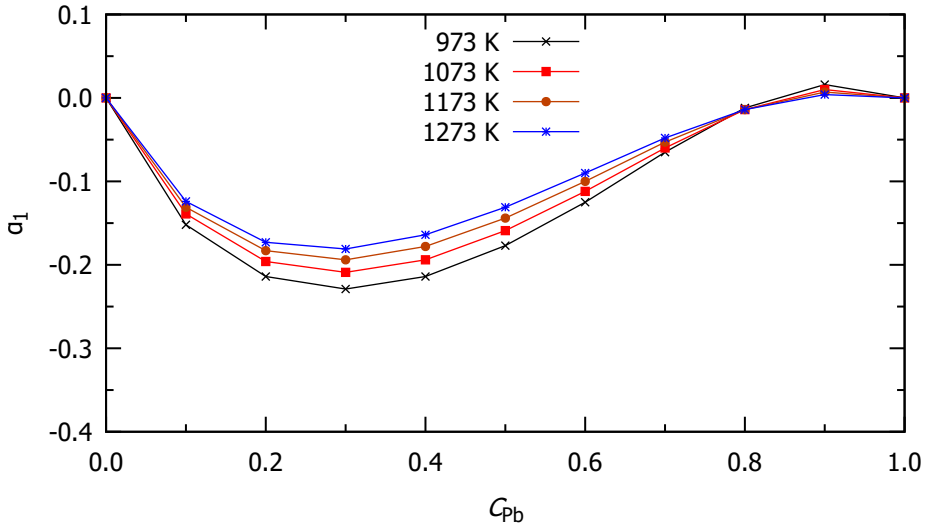

Figure 53: Chemical short range order parameter for Pb-Mg liquid alloy at different temperatures.

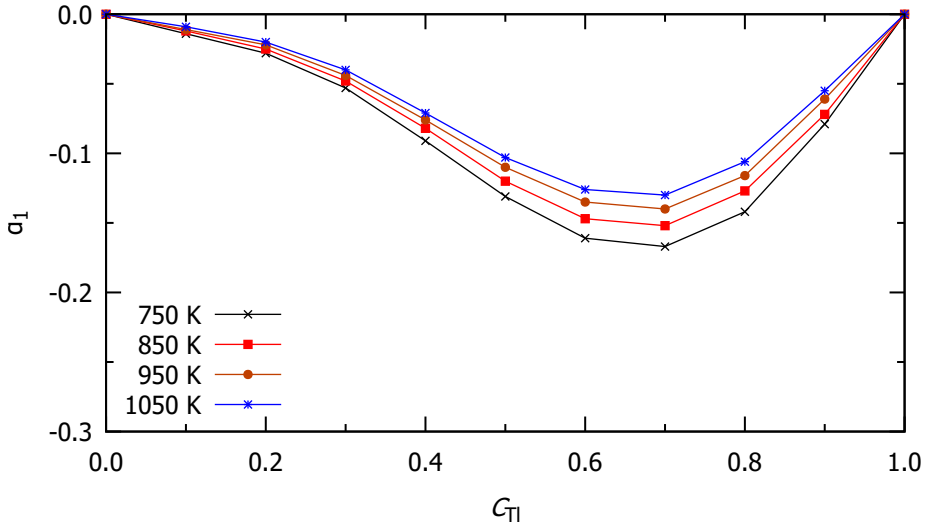

Figure 54: Chemical short range order parameter for Bi-Tl liquid alloy at different temperatures.

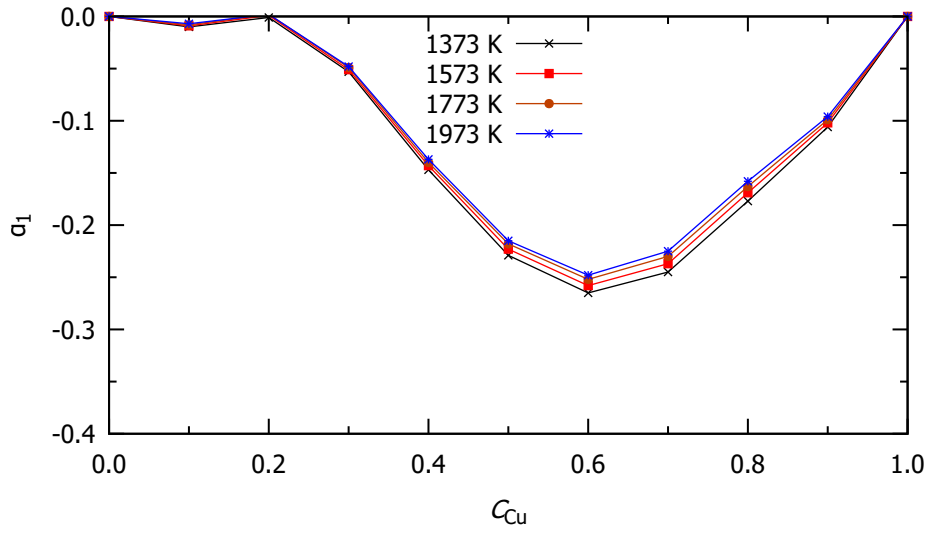

Figure 55: Chemical short range order parameter for Cu-Al liquid alloy at different temperatures.

4.9.6 Viscosity

It was already covered in Chapter 1 that measuring the thermophysical characteristics of metals and alloys is difficult, time-consuming and expensive. On the other hand, composition and temperature dependency of alloys are considerably important in the case of metallurgical science. Mixing the components by altering composition and temperature brings the variation in the properties, changing the interactions among the components. Therefore, the estimated values of various physical properties are often used during developing and solving metallurgical activities. These are obtained based on thermophysical properties of liquid alloys. One of such property is the viscosity of liquid alloys.

Table 50: Viscosity for Pb-Mg liquid alloy at different temperatures for different concentrations of lead.

Concentration of Pb	Viscosity(η) (mN s m^{-2})			
C_{Pb}	973 K	1073 K	1173 K	1273 K
0.1	1.248	0.900	0.685	0.548
0.2	1.319	0.983	0.768	0.630
0.3	1.365	1.052	0.845	0.711
0.4	1.386	1.106	0.916	0.790
0.5	1.385	1.148	0.980	0.866
0.6	1.369	1.178	1.039	0.941
0.7	1.344	1.202	1.095	1.017
0.8	1.321	1.228	1.156	1.100
0.9	1.309	1.264	1.228	1.198

In this section, we focus on the theoretical analysis and prediction of the viscosity for

Pb-Mg, Bi-Tl, and Cu –Al liquid alloys at various temperatures. The basic variable input parameters for calculating the viscosity of the alloys are Gibbs activation energy of viscous flow and enthalpy of mixing. The Gibbs activation energy of each component of the alloy at preferred temperatures can be obtained by taking molar volume and viscosity of each component using Equations (3.103) and (3.104) for respective temperatures. Similarly, the enthalpy of mixing as calculated in different temperatures in Section 4.9.3 are used for various alloys. The computed values of viscosities for these alloys are respectively given in Tables 50, 51 and 52. The variations of viscosities with temperatures of the are alloys shown in Figures 56, 57 and 58 respectively for Pb-Mg,Bi-Tl and Cu-Al liquid alloys.

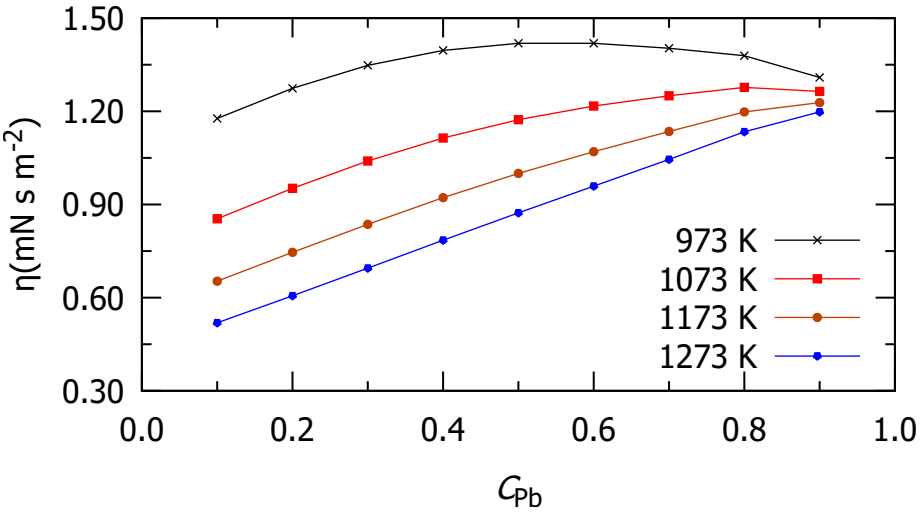

Figure 56: Viscosity for Pb-Mg liquid alloy at different temperatures.

Table 51: Viscosity for Bi-Tl liquid alloy at different temperatures for different concentrations of thallium.

Concentration of Tl	Viscosity(η) (mN s m^{-2})			
C_{Tl}	750 K	850 K	950 K	1050 K
0.1	1.319	1.155	1.040	0.956
0.2	1.386	1.201	1.072	0.979
0.3	1.452	1.245	1.103	1.000
0.4	1.515	1.287	1.131	1.019
0.5	1.573	1.324	1.156	1.035
0.6	1.621	1.353	1.173	1.045
0.7	1.653	1.370	1.182	1.048
0.8	1.664	1.372	1.178	1.041
0.9	1.649	1.354	1.160	1.023

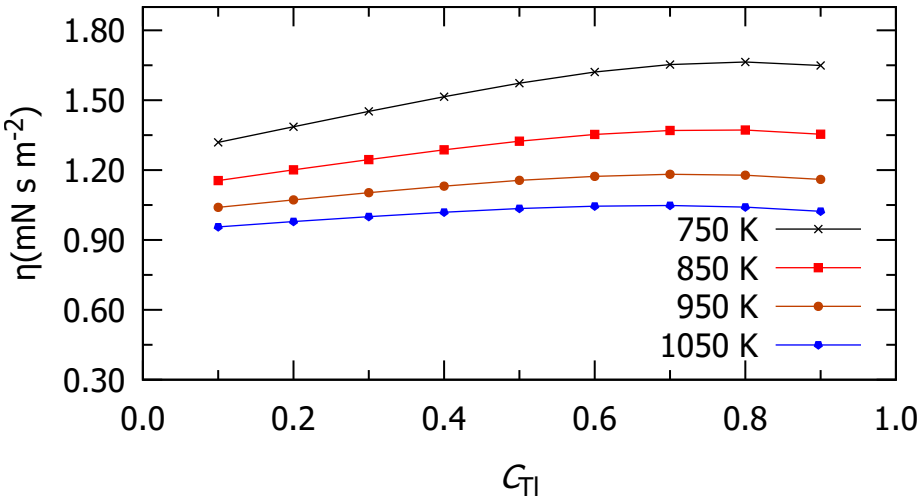

Figure 57: Viscosity for Bi-Tl liquid alloy at different temperatures.

The study shows that the viscosity of the preferred alloys decrease with increase in temperatures. This is due to the fact that the bonding strength between the atoms of the complex atoms reduces with increasing temperature causing the declination of complex formation of the alloys.

Equation (3.104) suggests that the variation on the viscosity is found to be more for the large value of activation energy (∋) for same temperature change. The value of ∋ of Pb is less than that of Mg (Brandes & Brook, 2013). Thus there is large gap among the viscosities towards Mg rich end than that of Pb rich end as shown in the Figure 56. The case is identical in the graphs shown in Figures 57 and 58.

Table 52: Viscosity for Cu-Al liquid alloy at different temperatures for different concentrations of copper

Concentration of Cu	Viscosity(η) (mN s m^{-2})			
C_{Cu}	1373 K	1573 K	1773 K	1973 K
0.1	0.775	0.633	0.541	0.478
0.2	0.947	0.760	0.641	0.560
0.3	1.156	0.913	0.760	0.657
0.4	1.410	1.097	0.902	0.771
0.5	1.724	1.317	1.069	0.905
0.6	2.099	1.578	1.264	1.060
0.7	2.542	1.882	1.491	1.238
0.8	3.059	2.233	1.750	1.440
0.9	3.658	2.636	2.045	1.670

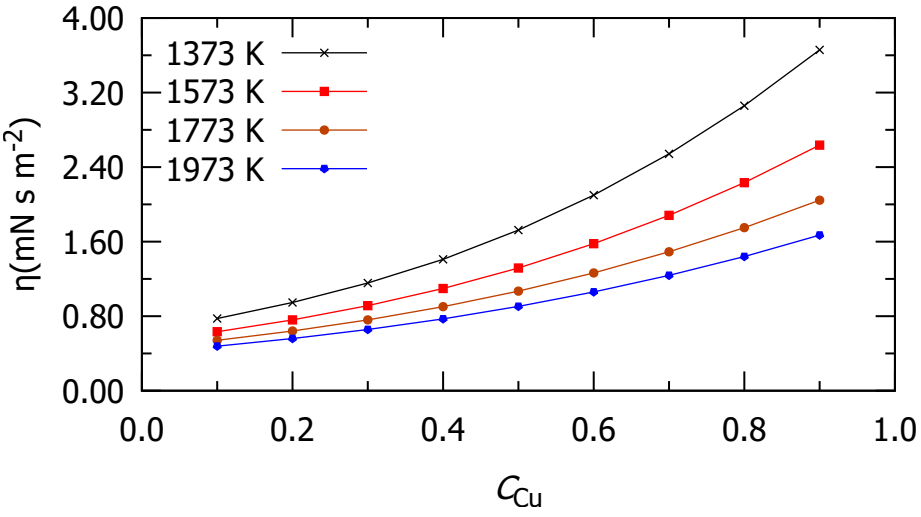

Figure 58: Viscosity for Cu-Al liquid alloy at different temperatures.

4.9.7 Surface Properties

Free surface and fluid phase produced at high temperatures are used in numerous metallurgical operations. On the other hand, clean conditions especially, the absence of foreign materials that could contaminate the surface or bulk of the sample is essential for the accurate measurement of thermophysical properties of metallic alloys in their liquid phase at high temperatures. In this regard the theoretical study of thermophysical properties of liquid alloy becomes significant for achieving the required data for metallurgical processes.

In the present section, we aim to study and predict the surface segregation and surface tension of three binary liquid alloys Pb-Mg, Bi-Tl and Cu-Al at high temperatures. For this purpose the values of bulk partial excess free energies of components at different temperatures are obtained from the Equation (3.121) as given in the Appendix. Similar to procedure as done in Section 4.8, the middle and right sides of Equation (3.120) are solved to obtain the surface concentration of the components of the alloys at working temperature for whole bulk concentration range. Using the findings of such surface concentrations as well as bulk concentrations of components of the alloys, the composition dependent surface tensions of the corresponding alloys at different temperatures are determined.

Theoretically calculated values of the composition dependent surface concentrations of components Pb and Mg for Pb-Mg liquid alloy at different temperatures are presented in Table 53 and plots of values calculated in this manner are displayed in Figure 59. The figure shows that as temperature rises above the melting temperature, the values of C^S_{Mg} gradually climb while those of C^S_{Pb} gradually fall with increase in temperatures of the alloy beyond its melting temperatures. These studies suggest that at higher temperatures,

Mg atoms fall from the bulk to the surface and Pb atoms move from the surface to the bulk.

Table 53: Surface concentration of Pb and Mg for liquid Pb-Mg alloy at different temperatures for different concentrations of lead.

Conc. of	Surface concentration of Pb(C^S_{Pb})				Surface concentration of Mg(C^S_{Mg})			
Pb(C_{Pb})	973 K	1073 K	1173 K	1273 K	973 K	1073 K	1173 K	1273 K
0.1	0.119	0.102	0.089	0.083	0.881	0.898	0.911	0.917
0.2	0.294	0.256	0.226	0.207	0.706	0.744	0.774	0.793
0.3	0.479	0.428	0.385	0.352	0.521	0.572	0.615	0.648
0.4	0.637	0.584	0.537	0.495	0.363	0.416	0.463	0.505
0.5	0.754	0.707	0.664	0.621	0.246	0.293	0.336	0.379
0.6	0.837	0.800	0.764	0.726	0.163	0.200	0.236	0.274
0.7	0.895	0.868	0.841	0.811	0.105	0.132	0.159	0.189
0.8	0.937	0.920	0.903	0.883	0.063	0.080	0.097	0.117
0.9	0.971	0.962	0.954	0.944	0.029	0.038	0.046	0.056

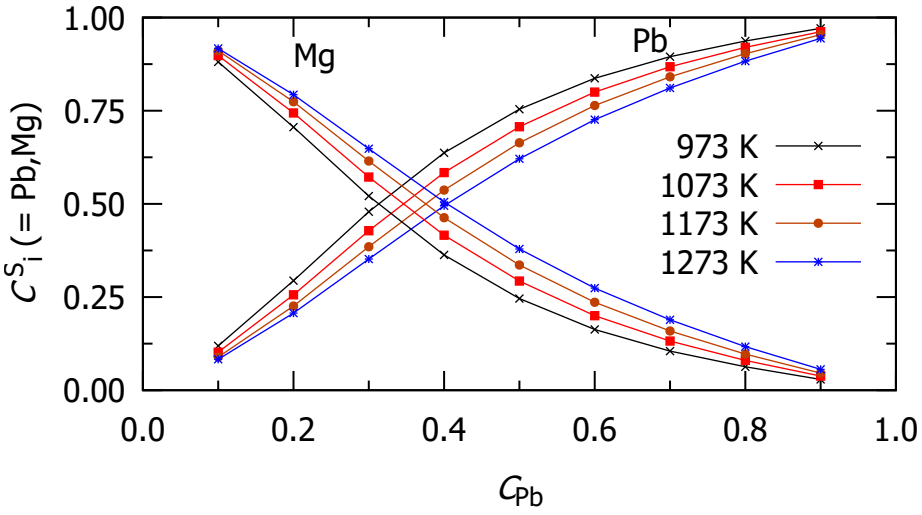

Figure 59: Surface concentrations of Pb and Mg for Pb-Mg liquid alloy at different temperatures.

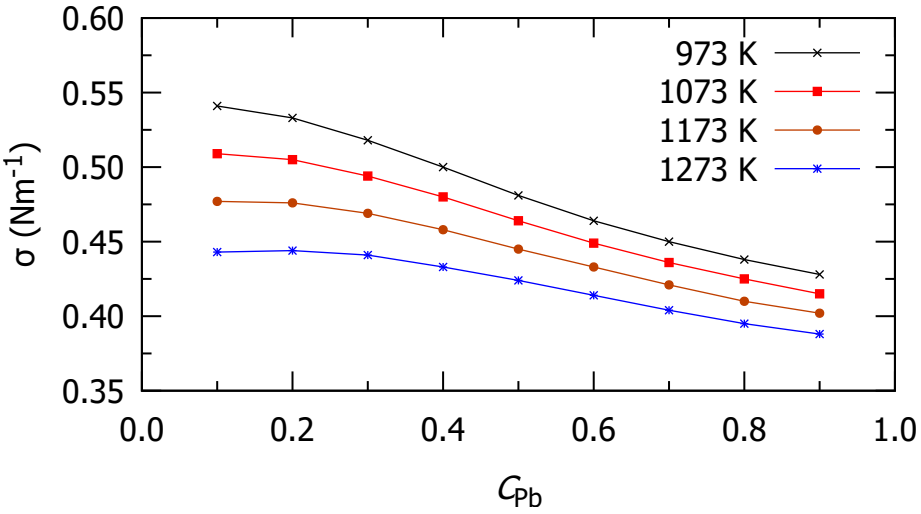

Figure 60: Surface tension for Pb-Mg liquid alloy at different temperatures.

The calculated values of surface tensions of Pb-Mg liquid alloy at preferred temperatures are given in the Table 54 and the plots of values so computed are given in Figure 60. It depicts that the surface tension of the alloy falls as temperature rises. According to earlier predictions from thermodynamic and structural properties, one of the prime reasons of this behavior may be loss of cohesive force of the constituents of the alloy at higher temperatures.

Table 54: Surface tension for liquid Pb-Mg alloy at different temperatures for different concentrations of lead.

Conc. of	Surface Tension(σ) (N m^{-1})			
Pb (C_{Pb})	973 K	1073 K	1173 K	1273 K
0.1	0.541	0.509	0.477	0.443
0.2	0.533	0.505	0.476	0.444
0.3	0.518	0.494	0.469	0.441
0.4	0.500	0.480	0.458	0.433
0.5	0.481	0.464	0.445	0.424
0.6	0.464	0.449	0.433	0.414
0.7	0.450	0.436	0.421	0.404
0.8	0.438	0.425	0.410	0.395
0.9	0.428	0.415	0.402	0.388

At the Mg-rich end, the surface tension of magnesium has a greater impact and it decreases at a faster rate with rising temperatures than does the surface tension of lead. (Brandes & Brook, 2013). Thus there is large variation on surface tensions towards right end of the Figure 60 with increase in temperatures.

Table 55: Surface concentration of Tl and Bi for liquid Bi-Tl alloy at different temperatures for different concentrations of thallium.

Conc. of	Surface concentration of Tl (C^S_{Tl})				Surface concentration of Bi (C^S_{Bi})			
Tl(C_{Tl})	750 K	850 K	950 K	1050 K	750 K	850 K	950 K	1050 K
0.1	0.032	0.037	0.041	0.045	0.968	0.963	0.959	0.955
0.2	0.071	0.080	0.089	0.096	0.929	0.920	0.911	0.904
0.3	0.119	0.134	0.146	0.157	0.881	0.866	0.854	0.843
0.4	0.181	0.201	0.218	0.232	0.819	0.799	0.782	0.768
0.5	0.264	0.289	0.309	0.325	0.736	0.711	0.691	0.675
0.6	0.377	0.403	0.424	0.441	0.623	0.597	0.576	0.559
0.7	0.522	0.546	0.564	0.579	0.478	0.454	0.436	0.421
0.8	0.690	0.706	0.718	0.728	0.310	0.294	0.282	0.272
0.9	0.856	0.863	0.868	0.872	0.144	0.137	0.132	0.128

Similarly, computed values of C^S_{Bi} and C^S_{Tl} for Bi-Tl liquid alloy and C^S_{Bi} and C^S_{Tl} for Cu-Al liquid alloys at concerned temperatures are presented in Tables 55 and 57 and their corresponding plots are shown in Figures 61 and 63.

Table 56: Surface tension for liquid Bi-Tl alloy at different temperatures for different concentrations of thallium.

Conc. of	Surface Tension(σ) (Nm^{-1})			
Tl(C_{Tl})	750 K	850 K	950 K	1050 K
0.1	0.370	0.364	0.357	0.350
0.2	0.378	0.372	0.365	0.358
0.3	0.386	0.380	0.374	0.367
0.4	0.395	0.389	0.383	0.377
0.5	0.406	0.400	0.394	0.387
0.6	0.417	0.411	0.405	0.398
0.7	0.429	0.422	0.415	0.408
0.8	0.439	0.432	0.424	0.416
0.9	0.446	0.438	0.430	0.422

Figure 61, when examined, shows that the surface concentration of Tl steadily rises whereas the surface concentration of Bi gradually falls as temperature rises. Likewise examining Figure 63 reveals that as temperature increases, the surface concentration of Cu steadily increases whereas the surface concentration of Al gradually decreases.

The computed surface tensions of the Bi-Tl and Cu-Al liquid alloys are displayed in Tables 56 and 58, respectively, along with the related graphs in Figures 62 and 64. Due to the loss of cohesive force of the constituents of the alloy at higher temperatures, as mentioned for the Pb-Mg liquid alloy, the surface tensions of both liquid alloys fall as temperature rises.

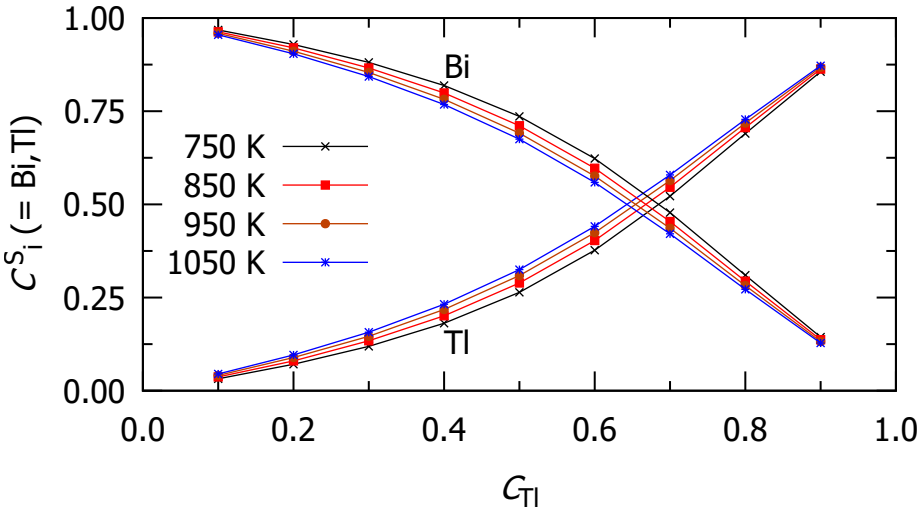

Figure 61: Surface concentrations of Bi and Tl for Bi-Tl liquid alloy at different temperatures.

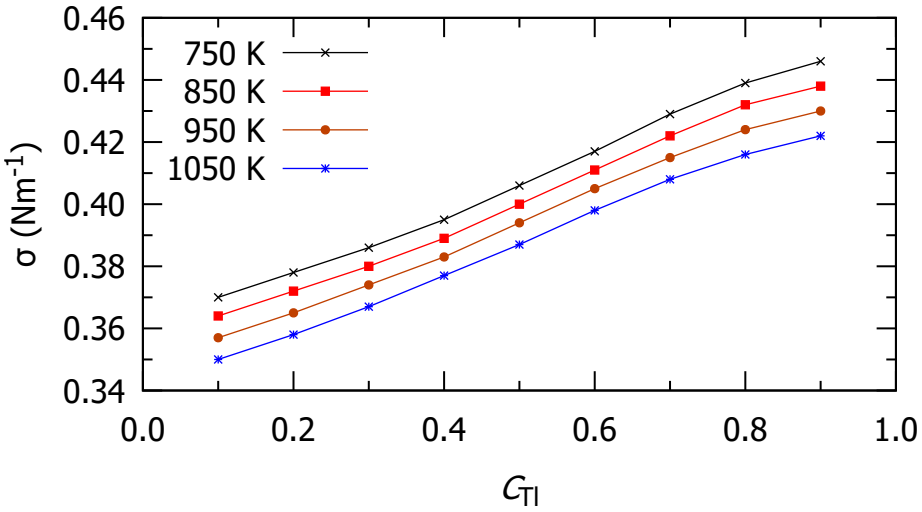

Figure 62: Surface tension for Bi-Tl liquid alloy at different temperatures.

Table 57: Surface concentration for liquid Cu-Al alloy at different temperatures for different concentrations of copper.

Conc. of	Surface concentration of Cu(C^S_{Cu})				Surface concentration of Al(C^S_{Al})			
Cu(C_{Cu})	1373 K	1573 K	1773 K	1973 K	1373 K	1573 K	1773 K	1973 K
0.1	0.013	0.014	0.015	0.016	0.987	0.986	0.985	0.984
0.2	0.028	0.030	0.032	0.034	0.972	0.970	0.968	0.966
0.3	0.046	0.050	0.053	0.055	0.954	0.950	0.947	0.945
0.4	0.074	0.079	0.084	0.087	0.926	0.921	0.916	0.913
0.5	0.119	0.127	0.133	0.138	0.881	0.873	0.867	0.862
0.6	0.196	0.207	0.215	0.221	0.804	0.793	0.785	0.779
0.7	0.318	0.331	0.341	0.348	0.682	0.669	0.659	0.652
0.8	0.492	0.504	0.514	0.519	0.508	0.496	0.486	0.481
0.9	0.719	0.728	0.733	0.736	0.281	0.272	0.267	0.264

Table 58: Surface tension for liquid Cu-Al alloy at different temperatures for different concentrations of copper.

Conc. of	Surface Tension(σ) (Nm^{-1})			
Cu(C_{Cu})	1373 K	1573 K	1773 K	1973 K
0.1	0.783	0.699	0.618	0.561
0.2	0.808	0.727	0.648	0.594
0.3	0.838	0.760	0.684	0.632
0.4	0.876	0.804	0.734	0.685
0.5	0.927	0.864	0.801	0.750
0.6	0.993	0.939	0.886	0.840
0.7	1.067	1.023	0.978	0.932
0.8	1.143	1.106	1.068	1.030
0.9	1.216	1.185	1.153	1.122

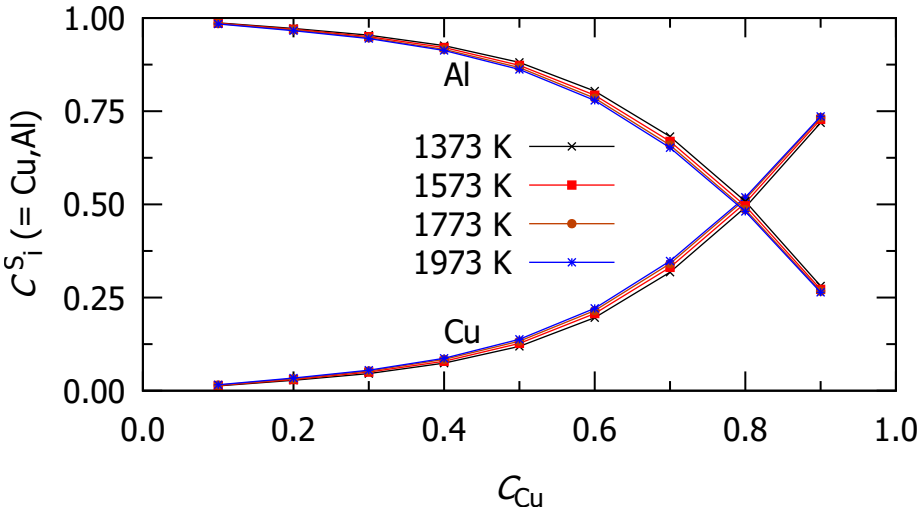

Figure 63: Surface concentrations of Cu and Al for Cu-Al liquid alloy at different temperatures.

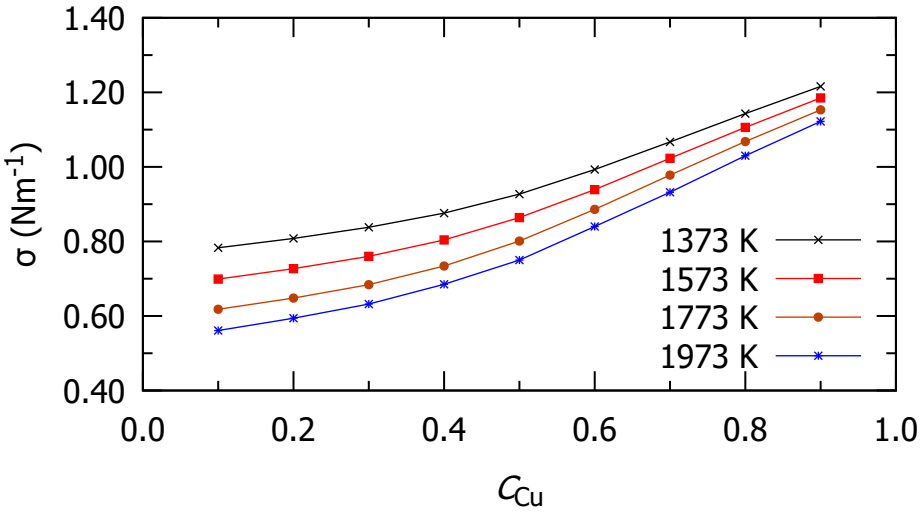

Figure 64: Surface tension for Cu-Al liquid alloy at different temperatures.

CHAPTER 5

5. CONCLUSION AND RECOMMENDATIONS

5.1 Conclusion

The mixing properties of binary alloys show anomalous behaviour as a function of concentration. The formation of such alloy is analyzed from the observed thermodynamic characteristics that deviates from the ideal mixing. Such characteristic behaviours are the reflection of interaction of the energetic and structural readjustment of atoms of the constituent elements. The empirical rules like electronegativity difference, ionic character, electron per atom ratio, size mismatch etc. can be used to study mixing behaviour of alloys. However, the mixing nature of segregating or ordering alloy systems and their corresponding phenomena like phase separation or compound formation are not properly described by such rules. (T. G. Iida, 1993; Novakovic et al., 2005).

The anomalies or asymmetric phenomena is due to the presence of strong interactions between the dissimilar constituent atoms of the liquid mixtures resulting the intermetallic compounds at one or more stoichiometric composition (Bhatia & Hargrove, 1974; Sommer, 1990; Prasad & Singh, 1990) . It is also termed as the existence of chemical short range order (Wilson, 1965). The departure of thermodynamic and microscopic functions of compound forming alloys from regular solution is caused by the existence of this chemical short range order. Similarly, there is no easy way to discern the arrangement of constituent atoms and hence the identification of neighboring pairs is complicated. Based on these facts, a large number of statistical approaches (Jordan, 1970; Bhatia et al., 1973; Bhatia & Singh, 1982, 1984) have been developed to explain the energetic of different liquid alloys.

The study of binary liquid alloys of type $A_\mu B_\nu$ by Quasi-Chemical Approximation has been the main emphasis of the research effort described in this thesis. Here, μ and ν are two small integers whose values are derived from knowledge of the phase diagram of the particular alloy in the solid state and depend on the stoichiometric composition at which the majority of intermetallic compounds are formed. For the study, we have selected four different types of alloys Na-Hg, Pb-Mg, Bi-Tl and Cu-Al. The analytical expressions for thermodynamic functions such as free energy of mixing, enthalpy of mixing, activity, entropy of mixing and structural functions such as concentration fluctuation in long wavelength limit and chemical short range order parameter have been obtained using the grand partition function. These functions help to understand the concentration

dependent properties in terms of interaction energy parameters. The relationship between microscopic and bulk characteristics has been established using the structural properties. For the validity of the preferred model, the computed thermodynamic and structural results are compared with the experimental values. The Kaptay's equation is employed to determine and study the viscosity of the liquid alloys. Similarly Kaptay's modified form of Butler equation has been used to compute and evaluate surface properties such as surface tension and surface segregation of preferred liquid alloys.

The present research work is also an attempt to extend the model equations of Quasi-Chemical Approximation, Kaptay equation and improved Butler equation to predict and explain the thermodynamic, transport and surface properties of Pb-Mg, Bi-Tl and Cu-Al liquid alloys at different temperatures. The Na-Hg alloy is not explored in this attempt since the Hg component evaporates at temperatures higher than that stated for the liquid alloy.

The liquid alloys selected for the study show asymmetry in the thermodynamic and structural properties. These alloys are widely used in modern technological advancements (details of applications are mentioned in chapter 1). Eventually, metallurgical processing, characterisation, and design all have a basic interest in the investigation and explanation of the anomalies in the mixing characteristics of these alloys. The prediction of the thermodynamic, structural and transport characteristics for the relevant systems will serve as a database in the absence of experimental data because the experimental methods are tedious and challenging to use at various higher temperatures. Similarly, during the assessment of surface tension of liquid alloys, oxide contamination of metallic surfaces, the strong reactivity of metallic melts at high temperature and high sensitivity of surface tension to impurities increase the risk of inaccuracy. Impurities having lower surface tension than that of the components of the alloys segregate at the surface and significantly diminish the surface tension of the system (Egry et al., 2010). In this spotlight, identifying the surface properties of binary systems and subsequently predicting these properties based on modeling equations at higher temperatures would unquestionably provide the groundwork for the study of surface science.

For the study of alloys by the preferred model, it is key task to determine interaction energy parameters. Such interaction energy parameters have been determined for all of the chosen binary liquid alloys by successive approximation method using a Quasi-Chemical Approximation and experimental data. The model makes the assumption that the interaction energy parameters depend on temperature. The temperature derivative interaction parameters have been obtained from the modelling equation by using observed enthalpy of mixing for the concerned liquid alloys. But for higher temperatures, it is assumed that the concentrations or mole fractions of complexes and the temperature derivative interaction energy parameters are independent on temperature. The values of

the interaction energy parameters are estimated for each of the aforementioned systems at higher temperatures using the modeling equations by extending the Quasi-Chemical Approximation under specific limited conditions.

We investigated several properties using interaction energy parameters and found many interesting features pertaining to the thermodynamic, structural, transport and surface properties of the alloys considered for the investigation of type $A_\mu B_\nu$. Following is a summary of some of the key findings from the research done for this thesis:

5.1.1 Gibbs Free Energy of Mixing

1. The theoretical values of Gibbs free energy of mixing are in agreement with their corresponding experimental values for all the liquid alloys at their respective melting temperatures. The asymmetric nature of free energy of mixing of compound forming alloys are well explained by preferred statistical model.
2. The position of maximum asymmetry appears directly linked to the nature of chemical complexes i.e. the values of μ and ν. The minimum values of the free energy of mixing have been found to occur at or close to compound forming concentration($C_C = \mu/(\mu + \nu)$).
3. The Gibbs free energy of mixing of all preferred liquid alloys becomes less negative with rise in temperature indicating that the alloy systems are less interactive at higher temperatures.
4. The interaction tendencies of the liquid alloys at their respective melting temperatures can be ordered as Na-Hg, Cu-Al, Pb-Mg, and Bi-Tl on the ground of the comparative analysis of the free energy of mixing.

5.1.2 Enthalpy of Mixing

1. The computed values of enthalpy of mixing are in reasonable agreement with their corresponding experimental values for all the liquid alloys at their respective melting temperatures.
2. The negative values of enthalpy of mixing of preferred alloy systems indicate that the mixing is exothermic.
3. For all preferred liquid alloys, the enthalpy of mixing becomes less negative as temperature rises indicating that the alloy systems interact less at higher temperatures.

5.1.3 Activity

1. The same interaction energy parameters that were utilized to estimate the free energy of mixing were also employed to compute the activity of the selected liquid alloys.
2. The computed values of activity for the liquid alloys under examination are composition-dependent and they agree well with the corresponding experimental values at their respective melting temperatures.
3. The computed values of activities increase with increase in temperature of the components of the alloys revealing less compound forming nature of the alloys.

5.1.4 Entropy of Mixing

1. To maintain consistency, we have used the same interaction energy parameters that have been used for the analysis of aforementioned thermodynamic properties to compute the entropy of mixing of the liquid alloys.
2. The computed as well as the experimental values of entropy of mixing as a function of concentration are in well agreement for the alloys at their respective melting temperatures.

5.1.5 Structural Properties

1. To understand the microscopic structure of the alloys, we have studied the concentration fluctuation in long wavelength limit and chemical short range order parameter. For this, the same interaction energy parameters that were used to compute aforementioned thermodynamic properties have been used.
2. The computed values of concentration fluctuation in long wavelength limit is found to be smaller than ideal concentration fluctuation in long wavelength limit except slight discrepancy in Pb-Mg liquid alloy at higher concentration of Pb. The chemical short range order parameter is negative for all the concerned alloy systems except behind 0.8 concentration of Pb in Pb-Mg liquid alloy . This reveals that the systems are mainly ordering in nature at their respective melting temperatures and the maximum deviation of Scc(0) from ideal values has occurred at the vicinity of compound forming concentration for all of the alloys.
3. The calculated values of Scc(0) gradually increase as the temperatures increase above the melting points of respective alloys. As a result, it can be predicted that the systems interact most when they are melting, and that propensity reduces as the temperature rises. These predictions are further quantified by the values of chemical short range order parameter.

5.1.6 Transport Properties

1. The transport properties (viscosity) of alloys have been studied using Kaptay's model (Kaptay, 2003) and theoretically computed enthalpy of mixing of the preferred alloys at different temperatures have been used to explain their transport behavior at different temperatures.

2. The computed values of viscosities for Na-Hg, Pb-Mg and Bi-Tl liquid alloys are positively deviated and for Cu-Al, it is negatively deviated from ideal behavior at their melting temperatures.

5.1.7 Surface Properties

1. The surface properties of alloys have been studied in the framework of Kaptay's modified form of Butler equation (Kaptay, 2019) and theoretically computed partial excess free energy of each component of preferred alloy system at different temperatures have been used to explain their surface tension and surface concentration of components of each alloys at different temperatures.

2. The component of the alloy having lower surface tension is found to segregate on the surface of the alloy for all preferred systems.

3. The surface tension of the alloy system decreases with increase in temperature.

5.2 Recommendations

1. This research is only a small beginning. We encourage the other researchers to look beyond our calculations in order to look at additional properties, even though they are useful for the investigation of compound forming binary liquid alloys.

2. With the help of experimental data, thermodynamic calculations are employed to assess the reliability of the theoretical models. For this, the adjustable parameters (i.e. interaction energy parameters) are determined by successive approximation method. However, theoretical models cannot be developed if the observed databases are not available. Therefore, more methods should be developed for the experimental measurements.

3. The mixing behavior of ternary liquid alloys cannot be explained by the Quasi-Chemical Approximation due to the complexity in the formulations. Therefore, for proper understanding of the properties of ternary liquid alloys, further modifications to the model are needed.

4. The viscocity of Cu-Al liquid alloy is negatively deviated from the ideal behaviour. For most of the interacting alloys, it is positively deviated. Thus, experimental data

of thermodynamic properties and phase diagram of Cu-Al liquid alloy should be revisited.

CHAPTER 6

6. SUMMARY

In the present thesis, we have studied and analyzed the thermodynamic, structural, transport (viscosity) and surface(surface segregation and surface tension) properties of compound forming binary liquid alloys of type $A_\mu B_\nu$ at their melting temperatures. For this, we have selected four different alloys (Na-Hg, Pb-Mg,Bi-Tl and Cu-Al) considering $NaHg_2$, $PbMg_2$, $BiTl_3$ and Cu_3Al_2 as their most stable intermetallic compounds. The thermodynamic and structural properties of the alloys have been studied in the framework of Quasi-Chemical Approximation. The viscosity and surface properties are studied by Kaptay's model and Kaptay's modified form of Butler equation respectively. The models are again extended to predict the aforementioned properties of Cu-Al, Pb-Mg and Bi-Tl liquid alloys at higher temperatures.

The major and important achievements from the present study are summarized in the following points:

1. We have first studied thermodynamic properties such as free energy of mixing, enthalpy of mixing, activity and entropy of mixing of preferred liquid alloys by determining interaction energy parameters with the help of experimental values at the melting temperatures of the alloy system. From the study, we concluded that the agreement between the computed and experimental values of aforementioned properties at melting temperature of concerned liquid alloys verifies the validity of the model used for the study. The compound forming alloys have maximum asymmetry as well as the minimum values of the free energy of mixing have been found to occur at or close to compound forming concentration. From the less negative values of the free energy and enthalpy of mixing and gradual increase in the values of activity of components of the liquid alloys at higher temperatures, we concluded that the alloy systems are less interactive and compound forming tendencies of the alloys gradually decline at higher temperatures.

2. The interaction energy parameters thus determined are used to study the structural properties such as concentration fluctuation in long wavelength limit and chemical short range order parameter. From the microscopic point of view, we concluded that the systems are mostly ordering in nature at their respective melting temperatures. The computed values of concentration fluctuation in long wavelength gradually increase with increase in temperature for the alloys . This made the conclusion that the alloy systems tend to change from ordering to segregating with increase in

temperatures.

3. The computed values of viscosity for the alloys Na-Hg, Pb-Mg and Bi-Tl deviate positively from the ideal behaviour but it it is negatively deviated for Cu-Al liquid alloy. Similarly, the viscosity of the alloy system decreases with increase in temperature. This is due to the fact that atoms gain more thermal energy and can easily overcome the attraction forces holding them together.

4. From the study of surface property, we concluded that the component of the alloy having lower surface tension is found to segregate on the surface of all preferred systems at their melting temperatures. The surface tension of the alloy system gradually decreases at elevated temperatures which is due to decrease in the strength of bonding between the atoms to form the complex as predicted by thermodynamic and structural properties.

5. Finally, we would like to point out that the interatomic interaction is crucial to the compound formation of alloys of types $A_\mu B_\nu$. These alloys in the solid state attain intermetallic compounds at one or more stoichiometric compositions owing to the strong interatomic interaction present. The alloys under the study mostly exhibit compound forming and ordering nature at their respective melting temperatures nevertheless as temperature rises, both the compound forming or ordering propensity weaken.

REFERENCES

Adhikari, D., Jha, I., & Singh, B. (2010). Structural Asymmetry in Liquid Fe-Si Alloys. *Philosophical Magazine*, *90*(20), 2687–2694.

Adhikari, D., Yadav, S., & Jha, L. (2014). Thermo-Physical Properties of Al-Fe Melt. *Journal of the Chinese Advanced Materials Society*, *2*(3), 149–158.

Akinlade, O., Ali, I., & Singh, R. (2001). Correlation Between Bulk and Surface Phenomena in Ga-(Bi, In) and In-Bi Liquid Alloys. *International Journal of Modern Physics B*, *15*(22), 3039–3053.

Alblas, B. P. (1983). *Order and Disorder in Liquid Alloys* (Unpublished doctoral dissertation). Rijksuniversiteit te Groningen, Netherlands.

Alonso, J., & March, N. (1982). Concentration Fluctuations in Simple Metallic Liquid Alloys. *Physica B+ C*, *114*(1), 67–70.

Altıntas, Y., Aksöz, S., Keşlioğlu, K., & Maraşlı, N. (2015). Determination of Thermodynamic Properties of Aluminum Based Binary and Ternary Alloys. *Journal of Alloys and Compounds*, *649*, 453–460.

Anusionwu, B. (2003). Surface Properties of Some Sodium-Based Binary Liquid Alloys. *Journal of alloys and compounds*, *359*(1-2), 172–179.

Anusionwu, B. (2006). Thermodynamic and Surface Properties of Sb-Sn and In-Sn Liquid Alloys. *Pramana*, *67*(2), 319–330.

Anusionwu, B., Adebayo, G., & Madu, C. (2009). Thermodynamics and Surface Properties of Liquid Al-Ga and Al-Ge Alloys. *Applied Physics A*, *97*(3), 533–541.

Arzpeyma, G., Gheribi, A. E., & Medraj, M. (2013). On the Prediction of Gibbs Free Energy of Mixing of Binary Liquid Alloys. *The Journal of Chemical Thermodynamics*, *57*, 82–91.

Azakami, T., & Yazawa, A. (1976). Activity Measurements of Liquid Copper Binary Alloys. *Canadian Metallurgical Quarterly*, *15*(2), 111–122.

Balej, J. (1979). Phase Diagram of the System Na—Hg in the Region of Dilute Sodium Amalgams. *Chem. zvesti*, *33*(5), 585–593.

Bardeen, J. (1937). Conductivity of Monovalent Metals. *Physical Review*, *52*(7), 688–697.

Bhandari, I. B., Koirala, I., & Adhikari, D. (2021). Temperature-Dependent Mixing Behaviours of Bi-Mg Liquid Alloys. *Physics and Chemistry of Liquids*, *59*(6), 918–931.

Bhandari, I. B., Panthi, N., & Koirala, I. (2021). Investigation on Thermo-Physical Properties of Liquid In-Tl Alloy. *Bibechana*, *18*(1), 149–158.

Bhandari, I. B., Panthi, N., Koirala, I., & Adhikari, D. (2021). Phase Segregating and Complex Forming Pb-Based (= X-Pb) Liquid Alloys. *Phase Transitions*, *94*(5), 338–352.

Bhatia, A., & Hargrove, W. (1974). Concentration Fluctuations and Thermodynamic Properties of Some Compound Forming Binary Molten Systems. *Physical Review B*, *10*(8), 3186–3196.

Bhatia, A., Hargrove, W., & March, N. (1973). Concentration Fluctuations in Conformal Solutions and Partial Structure Factor in Alloys. *Journal of Physics C: Solid State Physics*, *6*(4), 621–630.

Bhatia, A., Hargrove, W., & Thornton, D. (1974). Concentration Fluctuations and Partial Structure Factors of Compound-Forming Binary Molten Alloys. *Physical Review B*, *9*(2), 435–444.

Bhatia, A., & March, N. (1975). Size Effects, Peaks in Concentration Fluctuations and Liquidus Curves of Na-Cs. *Journal of Physics F: Metal Physics*, *5*(6), 1100–1106.

Bhatia, A., & Singh, R. (1982). Thermodynamic Properties of Compound Forming Molten Alloys in a Weak Interaction Approximation. *Physics and Chemistry of Liquids an International Journal*, *11*(4), 343–351.

Bhatia, A., & Singh, R. (1984). A Quasi-Lattice Theory for Compound Forming Molten Alloys. *Physics and Chemistry of Liquids an International Journal*, *13*(3), 177–190.

Bhatia, A., & Thornton, D. E. (1970). Structural Aspects of the Electrical Resistivity of Binary Alloys. *Physical Review B*, *2*(8), 3004–3012.

Bhuiyan, G., Alam, M. S., Ahmed, A. Z., Syed, I. M., & Rashid, R. (2009). Entropy of Mixing for Ag_xIn_{1-x} and Ag_xSn_{1-x} Liquid Binary Alloys. *The Journal of Chemical Physics*, *131*(3), 034502.

Bhuiyan, G., Ali, I., & Rahman, S. M. (2003). Atomic Transport Properties of Ag-In Liquid Binary Alloys. *Physica B: Condensed Matter*, *334*(1-2), 147–159.

Born, M., & Green, H. (1947). A General Kinetic Theory of Liquids III. Dynamical Properties. *Proceedings of the Royal Society of London. Series A. Mathematical and Physical Sciences*, *190*(1023), 455–474.

Brandes, E. A., & Brook, G. (2013). *Smithells Metals Reference Book*. Elsevier.

Butler, J. A. V. (1932). The Thermodynamics of the Surfaces of Solutions. *Proceedings of the Royal Society of London. Series A, Containing Papers of a Mathematical and Physical Character*, *135*, 348–375.

Costa, C., Delsante, S., Borzone, G., Zivkovic, D., & Novakovic, R. (2014). Thermodynamic and Surface Properties of Liquid Co-Cr-Ni Alloys. *The Journal of Chemical Thermodynamics*, *69*, 73–84.

Cowley, J. (1950). An Approximate Theory of Order in Alloys. *Physical Review*, *77*(5), 667–675.

Curioni, M., Roeth, F., Garcia-Vergara, S., Hashimoto, T., Skeldon, P., Thompson, G., & Ferguson, J. (2010). Enrichment, Incorporation and Oxidation of Copper During Anodising of Aluminium–Copper Alloys. *Surface and Interface Analysis: An International Journal devoted to the development and application of techniques for the analysis of surfaces, interfaces and thin films*, *42*(4), 234–240.

Darken, L. (1950). Application of the Gibbs-Duhem Equation to Ternary and Multicomponent Systems. *Journal of the American Chemical Society*, *72*(7), 2909–2914.

Dębski, A., Dębski, R., Gąsior, W., & Góral, A. (2014). Formation Enthalpy of Intermetallic Phases From Ag–Ca System. Experiment vs. Modeling. *Journal of Alloys and Compounds*, *610*, 701–705.

Delsante, S., Borzone, G., & Novakovic, R. (2019). Experimental Thermodynamics, Surface and Transport Properties of Liquid Ag-Ge Alloys. *Thermochimica Acta*, *682*, 1–10.

Drude, P. (1900). Zur Elektronentheorie der Metalle. *Annalen der physik*, *306*(3), 566–613.

Dubinin, N., Son, L., & Vatolin, N. (2007). Thermodynamic Properties of Liquid Binary Transition-Metal Alloys in the Bretonnet-Silbert Model. In *Defect and diffusion forum* (Vol. 263, pp. 105–110).

Egry, I., Ricci, E., Novakovic, R., & Ozawa, S. (2010). Surface Tension of Liquid Metals and Alloys—Recent Developments. *Advances in Colloid and Interface Science*, *159*(2), 198–212.

Faber, T. (1972). *An Introduction to the Theory of Liquid Metals and Alloys*. Cambridge University Press.

Flory, P. J. (1942). Thermodynamics of High Polymer Solutions. *The Journal of Chemical physics*, *10*(1), 51–61.

Fowler, R., & Guggenheim, E. (1939). *Statistical Thermodynamics*. Cambrige University.

Gąsior, W. (2014). Viscosity Modeling of Binary Alloys: Comparative Studies. *Calphad*, *44*, 119–128.

Gibbs, J. W. (1928). *Influence of Surfaces of Discontinuity Upon the Equilibrium of Heterogeneous Masses—Theory of Capillarity*. Longmans Green & Com. Newyork.

Guggenheim, E. (1952). *Mixtures.* Oxford University Press.

Harada, S., Takahashi, S., Takeda, S., Tamaki, S., Gray, P., & Cusack, N. (1988). Thermodynamic Properties of Liquid Na-Cd and Na-In. *Journal of Physics F: Metal Physics*, *18*(12), 2559–2567.

Harrison, W. A. (1966). *Pseudopotentials in the Theory of Metals*. P. W. A. BENJAMIN, INC., NEW YORK.

Hasegawa, M., & Young, W. (1977). Pseudopotential Theory of the Solid-Liquid Transition in Binary Alloys: Applications to CdxMg_{1-x} and NaxK_{1-x}. *Journal of Physics F: Metal Physics*, *7*(11), 2271–2283.

Heine, V., & Weaire, D. (1966). Structure of Di-and Trivalent Metals. *Physical Review*, *152*(2), 603–610.

Hendriks, E., Kontogeorgis, G. M., Dohrn, R., de Hemptinne, J.-C., Economou, I. G., Zilnik, L. F., & Vesovic, V. (2010). Industrial Requirements for Thermodynamics and Transport Properties. *Industrial & Engineering Chemistry Research*, *49*(22), 11131–11141.

Hildebrand, J., & Scott, R. (1950). Solutions of Nonelectrolytes. *Annual Review of Physical Chemistry*, *1*(1), 75–92.

Hirai, M. (1993). Estimation of viscosities of Liquid Alloys. *Isij International*, *33*(2), 251–258.

Hoar, T., & Melford, D. (1957). The Surface Tension of Binary Liquid Mixtures: Lead+Tin and Lead+Indium Alloys. *Transactions of the Faraday Society*, *53*, 315–326.

Hoshino, K., & Young, W. (1980). Entropy of Mixing of Compound Forming Liquid Binary Alloys. *Journal of Physics F: Metal Physics*, *10*(7), 1365–1374.

Huggins, M. L. (1942). Thermodynamic Properties of Solutions of Long-Chain Compounds. *Annals of the New York Academy of Sciences*, *43*(1), 1–32.

Hughes, E. A. M. (1961). *Physical Chemistry*. Pergamon Press.

Hultgren, R., Desai, P. D., Hawkins, D. T., Gleiser, M., & Kelley, K. K. (1973). *Selected Values of the Thermodynamic Properties of the Elements* (Tech. Rep.). National Standard Reference Data System.

Hume-Rothery, W., Mabbott, W., Gilbert, & Channel Evans, K. (1934). The Freezing Points, Melting Points, and Solid Solubility Limits of the Alloys of Sliver and Copper with the Elements of the b Sub-Groups. *Philosophical Transactions of the Royal Society of London. Series A, Containing Papers of a Mathematical or Physical Character*, *233*(721-730), 1–97.

Hume-Rothery, W., & Powell, H. M. (1935). On the Theory of Super-Lattice Structures in Alloys. *Zeitschrift für Kristallographie-Crystalline Materials*, *91*(1-6), 23–47.

Iida, T., Ueda, M., & Morita, Z.-i. (1976). On The Excess Viscosity of Liquid Alloys and the Atomic Interaction of Their Constituents. *Tetsu-to-Hagane*, *62*(9), 1169–1178.

Iida, T. G. (1993). *RIL: The Physical Properties of Liquid Metals.* Oxford, Clarendon Press.

Jha, I., Khadka, R., Koirala, R., Singh, B., & Adhikari, D. (2016). Theoretical Assessment on Mixing Properties of Liquid Tl-Na Alloys. *Philosophical Magazine*, *96*(16), 1664–1683.

Jha, N., & Mishra, A. (2001). Thermodynamic and Surface Properties of Liquid Mg-Zn Alloys. *Journal of Alloys and Compounds*, *329*(1-2), 224–229.

Jordan, A. S. (1970). A Theory of Regular Associated Solutions Applied to the Liquidus Curves of the Zn-Te and Cd-Te systems. *Metallurgical Transactions*, *1*(1), 239–249.

Kanibolotsky, D., Bieloborodova, O., Kotova, N., & Lisnyak, V. (2002). Thermodynamic Properties of Liquid Al-Si and Al-Cu Alloys. *Journal of Thermal Analysis and Calorimetry*, *70*(3), 975–983.

Kaptay, G. (2003). A New Equation to Estimate the Concentration Dependence of the Viscosity of Liquid Metallic Alloys From the Heat of Mixing Data. In *Proceedings of MicroCAD 2003 Conference. Section Metallurgy, University of Miskolc* (pp. 23–28).

Kaptay, G. (2008). A Unified Model for the Cohesive Enthalpy, Critical Temperature, Surface Tension and Volume Thermal Expansion Coefficient of Liquid Metals of bcc, fcc and hcp Crystals. *Materials Science and Engineering: A*, *495*(1-2), 19–26.

Kaptay, G. (2015). Partial Surface Tension of Components of a Solution. *Langmuir*, *31*(21), 5796–5804.

Kaptay, G. (2018). The Chemical (not Mechanical) Paradigm of Thermodynamics of Colloid and Interface Science. *Advances in Colloid and Interface Science*, *256*, 163–192.

Kaptay, G. (2019). Improved Derivation of the Butler Equations for Surface Tension of Solutions. *Langmuir*, *35*(33), 10987–10992.

Kaptay, G., Csicsovszki, G., & Yaghmaee, M. S. (2003). An Absolute Scale for the Cohesion Energy of Pure Metals. In *Materials Science Forum* (Vol. 414, pp. 235–240).

Khanna, K. (1984). Entropy of Mixing Calculations for Na-Hg and Sb-Zn Liquid Alloys in the Hard-Sphere System. *Journal of Physics F: Metal Physics*, *14*(8), 1827–1832.

Kittel, C. (1966). *Introduction to Solid State Physics*. John Wiley & Sons.

Kleppa, O. (1958). Thermodynamic Analysis of Binary Liquid Alloys of Group IIB Metals—II The Alloys of Cadmium with Gallium, Indium, Tin, Thallium, Lead and Bismuth. *Acta Metallurgica*, *6*(4), 233–242.

Koirala, I. (2016). *Ordering and Segregation in Binary Liquid Alloys* (Unpublished doctoral dissertation). T.M. Bhagalpur University,Bhagalpur.

Koirala, I. (2018). Chemical Ordering of Ag-Au Alloys in the Molten State. *Journal of Institute of Science and Technology*, *22*(2), 191–201.

Koirala, I., Singh, B., & Jha, I. (2014). Theoretical Assessment on Segregating Nature of Liquid In-Tl Alloys. *Journal of Non-Crystalline solids*, *398*, 26–31.

Koirala, I., Singh, B., & Jha, I. (2016). Theoretical Investigation of Mixing Behavior of Al-Fe Alloys in Molten Stage. *The African Review of Physics*, *10*, 329–335.

Koirala, I., Singh, B., Jha, I., & Mallik, A. (2015). Theoretical Investigation of Energetic and its Effect on Cd-Hg Amalgam. *Journal of Nepal Physical Society*, *3*(1), 60–66.

Korozs, J., & Kaptay, G. (2017). Derivation of the Butler Equation From the Requirement of the Minimum Gibbs Energy of a Solution Phase, Taking into Account Its

Surface Area. *Colloids and Surfaces A: Physicochemical and Engineering Aspects*, *533*, 296–301.

Kozlov, L. Y., Romanov, L., & Petrov, N. (1983). Predicting the Viscosity of Multicomponent Metallic Melts. *Izv Vuzov Chernaya Met*, *3*(7), 7–11.

Lai, S., Matsuura, M., & Wang, S. (1983). Variational Thermodynamic Calculation for Simple Liquid Metals and Alkali Alloys. *Journal of Physics F: Metal Physics*, *13*(10), 2033–2051.

Lebowitz, J. (1964). Exact Solution of Generalized Percus-Yevick Equation for a Mixture of Hard Spheres. *Physical Review*, *133*(4A), 895–899.

Lele, S., & Ramachandrarao, P. (1981). Estimation of Complex Concentration in a Regular Associated Solution. *Metallurgical Transactions B*, *12*(4), 659–666.

Liang, S.-M., Wang, P., & Schmid-Fetzer, R. (2016). Inherently Consistent Temperature Function for Interaction Parameters Demonstrated for the Mg-Si Assessment. *Calphad*, *54*, 82–96.

Longuet-Higgins, H. (1951). The Statistical Thermodynamics of Multicomponent Systems. *Proceedings of the Royal Society of London. Series A. Mathematical and Physical Sciences*, *205*(1081), 247–269.

Loukil, N. (2021). Alloying Elements of Magnesium Alloys: a Literature Review. *Magnesium Alloys Structure and Properties*, 183–189.

Malan, R. C., & Vora, A. M. (2021). Investigation of Some Basic Thermodynamic Properties of Na-K Alloy. *Bibechana*, *18*(2), 1–8.

March, N. H., & Tosi, M. P. (1976). *Atomic Dynamics in Liquids*. Macmillan Press Ltd. London.

Matsunaga, S., Ishiguro, T., & Tamaki, S. (1983). Thermodynamic Properties of Liquid Na-Pb alloys. *Journal of Physics F: Metal Physics*, *13*(3), 587–595.

Matsunaga, S., Tamaki, S., & Takeda, S. (1999). Structural Study of Liquid Na-Pb Alloys by Hard-Sphere Model. *Physics and Chemistry of Liquids*, *37*(4), 395–408.

Mehta, U., Yadav, S., Koirala, I., & Adhikari, D. (2020). Thermo-Physical Properties of Ternary Al-Cu-Fe Alloy in Liquid State. *Philosophical Magazine*, *100*(19), 2417–2435.

Meyer, K. H. (1939). Über die Mischungsentropie von Systemen mit langkettigen Verbindungen und ihre statistische Erklärung. *Zeitschrift für Physikalische Chemie*, *44*(1), 383–391.

Mishra, K., Limbu, H., Dhungana, A., Jha, I., Adhikari, D., et al. (2018). Thermodynamic, Structural, Surface and Transport Properties of In-Tl Liquid Alloy at Different Temperatures. *World Journal of Condensed Matter Physics*, *8*(3), 91–108.

Morachevskii, A. (2014). Liquid Alloys of the Mercury-Sodium System: Thermodynamics, Structure, and Applications. *Russian Journal of Applied Chemistry*, *87*(7), 837–852.

Mukai, K., Matsushita, T., Mills, K. C., Seetharaman, S., & Furuzono, T. (2008). Surface Tension of Liquid Alloys—A Thermodynamic Approach. *Metallurgical and Materials Transactions B*, *39*(4), 561–569.

Nayeb-Hashemi, A., & Clark, J. (1985). The Mg- Pb (Magnesium-Lead) system. *Bulletin of Alloy Phase Diagrams*, *6*(1), 56–66.

Novakovic, R., Giuranno, D., Ricci, E., & Lanata, T. (2008). Surface and Transport Properties of In-Sn Liquid Alloys. *Surface Science*, *602*(11), 1957–1963.

Novakovic, R., Giuranno, D., Ricci, E., Tuissi, A., Wunderlich, R., Fecht, H.-J., & Egry, I. (2012). Surface, Dynamic and Structural Properties of Liquid Al-Ti Alloys. *Applied Surface Science*, *258*(7), 3269–3275.

Novakovic, R., Muolo, M., & Passerone, A. (2004). Bulk and Surface Properties of Liquid X-Zr (X= Ag, Cu) Compound Forming Alloys. *Surface Science*, *549*(3), 281–293.

Novakovic, R., Ricci, E., Gnecco, F., Giuranno, D., & Borzone, G. (2005). Surface and Transport Properties of Au-Sn Liquid Alloys. *Surface Science*, *599*(1-3), 230–247.

Okajima, K., & Sakao, H. (1968). Activity Measurements of Binary Pb-X Molten Alloys by the TIE Method. *Transactions of the Japan Institute of Metals*, *9*(5), 325–329.

Okamoto, H., Massalski, T., et al. (1990). Binary Alloy Phase Diagrams. *ASM International, Materials Park, OH, USA*, 12.

Osman, S., & Singh, R. (1993). Concentration Fluctuations at the Liquid-Vapour Coexistence in Ne-Ar Mixture. *Journal of Non-Crystalline Solids*, *156*, 459–462.

Osman, S., & Singh, R. (1995). Description of Concentration Fluctuations in Liquid Binary Mixtures with Nonadditive Potentials. *Physical Review E*, *51*(1), 332–338.

Panthi, N., B Bhandari, I. B., Jha, I., & Koirala, I. (2021). Complex Formation Behavior of Copper-Tin Alloys at its Molten State. *Advanced Materials Letters*, *12*(1), 1–7.

Panthi, N., Bhandari, I. B., & Koirala, I. (2021). Complex Formation of Sodium-Mercury Alloy at Molten State. *Journal of Physics Communications*, *5*(8), 1–11.

Panthi, N., Bhandari, I. B., Pangeni, R., & Koirala, I. (2020). High Temperature Assessment of K-Tl Binary Liquid Alloy. *Journal of Nepal Physical Society*, *6*(2), 20–25.

Parrinello, M., Tosi, M., & March, N. (1974). Partial Structure Factors and Atomic Dynamics in Conformal Solutions. *Proceedings of the Royal Society of London. A. Mathematical and Physical Sciences*, *341*(1624), 91–104.

Pelton, A. D., & Blander, M. (1986). Thermodynamic Analysis of Ordered Liquid Solutions by a Modified Quasichemical Approach—Application to Silicate Slags. *Metallurgical Transactions B*, *17*(4), 805–815.

Percus, J. K., & Yevick, G. J. (1958). Analysis of Classical Statistical Mechanics by Means of Collective Coordinates. *Physical Review*, *110*(1), 1–13.

Plevachuk, Y., Sklyarchuk, V., Gerbeth, G., Eckert, S., & Novakovic, R. (2011). Surface Tension and Density of Liquid Bi-Pb, Bi-Sn and Bi-Pb-Sn Eutectic Alloys. *Surface science*, *605*(11-12), 1034–1042.

Porter, D. A., & Easterling, K. E. (2009). *Phase Transformations in Metals and Alloys (Revised Reprint)*. CRC press.

Prasad, L., & Jha, R. (2005). Surface Tension and Viscosity of Sn-Based Binary Liquid Alloys. *Physica Status Solidi (a)*, *202*(14), 2709–2719.

Prasad, L., & Singh, R. (1990). A Quasi-Lattice Model for the Thermodynamic Properties of Au-Zn Liquid Alloys. *Physics and Chemistry of Liquids*, *22*(1-2), 1–9.

Prasad, L., & Singh, R. (1991). Surface Segregation and Concentration Fluctuations at the Liquid-Vapor Interface of Molten Cu-Ni Alloys. *Physical Review B*, *44*(24), 13768–133771.

Prasad, L., Singh, R., & Singh, G. (1994). The Role of Size Effects on Surface Properties. *Physics and Chemistry of Liquids*, *27*(3), 179–185.

Prasad, L., Singh, R., Singh, V., & Singh, G. (1998). Correlation Between Bulk and Surface Properties of AgSn Liquid Alloys. *The Journal of Physical Chemistry B*, *102*(6), 921–926.

Prasad, L., & Singh, V. (2000). Surface Properties and Concentration Fluctuations in Sn-Based Molten Alloys. *Zeitschrift für Naturforschung A*, *55*(11-12), 967–972.

Predel, B., & Oehme, G. (1974). Untersuchung der Auswirkung von Assoziationsgleichgewichten auf die Konzentrationsabhängigkeit der Mischungsenthalpie flüssiger Quecksilber-Indium-Legierungen. *International Journal of Materials Research*, *65*(8), 525–530.

Prigogine, I., & Defay, R. (1958). *Chemical Thermodynamics*. Jarrold & Sons.

Ramaswamy, R. (1971). Electronics of Solids: Part I. *IETE Journal of Education*, *12*(4), 147–152.

Rasch, M., Roider, C., Kohl, S., Strauß, J., Maurer, N., Nagulin, K. Y., & Schmidt, M. (2019). Shaped Laser Beam Profiles for Heat Conduction Welding of Aluminium-Copper Alloys. *Optics and Lasers in Engineering*, *115*, 179–189.

Redlich, O., & Kister, A. (1948). Algebraic Representation of Thermodynamic Properties and the Classification of Solutions. *Industrial & Engineering Chemistry*, *40*(2), 345–348.

Reijers, H., Saboungi, M.-L., Price, D., Richardson Jr, J., Volin, K., & Van der Lugt, W. (1989). Structural Properties of Liquid Alkali-Metal–Lead Alloys: NaPb, KPb, RbPb, and CsPb. *Physical Review B*, *40*(9), 6018–6029.

Rice, S. A., & Allnatt, A. R. (1961). On the Kinetic Theory of Dense Fluids. VI. Singlet Distribution Function for Rigid Spheres with an Attractive Potential. *The Journal of Chemical Physics*, *34*(6), 2144–2155.

Rice, S. A., & Kirkwood, J. G. (1959). On an Approximate Theory of Transport in Dense Media. *The Journal of Chemical Physics*, *31*(4), 901–908.

Ruppersberg, H., & Egger, H. (1975). Short-Range Order in Liquid Li-Pb Alloys. *The Journal of Chemical Physics*, *63*(10), 4095–4103.

Rushbrooke, G. (1963). On the Thermodynamics of the Critical Region for the Ising Problem. *The Journal of Chemical Physics*, *39*(3), 842–843.

Schwitzgebel, G., & Langen, G. (1981). Application of the Hard Sphere Theory to the Diffusion of Binary Liquid Alloy Systems. *Zeitschrift für Naturforschung A*, *36*(11), 1225–1232.

Seetharaman, S., & Sichen, D. (1994). Estimation of the viscosities of Binary Metallic Melts Using Gibbs Energies of Mixing. *Metallurgical and Materials Transactions B*, *25*(4), 589–595.

Sharma, N., Thakur, A., & Ahluwalia, P. (2014). Thermodynamic, Surface, and Structural Properties of Hg-Na and Hg-Zn Liquid Alloys. *Journal of Molecular Liquids*, *195*, 73–79.

Singh, R. (1987). Short-Range Order and Concentration Fluctuations in Binary Molten Alloys. *Canadian journal of Physics*, *65*(3), 309–325.

Singh, R., & Choudhary, R. (1981). Entropies of Molten Alloys. *Journal of Physics F: Metal Physics*, *11*(8), 1577–1583.

Singh, R., Jha, I., & Sinha, S. (1991). The Segregation-Order Transformation in Cd-Na Liquid Alloy. *Journal of Physics: Condensed Matter*, *3*(16), 2787–2793.

Singh, R., & Mishra, I. (1988). Conditional Probabilities and Thermodynamics of Binary Molten Alloys. *Physics and Chemistry of Liquids*, *18*(4), 303–319.

Singh, R., Mishra, I., & Singh, V. (1990). Local Order in Cd-Based Liquid Alloys. *Journal of Physics: Condensed Matter*, *2*(42), 8457–8462.

Singh, R., & Sommer, F. (1997). Segregation and Immiscibility in Liquid Binary Alloys. *Reports on Progress in physics*, *60*(1), 57–150.

Singh, R., & Sommer, F. (1998). Thermodynamic Investigation of Viscosity and Diffusion in Binary Liquid Alloys. *Physics and Chemistry of Liquids*, *36*(1), 17–28.

Singh, R., & Sommer, F. (2012). Viscosity of Liquid Alloys: Generalization of Andrade's Equation. *Monatshefte für Chemie-Chemical Monthly*, *143*(9), 1235–1242.

Sommer, F. (1990). Thermodynamic Properties of Compound-Forming Liquid Alloys. *Journal of Non-Crystalline Solids*, *117*, 505–512.

Sommer, F., Singh, R. N., & Witusiewicz, V. (2001). On the Entropy of Mixing. *Journal of Alloys and Compounds*, *325*(1-2), 118–128.

Speiser, R., Poirier, D., & Yeum, K. (1987). Surface Tension of Binary Liquid Alloys. *Scripta Metallurgica*, *21*(5), 687–692.

Suganuma, K. (2001). Advances in Lead-Free Electronics Soldering. *Current Opinion in Solid State and Materials Science*, *5*(1), 55–64.

Takeda, S., Harada, S., Tamaki, S., Matsubara, E., & Waseda, Y. (1987). Structural Study of Liquid Na-Pb Alloys by Neutron Diffraction. *Journal of the Physical Society of Japan*, *56*(11), 3934–3940.

Tanaka, T., Gokcen, N., & Morita, Z. (1990). Relationship Between Enthalpy of Mixing and Excess Entropy in Liquid Binary Alloys. *Zeitschrift für Metallkunde*, *81*(1), 49–54.

Tanaka, T., Hack, K., Iida, T., & Hara, S. (1996). Application of Thermodynamic Databases to the Evaluation of Surface Tensions of Molten Alloys, Salt Mixtures and Oxide Mixtures. *Zeitschrift für Metallkunde*, *87*(5), 380–389.

Thiele, E. (1963). Equation of State for Hard Spheres. *The Journal of Chemical Physics*, *39*(2), 474–479.

Tripathi, S., & Chandrasekharaiah, M. (1983). Thermodynamic Properties of Binary Alloys of Platinum Metals II: Ir-Pt System. *Journal of the Less Common Metals*, *91*(2), 251–260.

Trybula, M., Gancarz, T., Gasior, W., & Pasturel, A. (2014). Bulk and Surface Properties of Liquid Al-Li and Li-Zn Alloys. *Metallurgical and Materials Transactions A*, *45*(12), 5517–5530.

Trybula, M., Szafrański, P. W., & Korzhavyi, P. A. (2018). Structure and Chemistry of Liquid Al-Cu Alloys: Molecular Dynamics Study Versus Thermodynamics-Based Modelling. *Journal of Materials Science*, *53*(11), 8285–8301.

Van Hove, L. (1954). Correlations in Space and Time and Born Approximation Scattering in Systems of Interacting Particles. *Physical Review*, *95*(1), 249–262.

Verma, R. P., & Lila, M. K. (2021). A Short Review on Aluminium Alloys and Welding in Structural Applications. *Materials Today: Proceedings*, *46*, 10687–10691.

Vora, A. M. (2010). Study of Thermodynamic Properties of Liquid Binary Alloys by a Pseudopotential Method. *Journal of Engineering Physics and Thermophysics*, *83*(5), 1070–1079.

Warren, B. (1969). *X-ray diffraction*. Reading, Mass: Addison-Wesley Pub. Co.

Wilson, J. R. (1965). The Structure of Liquid Metals and Alloys. *Metallurgical Review*, *10*(3), 381-590.

Yadav, S., Jha, L., & Adhikari, D. (2015). Thermodynamic and Structural Properties of Bi-Based Liquid Alloys. *Physica B: Condensed Matter*, *475*, 40–47.

Yadav, S., Jha, L. N., Dhungana, A., Mehta, U., Adhikari, D., et al. (2018). Thermo-Physical Properties of Al-Mg Alloy in Liquid State at Different Temperatures. *Materials Sciences and Applications*, *9*(10), 812–828.

Yadav, S., Lamichhane, S., Jha, L., Adhikari, N., & Adhikari, D. (2016). Mixing Behaviour of Ni-Al Melt at 1873 K. *Physics and Chemistry of Liquids*, *54*(3), 370–383.

Yakymovych, A., Mudry, S., Luef, C., & Ipser, H. (2008). The Competition Between In-Bi and In_2Bi Like Atomic Distributions Before Solidification. *Chemistry of Metals and Alloys*, *1*(2), 159–162.

Yang, H., Tao, D., & Zhou, Z. (2009). Prediction of the Mixing Enthalpies of Binary Liquid Alloys by Molecular Interaction Volume Model. *Acta Metallurgica Sinica (English Letters)*, *21*(5), 336–340.

Yeh, J.-W. (2015). Physical Metallurgy of High-Entropy Alloys. *Jom*, *67*(10), 2254–2261.

Yeum, K., Speiser, R., & Poirier, D. (1989). Estimation of the Surface Tensions of Binary Liquid Alloys. *Metallurgical Transactions B*, *20*(5), 693–703.

Young, W. (1992). Structural and Thermodynamic Properties of NFE Liquid Metals and Binary Alloys. *Reports on Progress in Physics*, *55*(10), 1769–1851.

Zajaczkowski, A., & Botor, J. (1995). Thermodynamics of the Al-Sb System Determined by Vapour Pressure Measurements. *International Journal of Materials Research*, *86*(9), 590–596.

Zhang, F., Wen, S., Liu, Y., Du, Y., & Kaptay, G. (2019). Modelling the Viscosity of Liquid Alloys with Associates. *Journal of Molecular Liquids*, *291*, 1–7.

APPENDIX

A. Partial Excess Free Energy

Table 59: Partial excess free energies of Pb and Mg for Pb-Mg liquid alloy at different temperatures for different concentrations of lead.

Conc. of	Partial excess free energy($\Delta G^{\mathrm{Xs}}_{i,\mathrm{b}}$) (J mol^{-1})							
	For Pb				For Mg			
Pb (C_{Pb})	973 K	1073 K	1173 K	1273 K	973 K	1073 K	1173 K	1273 K
0.1	-37052	-37033	-37014	-34089	-821	-842	-864	-817
0.2	-24669	-24452	-24236	-22132	-2984	-3039	-3093	-2900
0.3	-15398	-15153	-14908	-13511	-6050	-6112	-6174	-5747
0.4	-8777	-8594	-8411	-7582	-9587	-9615	-9642	-8910
0.5	-4353	-4263	-4172	-3761	-13175	-13126	-13077	-12005
0.6	-1683	-1673	-1664	-1524	-16399	-16252	-16105	-14705
0.7	-334	-366	-398	-394	-18856	-18627	-18399	-16743
0.8	121	137	162	179	-20153	-19914	-19676	-17911
0.9	97	79	62	41	-19903	-19803	-19703	-18063

Table 60: Partial excess free energies of Bi and Tl for Bi-Tl liquid alloy at different temperatures for different concentrations of thallium.

Conc. of	Partial excess free energy($\Delta G^{\mathrm{Xs}}_{i,\mathrm{b}}$E) (J mol^{-1})							
	For Tl				For Bi			
Tl (C_{Tl})	750 K	850 K	950 K	1050 K	750 K	850 K	950 K	1050 K
0.1	-11625	-11748	-11872	-11996	-55	-52	-49	-47
0.2	-10750	-10892	-11034	-11175	-210	-204	-199	-194
0.3	-9737	-9869	-10002	-10135	-554	-552	-550	-548
0.4	-8380	-8484	-8589	-8694	-1297	-1310	-1323	-1336
0.5	-6652	-6719	-6785	-6852	-2728	-2773	-2818	-2863
0.6	-4696	-4723	-4751	-4778	-5141	-5234	-5327	-5420
0.7	-2779	-2777	-2774	-2772	-8725	-8873	-9021	-9168
0.8	-1218	-1204	-1189	-1175	-13423	-13605	-13788	-13970
0.9	-272	-263	-255	-246	-18756	-18899	-19043	-19187

Table 61: Partial excess free energies of Cu and Al for Cu-Al liquid alloy at different temperatures for different concentrations of copper.

Conc. of	Partial excess free energy($\Delta G^{\mathrm{Xs}}_{i,\mathrm{b}}$) (J mol^{-1})							
	For Cu				For Al			
Cu (C_{Cu})	1373	1573	1773	1973	1373	1573	1773	1973
0.1	-30965	-34011	-37057	-40132	-178	-191	-204	-218
0.2	-30831	-33943	-37056	-40194	-189	-190	-190	-192
0.3	-29931	-32983	-36035	-39105	-523	-548	-574	-602
0.4	-26401	-29075	-31748	-34433	-2490	-2727	-2963	-3208
0.5	-20437	-22461	-24485	-26511	-7452	-8229	-9005	-9797
0.6	-13456	-14740	-16024	-17304	-16051	-17739	-19426	-21135
0.7	-7271	-7935	-8600	-9258	-27550	-30385	-33220	-36080
0.8	-3100	-3385	-3671	-3951	-39984	-43945	-47905	-51886
0.9	-891	-986	-1082	-1176	-52477	-57517	-62557	-67599

B. Papers Published in International journals

Bhandari, I. B., Panthi, N., Gaire, S., & Koirala, I. (2021). Effect of Temperature on Mixing Behavior and Stability of Liquid Al-Fe Alloys. In *Journal of Physics: Conference Series* (Vol. 2070, p. 012025).

Bhandari, I. B., Panthi, N., Koirala, I., & Adhikari, D. (2021). Phase Segregating and Complex Forming Pb-based (= X-Pb) Liquid Alloys. *Phase Transitions*, *94*(5), 338–352.

Panthi, N., Bhandari, I. B., & Koirala, I. (2021). Complex Formation of Sodium-Mercury Alloy at Molten State. *Journal of Physics Communications*, *5*(8), 1–11.

Panthi, N. and Bhandari, I. B. and Koirala, I. (2022a). High Temperature Stability of K-Pb Liquid Alloy. In *Defect and Diffusion Forum* (Vol. 419, pp. 147–154).

Panthi, N. and Bhandari, I. B. and Koirala, I. (2022b). Thermophysical Behavior of Mercury-Lead Liquid Alloy. *Papers in Physics*, *14*, 140005(1)–140005(11).

Panthi, N. and Bhandari, I. B. and Koirala, I. (2022c). Thermophysical Study of Sodium–Indium Alloy. *Metallofizika i Noveishie Tekhnologii*, *44*(11), 1535–1549.

C. Papers Published in National journals

Bhandari, I., Panthi, N., & Koirala, I. (2019). Thermodynamics of Liquid Gallium-Zinc Alloy. *Himalayan Physics*, *8*, 33–38.

Bhandari, I., Panthi, N., & Koirala, I. (2021). Investigation on Thermo-Physical Properties of Liquid In-Tl Alloy. *Bibechana*, *18*(1), 149–158.

Panthi, N., Bhandari, I., Pangeni, R., & Koirala, I. (2021). Comparison of Thermophysical Properties of Mg-Ga and Mg-Pb Alloys at 1000 K. *Journal of Institute of Science and Technology*, *26*(1), 51–56.

Panthi, N., Bhandari, I. B., & Koirala, I. (2020). Theoretical Assessment on Hetero-Coordination of Alloys Silver-Antimony at Molten State. *Himalayan Journal of Science and Technology*, *3-4*, 68–73.

D. Participation in Conferences, Seminars and Workshops

Panthi, N. (2022, Apr 8-9). *Thermo-Physical Stability of K-Pb Liquid Alloy at Different Temperatures* [Oral presentation]. Fourth International Conference on Material Science and Manufacturing Technology (ICMSMT 2022), Akshya College of Engineering and Technology, Coimbatore, Tamil Nadu, India.

Panthi, N. (2022, Mar 14-18). *Thermophysical Behaviour of Sodium-Indium alloy* [Oral presentation]. The American Physical Society's March Meeting, American Physical Society, U.S.A.

Panthi, N. (2022, Jan 22-25). *High Temperature Study of Complex Lead Magnesium Alloy* [Oral presentation]. International Conference on Frontiers of Physics (ICFP-2022), Nepal Physical Society, Nepal.

Panthi, N. (2021, Sep 26-28). *Comparison of Thermophysical Properties of Mg-Ga and Mg-Pb Alloys at 1000 K* [Poster presentation]. International Conference on Material Science and Characterization Technology (ICMSCT), St. Xavier's College, Maitighar, Kathmandu, Nepal.

Panthi, N. (2019, May 8-11). Workshop on Research Writing and Publishing, Mahendra Morang Aadarsha Multiple Campus, Biratnagar, Nepal.

Taylor & Francis
Taylor & Francis Group

Phase Transitions
A Multinational Journal

ISSN: (Print) (Online) Journal homepage: https://www.tandfonline.com/loi/gpht20

Phase segregating and complex forming Pb-based (=X-Pb) liquid alloys

Indra Bahadur Bhandari, Narayan Panthi, Ishwar Koirala & Devendra Adhikari

To cite this article: Indra Bahadur Bhandari, Narayan Panthi, Ishwar Koirala & Devendra Adhikari (2021) Phase segregating and complex forming Pb-based (=X-Pb) liquid alloys, Phase Transitions, 94:5, 338-352, DOI: 10.1080/01411594.2021.1933485

To link to this article: https://doi.org/10.1080/01411594.2021.1933485

PHASE TRANSITIONS
2021, VOL. 94, NO. 5, 338–352
https://doi.org/10.1080/01411594.2021.1933485

Taylor & Francis
Taylor & Francis Group

Phase segregating and complex forming Pb-based (=X-Pb) liquid alloys

Indra Bahadur Bhandari[a,b], Narayan Panthi[a,c], Ishwar Koirala[a] and Devendra Adhikari [d]

[a]Central Department of Physics, Tribhuvan University, Kirtipur, Nepal; [b]Department of Applied Sciences, Purwanchal Campus, Tribhuvan University, Dharan, Nepal; [c]Department of Physics, Patan Multiple Campus, Tribhuvan University, Lalitpur, Nepal; [d]Department of Physics, M.M.A.M.C., Tribhuvan University, Biratnagar, Nepal

ABSTRACT

We have used a theoretical model based on the assumption of compound formation in binary alloys to study the thermodynamic, microscopic and surface properties of Bi-Pb and In-Pb liquid alloys. A review of the phase diagrams for these alloys shows that one of the stable complexes for Bi-Pb liquid alloy is $BiPb_3$; also that In-Pb is a stable phase in liquid In-Pb alloys. Using the same interaction parameters that are fitted for free energy of mixing, we have been able to compute the bulk and thermodynamic properties of the alloys. From our observations, we are able to show that the Bi-Pb liquid alloy exhibits compound formation over the whole concentration range and the In-Pb alloys undergo phase separation. With regard to surface properties Pb segregates more to the surface in In-Pb alloys than in Bi-Pb alloys. The viscosity isotherms have positive deviation from ideality for both Bi-Pb and In-Pb alloys.

ARTICLE HISTORY
Received 9 December 2020
Accepted 24 March 2021

KEYWORDS
Bi-Pb; In-Pb; asymmetry; interaction parameters; deviation

1. Introduction

Numerous available models [1–28] have been used by a number of researchers to study the thermodynamic, structural, transport and surface properties of binary liquid alloys; the deviation of the properties of alloys from the ideal mixing condition is discussed in such model formulations in terms of the energy interaction of the constituent species of the respective alloys. It follows from the above that the main parameter for selecting a thermodynamic alloy is how far the thermodynamic properties of liquid alloys deviate from the ideal properties. On the basis of its deviation from the ideal thermodynamic properties, an alloy can be considered either as a compound-forming liquid alloy (hetero-coordinated) or as a segregating (homo-coordinated) system. One of the basic advantages of using such a thermodynamic model is that it can be easily extended to investigate the compositional dependence of structural properties [14,29] such as long wavelength fluctuations, chemical short-range order parameters, transport properties [30,31] such as diffusion coefficient, viscosity and surface properties [16,32] such as surface tension and surface composition. Departures from ideality are visible as asymmetries in thermodynamic properties away from equiatomic composition and are usually attributed to one of the following factors: the size effect, the difference in electronegativity or the interactions between solute and solvent atoms or the combination of these factors [33]. The industrial applications of liquid alloys could also be a very important basis for a detailed study. Lead and lead alloys have frequently been the subject of numerous experimental and theoretical research studies [34–50].

CONTACT Devendra Adhikari adksbdev@yahoo.com; devendra.adhikari@mmamc.tu.edu.np

Lead (Pb) is among the top 10 essential commodities consumed in the industrial world. Lead has some exceptional properties: low melting point, easy casting, high density, softness, malleability, low strength, easy production, acid resistance and electrochemical reactions with sulfuric acid. Due to its excellent resistance to air, water and soil corrosion, Lead is one of the most stable materials produced. Lead is ductile and malleable and can be produced by rolling, extruding, forging, spinning and hammering in different shapes. Low tensile strength and very low creep strength make it unfit for use without the addition of alloy elements. Lead can be easily alloyed to a lot of other metals. Lead alloys with low melting points can be cast into many shapes using a variety of molding materials and casting processes. Antimony, calcium, tin, copper, tellurium, arsenic and silver are the main alloy elements used to strengthen lead. Minor alloy elements include selenium, sulfur, bismuth, cadmium, indium, aluminum and strontium. The main uses of lead alloys are lead-acid ammunition batteries; cable sheathing; construction of sheets, pipes and solders; bearings; gaskets; special castings; anodes; fusible alloys; shielding; and weights. Because of the corrosion resistance of lead and lead alloys, their applications are also associated with the formation of the protective corrosion film. Despite many useful applications, lead and its compounds are combined toxins and should be treated with recommended precautions. Such chemicals should not be used in diet or other consumption substances [51].

In-Pb alloys are generally recommended for soldering gold as alternative solders, as they do not easily leach or dissolve gold. In addition, In-Pb alloys are used as contact alloys for metal-glass or metal-ceramic connections due to their relatively low melting temperatures [40]. Elemental Pb and In are not easy to volatilize; therefore; the data obtained at high temperatures are sufficiently realistic and it is interesting to study the properties of Pb–In melts. Lead-bismuth alloys are of value for their corrosion protection and wear resistance properties [52]. The lead-bismuth alloy is a prospective heat transfer medium for nuclear power units [53].

The layout of the paper is as follows. Section 2 provides the theoretical basis for our work. Section 3 presents and discusses the results of this work. Finally, the conclusions are outlined in Section 4.

2. Theory

The advantages of complex formation model (CFM) [12,17,25,54] are that, it seeks to account stability of compound through concentration-dependent free energy of mixing G_M, heat of mixing H_M and concentration fluctuation in long wavelength limit $S_{cc}(0)$. Formalism in weak interaction approximation [55] was applied to liquid Bi-Pb and In-Pb alloys to describe the behavior of their mixing properties. In the framework of CFM, A-B liquid alloy is a pseudo-ternary mixture consisting of A-atoms, B-atoms and chemical complexes $A_\alpha B_\beta$ with intermetallic stoichiometry present in a solid state, all in chemical equilibrium with each other [56,57]. If there are x_1 number of A atoms, x_2 number of B atoms and x_3 number of $A_\alpha B_\beta$ complexes in the ternary mixture, then we have from the conservation of atoms,

$$x_1 = c - \alpha x_3,\ x_2 = (1-c) - \beta x_3 \text{ and } x = x_1 + x_2 + x_3 = 1 - (\alpha + \beta - 1)x_3 \tag{1}$$

where α and β are small integers determined from the stoichiometry of energetically favored compound and c is the atomic fraction of A atoms. The value of x_3 can be calculated at a given pressure and temperature from the equilibrium state of free mixing energy,G_M as

$$\left(\frac{\partial G_M}{\partial x_3}\right)_{T,P,c} = 0 \tag{2}$$

where G_M for binary alloys can be written as

$$G_M = -x_3\chi + RT\sum_{i=1}^{3} x_i \ln\left(\frac{x_i}{x}\right) + \sum_{i<j} \Psi_{ij}\left(\frac{x_i x_j}{x}\right) \tag{3}$$

Here the first term $-x_3\chi$ stands for lowering of free energy due to the formation of complex $A_\alpha B_\beta$, χ is the formation energy of the complex, Ψ_{ij} ($i = 1, 2, 3$) are the average interaction energies among the species i and j. From Equations (2) and (3), the equilibrium value of x_3 is given by the equation

$$(x_3 x^{\alpha+\beta-1} x_1^{-\alpha} x_2^{-\beta})^{-1} = \exp\left(\Phi - \frac{\chi}{RT}\right) \tag{4}$$

where

$$\begin{aligned}
\Phi =& \Phi_1 + \Phi_2 + \Phi_3 \\
\Phi_1 =& \left[(\alpha+\beta-1)\frac{x_1 x_2}{x^2} - \alpha\frac{x_2}{x} - \beta\frac{x_1}{x}\right]\frac{\Psi_{12}}{RT} \\
\Phi_2 =& \left[(\alpha+\beta-1)\frac{x_2 x_3}{x^2} - \beta\frac{x_3}{x} + \frac{x_2}{x}\right]\frac{\Psi_{23}}{RT} \\
\Phi_3 =& \left[((\alpha+\beta-1)\frac{x_1 x_3}{x^2} - \alpha\frac{x_3}{x} + \frac{x_1}{x}\right]\frac{\Psi_{13}}{RT}
\end{aligned} \tag{5}$$

The heat formation, H_M, can be obtained through Equation (3) and the relation

$$H_M = G_M - T(\partial G_M/\partial T)_{P,c,N} \tag{6}$$

Equations (3) and (6) yield

$$H_M = -x_3\left[\chi - T\left(\frac{\partial\chi}{\partial T}\right)\right] + \sum_{i<j}\sum\left(\frac{x_i x_j}{x}\right)\left[\Psi_{ij} - T\left(\frac{\partial\Psi_{ij}}{\partial T}\right)\right] \tag{7}$$

The other thermodynamic function entropy of mixing(S_M)can be expressed as

$$S_M = (H_M - G_M)/T \tag{8}$$

Using Equations (3) and (7) in Equation (8) we obtain

$$S_M = x_3\frac{\partial\chi}{\partial T} - R\sum_{i=1}^{3} x_i \ln\frac{x_i}{x} - \sum_{i<j}\sum\left(\frac{x_i x_j}{x}\right)\frac{\partial\Psi_{ij}}{\partial T} \tag{9}$$

Knowledge of surface properties is important for understanding surface-related properties such as wet joint capability, epitaxial growth, corrosion and phase transformation kinetics [58]. Centered on the assumption of a monatomic surface layer, Butler's method [59] for assessing surface tension, σ of liquid solution can be expressed as follows:

$$\sigma = \sigma_A + \frac{G_A^s - G_A^b}{S_A} + \frac{RT}{S_A}\ln\left(\frac{c^s}{c}\right) \tag{10}$$

$$= \sigma_B + \frac{G_B^s - G_B^b}{S_B} + \frac{RT}{S_B}\ln\left(\frac{1-c^s}{1-c}\right) \tag{11}$$

Equations (10) and (11) give the expression for surface tension in terms of partial excess free energy of mixing in bulk (G_i^b), partial excess free energy of mixing at the surface (G_i^s), bulk concentration (c) and surface concentration (c^s). Where σ_A and σ_B are the surface tensions of pure components A and B, respectively.

The monatomic surface area for each component is

$$S_i = 1.091 N_A^{1/3} V_i^{2/3} \tag{12}$$

where V_i is the molar volume of the component i that can be determined from its molar mass and density and N_A stands for Avogadro number. It is difficult to evaluate the coefficient in Equation

(12) for liquid alloys. For simplicity, it is usually set to 1.091 for liquid metals assuming close-packed structures [60].

The concentration fluctuations, in the long wavelength limit, $S_{cc}(0)$ indicate the preference for homo-coordination or hetero-coordination that defines the essence of mixing in liquid alloys in terms of chemical order and segregation. Once the Gibbs energy of mixing of the liquid phase, G_M is known, $S_{cc}(0)$ can be expressed by G_M as [61].

$$S_{cc}(0) = \left(\frac{1}{RT}\frac{\partial^2 G_M}{\partial c^2}\right)^{-1} \tag{13}$$

Theoretically computed values of $S_{cc}(0)$ can be compared with the observed values evaluated from the activity of constituent element at different composition by the following expression

$$S_{cc}(0) = \frac{c_B a_A}{(\partial a_A/\partial c_A)_{T,P,N}} = \frac{c_A a_B}{(\partial a_B/\partial c_B)_{T,P,N}} \tag{14}$$

Solving Equations (4) and (12) one obtains

$$S_{cc}(0) = \frac{RT}{RT\sum_{i=1}^{3}\left(\frac{(x'_i)^2}{x_i} - \frac{(x')^2}{x}\right) + 2x\sum_{i<j}\sum \Psi_{ij}\left(\frac{x_i}{x}\right)'\left(\frac{x_j}{x}\right)'} \tag{15}$$

where the prime on $x$denotes its first differentiation with respect to c.

For ideal mixture Equation (15) reduces to

$$S_{cc}^{id}(0) = c_A c_B \tag{16}$$

The degree of order in the liquid alloy can be viewed using the Warren–Cowley short-range order parameter (α_1) [62, 63]. Experimentally, these quantities are not easily quantifiable by diffraction experiments. From the knowledge of the nearest neighbor contacts of unlike atoms in the melt, the expression for α_1 can be simply obtained [27]. Knowledge of α_1 provides a direct insight into the nature of the mixture's local arrangement of atoms. $\alpha_1 < 0$ refers to unlike atoms pairing as nearest neighbors, $\alpha_1 > 0$ corresponds to like atoms pairing in the first coordination shell, while $\alpha_1 = 0$ corresponds to a random distribution. The limiting values of α_1 for equiatomic composition fall in the range $-1 \le \alpha_1 \le +1$. The minimum possible value of α_1 is $\alpha_{min} = -1$representing complete ordering. On the other hand, the maximum value$\alpha_{max} = +1$implies total segregation leads to phase separation. Singh et al. [64] suggested that α_1 can be estimated from$S_{cc}(0)$.

$$\alpha_1 = \frac{S-1}{S(z-1)+1},\ S = \frac{S_{cc}(0)}{S_{cc}^{id}(0)} \tag{17}$$

Here z is the coordination number of the alloy. It is taken as 10 for the present calculations, and the α_1 values are evaluated [6].

Viscosity is one of the most essential thermophysical properties of liquid alloys, deciding certain manufacturing processes and natural phenomena. By means of viscosity, the mixing behavior of binary melt can also be understood at the microscopic level. The Budai-Benko-Kaptay (BBK) model for viscosity of liquid alloy[65] is

$$\eta = P\,T^{1/2}\frac{\left(\sum_i c_i M_i\right)^{1/2}}{\left(\sum_i c_i V_i\right)^{2/3}}\exp\left[\frac{B}{T}\left(\sum_i c_i T_{m,i} - \frac{H_M}{qR}\right)\right] \tag{18}$$

The detailed formalism of the above-mentioned model and the values of the different parameters present in Equation (18) are explored in detail [66]. Here we have presented the main equation involved in the

measurement of viscosity. Many metallurgical processes and heterogeneous chemical reactions require transport properties, such as the diffusivity of liquid metals. For example, the rate of heterogeneous reactions between two liquid alloys, such as slag and metal, is limited by the diffusion of the reactant species [58]. The mixing behavior of the binary liquid alloys can also be explored at the microscopic level in terms of diffusion coefficient. The mutual diffusion coefficient (D_M) of liquid alloys can be displayed in terms of activity (a_i) and self-diffusion coefficient (D_{id}) of individual component applying Darken's equation [67].

$$D_M = c_i D_{id} \frac{d \ln a_i}{\mathrm{d}c_i} \tag{19}$$

Here

$$D_M = cD_B + (1 - c)D_A \tag{20}$$

where D_A and D_B are the self--diffusion coefficients of pure components A and B, respectively. The ratio of mutual diffusion coefficient (D_M) and self-diffusion coefficient (D_{id}) is also associated with concentration fluctuation in long wavelength limit ($S_{\mathrm{cc}}(0)$) as

$$\frac{D_M}{D_{\mathrm{id}}} = \frac{c_A c_B}{S_{\mathrm{cc}}(0)} \tag{21}$$

3. Results and discussion

3.1. Thermodynamic properties

In this work, we aim to investigate some of the transport and surface properties of Bi-Pb and In-Pb alloys, such as surface tension, surface concentration, mutual diffusivity and viscosity, using energetics derived from their experimental thermodynamic data. To use the CFM to obtain the required energy parameters, we consider the existence of a form $A_\alpha B_\beta$ chemical complex in the liquid state of the alloy. By choosing the values α and β, we continue to determine the free energy of the alloy mixing values by varying the energy parameters χ and Ψ_{ij}. The set of energy parameters that propagates to a reasonable extent the computed values of the free energy of mixing of liquid alloys will be used in the calculation of their enthalpy of formation H_M, mixing entropy S_M, concentration-concentration fluctuation at the long wavelength limit $S_{\mathrm{cc}}(0)$ and mutual diffusivitiesD_M/D_{id}. The values of α and β used for the computation are obtained from phase diagrams. For Bi-Pb, the phase diagram [68] shows the formation of intermetallic compounds of the type $BiPb_3$ in the solid phase. We, therefore, presume that the compound will stay stable and remain in the liquid phase and affect the thermodynamic properties of the liquid alloy to a reasonable amount. However in the case of the In-Pb liquid alloy, the selection of α and β corresponding to the In-Pb complex was capable of reproducing, to a reasonable degree, the reported free energy of the mixing values of the alloy. The plot of G_M/RT with respective concentration of Bi and In for Bi-Pb and In-Pb liquid alloys is shown in Figure 1.

The points are experimental data due to Ref. [68] and the lines are the calculated values, at 700 K for Bi-Pb and at 673 K for In-Pb. The energy parameters used for the calculation are presented in Table 1. It should be noted that within the framework of the models mentioned above certain parameters, i.e. the coordination number, z and the order energy parameters χ, Ψ_{ij} do not depend on concentration. The exponential dependence of the interaction energies with temperature was used to remove artifacts present in the thermodynamic properties of liquid alloys calculated using R-K polynomial [69, 70]. But in our case, using a CFM, no artifacts were observed in such a way that we have made use of linear dependency of interaction energies with temperature [71]. The value of z is selected from the structural data and the order energy parameters are fitted from the thermodynamic data.

Figure 1 demonstrates calculations made using $\alpha = 1$ and $\beta = 3$ for $BiPb_3$ complex and $\alpha = 1$ and $\beta = 1$ for In-Pb complex. To a reasonable extent, the measured free energy of the mixing of liquid alloys indicates that these complexes are likely to occur in the liquid phase of the alloy. Both complexes

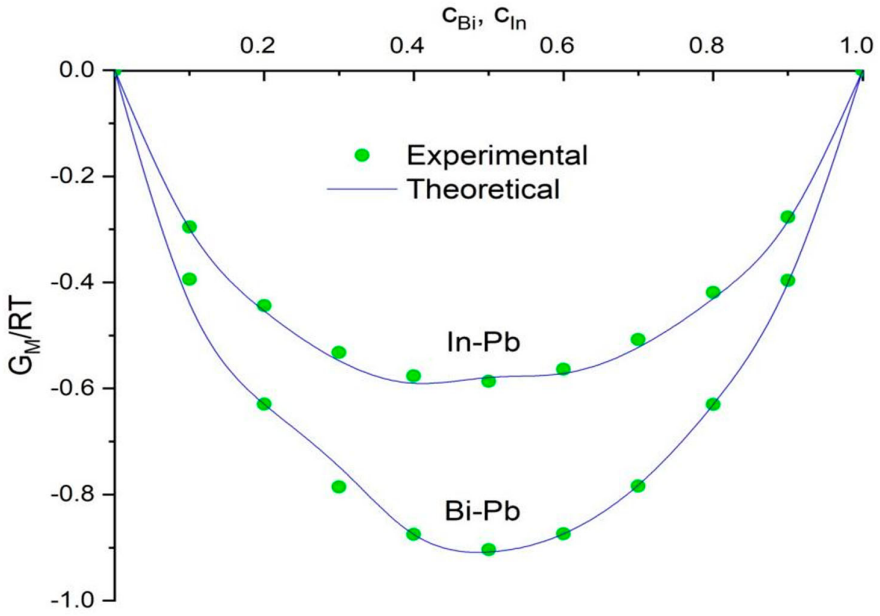

Figure 1. Free energy of mixing (G_M/RT) vs. bulk concentration for Bi-Pb and In-Pb alloys at 700 K and 673 K, respectively.

mentioned above show a good fit for the values of free energy at the given temperatures. We used experimental H_M values taken from Ref. [68] in conjunction with Equation (7) to fit the H_M versus concentration graph. Table 1 shows the values of the first derivatives of the interaction parameters with respect to temperature that give us the best fit for experimental H_M data. The values of H_M and S_M are in poor agreement with the experiment if energy parameters are taken as being temperature independent. We have, therefore, assumed the variation of these parameters with temperature to determine heat and entropy of formation with observed values [68]. Figure 2 illustrates that there is a good agreement between the experimental and calculated values of H_M/RT in both alloy systems. For the Bi-Pb system, the values of H_M/RT are negative throughout the whole concentration; this further confirms that Bi-Pb is a chemically favored system. However for In-Pb, the positive values of H_M/RT at all composition show that it is very weaker in complex formation than the previous system.

Table. 1 shows that only Ψ_{12} of the first system has a negative temperature coefficient between the two systems; all energy parameters have positive temperature coefficients. The same interaction parameters fitted for experimental values of G_M and H_M are further used to calculate S_M/R through Equation (9). Figure 3 shows the reasonable agreement between the experimental values and calculated values of S_M for both systems.

3.2. Surface properties

The surface compositions and surface tension values for Bi-Pb and In-Pb liquid alloys were computed numerically from the expressions in Equations (10) and (11). The partial excess free energy of

Table 1. Interaction parameters and their temperature derivatives.

System	α	β	χ/RT	Ψ_{12}/RT	Ψ_{23}/RT	Ψ_{13}/RT	$\frac{1}{R}\frac{\partial\chi}{\partial T}$	$\frac{1}{R}\frac{\partial\Psi_{12}}{\partial T}$	$\frac{1}{R}\frac{\partial\Psi_{13}}{\partial T}$	$\frac{1}{R}\frac{\partial\Psi_{23}}{\partial T}$
Bi-Pb	1	3	1.880	−0.887	−0.714	0.519	1.580	−0.150	0.500	0.900
In-Pb	1	1	0.730	0.480	1.376	1.230	1.110	9.500	0.650	0.500

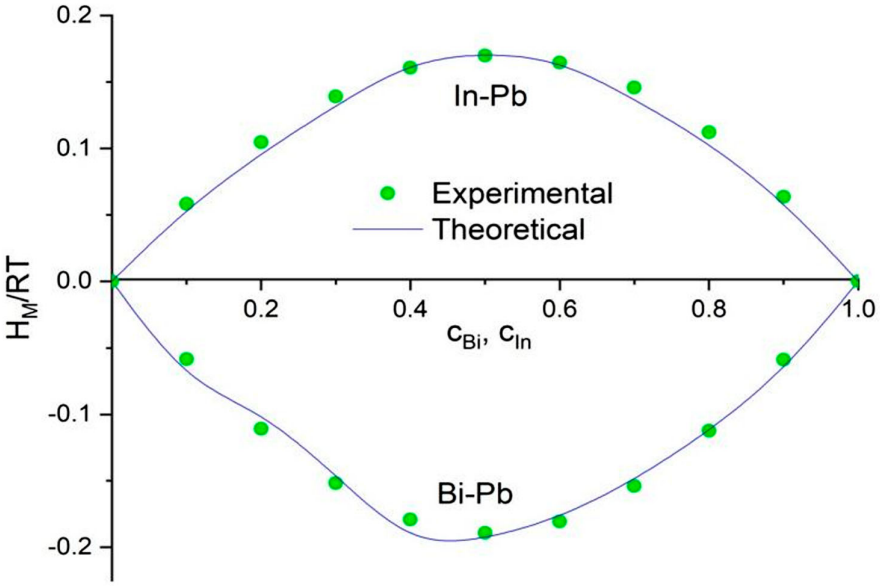

Figure 2. Heat of mixing (H_M/RT) vs. bulk concentration for Bi-Pb and In-Pb alloys at 700 K and 673 K, respectively.

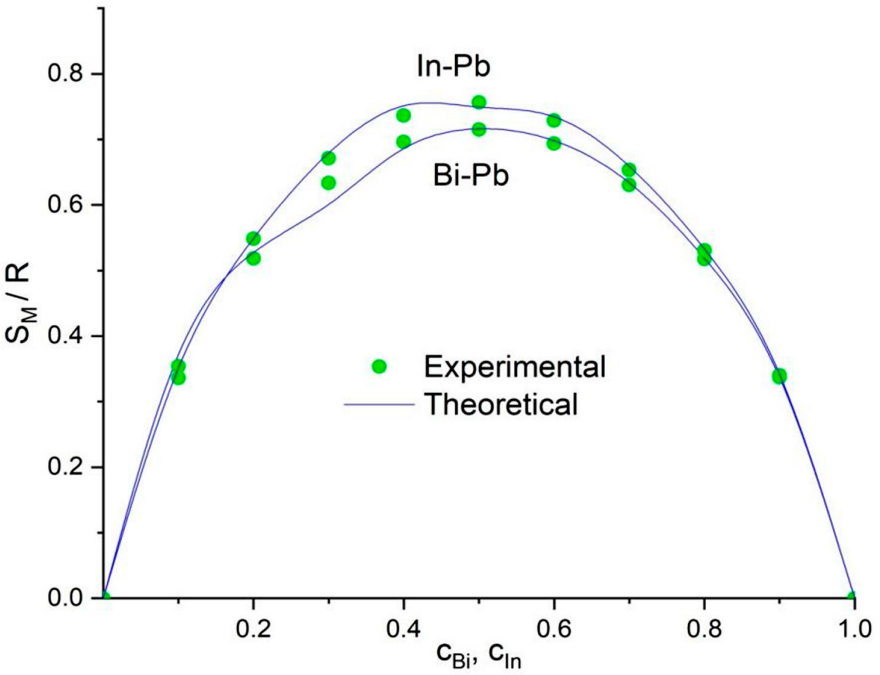

Figure 3. Entropy of mixing (S_M/R) vs. bulk concentration for Bi-Pb and In-Pb alloys at 700 K and 673 K, respectively.

Table 2. Input parameters for the calculation of surface tension and viscosity [72].

Element	$T_i^0(K)$	ρ_i^0 (kgm^{-3})	$\Delta\rho_i$(kgm$^{-3}K^{-1}$)	σ_i^0(Nm^{-1})	$\Delta\sigma_i$(Nm$^{-1}K^{-1}$)	η_i^0(Nsm^{-2})	E(J mol^{-1})
Bi	544	10,068	−1.33	0.378	-7×10^{-5}	4.458×10^{-4}	6450
In	429.6	7023	−0.6798	0.556	-9×10^{-5}	3.02×10^{-4}	6650
Pb	600	10,678	−1.3174	0.468	-1.3×10^{-4}	4.636×10^{-4}	8610

mixing in bulk (G_i^b) and partial excess free energy of mixing at the surface (G_i^s) for Bi, Pb and In in both alloys were taken from Ref. [68]. The surface tension (σ_i^0), density (ρ_i^0) at fixed temperature (T_i^0) of the components of the alloy system were taken from Ref. [72] (where i denote In, Pb and Mg) are presented in Table 2. However, to obtain surface tension and density at working temperatures of 700 K and 673 K for Bi-Pb and In-Pb, respectively, the relationship between the temperature dependence of the surface tension and the density of the liquid metals used is shown below.

$$\rho_i(T) = \rho_i^0 + (T - T_i^0)\Delta\rho_i \tag{22}$$

$$\sigma_i(T) = \sigma_i^0 + (T - T_i^0)\Delta\sigma_i \tag{23}$$

Here $\Delta\rho_i$ and $\Delta\sigma_i$ are the temperature coefficients of density and surface tension, respectively, for the metal component of the alloys, and T is the working temperature in Kelvins.

Variation of the surface concentration of Bismuth and Indium by their bulk concentration for both Bi-Pb and In-Pb liquid alloys is shown in Figure 4. The surface concentration plot for Bi-Pb alloy showed that there is a surface segregation of Bismuth in this alloy. Lead, on the other hand, segregates to the surface for the In-Pb alloy.

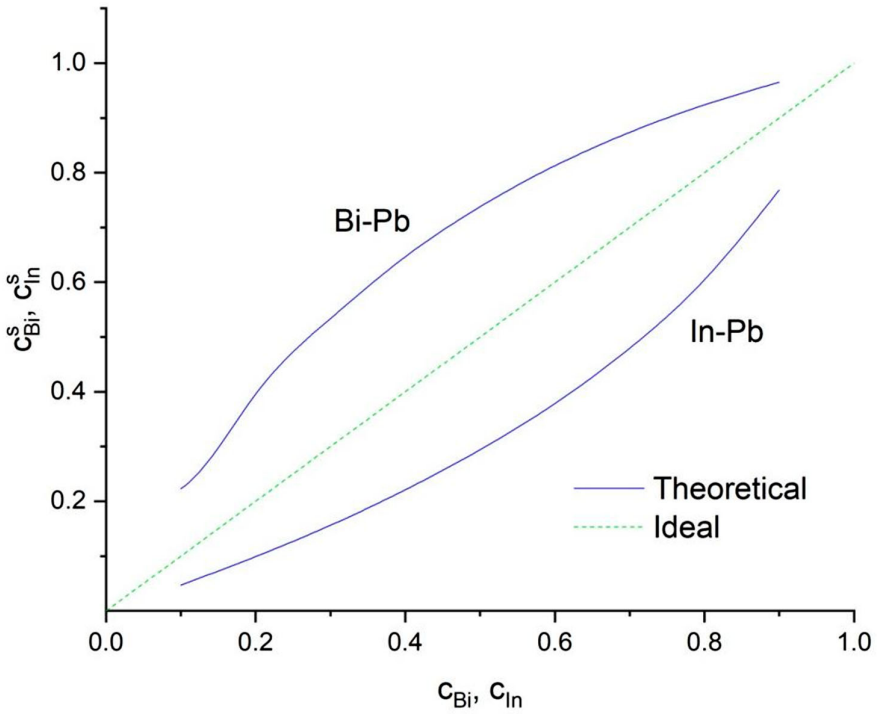

Figure 4. Surface concentrations (c^s_{Bi}, c^s_{In}) vs. bulk concentrations (c_{Bi}, c_{In}) for Bi-Pb and In-Pb alloys at 700 K and 673 K, respectively.

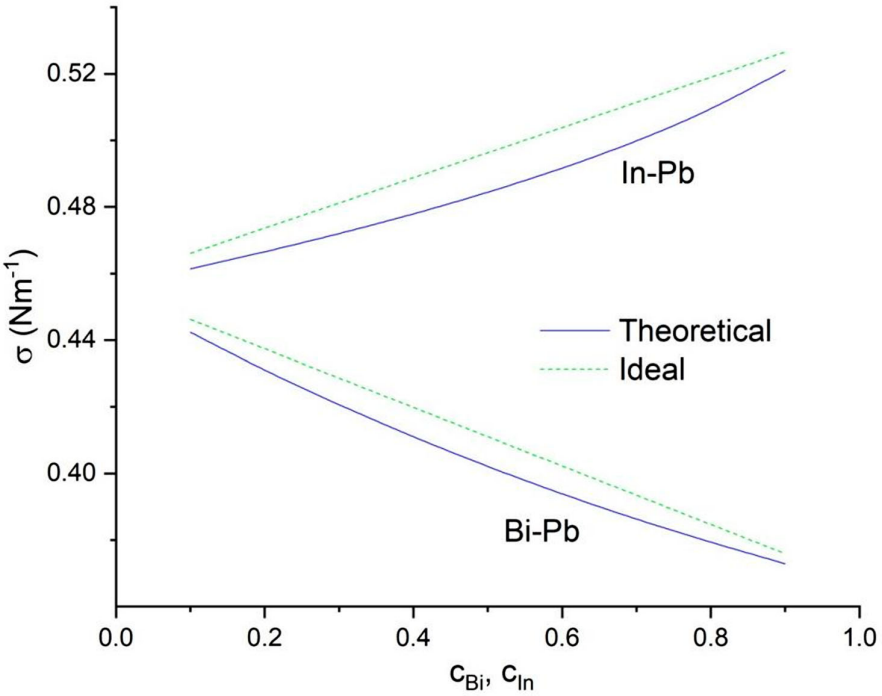

Figure 5. Surface tension (σ) vs. bulk concentration for Bi-Pb and In-Pb alloys at 700 K and 673 K, respectively.

Surface tension values for Bi-Pb and In-Pb liquid alloys over the entire bulk concentration range of the corresponding component are presented in Figure 5.

The surface tension values of Bi-Pb decrease with little addition of Bismuth atoms. The surface tension of Bi is less than that of Pb. As most Bismuth atoms migrate to the surface and populate it, the surface tension of the alloy reduces the value of Lead and approaches the surface tension value of pure Bismuth. An increase in surface tension with an increase in the bulk concentration of Indium was observed for In-Pb. The surface tension values increase with the bulk concentration and reach a largest value of about 0.5211 at 0.9 atomic fraction of indium, which is close to the surface tension of the individual indium component.

3.3. Structural properties

Due to the difficulties in diffraction experiments, the theoretical estimation of concentration fluctuations in the long wavelength limit $S_{cc}(0)$ is of great significance when the nature of the atomic interactions in the melt has to be investigated. We calculated $S_{cc}(0)$ and the Warren–Cowley short-range order parameter (α_1) using the energy parameters estimated from our earlier calculations. In general, for a liquid binary alloy, when $S_{cc}(0) > S^{id}_{cc}(0)$, the liquid alloy is said to be phase-segregating or exhibits homo-coordination. $S^{id}_{cc}(0)$ is the ideal value of $S_{cc}(0)$ which is associated with ideal mixture. When $S_{cc}(0) < S^{id}_{cc}(0)$, the liquid alloys have a tendency of compound formation or manifest the hetero-coordination. In addition, the chemical short-range order parameter (α_1) provides a measure of the degree of compound formation in the liquid alloy. The maximum value of α_1 is 1 which shows complete separation of alloy components, while the minimum value of α_1 is -1 which means complete ordering in a liquid alloy. The plots of $S_{cc}(0)$ and the chemical short-range order parameter (α_1) for Bi-Pb and In-Pb complexes are shown in Figures 6 and 7, respectively.

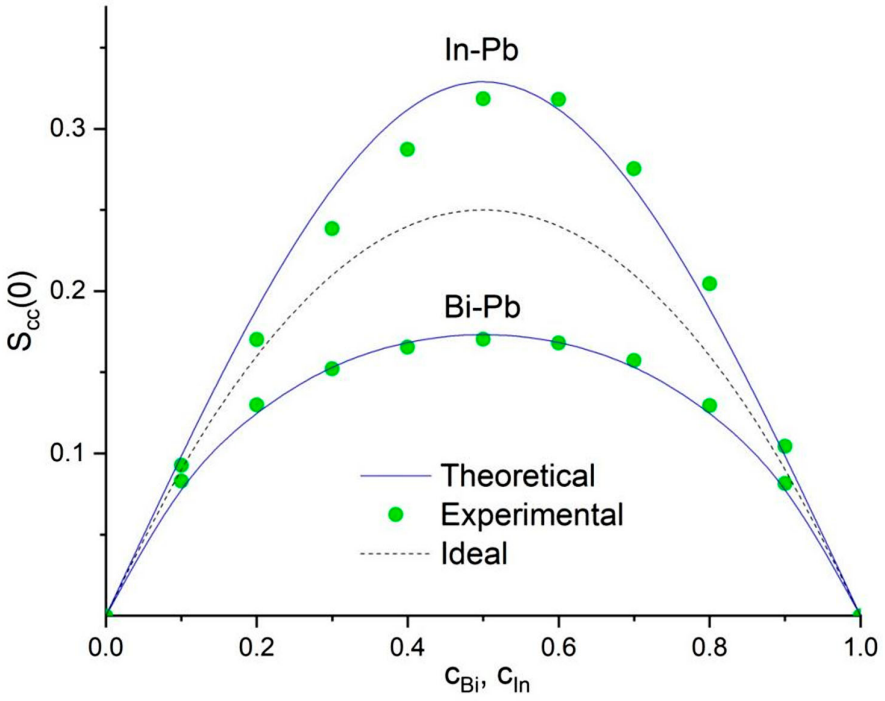

Figure 6. Concentration fluctuation at long wavelength limit ($S_{cc}(0)$) vs. bulk concentration for Bi-Pb and In-Pb alloys at 700 K and 673 K, respectively.

The lines are calculated values, while the points are experiment values calculated with Equation (14) using the activity data from Ref. [68] and the dashed line is for ideal values of $S_{cc}(0)$. Figure 6 shows that In-Pb is a phase-segregating almost the entire concentration range. This is supported by the chemical short-range order value, which has positive values throughout the entire region. For Bi-Pb liquid alloy, the computed $S_{cc}(0)$ values are smaller than the ideal values $S_{cc}^{id}(0)$ so the Bi-Pb liquid alloys have a good tendency for compound formation at all compositions. It can also be seen that α_1 values for Bi-Pb complex appear stronger with a minimum depth of $\alpha_1 = -0.0425$ at equiatomic composition. This strongly suggests that the first of the two Bi-Pb and In-Pb complexes have a higher tendency for complex formation.

3.4. Transport properties

Taking the necessary input data from Ref. [70, 72], the viscosity of the Bi-Pb liquid alloy at 700 K and the In-Pb alloy at 673 K is calculated out by Equation (18). The compositional dependency of the viscosity of both systems can be seen in Figure 8. The viscosity obtained for each alloy has opposite behavior. The viscosity value for Bi-Pb first increases with the bulk composition and achieves the highest value with the equiatomic composition. It decreases with a further rise in bismuth concentration. In the case of In-Pb, the viscosity isotherm almost displays the symmetric behavior with minima at $c_{In} = 0.5$. In comparison to the behavior seen in the previous one, the viscosity values for the In-Pb values decrease initially with the increase in corresponding composition. It is observed to decrease with more increase in concentration following equiatomic composition.

The computed values of $S_{cc}(0)$ for Bi-Pb and In-Pb were further used to evaluate the ratio of mutual diffusivities to intrinsic diffusivities (D_M/D_{id}) as a function of composition using Equation

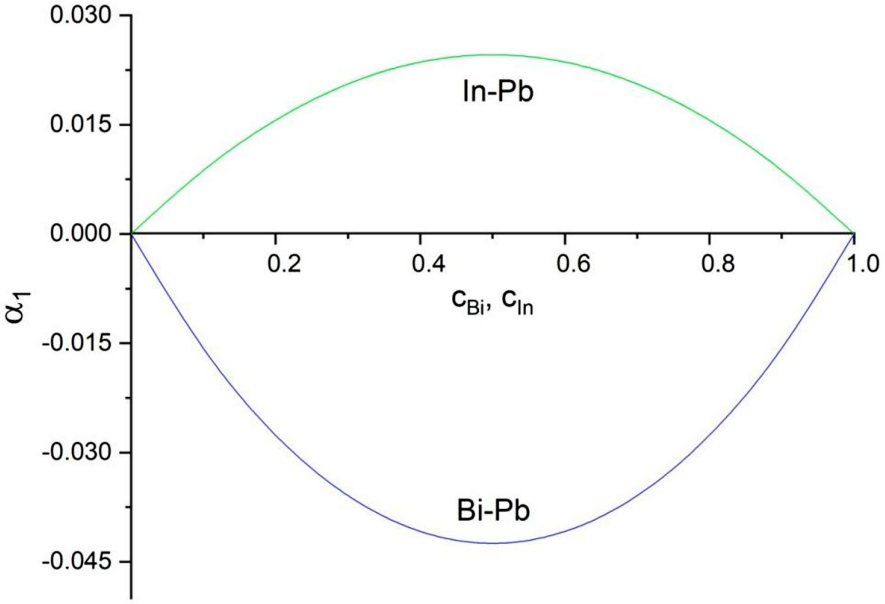

Figure 7. Chemical short-range order (α_1) vs. bulk concentration for Bi-Pb and In-Pb alloys at 700 K and 673 K, respectively.

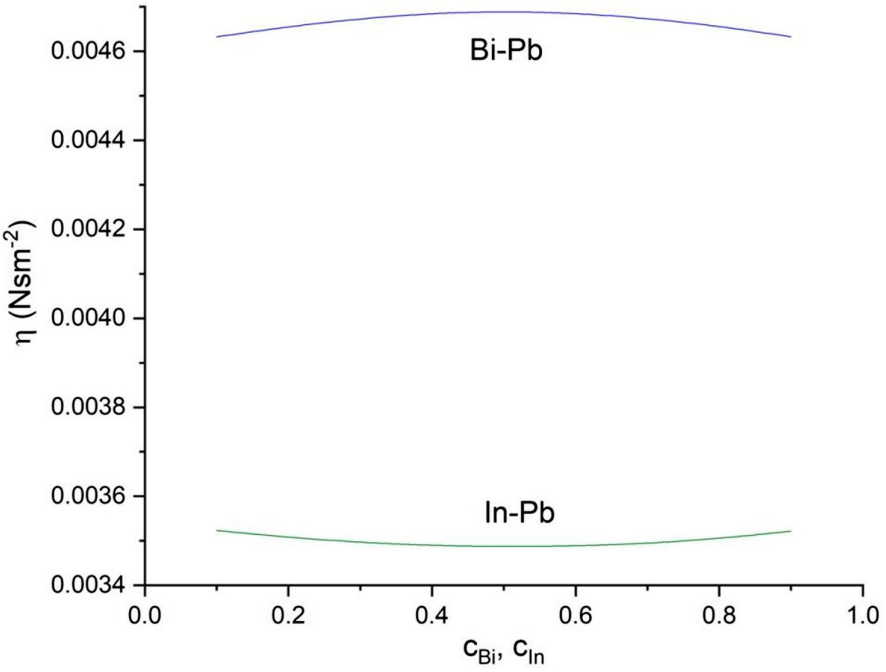

Figure 8. Viscosity (η) vs. bulk concentration for Bi-Pb and In-Pb alloys at 700 K and 673 K, respectively.

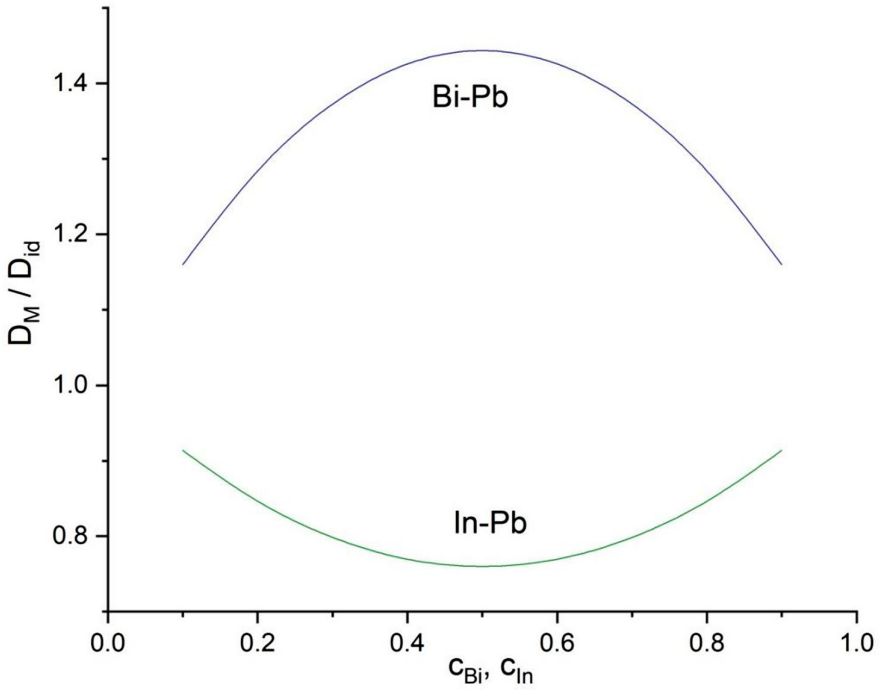

Figure 9. Ratio of mutual and intrinsic diffusion coefficients (D_M/D_{id}) vs. bulk concentration for Bi-Pb and In-Pb alloys at 700 K and 673 K, respectively.

(21). It is noted here that this ratio of diffusivities can also be used to indicate the level of order in a liquid binary alloy. If $D_M/D_{id} = 1$, the alloy has a regular mixture of components leading to the ideal solution. Hence $D_M/D_{id} > 1$ shows a tendency to hetero-coordination, while $D_M/D_{id} < 1$ shows a tendency to homo-coordination. The plots of D_M/D_{id} against concentration are presented in Figure 9.

The Bi-Pb alloy is stronger by better predicting the measured $S_{cc}(0)$. We, therefore, expect it to better emulate the other properties of the alloy. The values of D_M/D_{id} for Bi-Pb liquid alloy based on the energy parameters, due to the $BiPb_3$ complex, showed values that are greater than 1 throughout the concentration range. This undoubtedly showed that the Bi-Pb alloy is strongly compound-forming in the entire concentration range. For In-Pb, our calculated values of D_M/D_{id} suggest segregation throughout the whole composition range and, therefore, further support the very small tendency of compound formation in the alloy.

4. Conclusion

Thermodynamic and microscopic investigations of selected systems show that Bi-Pb alloys have a complex formation behavior, while the In-Pb system is undergoing phase separation. It has been observed that a component with a higher surface concentration, compared to its bulk concentration or a component with a lower surface tension segregates over the surface of the alloy. The evaluation of the coefficient of diffusion promotes the same tendency of the selected systems, as predicted in structural and thermodynamic properties. In the present study of viscosity, it is interesting to notice that both the alloys show symmetric behavior about equiatomic composition. However, in the case of variation with bulk composition, they exhibit opposite behavior.

Disclosure statement

No potential conflict of interest was reported by the author(s).

ORCID

Devendra Adhikari http://orcid.org/0000-0002-6022-3615

References

[1] Adhikari D, Jha IS, Singh BP. Structural asymmetry in liquid Fe-Si alloys. Philos Mag. 2010;90:2687–2694. DOI:10.1080/14786431003745302.
[2] Adhikari D, Singh BP, Jha IS. Structural and energetic anomaly in liquid Na–Sn alloys. J Mol Liq. 2012;167:52–56. DOI:10.1016/j.molliq.2011.12.010.
[3] Brillo J, Kolland G. Surface tension of liquid Al–Au binary alloys. J Mater Sci. 2016;51, DOI:10.1007/s10853-016-9794-x.
[4] Chatterjee SK, Prasad LC, Bhattarai A. Interionic pair potential and entropy of mixing of Al–Mg compound forming binary molten alloys. J Alloys Compd. 2010;496:100–104. DOI:10.1016/j.jallcom.2010.02.013.
[5] Egry I, Brillo J, Holland-Moritz D, et al. The surface tension of liquid aluminium-based alloys. Mater Sci Eng A. 2008;495:14–18. DOI:10.1016/j.msea.2007.07.104.
[6] Godbole RP, Jha SA, Milanarun M, et al. Thermodynamics of liquid Cu–Mg alloys. J Alloys Compd. 2004;363:187–193. DOI:10.1016/S0925-8388(03)00326-8.
[7] Jha IS, Koirala I, Singh BP, et al. Concentration dependence of thermodynamic, transport and surface properties in Ag–Cu liquid alloys. Appl Phys A. 2014;116:1517–1531.
[8] Jha N, Rafique SM, Mishra AK, et al. Thermodynamic properties and electrical resistivity of liquid MgZn alloys. Indian J Phys. 2001;75(A):519–523.
[9] Koirala I, Singh BP, Jha IS. Theoretical assessment on segregating nature of liquid In-Tl alloys. J Non Cryst Solids. 2014: 398–399. DOI:10.1016/j.jnoncrysol.2014.04.018.
[10] Koirala RP, Koirala I, Adhikari D. Energetics of mixing and transport phenomena in Cd-X (X = Pb, Sn) melts. Bibechana. 2017;15:113–120. DOI:10.3126/bibechana.v15i0.18751.
[11] Kumar A, Rafique SM, Jha N, et al. Structure, thermodynamic, electrical and surface properties of Cu–Mg binary alloy : complex formation model. Phys B. 2005;357:445–451. DOI:10.1016/j.physb.2004.12.031.
[12] Novakovic R, Giuranno D, Ricci E, et al. Bulk and surface properties of liquid Sb–Sn alloys. Surf Sci. 2011;605:248–255. DOI:10.1016/j.susc.2010.10.026.
[13] Akinlade O, Singh RN, Sommer F. Thermodynamics of liquid Al-Fe alloys. J Alloys Compd. 2000;299:163–168. DOI:10.1016/S0925-8388(99)00682-9.
[14] Novakovic R. Thermodynamics, surface properties and microscopic functions of liquid Al – Nb and Nb – Ti alloys. J Non Cryst Solids. 2010;356:1593–1598. DOI:10.1016/j.jnoncrysol.2010.05.055.
[15] Odusote Y.A., Hussain L.A., Awe O.E. Bulk and dynamic properties in Al–Zn and Bi–In liquid alloys using a theoretical model. J Non Cryst Solids. 2007;353:1167–1171. DOI:10.1016/j.jnoncrysol.2006.12.023.
[16] Prasad LC, Singh RN. Surface segrgation and concentration fluctuation at the liquid-vapor interface of molten Cu-Ni alloys. Phys Rev B. 1991;44:13768–13771.
[17] Sharma N, Thakur A, Ahluwalia PK. Thermodynamic, surface and transport properties of liquid Hg-Pb and Hg-In amalgams. J Mol Liq. 2013;188:104–112. DOI:10.1016/j.molliq.2013.10.004.
[18] Shrestha GK, Singh BK, Jha IS, et al. Optimization method for the study of the properties of Al-Sn binary liquid alloys. Phys B Condens Matter. 2017;514:1–7. DOI:10.1016/j.physb.2017.03.005.
[19] Sommer F. Thermodynamics of liquid alloys. Mater Sci Eng A. 1997;226:757–762.
[20] Yadav SK, Jha LN, Dhungana A, et al. Themo-Physical properties of Al-Mg alloy in liquid state at different temperatures. Mater Sci Appl. 2018;09:812–828. DOI:10.4236/msa.2018.910058.
[21] Yadav SK, Mehta U, Gohivar RK, et al. Reassessments of thermo-physical properties of Si-Ti melt at different temperatures. Bibechana. 2019;17:146–155. DOI:10.3126/bibechana.v17i0.26877.
[22] Anusionwu BC, Adebayo GA, Madu CA. Thermodynamics and surface properties of liquid Al–Ga and Al–Ge alloys. Appl Phys A. 2009;97:533–541. DOI:10.1007/s00339-009-5428-3.
[23] Attri KS, Ahluwalia PK, Sharma KC. Concentration fluctuations and thermodynamics of compound formation in mercury indium liquid alloy. Phys Chem Liq. 1994;26:225–235. DOI:10.1080/00319109408029495.
[24] Awe OE, Odusote YA, Hussain LA, et al. Temperature dependence of thermodynamic properties of Si–Ti binary liquid alloys. Thermochim Acta. 2011;519:1–5. DOI:10.1016/j.tca.2011.02.028.
[25] Bhatia AB, Hargrove WH. Concentration fluctuations and thermodynamic properties of some compound forming binary molten systems. Phys Rev B. 1974;10:3186–3196.

[26] Bhatia AB, Singh RN. Thermodynamic properties of compound forming molten alloys in a weak interaction approximation. Phys Chem Liq. 1982;11:343–351. DOI:10.1080/00319108208080755.
[27] Bhatia AB, Singh RN. A Quasi-lattice Theory for compound forming molten alloys. Phys Chem Liq. 1984;13:177–190. DOI:10.1080/00319108608078511.
[28] Boyo AO. The study of thermodynamic properties of liquid NaCs alloys. African J Sci Technol. 2005;6:73–80.
[29] Bhatia AB, Hargrove WH, Thornton DE. Concentration fluctuations and partial structure factors of compound-forming binary molten alloys. Phys Rev B. 1974;9:435–444. DOI:10.1103/PhysRevB.9.435.
[30] Koirala I, Jha IS, Singh BP. Theoretical investigation on ordering nature of Cd-Bi alloys in the molten state. Bibechana. 2014;11:70–78.
[31] Awe OE. Thermodynamic investigation of thermophysical properties of thallium-based liquid alloys. Phys Chem Liq. 2019;57:296–310. DOI:10.1080/00319104.2018.1443453.
[32] Prasad LC, Singh RN, Singh VN, et al. Correlation between bulk and surface properties of AgSn liquid alloys. J Phys Chem B. 1998;102:921–926. DOI:10.1021/jp971042l.
[33] Novakovic R, Giuranno D, Ricci E, et al. Surface and transport properties of In–Sn liquid alloys. Surf Sci. 2008;602:1957–1963. DOI:10.1016/j.susc.2008.03.033.
[34] Anusionwu BC, Adebayo GA. Mixing properties in the In-Pb and In-Mg liquid alloys. Phys B Condens Matter. 2010;405:880–887. DOI:10.1016/j.physb.2009.10.007.
[35] Kurata Y, Futakawa M, Kikuchi K, et al. Corrosion studies in liquid Pb-Bi alloy at JAERI: R & D program and first experimental results. J Nucl Mater. 2002;301:28–34. DOI:10.1016/S0022-3115(01)00720-6.
[36] Yu J, Zhang Y, Zu FQ, et al. The abnormal changes of electrical resistivity in liquid Pb-In alloys. Phys Chem Liq. 2006;44:401–408. DOI:10.1080/00319100600574127.
[37] Okajima K, Sakao H. On surface- and body-activities of components in the binary molten alloys. Trans Japan Inst Met. 1970;11:180–184. DOI:10.2320/matertrans1960.11.180.
[38] Jesser WA, Shneck RZ, Gile WW. Solid-liquid equilibria in nanoparticles of Pb-Bi alloys. Phys Rev B – Condens Matter Mater Phys. 2004;69:1–13. DOI:10.1103/PhysRevB.69.144121.
[39] Plevachuk Y, Sklyarchuk V, Gerbeth G, et al. Surface tension and density of liquid Bi-Pb, Bi-Sn and Bi-Pb-Sn eutectic alloys. Surf Sci. 2011;605:1034–1042. DOI:10.1016/j.susc.2011.02.026.
[40] Minic D, Zivkovic D, Zivkovic Z. Calorimetric investigation of the Pb–In binary system. Thermochim Acta. 2001;372:85–91. DOI:10.1016/S0040-6031(01)00443-9.
[41] Deloffre P, Balbaud-Célérier F, Terlain A. Corrosion behaviour of aluminized martensitic and austenitic steels in liquid Pb-Bi. J Nucl Mater. 2004;335:180–184. DOI:10.1016/j.jnucmat.2004.07.014.
[42] Bermúdez-Salguero C, Gracia-Fadrique J. Phase segregation at the liquid–air interface prior to liquid–liquid equilibrium. J Phys Chem B. 2015;119:10304–10315.
[43] Popović MP, Olmsted DL, Bolind AM, et al. A study of the effects of minor additives to Pb-Bi eutectic: designing novel Pb-Bi-X liquid alloys for heat transfer applications. Mater Des. 2018;159:240–251. DOI:10.1016/j.matdes.2018.08.044.
[44] Lukas HL. The Bi-Pb (Bismuth-Lead) system. Bull Alloy Phase Diagrams. 1980;1:67–70. DOI:10.1007/BF02881192.
[45] Awe OE, Odusote YA, Akinlade O, et al. Energetics of mixing in Bi-Pb and Sb-Sn liquid alloys. Phys B Condens Matter. 2008;403:2732–2739. DOI:10.1016/j.physb.2008.02.005.
[46] Ilinčev G. Research results on the corrosion effects of liquid heavy metals Pb, Bi and Pb-Bi on structural materials with and without corrosion inhibitors. Nucl Eng Des. 2002;217:167–177. DOI:10.1016/S0029-5493(02)00158-9.
[47] Odusote YA, Fayose OO, Odigie PJ. Mixing properties of X-Pb, (X = Cd, In) liquid binary alloys. J Non Cryst Solids. 2007;353:4666–4671. DOI:10.1016/j.jnoncrysol.2007.07.006.
[48] Fruehan RJ. Mass spectrometric determination of activities for alloys with complex vapor species: Bi-Pb and Bi-Tl. Metall Trans. 1971;2:1213–1218. DOI:10.1007/BF02664254.
[49] Awe OE, Akinlade O, Hussain LA. Thermodynamic investigations of Bi-Cd, In-Pb, and Ni-Pd liquid alloys. Zeitschrift Fuer Met Res Adv Tech. 2005;96:89–93. DOI:10.3139/146.018076.
[50] Klement W. Hexagonal close-packed structures in Bi-Pb alloys and the polymorphism of lead at high pressure. J Chem Phys. 1963;38:298–299. DOI:10.1063/1.1733654.
[51] King M, Ramachandran V, Prengaman RD, et al. Updated by staff, lead and lead alloys. Kirk-Othmer Encycl Chem Technol. 2005;14, DOI:10.1002/0471238961.1205010411091407.a01.pub2.
[52] Fratesi R, Roventi G, Maja M, et al. Electrodeposition of lead alloys from fluoborate baths. J Appl Electrochem. 1984;14:505–510. DOI:10.1007/BF00610816.
[53] Barbin N, Terentiev D, Alexeev S, et al. Thermodynamic modeling of the Pb + Bi melt evaporation under various pressures and temperatures. Comput Mater Sci. 2013;66:28–33. DOI:10.1016/j.commatsci.2012.06.013.
[54] Jha IS, Singh RN, Srivastava PL, et al. Stability of HgNa and HgK liquid alloys, philos. Mag. B phys. condens. matter; stat. mech. electron. Opt Magn Prop. 1990;61:15–24. DOI:10.1080/13642819008208649.
[55] Novakovic R, Ricci E, Giuranno D, et al. Thermodynamics and surface properties of liquid Bi–In alloys. CALPHAD. 2009;33:69–75. DOI:10.1016/j.calphad.2008.09.002.

[56] Novakovic R, Tanaka T, Muolo ML, et al. Bulk and surface properties of liquid Ag–X (X = Ti, Hf) compound forming alloys. Surf Sci. 2005;591:56–69. DOI:10.1016/j.susc.2005.06.022.
[57] Singh RN. Free energy and heat of mixing of alloys. J Phys F Met Phys. 1981;11:389–396. DOI:10.1088/0305-4608/11/2/011.
[58] Iida Takamichi IL, Rodericj G. The physical properties of liquid metals. Oxford University Press; 1988.
[59] Butler JAV. The Thermodynamics of the surfaces of solutions. R Soc A. 1932: 348–375. DOI:10.1098/rspa.1983.0054.
[60] Moser Z, Gasior W, Gasior J, et al. Surface tension of liquid Ag-Sn alloys: experiment versus modeling. J Phase Equilib. 2001;22(3):254–258.
[61] Bhatia AB, Thornton DE. Structural aspects of the electrical resistivity of binary alloys. Phys Rev B. 1970;2:3004–3012. DOI:10.1103/PhysRevB.2.3004.
[62] Warren BE. X-ray diffraction. New York: Dover Publication; 1990.
[63] Cowley JM. An approximate theory of order in alloys. Phys Rev. 1950;77:669–675. DOI:10.1103/PhysRev.77.669.
[64] Singh RN, Pandey DK, Sinha S, et al. Thermodynamic properties of molten salt solutions. Phys B. 1987;145:358–364. DOI:10.1007/978-94-009-3863-2_2.
[65] Budai I, Benkő MZ, Kaptay G. Comparison of different theoretical models to experimental data on viscosity of binary liquid alloys. Mater Sci Forum. 2007;537-538:489–496.
[66] Zhang F, Wen S, Liu Y, et al. Modelling the viscosity of liquid alloys with associates. J Mol Liq. 2019;291:111345.
[67] Darken LS, Gurry RW. Physical chemistry of metals. New York: McGraw Hill; 1953.
[68] Hultgren R, Desai PD, Hawkins DT, et al. Selected values of the thermodynamic properties of binary alloys. Metal Park, OH: American Society for Metals; 1973.
[69] Kaptay G. A coherent set of model equations for various surface and interface energies in systems with liquid and solid metals and alloys. Adv Colloid Interface Sci. 2020;283:102212.
[70] Kaptay G. The exponential excess Gibbs energy model revisited. Calphad. 2017;56:169–184.
[71] Bhandari IB, Koirala I, Adhikari D. Temperature-dependent mixing behaviours of Bi-Mg liquid alloys. Phys Chem Liq. 2020:1–14. https://doi.org/10.1080/00319104.2020.1863402.
[72] Brandes EA, Brook GB. Smithells Metals reference book, seventh, Butterw orth-Heinemann Linacre House. Oxford: Jordan Hill; 1992; DOI:10.1016/B978-075067509-3/50014-2.

Complex formation of sodium-mercury alloy at molten state

Journal of Physics Communications

PAPER

Complex formation of sodium-mercury alloy at molten state

N Panthi[1,2], I B Bhandari[1] and I Koirala[1,*]

[1] Central Department of Physics, Tribhuvan University, Kirtipur, Nepal
[2] Department of Physics, Patan Multiple Campus, Tribhuvan University, Nepal
[*] Author to whom any correspondence should be addressed.

E-mail: ikphysicstu@gmail.com

Keywords: complex formation, sodium-mercury alloy, molten state

OPEN ACCESS

RECEIVED
4 March 2021

REVISED
15 July 2021

ACCEPTED FOR PUBLICATION
22 July 2021

PUBLISHED
6 August 2021

Abstract

Thermodynamic properties of compound forming binary liquid sodium-mercury alloy at temperature 673 K have been analyzed as a function of concentration by considering $NaHg_2$ complex using quasi chemical approximation. The surface tension of the alloy has been studied by the compound formation model, Butler equation as improved by Kaptay, and Statistical mechanical approach. The mixing behavior of the alloy is studied in detail with more emphasis on the interaction energy parameters between neighboring atoms of the alloy. The study provides the information of moderately interacting as well as ordering nature on the entire range of concentration of the liquid alloy and the computed theoretical thermodynamic data are in good agreement with the corresponding experimental data at 673 K. The surface tension of the alloy computed predicts deviation from the ideal case.

1. Introduction

In metallurgical science, alloys are considered superior to individual metals due to their high mechanical strength, chemical resistance, and heat resistance. The formation of an alloy is due to the interaction and structural rearrangement of constituent atoms so that the chemical properties of each constituent element are repressed and new properties are evolved. Most of the alloys are far away from the ideal solution and show the micro-inhomogenous atomic arrangement and hence are difficult to realize as compared to the crystals. The mixing property of the alloy is mainly governed by the electrochemical effect, size of atoms and the concentration of constituent elements so that atoms of individual elements either tend to align showing self-coordinated tendency or a strong ordering tendency [1]. Thus the understanding of the mixing behavior of metals forming alloys has been of great interest to metallurgists and physicists. However, materials remained uninvestigated due to experimental difficulties and time constraints. In order to solve such problems, different theoretical models have been developed.

Alloys are widely used in industries as commercial materials and hence studied extensively in solid-state. The properties of the initial melt of mixing play a vital role in the formation of alloys. Various properties of the alloys in the liquid state are studied in metallurgy as well as for the discovery of new materials for high-temperature application.

Among the various alloys, sodium mercury alloy (sodium amalgam) is of great interest to researchers [2–8] where most of the studies are focused on thermodynamic properties at specified temperatures. It is used as a strong reducing agent in reactions. It is also used in the design of high-pressure sodium lamps where sodium and mercury produce the proper color and electrical characteristics respectively. The production of alkali and chlorine by electrolysis process with liquid mercury as a cathode is considered to be one of the important applications of sodium amalgam [9].

There are a number of solid intermetallic compounds of sodium amalgam. Balej [4] has suggested sodium concentration in the liquid amalgams below 18%, viz: $NaHg_4$, $NaHg_5$, $NaHg_6$, $NaHg_7$, $NaHg_8$, $NaHg_{10}$, $NaHg_{12}$ and $NaHg_{14}$. Similarly, mercury and sodium form a congruently melting compound in the form of $NaHg_2$ (mp. 626 K) [9]. It shows negative deviation from Raoult's law and also shows anomalous behavior that

some of its equilibrium mixing properties such as free energy of mixing, enthalpy of mixing, entropy of mixing, and concentration fluctuation in long-wavelength limit at 673 K are asymmetric at equiatomic composition. The alloys showing such behavior are usually known as compound forming binary alloys at one or more defined compositions [10].

The present work aims to study Na − Hg alloy theoretically to determine concentration-dependent thermodynamic properties at 673 K assuming $NaHg_2$ complex in the melt by using quasi chemical approximation [11] and study of surface tension by the compound formation model developed by Novakovic *et al* in which connection between surface and bulk properties has been developed through the grand partition functions[12] by the consideration of interaction energy parameters as that of the aforementioned method. Due to lack of experimental data, we intend to compare surface tension thus obtained with other two models: the Butler model as improved by Kaptay [13] and the Statistical approach [14].

The model used in the study assumes an alloy as a pseudo ternary mixture of X atoms, Y atoms, and $X_\mu Y_\nu$ group of atoms (μ and ν are small integers) of an energetically favored compound forming alloys all in chemical equilibrium with each other. The equilibrium properties of mixing binary alloy are governed by short-range atomic interaction energies ε_{XX}, ε_{YY} and ε_{XY} for *XX*, *YY*, and *XY* atomic pairs respectively [15]. Based on the pairing of atoms of the constituent elements, the alloys can be classified into two main categories, segregating where like atoms tend to be the nearest neighbor and the compound forming alloys (ordering) where unlike atoms tend to be the nearest neighbor.

The thermodynamic properties such as free energy of mixing, chemical activity, heat of mixing, and entropy of mixing, provide the information on the interaction, stability, and bonding strength among the constituent atoms of alloy whereas information on the structural ordering of atoms in binary alloys in the liquid state is provided by the quantitative analysis of microscopic functions., the concentration fluctuations in the long-wavelength limit ($S_{CC}(0)$), short-range order parameter (α_1) [16]. The surface tension is one of the important thermophysical properties studied in metallurgy to get the information of surface property of liquid alloy and is important in the casting process for getting different devices for better mechanical performance. Further, surface segregation, which mainly refers to the inequality in concentration between the surface and that of bulk materials of the alloy, is one of the important factors of the alloy which is to be studied in metallurgical science. The reason for this inequality is the difference in surface energy between the constituent elements of the alloy where the element with smaller surface energy has the tendency to segregate on the surface [17].

The organization of this paper is as follows. In section 2, the expressions required for the calculation are presented. In section 3, the result and general discussion of Na-Hg alloy are presented. Finally, the conclusions are presented in section 4.

2. Theoretical basis

2.1. Thermodynamical functions

Consider a binary alloy of N number of atoms with elements *X* and *Y*.The model (QCA) considers the existence of chemical complexes $X_\mu Y_\nu$ where

$$\mu X + \nu Y = X_\mu Y_\nu \tag{1}$$

With this consideration, grand partition function in terms of configurational energy '*E*' is simplified and excess free energy of mixing (G_M^{XS}) at temperature T is expressed as

$$G_M^{XS} = Nk_B T \int_0^C \Upsilon dc \tag{2}$$

Where Υ is ratio of activity coefficient of element $_X$ to $_Y$, $_C$ is the concentration of *X* atoms.

After simple mathematical calculation [11] the solution of equation (2) is given below.

$$G_M^{XS} = N[\theta\omega + \theta_{XY}\Delta\omega_{XY} + \theta_{XX}\Delta\omega_{XX} + \theta_{YY}\Delta\omega_{YY}] \tag{3}$$

Where $\theta = C(1 - C)$ and $\theta_{j,k}'s(j.k = X, Y)$ are the simple polynomials in C depending on the values of *X* and *Y*, $\theta\{=Z\varepsilon_{xy} - (\varepsilon_{XX}/2 + \varepsilon_{YY}/2)\})\}$ is interchange energy, $\Delta\omega_{jk}(=Z\Delta\varepsilon_{jk})$ are interaction energy parameters and *Z* is coordination number.

For $X =$ Na, $Y =$ Hg, $\mu = 1$, $\nu = 2$, the values of $\theta_{j,k}'s$ are found to be [11]

$$\theta_{XY}(c) = \frac{1}{6}C + C^2 - \frac{5}{3}C^3 + \frac{1}{2}C^4 \tag{4}$$

$$\theta_{XX}(C) = 0 \tag{5}$$

$$\theta_{YY}(C) = -\frac{1}{4}C + \frac{1}{2}C^2 - \frac{1}{4}C^4 \tag{6}$$

The Free energy of mixing for the complex alloy is given by

$$\begin{aligned} G_{\mathrm{M}} &= G_{\mathrm{M}}^{XS} + G_{\mathrm{M}}^{\mathrm{ideal}} \\ &= G_{\mathrm{M}}^{XS} + RT[C\ln C + (1-C)\ln(1-C)] \\ &= N[\theta\omega + \theta_{XY}\Delta\omega_{XY} + \theta_{XX}\Delta\omega_{XX} + \theta_{YY}\Delta\omega_{YY}] \\ &\quad + RT[C\ln C + (1-C)\ln(1-C)] \end{aligned} \tag{7}$$

Here θ_{XX} is taken zero because according to the model, for $\mu = 1$, the probability of X and X (or XX) pair to be part of the complex is zero so that the coefficient of $\frac{\Delta\omega_{XY}}{k_{\mathrm{B}}T}$ in equation (7) also tends to zero. If there are not complexes in the alloy then $\Delta\omega_{jk}$ is zero. In such case, the above equation takes the form as,

$$G_{\mathrm{M}} = N\theta\omega + RT[C\ln C + 1 - C\ln(1-C)] \tag{8}$$

The heat of mixing is found out by using standard thermodynamic relation:

$$\begin{aligned} H_{\mathrm{M}} &= G_{\mathrm{M}} - T\left(\frac{dG_{\mathrm{M}}}{dT}\right)_p \\ &= N\left[\begin{array}{c} \theta\left(\omega - T\frac{d\omega}{dT}\right) + \theta_{XY}\left(\theta\omega_{XY} - T\frac{d\Delta\omega_{XY}}{dT}\right) + \\ \theta_{XX}\left(\theta\omega_{XX} - T\frac{d\Delta\omega_{XX}}{dT}\right) + \theta_{YY}\left(\theta\omega_{YY} - T\frac{d\Delta\omega_{YY}}{dT}\right) \end{array}\right] \end{aligned} \tag{9}$$

The standard thermodynamic relation for the entropy of mixing is

$$S_{\mathrm{M}} = \frac{H_{\mathrm{M}}}{T} - \frac{G_{\mathrm{M}}}{T} \tag{10}$$

The activity of the constituent elements in the alloys is determined from following standard thermodynamic relation.

$$RT\ln a_j(j = X, Y) = G_{\mathrm{M}} + (1-C)\left[\frac{\partial G_{\mathrm{M}}}{\partial C_j}\right]_{T,P,N} \tag{11}$$

By solving equations (7) and (11), the theoretical values of activities of each component are given as follows,

$$RT\ln a_X = \frac{G_{\mathrm{M}}}{RT} + \frac{1-C}{k_{\mathrm{B}}T}\left[(1-2C)\omega + \theta'_{XY}\Delta\omega_{XY} + \theta'_{XX}\Delta\omega_{XX} + \theta'_{YY}\Delta\omega_{YY} + \ln\frac{C}{1-C}\right] \tag{12}$$

$$RT\ln a_Y = \frac{G_{\mathrm{M}}}{RT} - \frac{C}{k_{\mathrm{B}}T}\left[(1-2C)\omega + \theta'_{XY}\Delta\omega_{XY} + \theta'_{XX}\Delta\omega_{XX} + \theta'_{YY}\Delta\omega_{YY} + \ln\frac{C}{1-C}\right] \tag{13}$$

Where θ'_{XY}, θ'_{XX} and θ'_{YY} are concentration derivatives of θ_{XY}, θ_{XX} and θ_{YY} respectively.

2.2. Microscopic functions

The concentration fluctuation in long-wavelength limit for the alloy is derived from standard relation as [18].

$$S_{CC}(0) = RT\left[\frac{\partial^2 G_{\mathrm{M}}}{\partial C^2}\right]^{-1}_{T,P,N} \tag{14}$$

The value of $S_{CC}(0)$ can be obtained by using observed activities as

$$S_{CC}(0) = C_Y a_X\left[\frac{\partial a_X}{\partial C_Y}\right]^{-1}_{T,P,N} = C_X a_Y\left[\frac{\partial a_Y}{\partial C_Y}\right]^{-1}_{T,P,N} \tag{15}$$

Where $C_X (=C)$ and $C_Y (=1-C)$ are concentrations of elements X and Y respectively. The values of $S_{CC}(0)$ obtained from equation (15) are called experimental values.

Solving equations (7) and (14), the theoretical value of $S_{CC}(0)$ is found as follows.

$$S_{CC}(0) = \frac{C(1-C)}{1 + (1-C)\left[-2\frac{\omega}{k_{\mathrm{B}}T} + \theta''_{XY}\frac{\theta\omega_{XY}}{k_{\mathrm{B}}T} + \theta''_{XX}\frac{\theta\omega_{XX}}{k_{\mathrm{B}}T} + \theta''_{YY}\frac{\theta\omega_{YY}}{k_{\mathrm{B}}T}\right]} \tag{16}$$

Where θ''_{jk} is the second derivative of θ_{jk} with respect to concentration.

The Warren-Cowley short-range order parameter [19, 20] is related to concentration fluctuation in the long-wavelength limit as,

$$\alpha_1 = \frac{L-1}{L(Z-1)+1} \tag{17}$$

Where,

$$L = \frac{S_{CC}(0)}{S_{CC}^{id}(0)} \tag{18}$$

2.3. Surface tension

The surface tension is considered as an important factor in metallurgy for the processes such as molten-metal processing, fusion-welding, soldering, etc. in which liquid alloy or metal is involved. It concerns the problems related to the surface and interface in the liquid metal process [21, 22]. The interfacial motion caused by the surface tension of liquid plays a major role in many industrial phenomena and hence the surface and interfacial behavior of liquid metals are considered to have importance in metallurgical processes for solidification, controlling the processes of welding and casting [23].

In the present work, we try to study the surface tension of Na−Hg alloy at 673 K by using three different models: compound formation model improved Butler equation and Statistical mechanical approach.

2.3.1. Compound formation model

The model assumes the compound forming tendency in the binary liquid alloy in the form of short-ranged volume elements due to the formation of intermetallic compound $(X_\mu Y_\nu)$ in the melt like that of a compound forming tendency in solid-state. The equation of surface tension (σ) at temperature T is given below.

$$\begin{aligned}\sigma = \sigma_X + \frac{K_B T}{\rho} ln \frac{C_X^S}{C_X} + \frac{\omega}{\rho}[p(\varphi^S - \varphi) - q\varphi] \\ + \frac{\Delta\omega_{XY}}{\rho}[p(\varphi_{XY}^S - \varphi_{XY}) - q\varphi_{xy}] + \frac{\Delta\omega_{YY}}{\rho}[p(\varphi_{YY}^S - \varphi_{YY}) - q\varphi_{YY}]\end{aligned} \tag{19}$$

$$\begin{aligned}= \sigma_Y + \frac{K_B T}{\rho} \ln \frac{C_Y^S}{C_Y} + \frac{\omega}{\rho}[p(f^S - f) - qf] \\ + \frac{\Delta\omega_{XY}}{\rho}[p(f_{XY}^S - f_{XY}) - qf_{XY}] \\ + \frac{\Delta\omega_{YY}}{\rho}[p(f_{YY}^S - \varphi_{YY}) - qf_{YY}]\end{aligned} \tag{20}$$

Where σ_j and C_j^S (j = X, Y) are surface tensions and surface concentration of pure component X and Y respectively. Similarly φ, f, φ_{jk} and f_{jk} are bulk concentration functions and φ^S, f^S, φ_{jk}^S and f_{jk}^S are surface concentration functions. p and q are surface coordination fractions that indicate the fraction of the number of nearest neighbors of an atom within its own layer and adjoining layers respectively and are related as $p + 2q = 1$. For a closed packed crystal, $p = 1/2$ and $q = 1/4$. ρ is the mean surface area of the alloy and is calculated by:

$$\rho = \sum_j C_j \rho_j \tag{21}$$

with the surface area of each component ρ_j is given as [12]:

$$\rho_j = 1.012\left(\frac{V_j}{N_{Av}}\right)^{\frac{2}{3}} \tag{22}$$

Where $V_j$is the molar volume of pure metal and N_{Av} is Avogadro's number.

For $\mu = 1$ and $\nu = 2$, the bulk concentration functions are:

$$\varphi = C^2 \tag{23}$$

$$\varphi_{XY} = \frac{1}{6} + 2(1-C) - 6(1-C)^2 + \frac{16}{3}(1-C)^3 - \frac{3}{2}(1-C)^4 \tag{24}$$

$$\varphi_{YY} = -\frac{1}{4} + (1-C) - \frac{1}{2}(1-C)^2 + (1-C)^3 - \frac{3}{4}(1-C)^4 \tag{25}$$

$$f = (1-C)^2 \tag{26}$$

$$f_{XY} = -(1-C)^2 + \frac{10}{3}(1-C)^3 - \frac{3}{2}(1-C)^4 \tag{27}$$

$$f_{YY} = -\frac{1}{2}(1 - C)^2 + \frac{3}{4}(1 - C)^4 \tag{28}$$

The surface concentration functions φ^S, φ^S_{jk}, , f^S and f^S_{jk} are obtained from equations (23) to (28) by replacement of bulk concentration C by surface concentration C^S.

2.3.2. Improved butler equation

It is the layered interface concept that assumes the existence of a monoatomic layer (called surface monolayer) at the surface of a liquid as a separate phase and is in thermodynamic equilibrium with the bulk phase. The equation for binary liquid alloy at temperature T is given as:

$$\sigma = \frac{A^0_j}{A_i}\sigma_j + \frac{RT}{A_j}\ln\frac{C^S_i}{C^b_i} + \frac{G^{S,XS}_j - G^{b,XS}_j}{A_j} \tag{29}$$

Where A^0_j is the molar surface area of pure liquid metal, A_j is the partial molar surface area of component i respectively. $G^{S,XS}_j$, and $G^{b,XS}_j$ are the partial excess free energy of mixing in the surface and bulk of constituent components of the alloy, respectively

The molar surface area of each pure component j is given as [24].

$$A^0_j = g(V_j)^{2/3}(N_{Av})^{1/3} \tag{30}$$

Where g is geometrical constant and is given as,

$$g = \left(\frac{3f_V}{4}\right)^{2/3}\frac{\pi^{1/3}}{f_s} \tag{31}$$

Where f_V and f_S are volume packing fraction and surface packing fraction respectively. Their values are based on the crystal structure type of every pure component of the alloy. For liquid metal the values of f_V and f_S are 0.66 and 0.906 respectively [24].

2.3.3. Statistical mechanical approach

This method is also based on the layered structure concept near the interface and assumes a surface monolayer, as well as the layer just below the surface layer that bridges the surface monolayer to the bulk solution [25]. The model relates the surface tension to thermodynamic properties through interchange energy (ω) and activity coefficients (γ_j) between the elements of the alloy. The equation at temperature T is given as below.

$$\sigma = \sigma_j + \frac{k_B T}{\rho}\ln\frac{C^S_j}{\gamma_j C_j} + [p(1 - C^S_j)^2 + q(1 - C_j)^2]\frac{\omega}{\rho} \tag{32}$$

3. Results and discussion

3.1. Thermodynamic properties

The properties of binary liquid alloys depend on temperature, concentration, and pressure. The study of the binary alloy Na − Hg was carried out as a function of the concentration of the alloy at fixed atmospheric pressure and a temperature 673 K. For the calculations of thermodynamic as well as structural properties of liquid alloy by quasi chemical approximation, the main work is to calculate the interchange energy (ω) and interaction energy parameters ($\Delta\omega_{jk}$). During the calculation of parameters, no any statistical method like mean square deviation is applied in order to decide the best fit so that the parameters used here are considered as reasonable for the study. For the sake of consistency, the same theoretical parameters have been considered throughout the calculations of other mixing properties. The different results thus obtained from the study are outlined in the section below.

We utilized equations (7), (9), (10), (11), and (12) for the analysis of the thermodynamic property. For the free energy of mixing, the interaction energy parameters are determined by successive approximation method for a couple of concentrations, following the stoichiometry of the $NaHg_2$ by the help of experimental values in the concentration range (0.1 to 0.9) [26]. The approximate values of the parameters are as follows.

$$\frac{\omega}{k_B T} = -10.524\ ,\ \frac{\Delta\omega_{XY}}{k_B T} = 2.714,\ \frac{\Delta\omega_{YY}}{k_B T} = 9.987$$

The plot of free energy of mixing versus concentration of sodium (C_{Na}) is shown in figure1. The computed and experimental values of G_M/RT are in good agreement. The theoretical value of free energy of mixing is minimum $1.102RT$ at 0.4 concentration of Na. The theoretical calculation of free energy of mixing shows that

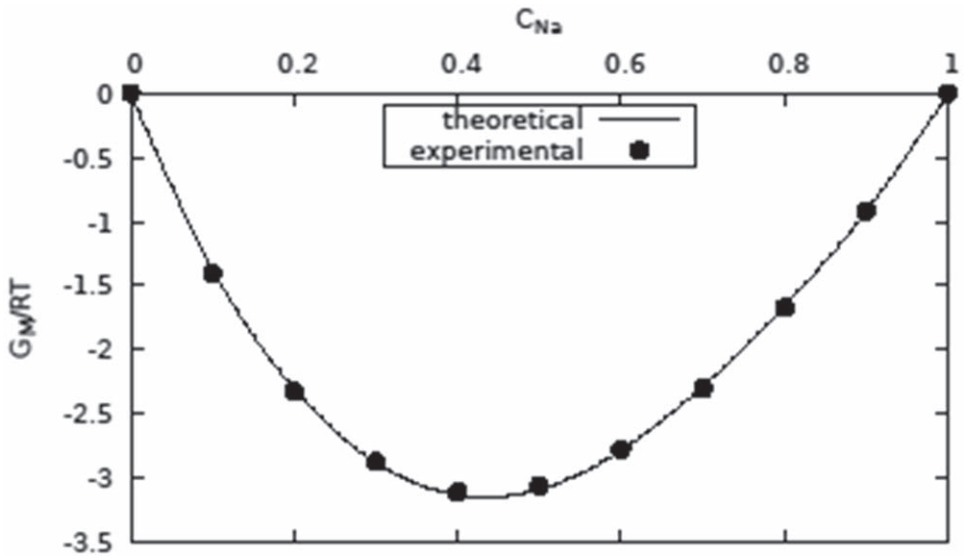

Figure 1. Gibb's free energy of mixing versus concentration of Na at 673 K.

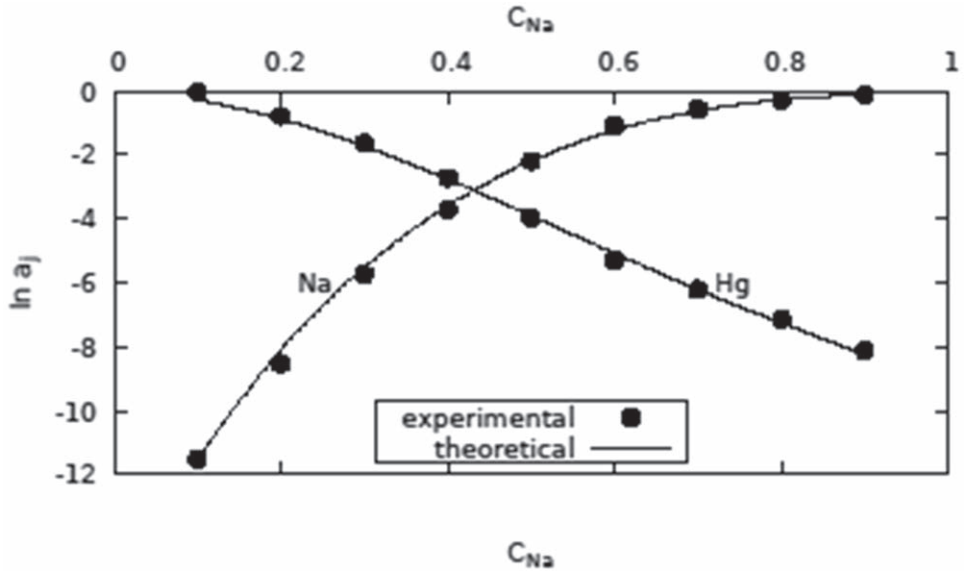

Figure 2. Chemical activity versus concentration of Na at 673K.

the alloy Na − Hg in the liquid state is moderately interacting and hence the tendency of compound formation is not so strong.

The deviation from the ideal behavior of alloy can be explained by chemical activities, a measure of effective concentration in the mixture, as its magnitude depends on the interaction of constituent binary components of the alloy. Equations (12) and (13) are used for the theoretical calculation of the chemical activity of constituent elements of alloy Na − Hg. Figure 2 shows the observed and theoretical value of the chemical activity of the alloy. There is good agreement between experimental and theoretical value of activities of Na and Hg in the alloy at 673 K for all concentrations of Na.

For the theoretical determination of heat of mixing, temperature derivatives of interaction parameters are required which are obtained by successive approximation method. The best fit values of parameters are

$$\frac{1}{k_B}\frac{d\omega}{dT} = -2.097,\ \frac{1}{k_B}\frac{d\Delta\omega_{AB}}{dT} = 8.971,\ \frac{1}{k_B}\frac{d\Delta\omega_{BB}}{dT} = -19.105$$

The plot of heat of mixing versus concentration of sodium (C_{Na}) is shown in figure 3. It is found that the heat of mixing is more negative at 0.4 concentration of sodium. The computed and experimental values of H_M/RT are in good agreement.

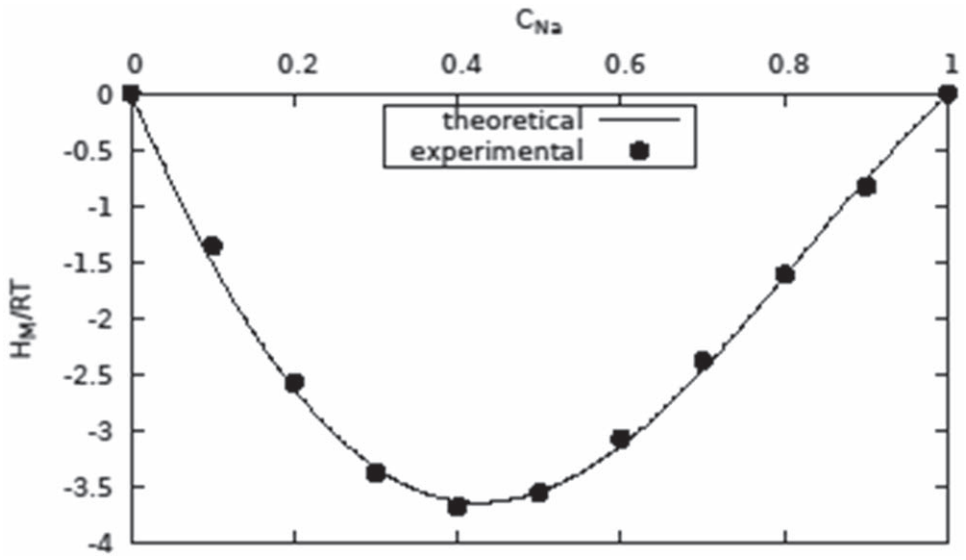

Figure 3. Heat of mixing versus concentration of Na at 673 K.

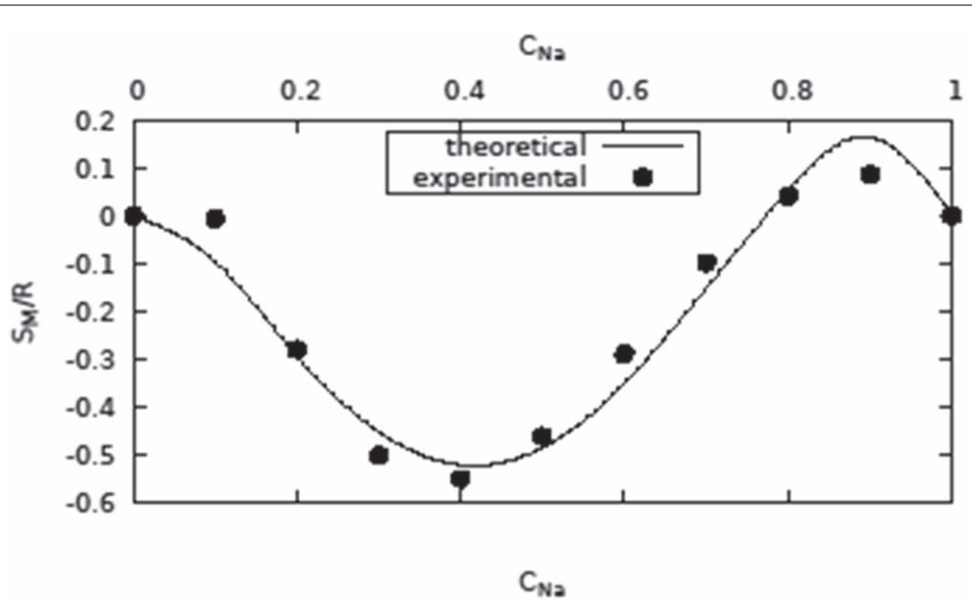

Figure 4. Entropy of mixing versus concentration of Na at 673K.

Using equations (7) and (9), the entropy of mixing (S_M) is computed. Energy parameters used in Gibb's free energy and heat of mixing of the alloy are used consistently throughout our calculation.

The plot of entropy of mixing (S_M/R) versus concentration of sodium is shown in figure 4 for both theoretical and observed values. From the figure, it is observed that theoretical values are in reasonable agreement with observed values.

3.2. Microscopic properties

One of the important functions for the study of nature of atomic order of the binary liquid is considered as the concentration fluctuations in the long-wavelength limit $S_{CC}(0)$ because it removes difficulties in the diffraction experiment [18]. For a given concentration if $S_{CC}(0) < S^{id}_{CC}(0)$, then complex formation tendencies are expected while $S_{CC}(0) > S^{id}_{CC}(0)$) points to the segregating tendencies. The experimental and theoretical values of $S_{CC}(0)$ at different concentrations of sodium are obtained from equations (15) and (16) respectively. The plot of experimental and theoretical along with ideal values of $S_{CC}(0)$ versus concentration of Na (C_{Na}) is shown in figure 5.

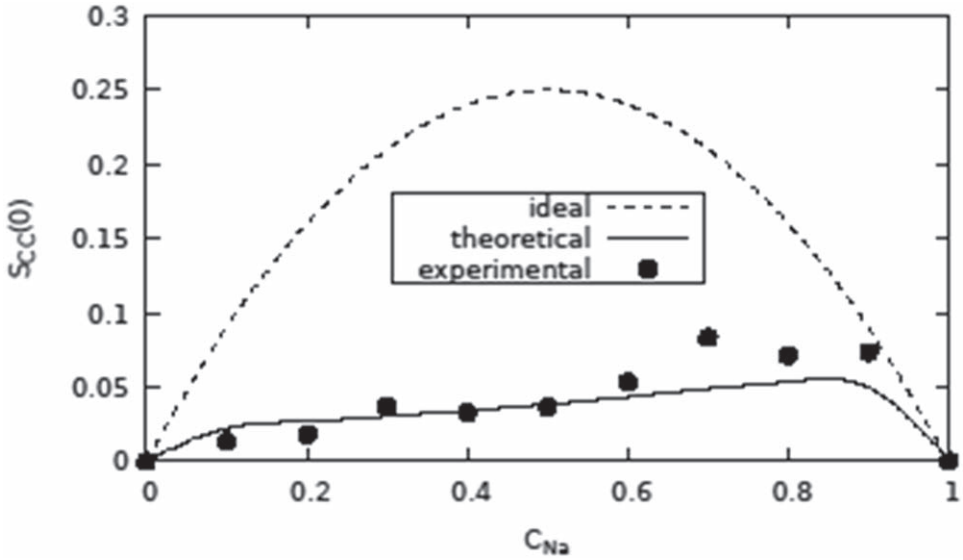

Figure 5 . Concentration fluctuation in long-wavelength versus concentration of Na at 673 K.

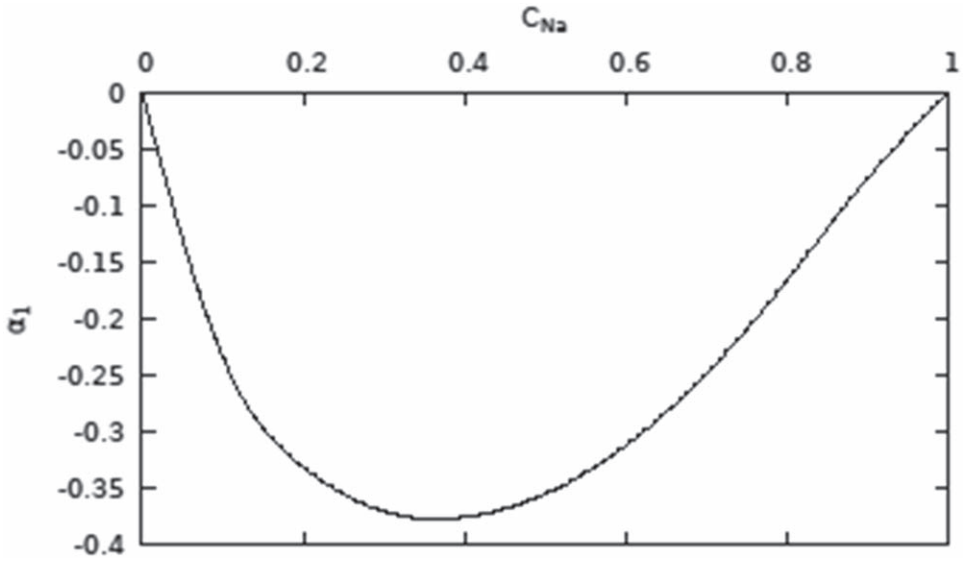

Figure 6 . Chemical short-range order parameter versus concentration of Na at 673 K.

It is clear from the figure that the theoretical value of lies below the ideal value of $S_{CC}(0)$ throughout the whole range of concentration of lead which is the good signature of ordering in the alloy.

The Warren-Cowley short-range order parameter (α_1) is another most powerful parameter to provide information on the local arrangement of the atoms in the molten alloys. Actually, it quantifies the degree of chemical order in the liquid alloys whose value lies between -1 to $+1$. The negative value of α_1 is an indication of the ordering nature of the alloy, which is complete for $\alpha_1 = -1$. The value $\alpha_1 = 0$ is the indication of the random distribution of the atoms in the mixture and similarly, positive values of α_1 is the indication of segregating nature, which is complete for $\alpha_1 = 1$. The value of α_1 has been computed as a function of the concentration of Na using equation (17). For this, we take coordination number $Z = 10$. The plot of theoretical values of α_1 versus concentration of Na (C_{Na}) is shown in figure 6. From the figure, it is observed that the value of α_1 is negative throughout the whole range of concentration of sodium with maximum negative at 0.4 concentration of sodium which signifies the strong tendency of ordering nature of the alloy.

3.3. Surface tension

To calculate the surface tension of Na $-$ Hg alloy the densities and surface tension of individual metals for all models required are calculated at 673 K by using relations given in reference [27].

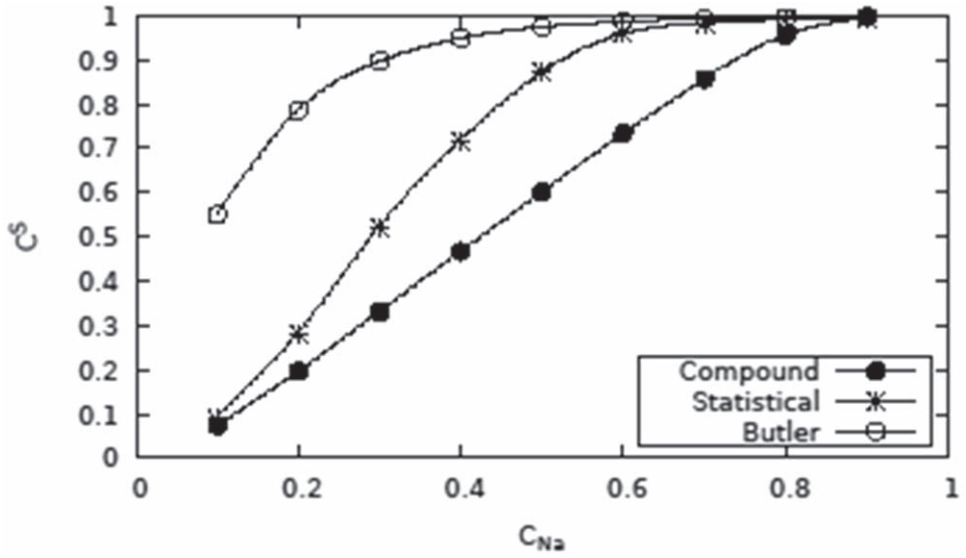

Figure 7. Surface concentration versus Concentration of Na at 673 K.

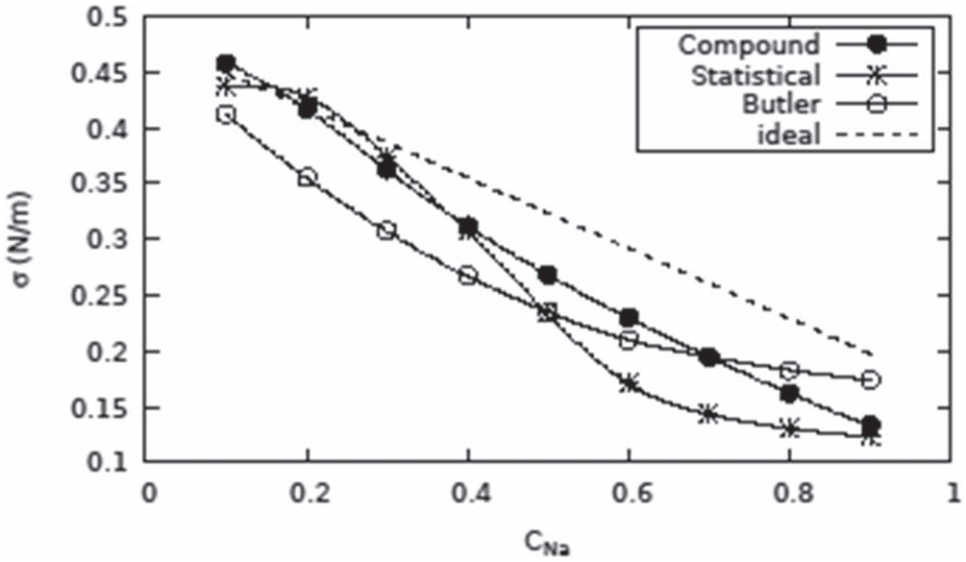

Figure 8. Surface tension (N/m) versus concentration of Na at 673 K.

For the unknown or negligible excess molar volume of the alloy, the partial molar volume is replaced by the molar volume of the pure component in the case of the improved Butler model and hence the partial surface area (A_j) of each component is definitely replaced by surface area (A_j^0) of the same pure component [13, 28]. The bulk and partial excess free energy of mixing of individual sodium and mercury in a liquid state at 673K are taken from reference [26]. The geometrical structure factor and ratio of surface excess energy to the bulk excess energy ($G_j^{s,xs}/G_j^{b,xs}$) are considered 1.061 and 0.818 [24] respectively. Now writing these values to both metals in equation (17) and solving them simultaneously, we first obtain surface concentrations of both metals, and then using each surface concentration of corresponding metals, the surface tension is obtained. Similar method is applied for the other two models as well.

For the statistical model, the interchange energy ($\omega = -9.564\ k_B T$) obtained from equation (7) is used since this method is not based on the complex of the alloys. Similarly, for the compound forming model, the same interaction energy parameters ω and ω_{jk} are used as in thermodynamic properties. The computed values of surface concentrations and surface tensions from different models are compared in figures 7 and 8 respectively.

Figure 7 shows the surface concentration increases with increasing bulk concentration of Na(C_{Na}) in all three models. The computed values of surface concentration suggest the segregation tendency of Na atoms to the surface but the segregation is more at higher bulk concentration of Na. This further suggests that at lower

bulk concentration of Na, the two different atoms of the alloy involve in the formation of chemical complexes or intermetallic compounds: possibly $NaHg_2$.

In figure 8, the surface tension of Na − Hg alloy decreases gradually with an increase in the bulk concentration of Na and is almost negatively deviated from the ideal value. In the compound formation model, the interaction energy parameters are considered which is the case of uniform deviation from the ideal one.

4. Conclusion

The present study is the theoretical analysis for the understanding of thermodynamic, structural, and surface behavior of binary liquid Na-Hg alloy at 673 K, under the assumption of the existence of $NaHg_2$ complex in the liquid mixture by quasi chemical approximation. The study explains the asymmetry behavior of the thermodynamic properties as a function of concentration. The theoretical study shows that the alloy exhibits ordered tendencies that become weaker with increasing temperature. It is noticed that segregating tendencies are not to be found in the bulk alloy for any concentrations. The sodium atoms segregate more on the surface at higher concentrations of sodium. The surface tension is negatively deviated from the ideal value.

Data availability statement

The data that support the findings of this study are available upon reasonable request from the authors.

Conflicts of interest

The authors declare no conflict of interest.

ORCID iDs

N Panthi https://orcid.org/0000-0001-7227-5888
I B Bhandari https://orcid.org/0000-0002-3607-5608

References

[1] Adhikari D, Singh B P and Jha I S 2012 Phase separation in Na–K liquid alloy *Phase Transit.* **85** 675–80
[2] Bent H E and Forziati A F 1936 The Activity of Sodium and Mercury in Solid Sodium Amalgams *JACS* **58** 2220–3
[3] Smirnov V A 1970 *Vosstanovlenie amal'gamami.* (Chimija: Izd)
[4] Balej J 1979 Phase diagram of the system Na—Hg in the region of dilute sodium amalgams *Chem. zvesti* **33** 585–93
[5] Hirayama C, Andrew K F and Kleinosky R L 1981 Activities and thermodynamic properties of sodium amalgams at 500–700 C *Thermochim. Acta* **45** 23–37
[6] Kozin L F 1992 Fiziko-khimiya i metallurgiya vysokochistoi rtuti i ee splavov *Physical Chemistry and Metallurgy of High Purity Mercury and Its Alloys)* (Kiev: Naukova Dumka)
[7] Deiseroth H J, Biehl E and Rochnia M 1997 Sodium amalgams: phase diagram, structural chemistry, and thermodynamic data, a summary of recent developments *J. Alloys Compd.* **246** 80–90
[8] Hoch C and Simon A 2012 Na11Hg52: Complexity in a polar metal *Angew. Chem. Int. Ed.* **51** 3262–5
[9] Morachevskii A G 2014 Liquid alloys of the Mercury-sodium system: Thermodynamics, structure, and applications *Russ. J. Appl. Chem.* **87** 837–52
[10] Adhikari D, Jha I S and Singh B P 2010 Structural asymmetry in liquid Fe–Si alloys *Philos. Mag.* **90** 2687–94
[11] Bhatia A B and Singh R N 1982 Thermodynamic properties of compound forming molten alloys in a weak interaction approximation *Physics and Chemistry of Liquids an International Journal* **11** 343–51
[12] Novakovic R, Ricci E, Giuranno D and Gnecco F 2002 Surface properties of Bi–Pb liquid alloys *Surf. Sci.* **515** 377–89
[13] Kaptay G 2019 Improved derivation of the Butler equations for surface tension of solutions *Langmuir* **35** 10987–92
[14] Prasad L C, Singh R N and Singh G P 1994 The role of size effects on surface properties *Phys. Chem. Liq.* **27** 179–85 LCRN
[15] Jha I S, Khadka R, Koirala R P, Singh B P and Adhikari D 2016 Theoretical assessment on mixing properties of liquid Tl–Na alloys *Philos. Mag.* **96** 1664–83
[16] Koirala I, Singh B P and Jha I S 2016 Theoretical investigation of mixing behavior of Al-Fe alloys in molten stage *The African Review of Physics* **10** 329–35
[17] Eldressi K A, Eltawahni H A, Moradi M, Twiname E R and Mistler R E 2019 *Energy Effects in Bulk Metals* (https://doi.org/10.1016/B978-0-12-803581-8.03346-4)
[18] Bhatia A B and Thornton D E 1970 Structural aspects of the electrical resistivity of binary alloys *Physical Review B* **2** 3004
[19] Warren B E 1969 *X-ray Diffraction Reading.* (MA: Addison-Wesley) 227
[20] Cowley J M 1960 Short-and long-range order parameters in disordered solid solutions *Phys. Rev.* **120** 1648
[21] Iida T 1994 Physical properties of liquid metals [IV] surface tension and electronic transport properties of liquid metals *Weld. Int.* **8** 766–70
[22] Koirala I, Singh B P and Jha I S 2014 Study of segregating nature in liquid Al-Ga alloys *Scientific World* **12** 14–20
[23] Brackbill J U, Kothe D B and Zemach C 1992 A continuum method for modeling surface tension *J. Comput. Phys.* **100** 335–54

[24] Kaptay G 2008 A unified model for the cohesive enthalpy, critical temperature, surface tension and volume thermal expansion coefficient of liquid metals of bcc, fcc and hcp crystals *Mater. Sci. Eng. A* **495** 19–26
[25] Yeum K S, Speiser R and Poirier D R 1989 Estimation of the surface tensions of binary liquid alloys *Metall. Trans. B* **20** 693–703
[26] Hultgren R, Desai P D, Hawkins D T, Gleiser M and Kelley K K 1973 *Selected Values Of The Thermodynamic Properties Of Binary Alloys.* (ASM, Metal Park, OH: National Standard Reference Data System)
[27] Brandes E A and Brook G B (ed) 2013 *Smithells Metals Reference Book.* (Amsterdam: Elsevier)
[28] Kaptay G 2020 A coherent set of model equations for various surface and interface energies in systems with liquid and solid metals and alloys *Adv. Colloid Interface Sci.* **283** 102212

Effect of temperature on mixing behavior and stability of liquid Al-Fe alloys

Effect of temperature on mixing behavior and stability of liquid Al-Fe alloys

I B Bhandari[1,2,*], N Panthi[1], S Gaire[3] and Ishwar Koirala[1]

[1]Central Department of Physics, Tribhuvan University, Kirtipur, Nepal
[2]Department of Applied Sciences, Purwanchal Campus, Tribhuvan University, Dharan, Nepal
[3]Everest Engineering College, Pokhara University, Lalitpur, Nepal

E-mail: bhandari.indra@gmail.com

Abstract. A theoretical model based on the assumption of compound formation in binary liquid alloy has been used to investigate the thermodynamic properties (free energy of mixing, enthalpy of mixing and entropy of mixing), microscopic properties (concentration fluctuation in long wavelength limit and chemical short range order parameter), surface properties (surface tension and surface composition) and dynamic properties (viscosity and diffusion coefficient). All the properties of Al_2Fe binary melt have been measured using the same energy parameters configured for experimental values of free energy of mixing. The energy parameters are detected as independent of concentration, but depend on temperature. The findings are well consistent with the experimental standards.

Keywords: Bulk properties; Ordering; Surface tension; Positive deviation

1. INTRODUCTION

The development of lightweight, energy-efficient materials is critical for mitigating the global energy crisis [1]. Aluminum alloys are intensively researched in the automotive and aerospace sectors as test specimens, structural components, and massive metal surfaces. Aluminum alloys are the most often utilized light alloys for structural component weight reduction. At room temperature, these materials are often distinguished by their low density, high thermal conductivity, and good corrosion resistance [2–5]. Because of the extent to which its microstructure may be changed, the Al - Fe alloy system is particularly appealing for aeronautical constructions [6]. Al-Fe alloys have good oxidation properties, a high melting point, and a cheap material cost, making them an economically attractive material for industrial use [7,8]. Al-Fe alloys are also significant in powder metallurgy and spray forming [7,9]. They are the primary components of metal-matrix composites. Additionally, by changing the composition and thermal treatments of Al-Fe alloys, especially when coupled with additional elements like Mg, Si, Cu, and Zn, stronger Al-Fe alloys can be produced [10]. When the thermodynamic characteristics of a binary liquid alloy deviate significantly from ideality, the theoretical models used to analyze it provide vital information. These deviations induce asymmetry in thermodynamic characteristics away from equiatomic composition. The asymmetry in the thermodynamic characteristics of binary melt is mostly due to the size effect [11] and the electronegativity difference [12]. The size ratio (≈1.4) and electronegativity difference (≈0.22) for Al - Fe liquid alloy are too small to produce significant asymmetry in thermodynamic characteristics. The phase diagram [13] shows that the Al - Fe alloy has many stable phases, including Al_3Fe, which has a complex end – centered monoclinic structure, Al_5Fe_2, which has an end – centered orthorhombic structure, AlFe, which has an ordered bcc (B_2) structure isotypic with CsCl, $AlFe_3$, which has an ordered bcc ($D0_3$)

structure isotypic with BiF_3, and Al_2Fe having a complex rhombohedral structure. Among these phases, the presence of Al_2Fe complex in the liquid state has been considered in this investigation, and its thermodynamic and microscopic characteristics at 1873 K have been calculated using the complex formation model [14]. The Moelwyn–Hughes method [15] has been used to investigate the viscosity of the selected alloy, whereas the Prasad model [16,17] was used to investigate the surface characteristics. Due to the lack of long-range atomic order, researching the characteristics of alloys in liquid form is challenging. As a result, theorists have used several models [18–24] to better explain the characteristics of binary liquid alloys. Theoreticians have previously studied the Al3Fe alloy in its liquid form at a constant temperature of 1873K [12]. The energetics of Al2Fe alloy at various temperatures have been investigated in this study utilizing a complex formation model [14]. To demonstrate the correctness of this technique in thermodynamic and structural description of the provided binary system, the results are examined and compared with published data [25].

2. Formulation

2.1 Thermodynamic Properties

To investigate the mixing behavior of Al - Fe compounds, the complex formation model has been used. According to this model, the Al-Fe alloy will be a ternary combination of three species: Al atoms, Fe atoms, and the chemical complex Al2Fe, all of which will be in chemical equilibrium with one another. Conformal solution is another name for this ternary combination. $N_{Al} = x$ number of Al atoms and $N_{Fe} = (1-x)$ number of Fe atoms make up the total number of atoms in the provided binary system, which equals $N = N_{Al} + N_{Fe}$. The thermodynamic characteristics of components Al and Fe are altered when they are combined to produce a binary Al-Fe solution. Because of compound formation in the melt, the quantity of free atoms will decrease. For n_1 g, n_2 g and n_3 g atoms of Al, Fe and Al_2Fe respectively,

$$n_1 = x - 2n_3 \text{ and } n_2 = 1 - x - n_3 \tag{1}$$

After mixing, the total number of atoms is

$$n = n_1 + n_2 + n_3 = 1 - 2n_3 \tag{2}$$

The free energy loss due to compound formation is given by $-n_3\psi$; the complex formation energy is denoted by ψ ; and the ternary mixture mixing free energy is denoted by G'. Then the binary mixture's free energy of mixing may be expressed as [14],

$$G_M = G' - n_3\psi \tag{3}$$

In the case of the ternary ideal solution,

$$G' = \frac{RT}{n}\sum_{i=1}^{3}(n_i \ln n_i) \tag{4}$$

Where the implications of the size differences in the mixture are not to be neglected and the interaction between species is limited, but not zero, the zeroth approximation of regular solutions [26] or conformal solution approximation [27] must be valid. In this approximation, G' in terms of interaction energy parameter, V_{ij} can be expressed as,

$$G' = \frac{RT}{n}\sum_{i=1}^{3}(n_i \ln n_i) + \frac{1}{n}\sum_{i<j} n_i n_j V_{ij} \tag{5}$$

The free energy of mixing for compound forming and regular binary alloys is now expressed as

$$G_M = \frac{RT}{n}\sum_{i=1}^{3}(n_i \ln n_i) + \frac{1}{n}\sum_{i<j} n_i n_j V_{ij} - n_3\psi \tag{6}$$

The equilibrium state at a particular pressure and temperature may be used to calculate the value of n_3.

$$\left(\frac{\partial G_M}{\partial n_3}\right)_{T,P,N,x} = 0 \tag{7}$$

Substituting G_M from equation 6 and doing some algebraic calculations, we get

$$\ln\left(n_3 n^2 n_1^{-2} n_2^{-1}\right) + \chi = \frac{\psi}{RT} \tag{8}$$

Which is the equilibrium equation, where

$$\chi = \left(\frac{2n_1n_2}{n} - 2n_2 - n_1\right)\frac{V_{12}}{nRT} + \left(\frac{2n_2n_3}{n} - n_3 + n_2\right)\frac{V_{23}}{nRT} + \left(\frac{2n_1n_3}{n} - 2n_3 + n_1\right)\frac{V_{13}}{nRT} \tag{9}$$

The heat of mixing H_M can be expressed as follows [14]:

$$H_M = G_M - T\left(\frac{\partial G_M}{\partial T}\right)_P \tag{10}$$

Using the value of G_M from equation 6, we obtain

$$H_M = -n_3\left[\psi - T\left(\frac{\partial \psi}{\partial T}\right)_P\right] + \frac{1}{n}\sum_{i<j}\sum n_i n_j\left[V_{ij} - T\left(\frac{\partial V_{ij}}{\partial T}\right)_P\right] \tag{11}$$

The entropy of mixing expression, S_M, may be written as

$$S_M = \frac{(H_M - G_M)}{T} = n_3\frac{\partial \psi}{\partial T} - R\sum_{i=1}^{3} n_i \ln\frac{n_i}{n} - \frac{1}{n}\sum_{i<j}\sum n_i n_j \frac{\partial V_{ij}}{\partial T} \tag{12}$$

2.2 Structural Properties

Any variation from the ideal value $S_{cc}^{id}(0)$ is crucial in understanding the nature of ordering and phase separation in molten alloys, therefore the concentration fluctuation at the long wavelength limit is of great importance. The free energy of mixing is linked to concentration variation at long wavelength limits by the formula [28],

$$S_{cc}(0) = RT\left(\frac{\partial^2 G_M}{\partial x^2}\right)^{-1} \tag{13}$$

Differentiating G_M twice with respect to x

$$\frac{\partial^2 G_M}{\partial x^2} = RT\sum_{i=1}^{3}\left(\frac{n_i'^2}{n_i} - \frac{n'^2}{n}\right) + 2n\sum_{i<j}\sum V_{ij}\left(\frac{n_i}{n}\right)'\left(\frac{n_j}{n}\right)'$$

$$S_{cc}(0) = \left[\sum_{i=1}^{3}\left(\frac{n_i'^2}{n_i} - \frac{n'^2}{n}\right) + \frac{2n}{RT}\sum_{i<j}\sum V_{ij}\left(\frac{n_i}{n}\right)'\left(\frac{n_j}{n}\right)'\right]^{-1} \tag{14}$$

In terms of composition, the prime on the n's refers to their first derivative. By using the following formula, the theoretically predicted values of $S_{cc}(0)$ may be compared to observed values computed from constituent element activity at different compositions.

$$S_{cc}(0) = x_{Fe}a_{Al}\left(\frac{\partial a_{Al}}{\partial x_{Al}}\right)^{-1}_{T,P,N} = x_{Al}a_{Fe}\left(\frac{\partial a_{Fe}}{\partial x_{Fe}}\right)^{-1}_{T,P,N} \tag{15}$$

$S_{cc}^{id}(0)$ represent the ideal value as,

$$S_{cc}^{id}(0) = x_{Al}x_{Fe} \tag{16}$$

In the following equation, α_1 indicates Warren – Cowely chemical short range order parameter which measures the degree of local order within the binary melt [29,30].

$$\alpha_1 = \frac{s-1}{s(z-1)+1} \text{ here, } s = \frac{s_{cc}(0)}{x_{Al}x_{Fe}} \tag{17}$$

In equation 17, z is coordination number.

2.3 Transport Properties

The molten alloy's mixing behavior can even be examined at the fundamental level in terms of diffusion coefficient. With the aid of Darken's equation [31], the mutual diffusion coefficient (D_M) of binary liquid alloys may be described in terms of activity (a_i) and self- diffusion coefficient (D_{id}) of individual component.

$$D_M = x_i D_{id} \frac{d\ln a_i}{dx_i} \tag{18}$$

with $D_M = x_{Al}D_{Fe} + x_{Fe}D_{Al}$

Where D_{Al} and D_{Fe} are the self – diffusion coefficients of Al and Fe respectively. In terms of $S_{cc}(0)$, the ratio of mutual diffusion coefficient (D_M) to self – diffusion coefficient (D_{id}) can be expressed as

$$\frac{D_M}{D_{id}} = \frac{S_{cc}^{id}(0)}{S_{cc}(0)} \tag{19}$$

The microscopic mixing behavior of liquid alloys may also be described in terms of viscosity. The Moelwyn – Hughes equation for liquid alloy viscosity is

$$\eta = \left(x_{Al}\eta_{Al} + x_{Fe}\eta_{Fe}\right)\left(1 - 2x_{Al}x_{Fe}\frac{H_M}{RT}\right) \tag{20}$$

Here η_i is the viscosity of individual elements Al and Fe. This value can be optimized for required temperature (T) as [32],

$$\eta_i = \eta_{i0}\exp\left(\frac{E}{RT}\right) \tag{21}$$

Here η_{i0} is a constant in the unit of viscosity and E is the activation energy.

2.4 Surface Properties

The surface characteristics of the liquid solution reveal metallurgical phenomena including crystal development, wielding, gas absorption, and gas bubble nucleation [33]. The surface tension equations provided by Prasad et al., [16, 17], have been simplified using the zeroth approximation as

$$\tau = \tau_{Al} + \frac{k_B T}{\xi}\ln\frac{x_{Al}^s}{x_{Al}} + \frac{\psi}{\xi}\left[p\left(x_{Fe}^s\right)^2 + (q-1)x_{Fe}^2\right] \tag{22}$$

$$\tau = \tau_{Fe} + \frac{k_B T}{\xi}\ln\frac{x_{Fe}^s}{x_{Fe}} + \frac{\psi}{\xi}\left[p\left(x_{Al}^s\right)^2 + (q-1)x_{Al}^2\right] \tag{23}$$

Where τ_i represents the surface tensions of pure Al and Fe, x_i and x_i^s denote the bulk and surface concentrations of alloy components while p and q represent the coordination fractions. These are the fraction of an atom's nearest neighbors generated within its own layer and those created by the next layer. The connection between the coordination fractions p and q is $p + 2q = 1$. For present

calculation, we assume the closed packed structure for which the p and q values are 0.5 and 0.25 respectively.

The mean atomic surface area (ξ) of the compound can be expressed in terms of component surface area (ξ_i) as,

$$\xi = \sum x_i \xi_i \tag{24}$$

Here

$$\xi_i = 1.102\left(\frac{\Omega_i}{N_A}\right)^{2/3} \tag{25}$$

Where Ω_i is the component i's molar volume and N_A is the Avogadro's number. Equations (22) and (23) may be solved for x_i^s as the function of x_i and hence surface tension compositional dependency can be examined.

3. RESULTS AND DISCUSSION

3.1 Thermodynamic Properties

The order energy values for the Al–Fe liquid phase were calculated using known experimental data on thermodynamic characteristics [25] as well as phase diagram information [13]. The mixing functions, i.e. the Gibbs free energy and the enthalpy of mixing (figure 1), are negative for all compositions and have a flat minimum of -1.4770 and -1.2775 at equiatomic composition, x_c = 0.5, showing the compositional site of an energetically favorable compound, the Al – Fe. The preferred configurations of Al and Fe component atoms facilitate the production of Al2Fe complexes (μ=2 and ν=1) in liquid alloys. All calculations were performed at T = 1873 K, taking into account the Al - Fe phase diagram [13] and the existence of the liquid phase across the entire concentration range. At T = 1873 K, the interaction energy parameters ψ , V_{12} , V_{13} and V_{23} as well as their temperature derivatives, were calculated using the Gibbs energy of mixing, G_M , of liquid Al - Fe alloys and the enthalpy of mixing, H_M [25]. The interaction energy parameters' values were tweaked to produce concentration dependences of G_M that closely matched the thermodynamic data. V_{12} = -3.095RT, V_{13} = -0.851RT, V_{23} = -1.970RT and ψ = 2.552RT are the estimated interaction energy parameters for liquid Al - Fe alloys, and they remain constant throughout all computations. The number of complexes, n_3 , was calculated using equations (8-9) and equations (1-2). The concentration dependence of the equilibrium values of chemical complexes, n_3 , reaches a maximum value of around 0.261 at the compound forming composition, x_c = 0.667.

If energy parameters are assumed to be temperature independent, the values of H_M and S_M are found to be in poor agreement with the experiment. As a result, we looked at how these parameters changed with temperature to see how heat and entropy of formation changed with observed values [25]. At T =1873K, the temperature-dependent energies are ∂V_{12} /∂T = 0.980R, ∂V_{13} /∂T = 2.591R, ∂V_{23} /∂T = 2.984R and $\partial\psi$ /∂T = 0.212R. Equations (11) and (12) have been used to calculate the enthalpy of mixing, H_M and the entropy of mixing, S_M and have been compared to existing experimental data [25]. A comparison of the anticipated values of H_M and S_M computed at T = 1873 K with published data of liquid Al - Fe alloys reveals a reasonable agreement (figure 1).

The temperature-dependent fluctuation of interaction energy parameters can be written as

$$V_{ij}(T_R) = V_{ij}(T) + (T - T_R)\frac{\partial V_{ij}}{\partial T} \tag{26}$$

Here T_R = 2073K, 2273K, 2473K and 2673K

Equation (26) was used to derive the interaction energy parameters at 2073K, 2273K, 2473K, and 2673K using the values of interaction energy parameters at 1873K and their temperature derivatives (figure 2). Table 1 shows the optimized values of interaction parameters at elevated temperatures.

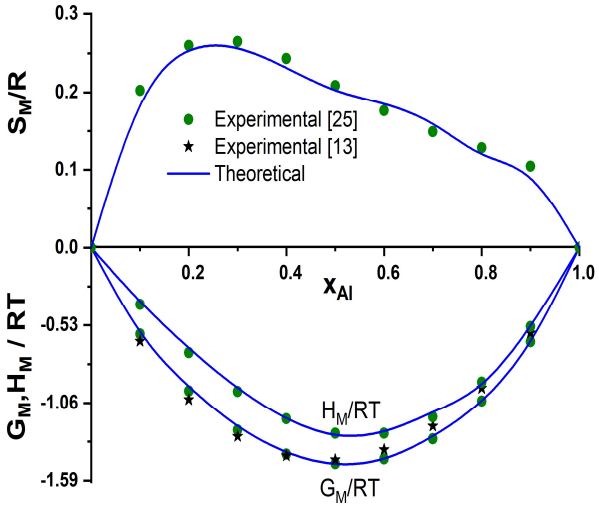

Figure 1. Gibb's free mixing energy (G_M / RT), heat of mixing (H_M / RT) and entropy of mixing (S_M / R) vs. concentration of aluminum (x_{Al}) in the liquid Al - Fe alloy at 1873K.

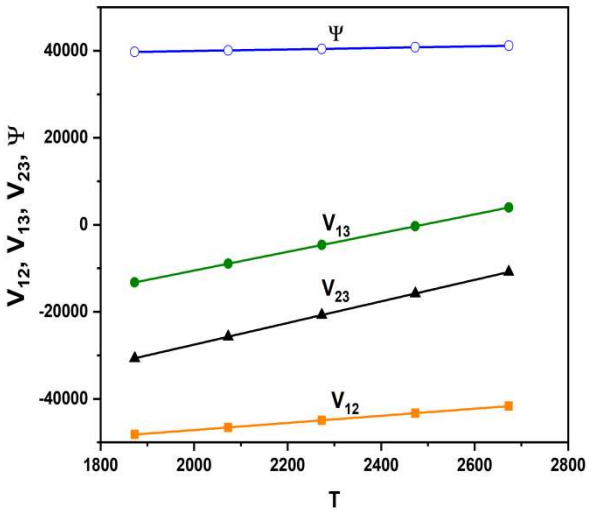

Figure 2. Temperature (T) effects on the interaction parameters (V_{ij} and ψ)

Table 1. Temperature-dependent optimization of the interaction energy parameters.

Parameter/ T	2073K	2273K	2473K	2673K
V_{12} / RT	-2.702	-2.378	-2.106	-1.875
V_{13} / RT	-0.519	-0.245	-0.016	0.179
V_{23} / RT	-1.492	-1.098	-0.768	-0.487
ψ / RT	2.326	2.140	1.984	1.852

The linear fit $V_{ij}(T) = a + bT$ for the temperature dependence of interaction energy parameters is excellent. Table 2 summarizes the a and b values for interaction parameters.

Table 2. Coefficient's values for linear fit of interaction parameters.

Coefficients	V_{12}	V_{13}	V_{23}	ψ
a (Joule)	-63456.4	-53599.2	-77144.3	36438.8
b (Joule K^{-1})	8.14772	21.5416	24.8090	1.76257

Equation (6) is used to obtain the variation of G_M with temperature using these interaction parameters at various temperatures (figure 3). When temperature rises from 1873K to 2673K, the maximum value of G_M / RT at equiatomic composition increases from -1.4770 to -1.0947, indicating a phase separation tendency at higher temperatures.

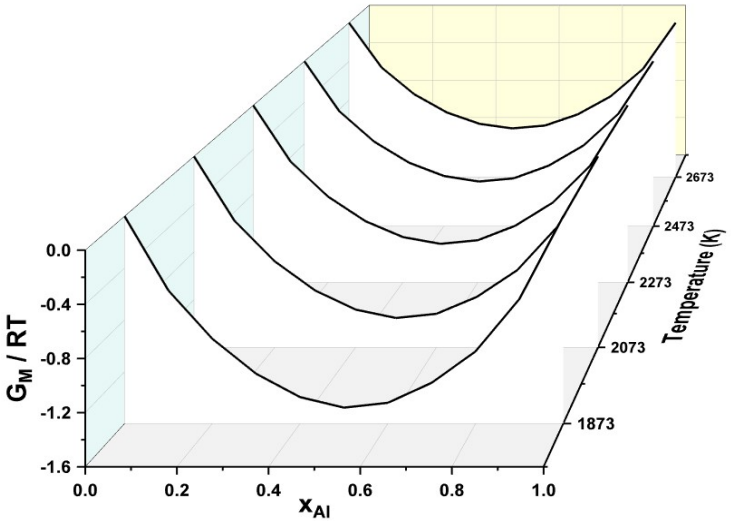

Figure 3. Temperature effects on G_M / RT with respect to bulk composition of Al.

3.2 Structural Properties

Concentration fluctuations in the long-wavelength limit, $S_{cc}(0)$, and chemical short-range order parameter, α_1, as functions of bulk concentration, have been used to investigate the ordering processes in the Al - Fe liquid phase. Equations (14) and (16) are used to derive the $S_{cc}(0)$ values and the values that characterize ideal mixing $S_{cc}^{id}(0)$ in weak approximation. Figure 4 plots these values along with the observed values from equation (15) using activity data. At x_c=0.5, the largest difference between theoretical and ideal concentration fluctuations in the long-wavelength limit is 0.1519. This means that x_c is the concentration at which the chemical can form [28]. As can be observed, $S_{cc}(0)$ is lower than $S_{cc}^{id}(0)$, showing that chemical order exists across the whole concentration range. With increasing temperature, the value of $S_{cc}(0)$ decreases, reducing the gap between ideal and theoretical values, indicating the tendency of similar atom pairing, leading to homo co-ordination (figure 5). As the temperature rises, the solution approaches its optimum state. At $T \approx$ 7788K, the regular solution becomes fully ideal, and $S_{cc}(0)$ is defined by the equation (16). The negative values of the Warren–Cowley parameter, α_1 over the whole concentration range support this conclusion (figure 4). The phase separating tendency is supported by the variation of α_1 with temperature, as evidenced by the variation of free energy of mixing with temperature.

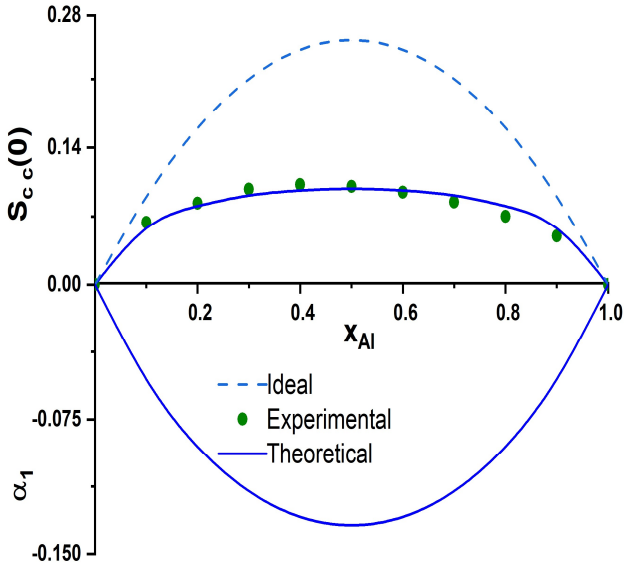

Figure 4. Concentration fluctuation at long wavelength limit ($S_{cc}(0)$) and chemical short range order (α_1) vs. concentration of aluminum (x_{Al}) in the liquid Al - Fe alloy at 1873K

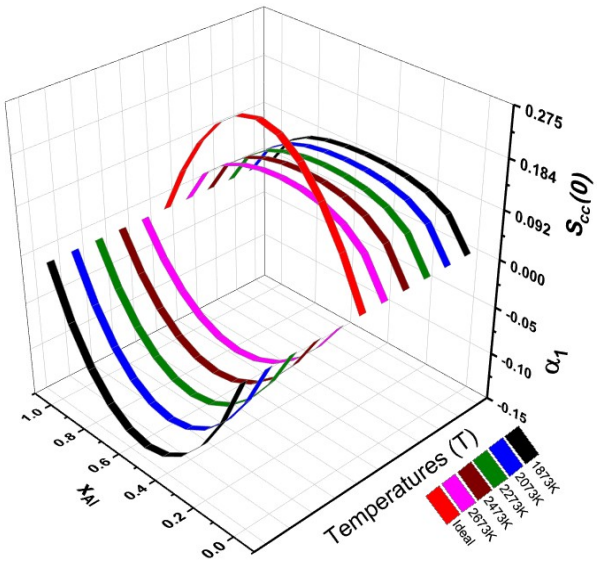

Figure 5. Temperature effects on $S_{cc}(0)$ and chemical short range order (α_1) of liquid Al - Fe alloy with respect to bulk composition of Al.

3.3 Transport Properties

The viscosities of the constituent elements, η_{i0} and the related activation energies at a fixed temperature were obtained from the literature [32]. Equation (21) is used to optimize these values for the temperature of research. Equation (20) is then used to calculate the viscosity of the liquid Al – Fe alloy at 1873K. Figure 6 depicts the viscosity's compositional dependence as well as the ideal value. Over the whole compositional range, the obtained viscosities are higher than ideal values. Up to x_{Al} = 0.4, the positive departure from ideality grows at which the deviation is maximum (= 0.001866) but sharply decreases below x_{Al} = 0.7. The plot of η at different temperature with respect to x_{Al} (figure 7.) shows that there is decreasing tendency of η as temperature increases.

At the fundamental level, the mixing tendency of the liquid alloy is investigated by determining the ratio of mutual and intrinsic diffusion coefficients (D_M / D_{id}). D_M / D_{id} > 1 denotes the likelihood of compound formation; D_M / D_{id} < 1 denotes phase separation; and D_M / D_{id} = 1 denotes the solution's ideality. The values of D_M / D_{id} are found to be positive and greater than unity throughout the compositions using equation (19) (figure 6). At the equiatomic composition, the maximum value (=2.5475) occurs. The theoretical examination of the presence of chemical order in the liquid state of Al-Fe alloy at 1873 K is now even clearer. Figure 8 shows that when the temperature raises, the amount of D_M / D_{id} decreases. The maximum difference (=0.6098) in D_M / D_{id} values for the temperatures 2673K and 1873K at equiatomic composition, x_{Al} = 0.5 again support high ordering tendency at that composition.

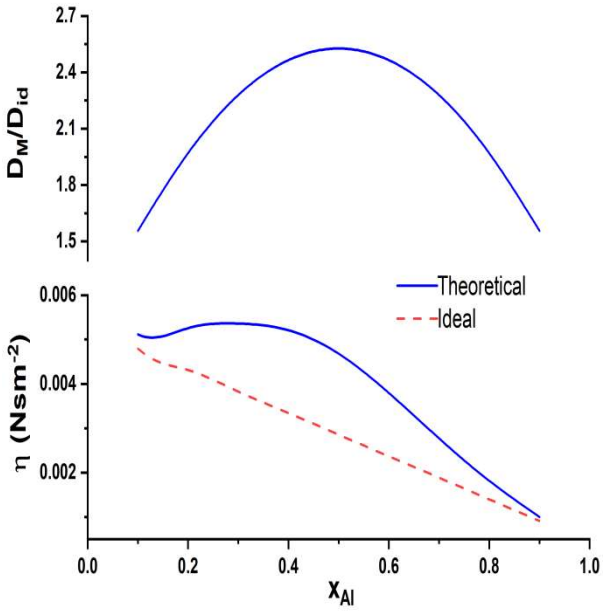

Figure 6. The mutual-to-intrinsic diffusion coefficient ratio (D_M / D_{id}) and viscosity (η) vs. concentration of aluminum (x_{Al}) in the liquid Al - Fe alloy at 1873K.

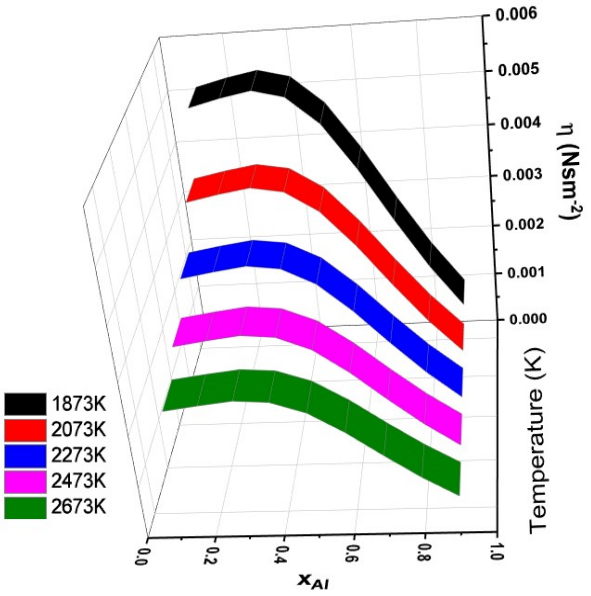

Figure 7. Temperature effects on viscosity (η) of liquid Al - Fe alloy with respect to bulk composition of Al.

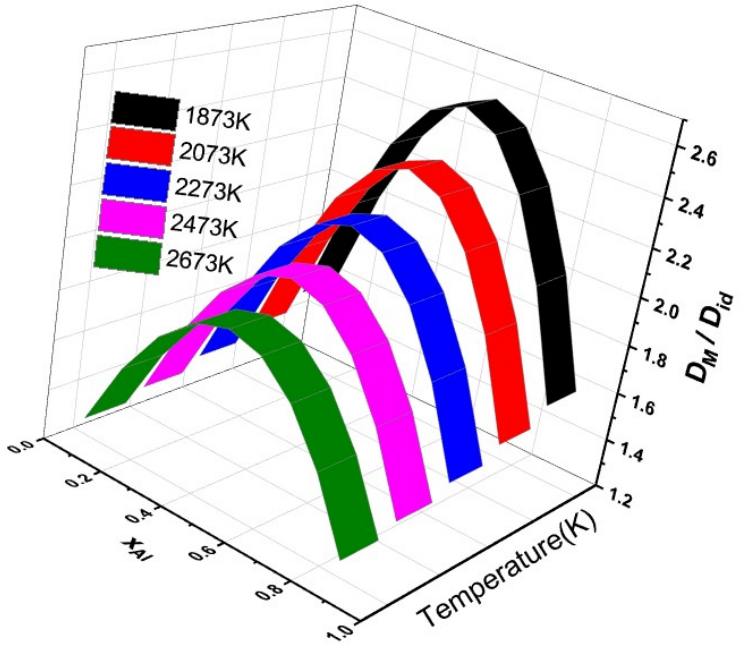

Figure 8. Temperature effects on the mutual-to-intrinsic diffusion coefficient ratio (D_M / D_{id}) of liquid Al - Fe alloy with respect to bulk composition of Al.

3.4 Surface Properties

The Prasad model [16,17] was used to compute the surface composition, x_{Al}^{s}, and surface tension, τ, of liquid Al_2Fe alloy as functions of bulk composition at various temperatures (T = 1873K, 2073K, 2273K, and 2473K). The surface composition values, x_{Al}^{s}, with regard to bulk concentration of Al, have been numerically solved using the expression derived by subtracting equation (23) from equation (22) (figure 9). Aluminum surface concentration in Al-Fe alloys is observed to rise as the bulk concentration of Al increases. The surface composition of Al deviates from ideality in a positive way. The surface compositions vs. concentration values were then utilized in the same equations to calculate the surface tension (figure 9). The same interaction energy parameters, surface coordination fractions (p = 0.5 and q = 0.25), mean atomic surface area, and surface tension data of pure components are used in both sets of equations (equations 24-25). The surface tensions of pure components at given temperatures, as well as the essential inputs for calculating mean atomic surface area and pure component element densities at fixed temperatures, were obtained from the literature [32]. Using the following formulas, these values have been evaluated at working temperature (T).

$$\rho_i(T) = \rho_i^0 + (T - T_i^0)\Delta\rho_i \quad (27)$$

$$\tau_i(T) = \tau_i^0 + (T - T_i^0)\Delta\tau_i \quad (28)$$

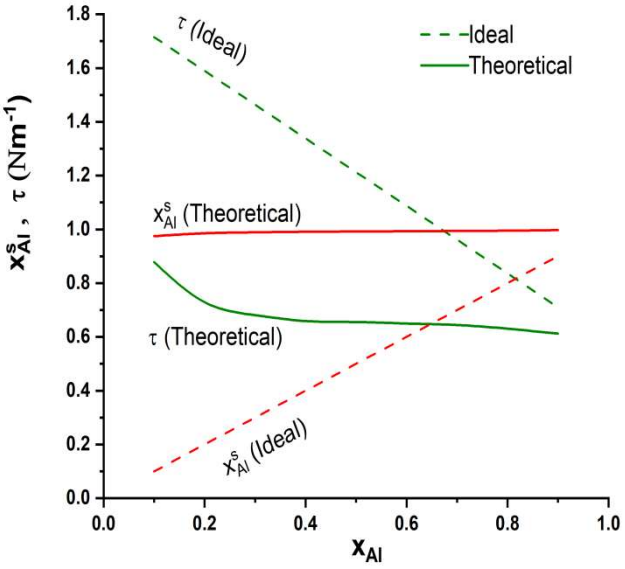

Figure 9. Surface concentration of aluminum (x_{Al}^{s}) and surface tension (τ) vs. bulk concentration of aluminum (x_{Al}) in the liquid Al - Fe alloy at 1873K.

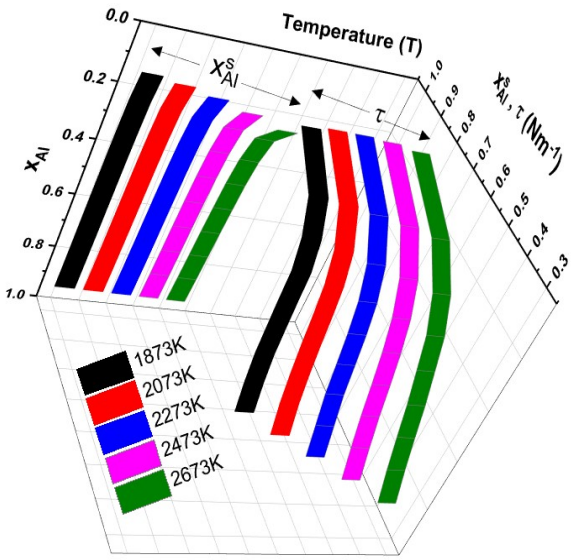

Figure 10. Compositional dependence of surface concentration of aluminum (x_{Al}^{s}) and surface tension (τ) in liquid Al - Fe alloy at different temperatures.

For the component metals of the alloys, $\Delta\rho_i$ and $\Delta\tau_i$ denote temperature coefficient of density and surface tension, respectively. Figure 10 shows the estimated surface concentration values for molten Al - Fe alloys at 1873 K and various temperatures. With increasing temperature, the surface concentration likewise decreases. The decreasing tendency of surface concentration with rise in temperature from 1873K to 2673K is maximum (=0.1310) at x_{Al} = 0.1 and minimum (=0.0060) at x_{Al} = 0.9. This implies the decreasing tendency of surface composition with respect to temperature, increases with decrease in bulk composition x_{Al}.

Furthermore, as shown in figure 9, the surface tension isotherm derived by the CFM for the regular solution deviates negatively from that calculated by the ideal solution model $\left(\tau_{ideal} = \tau_{Al}x_{Al} + \tau_{Fe}x_{Fe}\right)$ with regard to surface composition of Al. This strongly suggests that liquid alloys with negative excess Gibbs energy in the bulk have negative surface tension departures from their ideal solution [34]. Figure 10 shows the surface tensions of Al–Fe alloys as a function of Al content at various temperatures. The surface tension of the alloy has been found to decrease as the temperature rises. At temperatures ranging from 1873K to 2673K, the difference in surface tension values is greatest (=0.2732) at x_{Al} = 0.9 and smallest (=0.0217) at x_{Al} = 0.1. This means that as the bulk composition of Al increases, $\tau_{2673K} - \tau_{1873K}$ increases as well.

4. CONCLUSIONS

Different theoretical models have proven effective in explaining the thermodynamic, microscopic, transport, and surface characteristics of Al-Fe alloys. At all concentrations, the theoretical study of thermodynamic characteristics reveals a propensity for dissimilar atom pairing or ordering in liquid Al - Fe alloys. The energy parameters are found to be negative, suggesting that the component elements are attracted to one other. The interaction parameters are also discovered to be temperature dependent and concentration independent. With the exception of the formation energy parameter, the negativity of the rest of the interaction parameter diminishes as temperature increases. At all temperatures investigated, symmetry is seen in the free energy of mixing and the heat of mixing. For entropy of mixing, however, asymmetry is found about x_{Al} =0.2. The CSRO and concentration fluctuation studies reveal that there is a propensity for hetero co-ordination in liquid Al - Fe alloy. Viscosity isotherms show a positive divergence from Roult's law. At all compositions, the ratio of diffusion coefficients, $D_M / D_{id} > 1$, shows that there is a tendency for complex formation across the entire range of concentrations. The surface tension of the liquid alloy decreases as the bulk concentration of Al in the alloy increases at all temperatures studied. The surface tension of the Al-Fe alloy is found to be less than that of ideal solution. In the setting of varying temperatures, as the temperature of the investigation rises, it falls. Metals with lower surface tension tend to segregate on the surface of molten alloys, according to this research. The compound formation propensity of Al – Fe liquid alloy diminishes as temperature increases, according to temperature variation researches of all characteristics.

REFERENCES

[1]. Srivastava S and Mohan S 2011 *Tribol. Ind.* **33** 128
[2]. Bel'tyukov A L, Menshikova S G and Lad'yanov V I 2015 *J. Non. Cryst. Solids.* **410** 1. DOI: 10.1016/j.jnoncrysol.2014.11.028.
[3]. Il'inskii A, Slyusarenko S, Slukhovskii O, Kaban I and Hoyer W 2002 *Mater. Sci. Eng. A.* **325** 98. DOI: 10.1016/S0921-5093(01)01457-5
[4]. Audebert F 2005 Prop. *Appl. Nanocrystalline Alloy. from Amorph. Precursors*. 301. DOI: 10.1007/1-4020-2965-9_27.
[5]. Dobromyslov A V and Taluts N I 2017 *Phys. Met. Metallogr.* **118** 564. DOI: 10.1134/S0031918X17060023.
[6]. Cotton J D and Kaufman M J 1991 *Metall. Trans. A.* **22** 927. DOI: 10.1007/BF02659002.
[7]. Egry I, Brillo J, Holland-Moritz D and Plevachuk Y 2008 *Mater. Sci. Eng. A.* **495** 14. DOI: 10.1016/j.msea.2007.07.104.
[8]. Rosas G, Esparza R, Bedolla-Jacuinde A and Pérez R 2009 *J. Mater. Eng. Perform.* **18** 57. DOI: 10.1007/s11665-008-9254-0.
[9]. Xue Y, Shen R, Ni S, Song M and Xiao D 2015 *J. Alloys Compd.* **618**) 537. DOI: 10.1016/j.jallcom.2014.09.009.
[10]. Cubero-Sesin J M and Horita Z 2012 *Metall. Mater. Trans. A Phys. Metall. Mater. Sci.* **43**

5182. DOI: 10.1007/s11661-012-1341-z.
[11]. Singh R N 1987 *Can. J. Phys.* **65** 309. DOI: 10.1139/p87-038.
[12]. Akinlade O, Singh R N and Sommer F 2000 *J. Alloys Compd.* **299** 163. DOI: 10.1016/S0925-8388(99)00682-9.
[13]. Hultgren R, Desai P D, Hawkins D T, Gleiser M and Kelley K K 1973 *Selected values of the thermodynamic properties of the elements* National Standard Reference Data System
[14]. Bhatia A B and Hargrove W H 1974 *Phys. Rev. B.* **10** 3186. DOI: 10.1103/PhysRevB.10.3186
[15]. Moelwyn-Hughes E A. 1967 *A short course of physical chemistry* American Elsevier Publishing Company
[16]. Prasad L C and Singh R N 1991 *Phys. Rev. B.* **44** 768. DOI: 10.1103/PhysRevB.44.13768
[17]. Prasad L C, Singh R N, Singh V N and Singh G P 1998 *J. Phys. Chem. B.* **102** 921. DOI: 10.1021/jp9710421.
[18]. Adhikari D, Singh B P, Jha I S and Singh B K 2011 *J. Non. Cryst. Solids.* **357** 2892. DOI: 10.1016/j.jnoncrysol.2011.03.029.
[19]. Anusionwu B C 2003 *J. Alloys Compd.* **359** 172. DOI: 10.1016/S0925-8388(03)00213-5
[20]. Awe O E 2019 *Phys. Chem. Liq.* **57** 296. DOI: 10.1080/00319104.2018.1443453.
[21]. Jha I S, Koirala I, Singh B P and Adhikari D 2014 *Appl. Phys. A.* **116** (2014) 1517. DOI: 10.1007/s00339-014-8282-x
[22]. Koirala I, Jha I S, Singh B P and Adhikari D 2013 *Phys. B Condens. Matter.* **423** 49. DOI: 10.1016/j.physb.2013.04.051.
[23]. Novakovic R, Giuranno D, Ricci E, Delsante S, Li D and Borzone G 2011 *Surf. Sci.* **605** 248. DOI: 10.1016/j.susc.2010.10.026.
[24]. Singh B P, Koirala I, Jha I S and Adhikari D 2014 *Phys. Chem. Liq.* **52** 457. DOI: 10.1080/00319104.2013.871668.
[25]. Desai P D 1987 *J. Phys. Chem. Ref. Data.* **16** 109. DOI: 10.1063/1.555788.
[26]. Guggenheim E A 1952 *Mixtures: The theory of The Equilibrium Properties of Some Simple Classes of Mixture Solutions and Alloys.* Clarendon Press
[27]. Longuet-Higgins H C 1951 *Proc. R. Soc. London. Ser. A. Math. Phys. Sci.* **205** 247. DOI: 10.1098/rspa.1951.0028.
[28]. Bhatia A B and Thornton D E 1970 *Phys. Rev. B.* **2** 3004. DOI: 10.1103/PhysRevB.2.3004.
[29]. Warren B E 1990 *X-ray diffraction* New York Dover Publication
[30]. Cowley J M 1950 *Phys. Rev.* **77** 669. DOI: 10.1103/PhysRev.77.669.
[31]. Darken L S, Gurry R W and Bever M B 1953 *Physical chemistry of metals* McGraw-Hill.
[32]. Brandes E A, Brook G B 1998 *Smithells metals reference book*. Oxford ; Boston: Butterworth-Heinemann 7
[33]. Butler J A V *R. Soc. A.* 348. DOI: 10.1098/rspa.1983.0054.
[34]. Westbrook J H and Fleischer R L 1995. *Intermetallic compounds: principles and practice.* Chichester New York Wiley 3 p

Papers in Physics, vol. 14, art. 140005 (2022)

www.papersinphysics.org

Received: 7 July 2021, Accepted: 18 February 2022
Edited by: A. Goñi

DOI: https://doi.org/10.4279/PIP.140005

ISSN 1852-4249

Thermophysical behavior of mercury-lead liquid alloy

N. Panthi[1,2*], I. B. Bhandari[1], I. Koirala[1†]

Thermophysical properties of compound forming binary liquid mercury-lead alloy at temperature 600 K have been reported as a function of concentration by considering $HgPb_2$ complex using different modelling equations. The thermodynamic properties such as the Gibbs free energy, enthalpy of mixing, chemical activity of each component, and microscopic properties such as concentration fluctuation in long-wavelength limit and Warren-Cowley short range order parameter of the alloy are studied by quasi-chemical approximation. This research paper places additional emphasis on the interaction energy parameters between the atoms of the alloy. The theoretical and experimental data are compared to determine the model's validity. Compound formation model, statistical mechanical technique, and improved derivation of the Butler equation have all been used to investigate surface tension. The alloy's viscosity is investigated using the Kozlov-Ronanov-Petrov equation, the Kaptay equation, and the Budai-Benko-Kaptay model. The study depicts a weak interaction of the alloy, and the theoretical thermodynamic data derived at 600 K are in good agreement with the experimental results. The surface tension is slightly different in the compound formation model than in the statistical mechanical approach and the Butler equation at greater bulk concentrations of lead. The estimated viscosities in each of the three models are substantially identical.

I Introduction

The knowledge of thermophysical characteristics of alloys is regarded as a necessary foundation for developing novel materials. The creation of an alloy is linked to changes in the structure of a system as well as bonding between the constituent atoms. The subject is more intricately understood by studying the interaction and structural rearrangement of constituent atoms during alloy formation. The electrochemical effect, atom size, and constituent element concentration all influence the alloy's mixing properties, causing atoms of particular elements to align in either a self-coordinated or strong ordering pattern [1–4]. The alloying properties of liquid alloys vary as a function of composition, temperature, and pressure, all of which are important for the materials' strength, stability, and electrical resistivity. As a result, metallurgists and physicists have been interested in understanding the mixing behavior of metals that produce alloys. However, due to experimental difficulties as well as time limitations, the study of various alloys' characteristics is still incomplete. Different theoreticians have produced numerous concentration-dependent theoretical models to comprehend the alloying behavior of compound forming binary alloys in order to address such challenges and facilitate study as well as speed up the investigation process [5–7].

Because of their direct impact on human health, mercury and lead are the most studied metals. Our

*narayan.755711@cdp.tu.edu.np
†iswar.koirala@cdp.tu.edu.np

[1] Central Department of Physics, Tribhuvan University, Kirtipur, Kathmandu, Nepal.

[2] Department of Physics, Patan Multiple Campus, Tribhuvan University, Nepal.

study focuses on one of the lead alloys, Hg-Pb, to theoretically determine various properties at 600 K, assuming Hg_xPb_y ($x = 1$, $y = 2$) complex in the melt, by using compound formation models [6]. Lead, being very soft and ductile, is often used commercially as lead alloys [8]. Zabdyr [9] explored phase diagram, crystal structure and lattice parameter by varying atomic weight percentage of Hg but the detailed thermophysical investigation is incomplete.

The properties under investigation include the Gibbs free energy of mixing, enthalpy of mixing, chemical activity, concentration fluctuation in long-wavelength limit and Warren–Cowley short-range order parameter of the alloy. Similarly, concentration-dependent surface tension and viscosity of binary liquid alloys are investigated, these being the most desirable in metallurgical research for specifying the surface and transport properties of liquid mixtures: as such, scientists are attempting to investigate these aspects by proposing several models [10–16] . Furthermore, surface segregation, which primarily refers to the concentration disparity between the alloys' surface and bulk materials, is one of the most essential elements to be investigated in metallurgical research. The difference in surface energy between the alloy's constituent elements is the fundamental source of this disparity, the element with lower surface energy tending to segregate on the surface [17]. Theoretical study indicates that the atom with a larger size tends to segregate on the surface of liquid alloy [18].

The present work also aims to study the surface tension of the alloy with a compound formation model [13]. Due to a lack of experimental data, the computed result is compared with two other models: a statistical mechanical approach [12] and an improved derivation of the Butler equation [16]. For the study of viscosity, this study employs three models; the Kozlov-Ronanov-Petrov equation [11], the Kaptay equation and the Budai-Benko-Kaptay model [10].

II Theoretical formulation

i Thermodynamic functions

Let a binary alloy contain N_A and N_B number of A and B atoms respectively. The model assumes the existence of complexes A_xB_y in such a way that

$$xA + yB = A_xB_y \tag{1}$$

where x and y are small integers.

With this assumption, the grand partition function in terms of configurational energy [6] is solved and excess free energy of mixing is obtained as given in Eq. (2) by which various properties are obtained.

$$G_M^{XS} = RT \int_0^C \gamma dC \tag{2}$$

where γ is the activity coefficient ratio of atom A to B, C is the concentration of A atom and R is universal gas constant. After simple mathematical calculation, the solution of Eq. (2) is given as

$$G_M^{XS} = N[\theta\omega + \theta_{AB}\Delta\omega_{AB} + \theta_{AA}\Delta\omega_{AA} + \theta_{BB}\Delta\omega_{BB}] \tag{3}$$

where $\theta = C(1-C)$ and $\theta_{j,k}$'s are the simple polynomials in C that depend on the values of integers x and y, ω is interchange energy, and $\Delta\omega_{jk}$ are the interaction energy parameters.

For A =Hg, B =Pb, $x = 1$, $y = 2$, the values of $\theta_{j,k}$'s are found to be [6, 19]

$$\theta_{AA}(C) = 0 \tag{4}$$

$$\theta_{AB}(C) = \frac{1}{6}C + C^2 - \frac{5}{3}C^3 + \frac{1}{2}C^4 \tag{5}$$

$$\theta_{BB}(C) = -\frac{1}{4}C + \frac{1}{2}C^2 - \frac{1}{4}C^4 \tag{6}$$

The Gibbs free energy of mixing for complex formation is given by

$$\begin{aligned} G_M &= G_M^{XS} + G_M^{ideal} \\ &= G_M^{XS} + RT(C\ln C + (1-C)\ln(1-C)) \\ &= RT\left[\theta\frac{\omega}{k_BT} + \theta_{AB}\frac{\Delta\omega_{AB}}{k_BT} + \theta_{AA}\frac{\Delta\omega_{AA}}{k_BT}\right. \\ &\quad \left. + \theta_{BB}\frac{\Delta\omega_{BB}}{k_BT} + C\ln C + (1-C)\ln(1-C)\right] \end{aligned} \tag{7}$$

Here θ_{AA} is taken as zero because, according to the model used, the value of x is 1. In this case, the probability of A and A pair to be part of the complex is zero, such that the coefficient of $\frac{\Delta\omega_{AA}}{k_BT}$ in Eq. (6) also tends to zero. If there are no complexes in the alloy, then $\Delta\omega_{jk}$ is zero. In such a case, the above equation takes the form as given below:

$$G_M = RT\left[\theta\frac{\omega}{k_BT} + C\ln C + (1-C)\ln(1-C)\right] \tag{8}$$

The enthalpy of mixing is calculated with the standard thermodynamic relation:

$$\begin{aligned}\frac{H_M}{RT} &= \frac{G_M}{RT} - \left[\frac{dG_M}{RdT}\right]_{C,N,P} \\ &= \theta\left[\frac{\omega}{k_BT} - \frac{1}{k_B}\frac{d\omega}{dT}\right] \\ &\quad + \theta_{AB}\left[\frac{\Delta\omega_{AB}}{K_BT} - \frac{1}{k_B}\frac{d\Delta\omega_{AB}}{dT}\right] \\ &\quad + \theta_{BB}\left[\frac{\Delta\omega_{BB}}{K_BT} - \frac{1}{k_B}\frac{d\Delta\omega_{BB}}{dT}\right]\end{aligned} \tag{9}$$

The activity of each constituent element of the alloy is revealed following the standard thermodynamic relation,

$$RT\ln a_j(j=A,B) = G_M + (1-C)\left[\frac{\partial G_M}{\partial C_j}\right]_{T,P,N} \tag{10}$$

Now, by solving Eqs. (7) and (10), the theoretical value of activity of each constituent component is given as follows:

$$\begin{aligned}\ln a_A &= \frac{G_M}{RT} + \frac{1-C}{k_BT}\left[(1-2C)\omega + \theta'_{AB}\Delta\omega_{AB}\right. \\ &\quad \left. + \theta'_{BB}\Delta\omega_{BB} + \ln\frac{C}{1-C}\right]\end{aligned} \tag{11}$$

$$\begin{aligned}\ln a_B &= \frac{G_M}{RT} - \frac{C}{k_BT}\left[(1-2C)\omega + \theta'_{AB}\Delta\omega_{AB}\right. \\ &\quad \left. + \theta'_{BB}\Delta\omega_{BB} + \ln\frac{C}{1-C}\right]\end{aligned} \tag{12}$$

where, θ'_{AB}, θ'_{AA} and θ'_{BB}, respectively, are derivatives of θ_{AB}, θ_{AA} and θ_{BB} with respect to concentrations.

ii Microscopic Functions

The concentration fluctuation in the long-wavelength limit $S_{CC}(0)$for the alloy is given from the relation as [20],

$$S_{CC}(0) = RT\left[\frac{\partial^2 G_M}{\partial C^2}\right]_{T,P,N} \tag{13}$$

The value of $S_{CC}(0)$ can be obtained by using experimentally observed activities with the help of the following Eq. (14). Hence the values of $S_{CC}(0)$ obtained from this equation are called experimental values.

$$\begin{aligned}S_{CC}(0) &= a_A(1-C)\left[\frac{\partial a_A}{\partial C_A}\right]^{-1}_{T,P,N} \\ &= a_BC\left[\frac{\partial a_B}{\partial C_B}\right]^{-1}_{T,P,N}\end{aligned} \tag{14}$$

where a_A and a_B are observed activities of elements A and B respectively. For simplicity, we can write C and 1-C in place of C_A and C_B, respectively. Solving Eqs. (7) and (14), the value of $S_{CC}(0)$ is found as,

$$\begin{aligned}S_{CC}(0) = C(1-C)\Bigg[1 + C(1-C)\Bigg(&-2\frac{\omega}{K_BT} \\ &+ \theta"_{AB}\frac{\Delta\omega_{AB}}{K_BT} + \theta"_{BB}\frac{\Delta\omega_{BB}}{K_BT}\Bigg)\Bigg]^{-1}\end{aligned} \tag{15}$$

Where $\theta"_{jk}$ are second concentration derivatives of θ_{jk}.

The Warren-Cowley short-range order parameter (α_1) is related to concentration fluctuation in the long-wavelength limit [21, 22] as:

$$\alpha_1 = (S-1)[S(Z-1)+1]^{-1} \tag{16}$$

where Z is coordination number and

$$S = \frac{S_{CC}(0)}{S^{id}_{CC}(0)} \tag{17}$$

iii Transport property: viscosity

At the microscopic level, the mixing nature of molten alloy may be examined in terms of viscosity, which provides basis for some of the most fundamental theories concerning atomic transport qualities. It is regarded as one of the most important thermophysical qualities in metallurgical research, which primarily deals with industrial processes and a variety of natural occurrences. It is influenced by factors such as the liquid's composition, cohesion energy, and molar volume [23, 24]. The composition dependence of viscosity at 600 K is computed to examine the atomic transport features of the Hg-Pb alloy. But due to the lack of experimental data, viscosity is compared using three different models: the Kozlov-Ronanov-Petrov equation, the Kaptay equation, and the BBK (Budai-Benko-Kaptay) model.

a Kozlov-Ronanov-Petrov equation

In liquids, viscous flow depends on cohesive interaction, this interaction results from geometric and electronic shell effects [25]. The KRP equation has been developed to incorporate cohesion interaction in terms of enthalpic effect in order to consider the viscous flow in a liquid alloy. At temperature T, the equation is given as:

$$\ln \eta = C \ln C \ln \eta_A + (1-C) \ln \eta_B - \frac{H_M}{3RT} \quad (18)$$

where η and η_j are viscosity of the alloy and viscosity of individual elements A and B, respectively. For the metals, the variation of viscosity with temperature is given as [26]

$$\eta_j = \eta_0 \exp \frac{\epsilon}{RT} \quad (19)$$

where η_0 and ϵ are constants of each metal's units of viscosity and energy per mole.

b Kaptay equation

Kaptay developed an equation by considering the theoretical relationship between the cohesive energy and activation energy of the viscous flow. At temperature T, the equation is:

$$\eta = \frac{hN_{Av}}{CV_A + (1-C)V_B + V^E} \times exp\left(\frac{CG_A + (1-C)G_B - \Phi H_M}{RT}\right) \quad (20)$$

where h is Plank's constant, N_{Av} is Avogadro's number, $V_j (j = A, B)$ is the molar volume of pure metal, V^E is excess molar volume upon alloy formation, G_j is Gibb's energy of activation of the viscous flow in pure metals, and ϕ is a constant whose value is (0.155±0.015) [27]. The Gibb's energy of activation of pure metal is calculated by the following equation:

$$G_j = RT \ln\left(\frac{\eta_j V_j}{hN_{Av}}\right) \quad (21)$$

c BBK (Budai-Benko-Kaptay) model

The BBK model is used for the viscosity of multicomponent alloys. At temperature, it is given as:

$$\eta = LT^{1/2}(CM_A + (1-C)M_B)^{1/2} \times (CV_A + (1-C)V_B + V^E)^{-2/3} \times exp\left[(CT_{m,A} + (1-C)T_{m,B} - \frac{H_M}{\chi R})\frac{I}{T}\right] \quad (22)$$

where L and I are constants whose values are $(1.80\pm0.39)\times10^{-8} j/Kmol^{1/3})^{1/2}$ and (2.34±0.02), respectively, and χ is a semi-empirical parameter having a value equal to 25.4. Similarly M_j and T_{mJ} are, respectively, molar mass and the effective melting temperature of constituent elements of the alloy.

iv Surface property

In metallurgy and industry, the surface properties (surface tension and surface concentration) of liquid alloy or liquid metal are considered to be prime factors for the processing, as well as for the production, of new materials due to their relation with both surface and interface in the liquid metal process [28, 29]. The interfacial motion caused by the surface tension of liquid plays a major role in many industrial phenomena, hence the importance given

to the surface and interfacial behaviors of liquid metals in the metallurgical process for solidification, controlling the processes of welding and casting [30].

a Compound Formation model

The model assumes that there is a compound forming tendency in the binary liquid alloy similar to that of the compound forming tendency in the solid state, in the form of short-ranged volume elements, due to the formation of intermetallic compound A_xB_y in the melt. The equation in this model is developed by using the grand partition function similar to the quasi chemical approximation. The equation at temperature T is given below:

$$\begin{aligned}\sigma &= \sigma_A + \frac{k_BT}{\rho}\ln\frac{C^s}{C} + \frac{\omega}{\rho}[p(f^S - f) - qf] \\ &\quad + \frac{\Delta\omega_{AB}}{\rho}[p(f^S_{AB} - f_{AB}) - qf_{AB}] \\ &\quad + \frac{\Delta\omega_{BB}}{\rho}[p(f^S_{BB} - f_{BB}) - qf_{BB}] \qquad (23) \\ &= \sigma_B + \frac{k_BT}{\rho}\ln\frac{1-C^s}{1-C} + \frac{\omega}{\rho}[p(\varphi^S - \varphi) - q\varphi] \\ &\quad + \frac{\Delta\omega_{AB}}{\rho}[p(\varphi^S_{AB} - \varphi_{AB}) - q\varphi_{AB}] \\ &\quad + \frac{\Delta\omega_{BB}}{\rho}[p(\varphi^S_{BB} - \varphi_{BB}) - q\varphi_{BB}] \qquad (24)\end{aligned}$$

where φ, f, φ_{jk} and f_{jk} are bulk concentration functions. Similarly, φ^S, f^S, φ^S_{jk} and f^S_{jk} are surface concentration functions, and ρ is the mean area of the surface per atom. For $x = 1$ and $y = 2$, the bulk concentration functions are [13, 31]:

$$\varphi = C^2 \qquad (25)$$

$$\varphi_{AB} = \frac{1}{6} + 2(1-C) - 6(1-c)^2 + \frac{16}{3}(1-C)^3 - \frac{3}{2}(1-C)^4 \qquad (26)$$

$$\varphi_{BB} = -\frac{1}{4} + (1-C) - \frac{1}{2}(1-C)^2 + (1-C)^3 - \frac{3}{4}(1-C)^4 \qquad (27)$$

$$f = (1-C)^2 \qquad (28)$$

$$f_{AB} = (1-C)^2 + \frac{10}{3}(1-C)^3 - \frac{3}{2}(1-C)^4 \qquad (29)$$

$$f_{BB} = -(1-C)^2 + \frac{3}{4}(1-C)^4 \qquad (30)$$

The functions φ^s, φ^S_{jk}, f^s and f^s_{jk} can be obtained from Eqs. (26) to (30) by replacing bulk concentration C with surface concentration C^S, while p and q are surface coordination fractions that indicate the fraction of the number of nearest neighbors of an atom within its own layer and in the adjoining layers, respectively, and and are related as $p + 2q = 1$. In a simple cubic crystal, $p = 2/3$ and $q = 1/6$. In a bcc crystal, $p = 3/5$ and $q = 1/5$, and in close packed crystal, $p = 1/2$ and $q = 1/4$. The mean atomic surface area is given by following relation [13]:

$$\rho = \sum_j C_j\rho_j \qquad (31)$$

The atomic surface area of each component is given as

$$\rho_j = 1.012\left(\frac{V_j}{N_{Av}}\right)^{2/3} \qquad (32)$$

b Statistical mechanical approach

This method is mainly based on the concept of layered structure near the interface. The model connects the surface tension to thermodynamic properties through the activity coefficient (γ_j) and the interchange energy between the components of an alloy. The equation at temperature T is given as below:

$$\sigma = \sigma_j + \frac{K_B T}{\rho} \ln \frac{C_j^S}{C_j \gamma_j} + \left[p(1-C_j^S)^2 - q(1-C_j)^2\right] \frac{\omega}{\rho} \quad (33)$$

c Improved Derivation of the Butler equation

According to this model, there exists a monoatomic layer, called surface monolayer, at the surface of a liquid as a separate phase, and it is in thermodynamic equilibrium with the bulk phase. The surface tension (σ) of binary alloy at temperature T is given by the improved Butler equation as:

$$\sigma = \frac{S_j^0}{S_j}\sigma_j^0 + \frac{RT}{S_j} \ln \frac{C_j^S}{C_j^b} + \frac{G_j^{S,XS} - G_j^{b,XS}}{S_j} \quad (34)$$

where, σ_j^0, S_j^0, S_j are surface tension of pure liquid metal, molar surface area of pure liquid metal, and partial molar surface area of j^{th} component, respectively. $G_j^{S,Xs}$ and $G_j^{b,Xs}$ are partial excess free energy of mixing in the surface and bulk of constituent elements of the alloy, respectively. The molar surface area of pure component is given as:

$$S_j^0 = \delta \left(\frac{M_j^0}{\lambda_j^0}\right)^{2/3} N_{Av}^{1/3} \quad (35)$$

where δ, M_j^0, λ_j^0, δ and $N_A v$ are geometrical constant, molar mass, density of each constituent element at its melting temperature, and Avogadro's number, respectively. The value of geometrical constant is expressed as,

$$\delta = \left(\frac{3f_v}{4}\right)^{2/3} \frac{\pi}{f_s} \quad (36)$$

where f_v is volume packing fraction and f_s is surface packing fraction. For liquid metal, the values of f_v and f_s are 0.66 and 0.906 respectively [33].

III Results and discussion

i Thermodynamic and microscopic properties

Generally, the properties of binary liquid alloys depend on temperature, composition, and pressure.

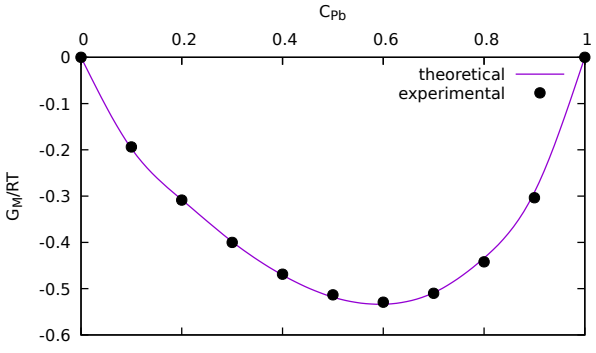

Figure 1: Gibbs free energy of mixing versus bulk concentration of Pb.

Our study of the binary alloy Hg-Pb is carried out at fixed atmospheric pressure and fixed temperature of 600 K as a function of the composition of the alloy. During the study, we assumed complexity with $x = 1$ and $y = 2$ and computed different thermodynamic and structural properties for compound forming molten alloys. The different results thus obtained from the study are outlined in the sections below.

a Thermodynamic Properties

For the analysis of the thermodynamic properties, we consider Eqs. (7), (9), (11), and (12), as mentioned above. For the Gibbs free energy of mixing, the interaction energy parameters are determined by the method of successive approximation for several concentrations, following stoichiometry of the $HgPb_2$ alloy with the help of experimental values in the concentration range (0.1 to 0.9) [34]. The approximated values of energy parameters are as follows:

$$\frac{\omega}{k_B T} = 2.139,$$
$$\frac{\Delta\omega_{AB}}{k_B T} = -2.264,$$
$$\frac{\Delta\omega_{BB}}{k_B T} = 0.392$$

To calculate the interaction energy parameters, no statistical methods such as mean square deviation were used to decide the best fit values, hence the

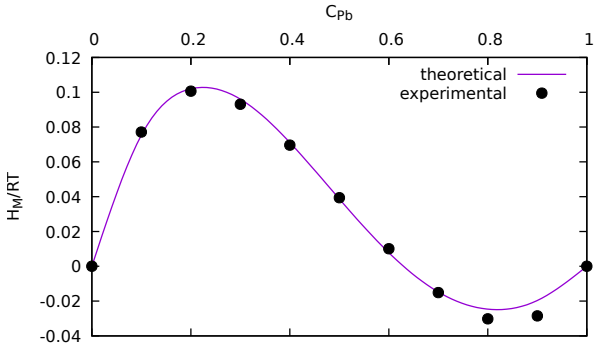

Figure 2: Enthalpy of mixing versus bulk concentration of Pb

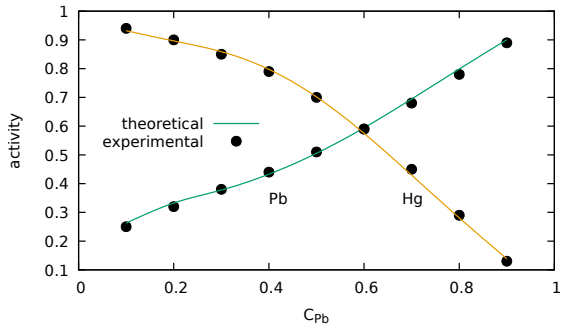

Figure 3: Chemical activity versus bulk concentration of Pb

parameters thus obtained are considered reasonable for analysis and have been considered throughout the study of different mixing properties. The computed values of G_M/RT are in good agreement with experimental values as shown in Fig. 1. The theoretically computed value of free energy of mixing is a minimum of $-0.533RT$ at 0.6 concentration of Pb. The calculation of free energy of mixing indicates that the alloy HgPb at molten state is weakly interacting. Similarly, being asymmetric at 0.5 concentration, it is classified as an irregular alloy.

The temperature derivatives of interaction energy parameters which are used for the theoretical calculation of enthalpy of mixing are obtained by the method of successive approximation. The best fit approximated values of such parameters are:

$$\frac{1}{k_B}\frac{d\omega}{dT} = 0.767,$$
$$\frac{1}{k_B}\frac{d\Delta\omega_{AB}}{dT} = -0.3128,$$
$$\frac{1}{k_B}\frac{d\Delta\omega_{BB}}{dT} = 0.429$$

The plot of enthalpy of mixing versus concentration of lead is shown in Fig. 2. It is positive below 0.6 concentration of lead, while above this concentration it is negative, and both computed and experimental values of enthalpy of mixing are in agreement, with small discrepancies.

The deviation of alloy from ideal behavior can be examined by chemical activity, a measure of effective concentration in the mixture, as its magnitude depends on the interaction of constituent binary components of the alloy. Equations (11) and (12) are used for the calculation of the chemical activity of elements of alloy Hg-Pb. Figure 3 plots experimental and theoretically computed values of the chemical activity of the components of the alloy, showing good agreement between the experimental and theoretical activities of the components in the alloy at temperature 600 K at all concentrations of Pb.

b Microscopic Properties

It is difficult to perform diffraction experiments on materials at high temperatures. Thus, to make the study of local arrangement of atoms in the binary alloy more effective, the concentration fluctuations in the long-wavelength limit ($S_{CC}(0)$) are

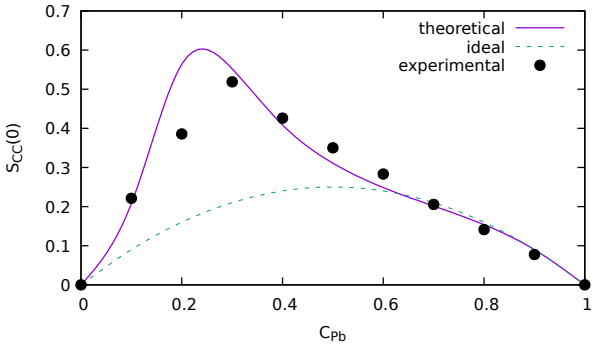

Figure 4: Concentration fluctuation in long-wavelength limit versus bulk concentration of Pb

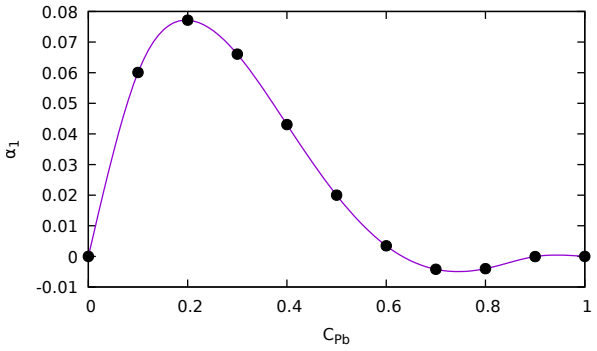

Figure 5: Warren-Cowley short-range order parameter versus bulk concentration of Pb

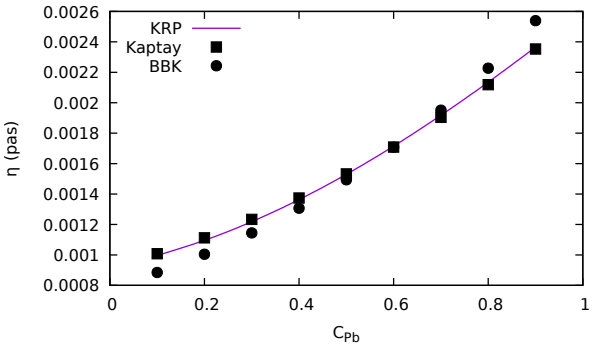

Figure 6: Viscosity versus bulk concentration of Pb

considered some of the most important microscopic functions [20, 35]. For any given concentration, if $S_{CC}(0) < S^{id}_{CC}(0)$, the alloy is expected to have complex formation in nature and if $S_{CC}(0) > S^{id}_{CC}(0)$, the expected nature of the alloy is segregating. The graph of experimental, theoretical and ideal values of $S_{CC}(0)$ versus concentration of Pb is shown in Fig. 4. In the figure, both the experimental and theoretical values of $S_{CC}(0)$ lie above the ideal value for lead concentration values below 0.6 , indicating that the alloy has a segregating nature below this concentration of lead, while above this concentration it exhibits an ordering nature.

The Warren-Cowley short range parameter (α_1) is considered one of the most powerful parameters for information regarding the arrangement of atoms in the liquid alloys. It provides quantitative information about the degree of local arrangement of atoms in the alloys. Its value lies between +1 and -1. The positive value of α_1 is considered an indication of a segregating nature, which is complete for $\alpha_1 = 1$, whereas its negative value indicates an ordering nature, and is complete for $\alpha_1 = -1$. Similarly the value $\alpha_1 = 0$ indicates the random arrangements of atoms in the liquid mixture. The value of α_1 computed as a function of the concentration of Pb using Eq. (16) is shown in Fig. 5 where we took coordination number $Z = 10$. It is observed that the α_1 is positive up to 0.6 concentration range of lead, with highest values at a concentration of 0.2, indicating the strong segregating tendency of the alloy. But above a 0.6 concentration of lead, the value of α_1 goes on decreasing, showing the ordering tendency of the alloy.

ii Viscosity

For the theoretical calculation of viscosity of Hg-Pb alloy at 600 K, the viscosities of each component (Pb and Hg) are required for KRP and Kaptay models. These values are obtained from Eq. (19) after substituting the values of η_0 and ϵ of the metals as given in reference [26]. The value of enthalpy for different concentrations is used as obtained from Eq. (9) and the Gibbs energy of activation of each pure metal is obtained from Eq. (21). Due to the lack of an experimental value for V^E, it is taken as zero. In fact, the value of V^E is non-zero for a non-ideal alloy, but the contribution of this term is very small for the determination of viscosity [15].

The results obtained from three models are compared as shown in Fig. 6. In the models, the viscosity of the liquid alloy increases with the increase in concentration of lead. The figure shows that there is a small deviation of the viscosity computed by BBK model as compared to the others. Due to the inability to compare theoretically computed results with experimental results, it becomes difficult to draw conclusions based on the models for the concentration dependence of the viscosity of Hg-Pb liquid alloy at temperature 600 K.

iii Surface segregation and surface tension

To calculate the surface tension of the alloy Hg-Pb, the densities and surface tension of individual metals for all models required at 600 K are calculated by using the relations given in reference [26].

For the compound formation model, the same interaction parameters ω and ω_{jk} used in thermody-

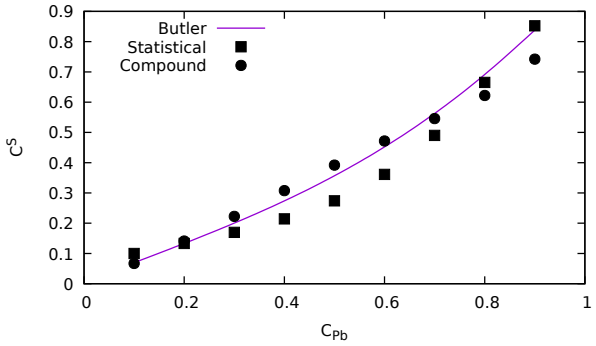

Figure 7: Surface concentration of lead versus bulk Pb concentration

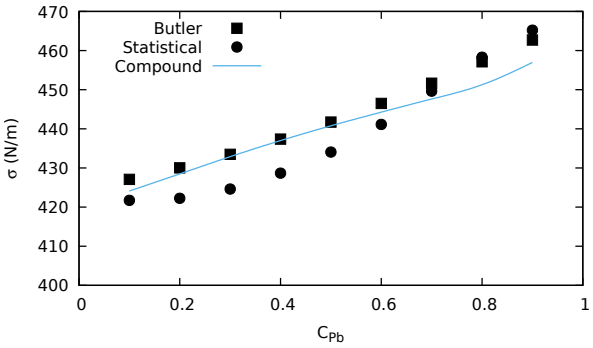

Figure 8: Surface tension versus bulk Pb concentration

namic properties are used. Now, writing these values and values of other quantities of both metals in Eqs. (23) and (24) and solving them simultaneously, we first obtain surface concentrations of both metals, and then using each surface concentration of the corresponding metals, the surface tension is obtained. A similar method is applied to the other models. For statistical mechanical approach interchange energy, $\omega = 0.699$, obtained from Eq. (8), is used.

For the improved derivation of the Butler model, the bulk and partial excess free energy of mixing of individual lead and mercury in a liquid state at 600 K are taken from reference [34]. The geometrical constant and the ratio of surface excess energy to the bulk excess energy ($G_i^{S,Xs}/G_i^{b,Xs}$) are respectively considered as 1.061 and 0.818 [33]. Kaptay suggested that, in the case of negligible or unknown excess molar volume of the mixture, the partial molar volume can be replaced by the molar volume of the same component. In such a situation, the partial surface area (S_i) is replaced by the surface area (S_i^0) of the same pure component [16,36]. The computed values of surface concentrations and surface tensions from all three models are compared in Figs. 7 and 8 respectively.

Figure 7 shows the increasing pattern of the surface concentration of Pb with the increase in bulk concentration of Lead in all models. At 600 K the surface tension of mercury is less than the surface tension of lead. This suggests the surface segregating tendency of Hg. Thus, at higher bulk concentration of Pb, two different atoms of the alloy are involved in the formation of chemical complexes or intermetallic compounds assumed to be $HgPb_2$, but at lower bulk concentration of Pb, the surface of the alloy is enriched with Hg atoms.

In Fig. 8, the surface tension of alloy Hg-Pb increases gradually with the increase in bulk concentration of Pb. The variation of surface tension in the compound formation model at higher bulk concentration of Pb than in the other two models is believed to be the cause of consideration of set of the interaction energy parameters because, as we already mentioned, there is the possibility of compound formation at higher bulk concentrations of Pb. The compound formation model is expected to give better results than the other two models due to the presence of interaction parameters. However, due to the lack of experimental results, computed results cannot be compared.

IV Conclusions

The present study is a theoretical analysis for the understanding of thermodynamic, structural, transport and surface behavior of the binary liquid alloy Hg-Pb at 600 K under the assumption of the existence of the $HgPb_2$ complex in the liquid mixture by compound formation model. The study explains the asymmetric behavior of the thermodynamic properties as a function of concentration as well as of a weakly interacting alloy. The theoretical study shows that the alloy has the nature of segregating at a lower concentration of Pb, but it shows an ordering nature at higher concentration of Pb at 600 K. Similarly, the viscosity and surface tension increases with the increase in the concentration of lead.

Acknowledgements - We are grateful to University Grants Commission of Nepal for research grant.

[1] N Panthi, I B Bhandari, I S Jha, I Koirala, *Thermophysical behavior of sodium lead alloy at different temperature*, Adv. Stud. Theor. Phys. **15**, 153 (2021).

[2] Y Plevachuk, V Sklyarchuk, G Pottlacher, A Yakymovych, O Tkach, *Thermophysical properties of some liquid binary Mg-based alloys*, J. Min. Metall. B **53**, 279 (2017).

[3] I Koirala, *Chemical ordering of Ag-Au alloys in the molten state*, J. I. S. T. **22**, 191 (2018).

[4] D Adhikari, B P Singh, I S Jha, *Phase separation in Na–K liquid alloy*, Phase Transit. **85**, 675 (2012).

[5] P J Flory, *Thermodynamics of high polymer solutions*, J. Chem. Phys. **10**, 51 (1942).

[6] A B Bhatia, R N Singh, *Thermodynamic properties of compound forming molten alloys in a weak interaction approximation*, Phys. Chem. Liq. **11**, 343 (1982).

[7] A B Bhatia, R N Singh, *A quasi-lattice theory for compound forming molten alloys*, Phys. Chem. Liq. **13**, 177 (1984).

[8] A A Nayeb-Hashemi, J B Clark, *The Mg-Pb (Magnesium-lead) system*, Bull. Alloy Phas. Diagr. **6**, 56 (1985).

[9] L A Zabdyr, C Guminski, *The Hg-Pb (Mercury-lead) system*, J. Phase Equilib. **14**, 734 (1993).

[10] J A V Butler, *The thermodynamics of the surfaces of solutions*, Proc. R. Soc. Lond. A **135**, 348 (1932).

[11] L Y Kozlov, L M Romanov, N N Petrov, *Prediction of multicomponent metallic melt viscosity*, Izv. Vuz. Chern Metallurg **3**, 7 (1983).

[12] L C Prasad, R N Singh, *A quasi-lattice model for the thermodynamic properties of Au-Zn liquid alloys*, Phys. Chem. Liq. **22**, 1 (1990).

[13] R Novakovic, E Ricci, D Giuranno, F Gnecco, *Surface properties of Bi–Pb liquid alloys*, Surf. Sci. **515**, 377 (2002).

[14] R Novakovic, M L Muolo, A Passerone, *Bulk and surface properties of liquid X–Zr (X= Ag, Cu) compound forming alloys*, Surf. Sci. **549**, 281 (2004).

[15] I Budai, M Z Benkő, G Kaptay, *Comparison of different theoretical models to experimental data on viscosity of binary liquid alloys*, Mater. Sci. Forum **537**, 489 (2007).

[16] G Kaptay, *Improved derivation of the Butler equations for surface tension of solutions*, Langmuir **35**, 10987 (2019).

[17] K A Eldressi, H A Eltawahni, M Moradi, E R Twiname, R E Mistler, *Energy effects in bulk metals*, In: Reference module in materials science and materials engineering, Elsevier (2019).

[18] L C Prasad, R N Singh, G P Singh, *The role of size effects on surface properties*, Phys. Chem. Liq. **27**, 179 (1994).

[19] R N Singh, *Short-range order and concentration fluctuations in binary molten alloys*, Can. J. Phys. **65**, 309 (1987).

[20] A B Bhatia, D E Thornton, *Structural aspects of the electrical resistivity of binary alloys*, Phys. Rev. B **2**, 3004 (1970).

[21] M Cowley, *Short- and long-range order parameters in disordered solid solutions*, Phys. Rev. **120**, 1648 (1960).

[22] B E Warren, *X-ray Diffraction*, Addison-Wesley Pub. Co., Reading (1969).

[23] D R Poirier, G H Geiger, *Transport phenomena in materials processing*, TMS Publications, Warrendale PA (1994).

[24] T Iida, R I Guthrie, *The thermophysical properties of metallic liquids: Fundamentals*, Oxford University Press, USA (2015).

[25] A K Starace, C M Neal, B Cao, M F Jarrold, A Aguado, J M López, *Correlation between the latent heats and cohesive energies of metal clusters*, J. Chem. Phys. **129**, 144702 (2008).

[26] E A Brandes, G B Brook, *Smithells metals reference book*, Butterworth-Heinemann, Oxford (1992).

[27] G Kaptay, *A unified equation for the viscosity of pure liquid metals*, Int. J. Mater. Res. **96**, 24 (2005).

[28] T Iida, *Physical properties of liquid metals [IV] surface tension and electronic transport properties of liquid metals*, Weld. Int. **8**, 766 (1994).

[29] I Koirala, B P Singh, I S Jha, *Study of segregating nature in liquid Al-Ga alloys*, Scientific World **12**, 14 (2014).

[30] J U Brackbill, D B Kothe, C Zemach, *A continuum method for modeling surface tension*, J. Comput. Phys. **100**, 335 (1992).

[31] N Jha, A K Mishra, *Thermodynamic and surface properties of liquid Mg–Zn alloys*, J. Alloys Compd. **329**, 224 (2001).

[32] P Laty, J C Joud, P Desre, *Surface tensions of binary liquid alloys with strong chemical interactions*, Surf. Sci. **60**, 109 (1976).

[33] G Kaptay, *A unified model for the cohesive enthalpy, critical temperature, surface tension and volume thermal expansion coefficient of liquid metals of bcc, fcc and hcp crystals*, Mater. Sci. Eng. A **495**, 19 (2008).

[34] R Hultgren, P D Desai, D T Hawkins, M Gleiser, KK Kelley, *Selected values of the thermodynamic properties of binary alloys*, ASM, Metals Park, Ohio (1973).

[35] R Novakovic, J Brillo, *Thermodynamics, thermophysical and structural properties of liquid Fe–Cr alloys*, J. Mol. Liq. **200**, 153 (2014).

[36] G Kaptay, *A coherent set of model equations for various surface and interface energies in systems with liquid and solid metals and alloys*, Adv. Colloid Interface Sci. **283**, 102212 (2020).

Defect and Diffusion Forum
ISSN: 1662-9507, Vol. 419, pp 147-154

Submitted: 2022-03-29
Revised: 2022-07-18
Accepted: 2022-07-20
Online: 2022-10-20

High Temperature Stability of K-Pb Liquid Alloy

Narayan Panthi[a*] Indra Bahadur Bhandari[b], Ishwar Koirala[c]

Patan Multiple Campus, Patandhoka, Lalitpur, Nepal

[a]narayan.panthi321@gmail.com, [b]bhandari.indra@gmail.com, [c]ikphysicstu@gmail.com

Keywords: Thermo-physical properties; Ordering; Complex formation; Interaction Parameters

Abstract. The study explores the cocentration dependent thermo-physical properties of complex potassium-lead binary liquid alloy at temperature 848 K by assuming KPb_2 complex from the different model equations. The Quasi Chemical approximation and the Redlich and Kister equation are used to investigate features such as free energy, heat of mixing, chemical activity, and concentration fluctuation in long wave limit at temperature 848 K. However, at 900 K and 1000 K, these are exclusively examined using the R-K equation. The temperature dependent exponential interaction parameters proposed by Kaptay are taken into account in the RK equation. The study goes on to look at the alloy's viscosity and surface tension using the Budai-Benko-Kaptay model and the Kaptay's new derivation of Butler equation. The alloy system is investigated in depth, with a focus on the interaction energy parameters between the alloy's surrounding atoms. The work investigates the fact that the liquid alloy has a moderately interacting as well as an ordering character throughout the whole concentration range. The theoretically investigated thermodynamic facts are in reasonably agree with the corresponding experimental results at 848 K. At greater temperatures, the alloy's tendency goes from ordering to segregating. The alloy's viscosity and surface tension decrease as the temperature rises.

Introduction

In metallurgy and engineering, the alloys are considered advanced materials than individual metals thanks to their good heat resistance, mechanical strength and so on. The formation of alloy is usually related to changes in the bonding and structure of a given system. The interaction and structural reorganization of the component atoms throughout the formation of the alloy create it totally different from crystals and therefore it becomes tough to understand the alloy in comparison to the metallic structure. The unique nature of the alloy is principally ruled by concentration, size of constituent elements and electrochemical effect and hence atoms of the alloy either tend to align showing heterocoordination nature or a powerful ordering tendency [1-4]. Hence the metallurgists and the physicists have both shown a keen interest in learning more about the mixing behavior of alloys. However, owing to the experimental difficulties and time constraint, the investigation of various behaviors of alloys is still incomplete. In order to resolve such problem and to speed up the investigation process, vital efforts are done by developing different model equations [5-11]. The goal of this study is to use the Quasi chemical approximation [8] to investigate the thermodynamics of potassium-lead alloy taking KPb_2 complex and the Redlich-Kister equation [6] at temperature 848 K. Further the study also aims to investigate thermophysical properties, viscosity and surface tension at higher temperatures 900 K and 1000 K which are two important thermo-physical characters that are studied in metallurgy in order to acquire the knowledge of surface and transport properties of molten alloy. Both of these are crucial to the casting process in order to produce various devices with improved mechanical performance. [12,13]. The Budai-Benko-Kaptay (BBK) model [14] and the new derivation of the Butler equation [15] are used to investigate the viscosity and surface tension of the alloy at various temperatures in this research article.

According to the Quasi chemical approximation there is an energetically favored pseudoternary combination of X atoms, Y atoms and X_mY_n group of atoms (m and n are integers) in the binary alloy. The X_mY_n group of atoms is called complex. The equilibrium mixing behaviours of the binary alloy are controlled by short-range atomic interaction energies ε_{XX}, ε_{YY}, and ε_{XY} for XX, YY, and X_mY_n

atomic pairs respectively. But the Redlich and Kister equation does not consider the complex nature of the alloy and generally depends on the temperature dependent linear interaction energy parameters called R-K polynomials. In some of the alloys there appears artificial miscibility gap (artefact) for high temperature study by using such linear interaction parameters [16 -18]. To remove such difficulty, George Kaptay [19, 20] has suggested the use of temperature dependent exponential interaction parameter rather than linear interaction parameter. Thus, we investigate the alloy's behavior assuming temperature-dependent exponential interaction parameters in the Redlich and Kister equation.

Potassium is an interesting element for researchers as it can be used as alternative energy storage device. Due to high cost, uneven distribution and limited nature of sources, the lithium ion batteries may not fulfill the growing demand of energy storage devices. As a result, it is vital to look for alternative energy storage systems that are mostly focused on the low-cost and affluent elements. Hence the researchers are showing more attention towards the Potassium-ion batteries due to its low price and enough amount on the earth, and also similar type of chemical and physical properties of potassium in comparison to lithium and sodium [21]. On the other hand, due to extreme ductility and softness, lead is frequently employed in industry as lead alloys.

Theoretical Basis

Consider a binary alloy of elements X and Y. Following QCA model [8], the excess free energy of mixing is obtained as,

$$G_{\mathrm{M}}^{XS} = N[\Theta\,\omega + \Theta_{XY}\Delta\omega_{XY} + \Theta_{XX}\Delta\omega_{XX} + \Theta_{YY}\Delta\omega_{YY}] \quad (1)$$

Where θ is product of concentration of constituents of binary alloy, ω and $\Delta\omega_{jk's}$ are interaction energy parameters.

For $X = \mathrm{K}, Y = \mathrm{Pb}$, $m = 1$, $n = 2$, the values of $\theta_{j,k}{}'s$ are [8]

$$\Theta_{XX}(C) = 0,\ \Theta_{XY}(c) = \frac{1}{6}C + C^2 - \frac{5}{3}C^3 + \frac{1}{2}C^4, \qquad \Theta_{YY}(C) = -\frac{1}{4}C + \frac{1}{2}C^2 - \frac{1}{4}C^4 \quad (2)$$

Where $C = C_X$ and $(1 - C) = C_Y$ are concentrations of X and Y components of the alloy respectively

Now the free energy (G_{M}) of compound forming alloy is given by

$$G_{\mathrm{M}} = RT\left[\Theta\frac{\omega}{k_{\mathrm{B}}T} + \Theta_{XY}\frac{\Delta\omega_{XY}}{k_{\mathrm{B}}T} + \Theta_{XX}\frac{\Delta\omega_{XX}}{k_{\mathrm{B}}T} + \Theta_{YY}\frac{\Delta\omega_{YY}}{k_{\mathrm{B}}T} + C\ln C + (1 - C)\ln(1 - C)\right] \quad (3)$$

The standard thermodynamic relation for heat of mixing is:

$$\frac{H_{\mathrm{M}}}{RT} = \Theta\left[\frac{\omega}{k_{\mathrm{B}}T} - \frac{1}{k_{\mathrm{B}}}\frac{d\omega}{dT}\right] + \Theta_{XY}\left[\frac{\Delta\omega_{XY}}{k_{\mathrm{B}}T} - \frac{1}{k_{\mathrm{B}}}\frac{d\Delta\omega_{XY}}{dT}\right] + \Theta_{XX}\left[\frac{\Delta\omega_{XX}}{k_{\mathrm{B}}T} - \frac{1}{k_{\mathrm{B}}}\frac{d\Delta\omega_{XX}}{dT}\right] + \Theta_{YY}\left[\frac{\Delta\omega_{YY}}{k_{\mathrm{B}}T} - \frac{1}{k_{\mathrm{B}}}\frac{d\Delta\omega_{YY}}{dT}\right] \quad (4)$$

Similarly the standard relation for the chemical activity of each element of the alloys is given as,

$$\ln a_j\ (j = X, Y) = \frac{G_M}{RT} + \frac{1 - C_j}{RT}\left[\frac{\partial G_{\mathrm{M}}}{\partial C_j}\right]_{T,P,N} \quad (5)$$

Following equations (7) and (11), the activities (a_X and a_Y) of each component are given as follows,

$$\ln a_X = \frac{G_{\mathrm{M}}}{RT} + \frac{1 - C}{k_{\mathrm{B}}T}\left[(1 - 2C)\omega + \Theta'_{XY}\Delta\omega_{XY} + \Theta'_{XX}\Delta\omega_{XX} + \Theta'_{YY}\Delta\omega_{YY} + \ln\frac{C}{1 - C}\right] \quad (6)$$

$$\ln a_Y = \frac{G_{\mathrm{M}}}{RT} - \frac{C}{k_{\mathrm{B}}T}\left[(1 - 2C)\omega + \Theta'_{XY}\Delta\omega_{XY} + \Theta'_{XX}\Delta\omega_{XX} + \Theta'_{YY}\Delta\omega_{YY} + \ln\frac{C}{1 - C}\right] \quad (7)$$

Where Θ'_{XY} , Θ'_{XX} and Θ'_{YY} are concentration derivatives of Θ_{XY} , Θ_{XX} and Θ_{YY} respectively.
The concentration fluctuation in long wavelength limit of liquid alloys is computed using the Gibbs free energy of mixing, as shown below. [22].

$$S_{CC}(0) = RT\left[\frac{\partial^2 G_{\mathrm{M}}}{\partial C^2}\right]^{-1}_{T,P,N} \tag{8}$$

The value of $S_{CC}(0)$ is found by solving equations (2) and (8) as,

$$S_{CC}(0) = \frac{C_X C_Y}{1 + (1 - C_X)\left[-2\,\frac{\omega}{k_{\mathrm{B}}T} + \Theta''_{XY}\frac{\Delta\omega_{XY}}{k_{\mathrm{B}}T} + \Theta''_{XX}\frac{\Delta\omega_{XX}}{k_{\mathrm{B}}T} + \Theta''_{YY}\frac{\Delta\omega_{YY}}{k_{\mathrm{B}}T}\right]} \tag{9}$$

Where θ''_{jk} is the concentration-related second derivative of θ_{jk} .
Again the excess free energy of liquid alloy by Redlich and Kister equation is [6]

$$G_{\mathrm{M}}^{XS} = C_X C_Y \sum_{i=0}^{n} K_i\,(C_X - C_Y)^i \tag{10}$$

Where K_i temperature dependent interaction parameters.
The temperature-dependent interaction parameters of binary alloys are as follows, [19, 20].

$$K_i = h_i \exp\left(-\frac{T}{t_i}\right) \tag{11}$$

Where h_i and t_i are semi-empirical parameters
The excess Gibbs free energy (G_{M}^{XS}), enthalpy (H_{M}) and excess entropy (S_{M}^{XS}) of mixing are related as,

$$G_{\mathrm{M}}^{XS} = H_{\mathrm{M}} - TS_{\mathrm{M}}^{XS} \tag{12}$$

From equations (19), (20) and (21), the mathematical expressions for heat and excess entropy of the alloy can be obtained as given below.

$$H_{\mathrm{M}} = C_X C_Y \sum_{i=0}^{n}\left(1 + \frac{T}{t_i}\right) h_i \exp\left(-\frac{T}{t_i}\right)(C_X - C_Y)^i \tag{13}$$

$$S_{\mathrm{M}}^{XS} = C_X C_Y \sum_{i=0}^{n}\frac{h_i}{t_i}\exp\left(-\frac{T}{t_i}\right)(C_X - C_Y)^i \tag{14}$$

The activity (a_j) of each component of the alloy is expressed in terms of interaction parameters as;

$$\ln a_{\mathrm{X}} = \frac{G_M}{RT} + (1 - C_X)[(1 - 2C_X)K_0 + (6C_X^2 + 6C_X - 1)K_1 + (-4C_X^4 + 8C_X^3 - 5C_X^2 + C_X)K_2] \tag{15}$$

$$\ln a_{\mathrm{Y}} = \frac{G_M}{RT} - C_X[(1 - 2C_X)K_0 + (6C_X^2 + 6C_X - 1)K_1 + (-4C_X^4 + 8C_X^3 - 5C_X^2 + C_X)K_2] \tag{16}$$

By replacing the Gibbs free energy (G_M) in terms of interaction parameters in equation (14), the $S_{CC}(0)$ is obtained as

$$S_{CC}(0) = RT\left[\frac{RT}{C_X C_Y} - 2K_0 + (-12C_X + 6)K_1 + (-48C_X^2 + 48C_X - 10)K_2\right]^{-1} \tag{17}$$

The BBK model gives the alloy's viscosity as

$$\eta = E\{\,T\,(C_X M_X^0 + C_Y M_Y^0)\,\}^{\frac{1}{2}}\,(\,C_X V_X + C_Y V_Y + V^E)^{\frac{-2}{3}} \times \exp\left\{\left(C_X T_{0,X} + C_Y T_{0,Y} - \frac{H_M}{\varphi R}\right)\frac{F}{T}\right\} \tag{18}$$

Where φ is a semi-empirical parameter with a value of 25.4, E and F are constants with values of $(1.80 \pm 0.39) \times 10^{-8}(\mathrm{j/Kmol^{1/3}})^{1/2}$ and 2.34 ± 0.20 respectively. M_j^0, V_j , are molar mass,volume of each component respectively, $T_{0,j}$ is melting temperature of elements of the alloy (j=X, Y), V^E excess molar volume of the alloy and R is gas constant,.

The surface tension (σ) of binary alloy by the Kaptay's new derivation of Butler equation is given as

$$\sigma = \frac{A_j^0}{A_j}\sigma_j^0 + \frac{RT}{A_j}\ln\frac{C_j^S}{C_j^b} + \frac{G_j^{S,XS} - G_j^{b,XS}}{A_j} \tag{19}$$

Where σ_j^0 and A_j^0, represent surface tension, molar surface area of pure liquid metal, A_j stands for partial molar surface area, C_j^S and C_j^b are surface concentration and bulk concentration of jth component respectively. $G_j^{S,XS}$ and $G_j^{b,XS}$ indicate the partial excess free energy in the surface and bulk of elements of the alloy respectively. As bulk concentrations of components of the alloy, the sum of surface concentrations of the components of alloy is one i.e. $\sum_j C_j^S = 1$.The molar surface area of J^{th} component is expressed as [23],.

$$A_j^0 = \chi \mathrm{Na}^{1/3}\left(\frac{M_j^0}{\rho_j^0}\right)^{2/3} \tag{20}$$

Where ρ_j^0 is density of each metal of the alloy at its melting point. Similarly χ and N_a are geometrical constant and Avogadro's number respectively. χ is related to the volume packing fraction (f_V) and surface packing fraction (f_S) of pure component as given below

$$\chi = \left(\frac{3f_V}{4}\right)^{\frac{2}{3}}\frac{\pi^{\frac{1}{3}}}{f_S} \tag{21}$$

At any temperature T, the density (ρ_j) and surface tension (σ_j) of each metal can be written as [24]

$$\rho_j = \rho_j^0 + \frac{\partial\rho}{\partial T}\left(T - T_{0J}\right) \tag{22}$$

$$\sigma_j = \sigma_j^0 + \frac{\partial\sigma}{\partial T}\left(T - T_{0J}\right) \tag{23}$$

Result and Discussion

Thermodynamic property

Eqs. (1), (4), and (5) are handled to compute thermodynamic parameters like free energy of mixing, heat of mixing, and activity using the quasi-chemical approximation. The interaction as well as temperature derivatives of interaction parameters are derived by iterative approach with the use of observed values [25] in the concentration range 0.1 to 0.9 for the free energy of mixing and the heat of mixing respectively. The best fit values of parameters are

$$\frac{\omega}{K_BT} = -1.023\,,\quad \frac{\Delta\omega_{AB}}{K_BT} = -11.058\,,\quad \frac{\Delta\omega_{AB}}{K_BT} = -16.049$$

$$\frac{1}{K_B}\frac{d\omega}{dT} = 3.913\,,\quad \frac{1}{K_B}\frac{d\Delta\omega_{AB}}{dT} = 1.556\,,\frac{1}{K_B}\frac{d\Delta\omega_{AA}}{dT} = -9.992$$

Similarly, observed enthalpy of mixing and excess entropy of mixing [25] are used to optimize temperature-dependent parameters for the liquid alloy within the framework of R-K polynomials using Eqs. (10), (11), (13), (15), and (16). The results are presented as shown below.

$K_0 = -82590.842\exp(-6.011\times10^{-4}T)$

$K_1 = -76062.258\exp(-7.201\times10^{-3}T)$

$K_2 = 25530.7248\exp(5.015\times10^{-4}T)$

The optimized exponential interaction parameters are used to calculate free energy, enthalpy, activity and concentration fluctuation in long wavelength limit of the preferred alloy at different temperatures. The values of the excess Gibbs free energy, the heat of mixing and the activity of each component using Quasi-chemical approximation, the Redlich and Kister equation as well as the

experimental results at 848 K, 900 K and 1000 K are presented in Figs. 1, 2 and 3 respectively. In Fig. 1, the calculated excess free energy is almost in agreement with the experimental values where there is a slight discrepancy in the heat of mixing calculated by Quasi-chemical approximation and RK equation with respect to that of the experimental values after 0.4 concentration of Potassium. However the computed activities of each component of the alloy by Quasi-chemical approximation and RK equations are in good agreement with experimental values. These results validate the used models.

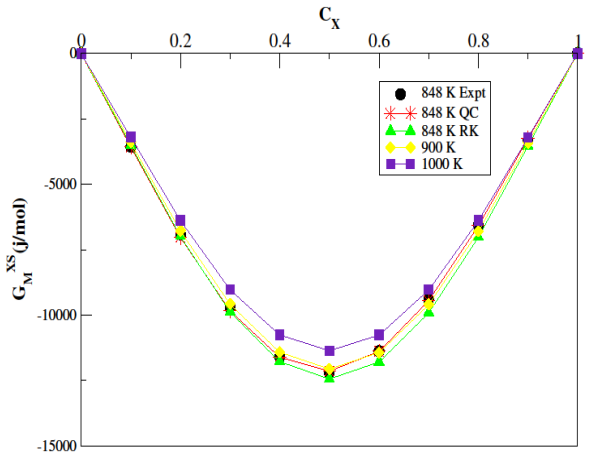

Fig. 1. Excess Gibbs free energy vs. concentration of potassium in the K-Pb alloy.

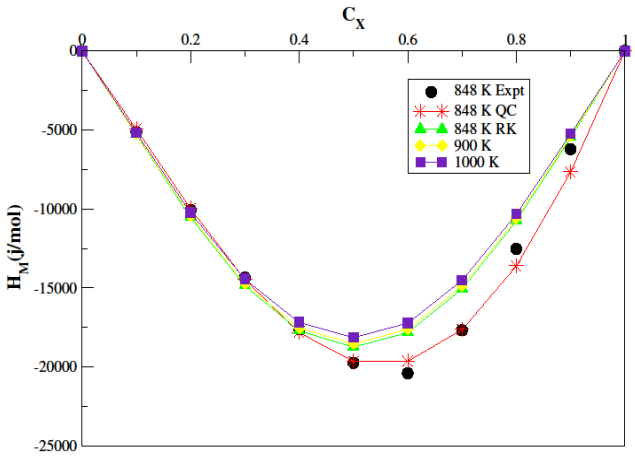

Fig. 2. Heat of mixing vs. concentration of potassium in the K-Pb alloy.

Structural property

There is no easy way to tell whether a mixture's constituent atoms are grouped together or not. As a result, determining the arrangement of atoms is extremely challenging. However, the local arrangement of atoms in constituents of a mixture may be investigated using the diffraction method, but this is a tough process. The determination of concentration fluctuations in long-wavelength limit (Scc(0)) is considered a major way for overcoming this challenge or studying the local arrangement of constituent atoms theoretically[21]. For a given concentration the alloy has complex formation nature if $S_{CC}(0) < S_{CC}^{id}(0)$, whereas the alloy has segregating nature if $S_{CC}(0) > S_{CC}^{id}(0)$. The theoretical values of $S_{CC}(0)$ at different concentrations of potassium for the alloy by Quasi-chemical approximation and RK equation along with experimental values is shown in Fig. 4 and suggests that the computed values of $S_{CC}(0)$ at all temperatures lie below the ideal value of $S_{CC}(0)$ within entire concentration range of potassium. This indicates that the alloy is strongly ordering at all temperatures of investigation.

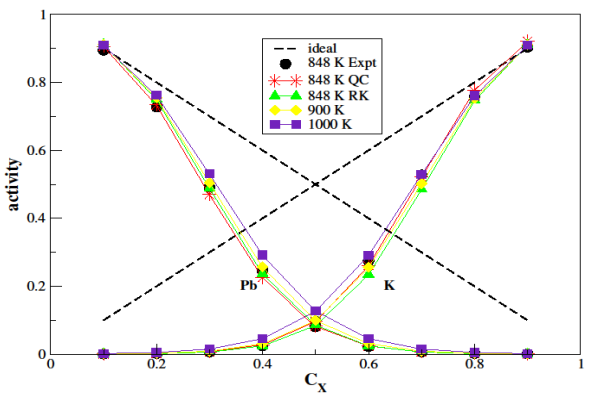

Fig. 3. Activity vs. concentration of potassium in the K-Pb alloy

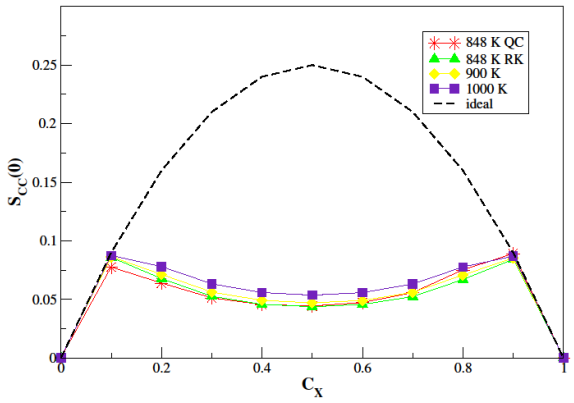

Fig. 4. Concentration fluctuation in long wavelength limit vs. concentration of potassium in the K-Pb alloy

Viscosity

We utilize Eq. (18) for the theoretical value of the alloy's viscosity at various temperatures. The densities at different temperatures are used to calculate the molar volume of the components of the alloy at various temperatures. The Eq. (22) is used to determine each component's density at temperatures of 848 K, 900 K, and 1000 K. The excess molar volume (V^E) is set to zero due to a lack of experimental data. Although the value of V^E is not zero for non-ideal alloys, its contribution is insignificant [26]. The viscosity of the alloy reduces as the temperature rises, as indicated in the Fig. (5). However, due to limited or no available data for certain compositions and temperatures, it is difficult to establish the accuracy of viscosity with certainty.

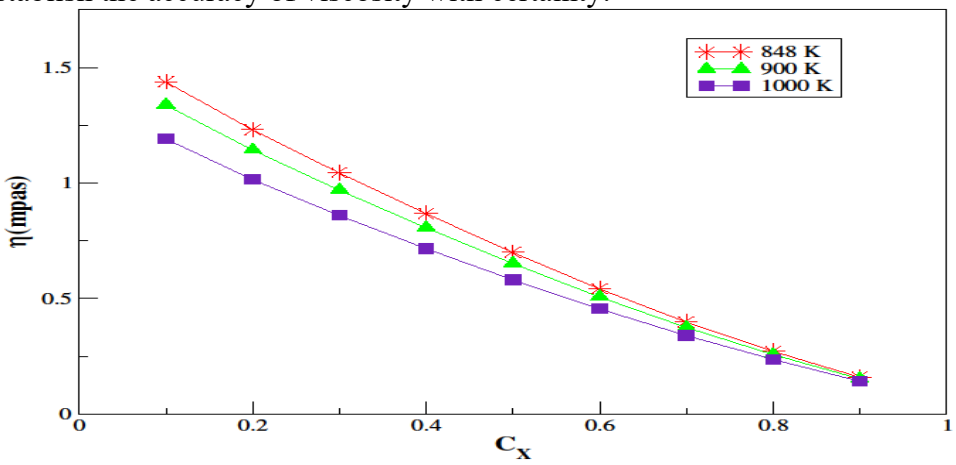

Fig. 5. Viscosity vs. concentration of potassium in the K-Pb alloy.

Surface property; Surface segregation and surface tension

In order to calculate the surface tension of the alloy, Individual metals' surface tensions are estimated at different temperatures (848 K, 1000 K, 1200 K, and 1500 K) by using Eq. (23) at first. The value of geometrical structure factor is 1.061 and ratio $(\frac{G_j^{s,xs}}{G_j^{b,xs}})$ is taken 0.818 [23].

The partial molar volume is substituted by the molar volume of the same component when the excess molar volume of the combination is minor or unknown. The pure surface area (A_j^0) of the same pure component obviously substitutes for the partial surface area (A_j) of the same pure component in this example [27]. We may now acquire surface concentrations for both metals by using such values to the expression for both metals in Eq. (19) and solving them concurrently, and then calculating the surface tension of the alloy using each surface concentration of corresponding metals. Figs. (6) and (7) depict graphs of potassium surface concentration and alloy surface tension versus potassium concentration respectively.

Fig. (6) illustrates that potassium atoms segregate on the surface, but this tendency decreases as temperature rises because another component, Pb, gains energy and seeks to move closer to the surface. As seen in Fig. (7), the surface tension of the liquid alloy falls as the temperature rises.

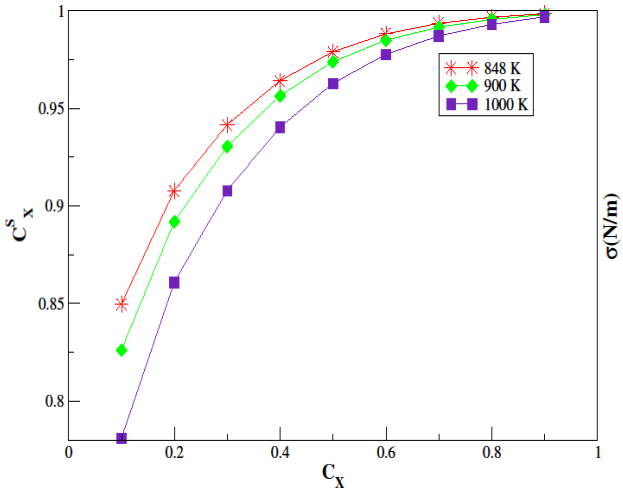

Fig. 6. Surface segregation vs. concentration of potassium in the K-Pb alloy.

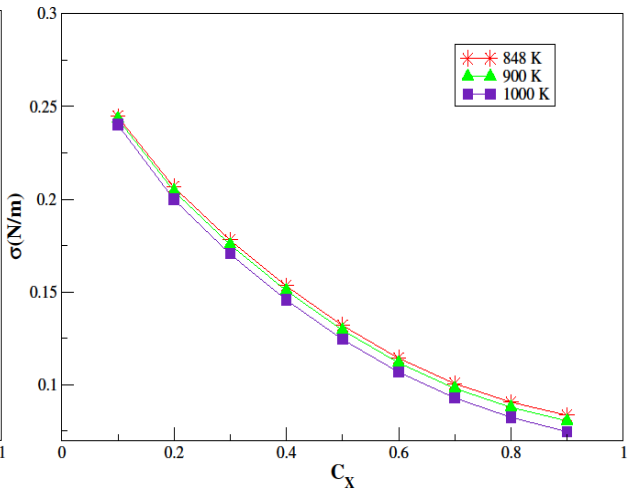

Fig.7. Surface tension vs. concentration of potassium in the K-Pb alloy

Conclusion

1. The alloy's thermodynamic and structural properties calculated using the quasi chemical approximation and RK equation are very close to experimental results at 848 K.

2. The alloy is less interactive, and its interaction ability declines as temperature rises.

3. It is totally ordering at all temperatures of interest, but as the temperature rises, it becomes less.

4. At 848 K, potassium atoms segregate on the alloy's surface, but this segregation decreases as the alloy's temperature rises.

5. As the concentration of potassium in the alloy rises, the case of viscosity and surface tension becomes exactly opposite. So is the case when we take temperature at one hand and viscosity and surface tension at the other.

Acknowledgement

N. Panthi, one of the authors, is appreciative of the research support from the University Grants Commission of Nepal.

References

[1] B. Predel, Thermodynamic properties and structure of liquid alloys, Berichte der Bunsengesellschaft für physikalische Chemie.80 (8) (1976) 695-704.

[2] I.B. Bhandari, N. Panthi, I. Koirala and D. Adhikari, Phase segregating and complex forming Pb-based (= X-Pb) liquid alloys, Phase Transit. 1 (2021) 338-352.

[3] D. Adhikari, B.P. Singh and I.S. Jha, Phase separation in Na–K liquid alloy, Phase Transit.. 85(8), (2012) 675-680.

[4] N. Panthi, I.B. Bhandari and I. Koirala, Theoretical assessment on hetero-coordination of Alloys Silver-Antimony at Molten State, Himalayan Journal of Science and Technology, 3-4 (2020) 68-73.

[5] P.J. Flory, Thermodynamics of high polymer solutions, J. Chem. Phys. 10(1) (1942) 51-61.

[6] O. Redlich and A.T. Kister. Algebraic representation of thermodynamic properties and the classification of solutions, Ind Eng Chem .40(2) (1948) 345-348.

[7] A.B. Bhatia and N.H. March. Size effects, peaks in concentration fluctuations and liquidus curves of Na-Cs, *J. Phys. F: Met. Phys*. 5(6) (1975) 1100-1106.

[8] A.B. Bhatia and R.N. Singh. Thermodynamic properties of compound forming molten alloys in a weak interaction approximation, Phys Chem Liquids.11 (1982) 343-353.

[9] A.B. Bhatia and R.N. Singh. A quasi-lattice theory for compound forming molten alloys. Phys Chem Liquids, 13 (3) (1984) 177-190.

[10] R.N. Singh and I.K. Mishra. Conditional probabilities and thermodynamics of binary molten alloys, Phys Chem Liquids.18 (4) (1988)303-319.

[11] R. Novakovic. Thermodynamics, surface properties and microscopic functions of liquid Al–Nb and Nb–Ti alloys. Journal of Non-Crystalline Solids. 31-32 (2010) 1593-1598.

[12] R. Novakovic, T. Tanaka, M.L.Muolo, J. Lee and A. Passerone. Bulk and surface properties of liquid Ag–X (X= Ti, Hf) compound forming alloys, Surf. Sci.1-3 (2005)56-59.

[13] Panthi, N., Bhandari, I. B. & Koirala, I.Thermophysical behavior of mercury-lead liquid alloy, Papers in Physics.14(2022)14005.

[14] I. Budai, M.Z. Benkő and G. Kaptay. Comparison of different theoretical models to experimental data on viscosity of binary liquid alloys, In Materials science forum. 537 (2007) 489-496.

[15] G.Kaptay.Improved derivation of the Butler equations for surface tension of solutions, Langmuir. 35(33) (2019)10987-10992.

[16] S.L. Chen, S.S. Daniel, F. Zhang, Y.A.Chang, W.A.Oates and R. Schmid-Fetzer. On the calculation of multicomponent stable phase diagrams, J. Ph. Equilibria Diffus. 22 (4) (2001) 373-378.

[17] R.K. Gohivar, S. K., Yadav, R.P. Koirala and D. Adhikari. Assessment of thermo-structural properties of Al-Fe and Fe-Si alloys at high temperatures, Phys Chem Liquids. 1 (2020) 679-689.

[18] N. Panthi, I.B. Bhandari, R.K. Rai, and I. Koirala. Thermophysical Behavior of Sodium Lead Alloy at Different Temperature, Adv. Stud. Theor. Phys. 15 (4) (2021) 153-165.

[19] G. Kaptay. A new equation for the temperature dependence of the excess Gibbs energy of solution phases, Calphad. 28(2) (2004) 115-124.

[20] G.Kaptay. The exponential excess Gibbs energy model revisited. Calphad.56 (2017)169-184.

[21] Q. Zhang, J. Mao, W.K. Pang, T. Zheng, V. Sencadas, Y. Chen and Z. Guo. Boosting the potassium storage performance of alloy-based anode materials via electrolyte salt chemistry, Adv. Energy Mater. 8(15) (2018) 1703288.

[22] A.B. Bhatia and D.E. Thornton. Structural aspects of the electrical resistivity of binary alloys, Phys. Rev. B. 2(8) (1970) 3004-3012.

[23] G. Kaptay. A unified model for the cohesive enthalpy, critical temperature, surface tension and volume thermal expansion coefficient of liquid metals of bcc, fcc and hcp crystals, Mater. Sci. Eng. A. 495(1-2) (2008) 19-26.

[24] E.A. Brandes and G.B. Brook (Eds.). Smithells metals reference book, Elsevier, 2013.

[25] R.Hultgren, P.D. Desai, D.T. Hawkins, M. Gleiser and K.K. Kelley. Selected values of the thermodynamic properties of binary alloys, National Standard Reference Data System, Ohio, 1973.

[26] I.S.Jha, R. Khadka, R.P. Koirala, B. P.Singh, and D. Adhikari. Theoretical assessment on mixing properties of liquid Tl–Na alloys, Philos. Mag. 96(16) (2016) 1664-1683.

[27] G. Kaptay. A coherent set of model equations for various surface and interface energies in systems with liquid and solid metals and alloys, Adv. Colloid Interface Sci.283 (2020) 102212.

Metallophysics and Advanced Technologies
Металофіз. новітні технол.
Metallofiz. Noveishie Tekhnol.
2022, vol. 44, No. 11, pp. 1535–1549
https://doi.org/10.15407/mfint.44.11.1535
Reprints available directly from the publisher

PACS numbers: 61.82.bg, 66.20.-d, 71.20.Be, 71.20.Gj, 71.55.Ak

Thermophysical Study of Sodium–Indium Alloy

N. Panthi, I. B. Bhandari*, and I. Koirala*

Patan Multiple Campus, Tribhuvan University,
44618 Kirtipur, Nepal
**Central Department of Physics, Tribhuvan University,*
44618 Kirtipur, Nepal

This study explores the mixing nature of sodium–indium liquid alloy at temperatures of 713 K, 850 K, 950 K and 1050 K. It uses quasi-lattice approximation for the thermodynamic analysis of concentration dependent mixing behaviours of sodium–indium liquid alloy under the assumption of Na_3In complex. It compares the obtained theoretical results with the experimental result and result of Redlich–Kister (R–K) equation for the validity. The researchers concentrate on the viscosity and surface tension of the alloy under the modelling equations as suggested by Kaptay and improved derivation of Butler equation, respectively. This paper focuses on the interaction energy parameters among neighbouring atoms of the alloy. It observes that the alloy is moderately interacting and ordering nature at the lower concentration of sodium. The theoretical results of the thermodynamic properties are nearly in agreement with the corresponding experimental data as well as results obtained by R–K equation at 713 K. It claims that the ordering behaviour, viscosity and surface tension of the alloy decreases with the increase in temperature.

Key words: liquid alloys, thermodynamic properties, R–K equation, energy parameters, ordering.

Досліджено характер змішування рідкого стопу натрій–індій за температур у 713 К, 850 К, 950 К і 1050 К. Було використано квазиґратницеве наближення для термодинамічної аналізи залежних від концентрації характеристик змішування рідкого стопу натрій–індій за припущенням наяв-

Corresponding author: Narayan Panthi
E-mail: narayan.755711@cdp.tu.edu.np

Citation: N. Panthi, I. B. Bhandari, and I. Koirala, Thermophysical Study of Sodium–Indium Alloy, *Metallofiz. Noveishie Tekhnol.*, **44**, No. 11: 1535–1549 (2022). DOI: 10.15407/mfint.44.11.1535

ности комплексу Na_3In. Порівняно одержані теоретичні результати з експериментальними та результатами, що дає рівняння Редліха–Кістера. Дослідники переважно зосереджуються на вивченні в'язкости та поверхневого натягу стопу відповідно до рівнянь, запропонованих Каптаєм, і вдосконаленого виведення рівняння Батлера. Цю статтю присвячено дослідженню енергетичних параметрів взаємодії між сусідніми атомами стопу. Зазначається, що взаємодія для цього стопу є помірною; крім того, наявне впорядкування за нижчої концентрації Натрію. Теоретичні результати для термодинамічних властивостей узгоджуються з відповідними експериментальними даними, а також результатами, одержаними за допомогою рівняння Редліха–Кістера для 713 К. Стверджується, що впорядкування, в'язкість і поверхневий натяг стопу зменшуються з підвищенням температури.

Ключові слова: рідкі стопи, термодинамічні властивості, рівняння Редліха–Кістера, енергетичні параметри, впорядкування.

(Received January 20, 2022; in final version, September 23, 2022)

1. INTRODUCTION

The properties of liquid alloys mainly depend on composition of constituent elements, temperature and pressure. The alloying phenomena play an important role on stability, strength, electrical character *etc*. of the materials. Thus, the study of mixing nature of elements forming alloys has been given great attention by researchers. However, detailed analysis of different behaviour of the alloys at high temperature and at all compositions of constituent elements becomes strenuous due to inconvenience in experimental task and time limitation. To overcome such difficulties and to speed up the study, many theoreticians have put forward different theoretical models [1–7].

The sodium element is highly reactive and makes complex alloys with other elements like lead, potassium, calcium and so on. Because of the development of such complexes, the thermodynamic properties of binary sodium alloys frequently deviate significantly from those of regular alloys. This makes it fascinating to investigate the properties of various alloys of sodium. Hence, different researchers [8–14] have investigated different properties of sodium alloys. However, the alloying nature of sodium with indium is found lacking till now except few experimental thermodynamic results explored by few experimentalists [15].

The present study aims to study the thermophysical behaviours of sodium–indium alloy at temperatures 713 K, 850 K, 950 K and 1050 K by assuming Na_3In complex. The thermodynamic behaviours of the alloy are analysed by quasi lattice approximation [4]. The validity of this model is tested comparing result obtained with theoretical results of

Redlich–Kister (R–K) equation [2] and experimental results at temperature 713 K. The viscosity and surface tension of the alloy have been studied at aforementioned temperature by Kaptay model [16] and improved Butler equation [17], respectively.

2. THEORETICAL DETAILS

2.1. Thermodynamic Properties

Let an alloy of constituent metals X and Y has chemical complexes $X_\mu Y_\vartheta$ in such a way that $\mu X + \vartheta Y = X_\mu Y_\vartheta$, where μ and ϑ are small integers. The excess Gibbs free energy of mixing G_M^{Xs} in the case of quasi lattice approximation [4] can be written as:

$$G_M^{Xs} = N(\theta\omega + \theta_{XY}\Delta\omega_{XY} + \theta_{XX}\Delta\omega_{XX} + \theta_{YY}\Delta\omega_{YY}), \tag{1}$$

where N is Avogadro's number, $\theta_{i,j}$ $(i, j = X,Y)$ are simple polynomials in concentration (C), ω is interchange energy and $\Delta\omega_{i,j}$ are interaction energy parameters.

The value of θ is always $C_X C_Y$, where C_X and C_Y are concentration of constituent elements X and Y respectively. The sum of concentration of two components is always one (*i.e.*, $C_X + C_Y = 1$). The values of $\theta_{i,j}$ in the case of $\mu = 3$ and $\vartheta = 1$ are found to be [4, 18]:

$$\theta_{XY} = \frac{1}{5}C_X + \frac{2}{3}C_X^3 - C_X^4 - \frac{1}{5}C_X^5 + \frac{1}{3}C_X^6, \tag{2}$$

$$\theta_{XX} = -\frac{3}{20}C_X + \frac{2}{3}C_X^3 - \frac{3}{4}C_X^4 + \frac{2}{5}C_X^5 - \frac{1}{6}C_X^6, \tag{3}$$

$$\theta_{YY} = 0. \tag{4}$$

The Gibbs free energy of complex formation of an alloy is given by standard equation as:

$$\begin{aligned} G_M = G_M^{Xs} + RT(C_X \ln C_X + C_Y \ln C_Y) = N(\theta\omega + \theta_{XY}\Delta\omega_{XY} + \\ +\theta_{XX}\Delta\omega_{XX} + \theta_{YY}\Delta\omega_{YY}) + RT(C_X \ln C_X + C_Y \ln C_Y). \end{aligned} \tag{5}$$

The enthalpy of mixing of an alloy is found out from Gibbs free energy by standard thermodynamic equation as:

$$H_M = G_M - T\left(\frac{\partial G_M}{\partial T}\right)_{C,N,P} = G_M - TN\left(\frac{\partial\omega}{\partial T}\theta + \frac{\partial\Delta\omega_{XY}}{\partial T}\theta_{XY} + \frac{\partial\Delta\omega_{XX}}{\partial T}\theta_{XX}\right). \tag{6}$$

The activity a_i of each constituent element of the alloy is related to Gibbs free energy by standard relation given as:

$$RT \ln a_{\mathrm{X}} = G_{\mathrm{M}} + C_{\mathrm{Y}} \left(\frac{\partial G_{\mathrm{M}}}{\partial C_{\mathrm{X}}} \right)_{T,P,N} \text{ and } RT \ln a_{\mathrm{Y}} = G_{\mathrm{M}} - C_{\mathrm{X}} \left(\frac{\partial G_{\mathrm{M}}}{\partial C_{\mathrm{Y}}} \right)_{T,P,N} . \quad (7)$$

Similarly, the partial excess Gibbs free energy is related to activity of each component by the following relation [19, 20]:

$$G_{\mathrm{t}}^{\mathrm{Xs}} = RT \ln(a_i / C_i) . \quad (8)$$

2.2. Structural Properties

For the theoretical study of arrangement of atoms in the binary alloy, we compute concentration fluctuation in long-wavelength limit and Warren–Cowley chemical short-range order parameter.

The concentration fluctuation in long-wavelength limit $S_{\mathrm{CC}}(0)$ is given as [21]:

$$S_{\mathrm{CC}}(0) = RT \left(\frac{\partial^2 G_{\mathrm{M}}}{\partial C^2} \right)^{-1}_{T,P,N} . \quad (9)$$

$S_{\mathrm{CC}}(0)$ can also be found out by observed activities as:

$$S_{\mathrm{CC}}(0) = C_{\mathrm{Y}} a_{\mathrm{X}} \left(\frac{\partial a_{\mathrm{X}}}{\partial C_{\mathrm{X}}} \right)^{-1}_{T,P,N} = C_{\mathrm{X}} a_{\mathrm{Y}} \left(\frac{\partial a_{\mathrm{Y}}}{\partial C_{\mathrm{Y}}} \right)^{-1}_{T,P,N} . \quad (10)$$

Thus, $S_{\mathrm{CC}}(0)$ obtained from observed activities is also called as experimental $S_{\mathrm{CC}}(0)$.

From equations (5) and (9), the theoretical $S_{\mathrm{CC}}(0)$ can be obtained as:

$$S_{\mathrm{CC}}(0) = \frac{RT}{(-2\omega + \theta''_{\mathrm{XY}} \Delta\omega_{\mathrm{XY}} + \theta''_{\mathrm{XX}} \Delta\omega_{\mathrm{XX}} + RT / C_{\mathrm{X}} C_{\mathrm{Y}})} . \quad (11)$$

The Warren–Cowley chemical short range order parameter α_1 is related to the ratio of concentration fluctuation in long-wavelength limit S to coordination number Z [22, 23] as:

$$\alpha_1 = (S - 1)[S(Z - 1) + 1]^{-1}, \quad (12)$$

where

$$S = \frac{S_{\mathrm{CC}}(0)}{S_{\mathrm{CC}}^{\mathrm{id}}(0)},$$

and $S_{\mathrm{CC}}^{\mathrm{id}}(0)$ is the concentration fluctuation in long-wavelength limit for an ideal alloy. Z is co-ordination number and its value is taken 10

[24, 25] for the liquid alloy study.

2.3. Transport Property: Viscosity

Kaptay considered the relationship between the cohesive energy and activation energy of the viscous flow and developed an equation of viscosity η for binary alloy as given below [16]:

$$\eta = \frac{hN}{C_X V_X + C_Y V_B + V^E} \exp\left(\frac{C_X G_X + C_Y G_Y - \Phi H_M}{RT}\right), \tag{13}$$

where h is Planck's constant, V_i (i = X, Y) is the molar volume of pure metal, V^E is excess molar volume upon alloy formation, G_i is Gibbs activation energy of viscous flow in pure metals and Φ is a constant whose value is (0.155 ± 0.015) [26]. The Gibbs energy of activation of pure metal i is calculated by the following equation:

$$G_i = RT \ln\left(\frac{\eta_i V_i}{hN}\right), \tag{14}$$

where η_i is viscosity of individual elements X and Y, respectively. The variation of viscosity of a metal with temperature is given as [27]:

$$\eta_i = \eta_0 \exp\left(\frac{\varepsilon}{RT}\right), \tag{15}$$

where η_0 and ε are constants of each metal having units of viscosity and energy per mole respectively.

2.4. Surface Properties: Surface Tension

According to this model, there is an existence of a monoatomic layer, called surface monolayer at the surface of the molten alloy as a separate phase and it is in thermodynamic equilibrium with that of the bulk phase. The surface tension σ of binary alloy at temperature T is given by the improved Butler equation [17] as:

$$\sigma = \frac{\gamma_i^0}{\gamma_i}\sigma_i^0 + \frac{RT}{\gamma_i}\ln\frac{C_i^S}{C_i^b} + \frac{G_i^{S,Xs} - G_i^{b,Xs}}{\gamma_i}, \tag{16}$$

where $\sigma_i^0, \gamma_i^0, \gamma_i$ are surface tension, molar surface area of each liquid metal and partial molar surface area of i^{th} component, respectively. $G_i^{S,Xs}$ and $G_i^{b,Xs}$ are partial excess free energy of mixing in the surface and bulk of constituent elements of the alloy respectively and are related as $G_i^{S,Xs} = \beta G_i^{b,Xs}$. For the liquid phase, the value of β is taken as

0.818 [28].

The molar surface area of i^{th} component is given as [26]:

$$\gamma_i^0 = \chi \left(\frac{M_i^0}{\rho_i^0} \right)^{2/3} N^{1/3}, \tag{17}$$

where M_i^0, ρ_i^0, χ are respectively molar mass, density of each constituent element at its melting temperature, and geometrical constant. The value of χ is obtained from volume packing fraction f_V and surface packing fraction f_S by the expression as [26]:

$$\chi = \left(\frac{3 f_V}{4} \right)^{2/3} \frac{\pi^{1/3}}{f_S}. \tag{18}$$

For the liquid metal, the values of both f_V and f_S are taken as 0.66 and 0.906, respectively [26, 28].

The density ρ_i^0 and surface tension σ_i^0 of each constituent metal of the liquid alloy at any temperature T are expressed as [27]:

$$\rho_i^0 = \rho_i + \frac{d\rho}{dT}(T - T_0), \tag{19}$$

$$\sigma_i^0 = \sigma_i + \frac{d\sigma}{dT}(T - T_0), \tag{20}$$

where ρ_i and σ_i are density and surface tension of each component at its melting temperature T_0. Similarly, $d\rho/dT$ and $d\sigma/dT$ are temperature coefficient of density and surface tension, respectively.

3. RESULTS AND DISCUSSION

3.1. Thermodynamic and Structural Properties

In order to analyse thermodynamic properties of an alloy under the quasi-chemical treatment, it is necessary to determine the interaction energy parameters and their temperature derivatives. The energy parameters between the atoms of the alloy at a temperature are carried out by successive approximation method using Eq. (1) and experimental results [15] within concentration range 0.1 to 0.9. Now such parameters at high temperatures are obtained using Eq. (21) under the assumption that the parameters are linearly dependent on temperature and independent on the concentration of each component of the alloy:

$$d[\omega_{ij}(T)]_{\text{C}} = \frac{\partial \omega_{ij}(T)}{\partial T} dT,\ i \neq j;\ \omega_{ij}(T_{\text{K}}) - \omega_{ij}(T) = \frac{\partial \omega_{ij}}{\partial T}(T_j - T). \tag{21}$$

TABLE 1. Interaction energy parameters (J/mol) at different temperatures.

Temperature, K	ω	$\Delta\omega_{XY}$	$\Delta\omega_{XX}$
713	–2641.197	–7800.238	77408.543
850	–2088.8403	–4156.642	65842.259
950	–1685.587	–1497.082	57399.716
1050	–1282.334	1162.477	48957.172

The parameters thus found at different temperature are shown in the Table 1.

Similarly, we optimized linear temperature dependent R–K polynomials [29] to compare our results with Redlich–Kister equation [2]. The R–K polynomials thus optimized are given below:

$$L_0 = -35087.119 + 27.878T,$$
$$L_1 = 8399.395 - 0.220T,$$
$$L_2 = 16556.200 - 12.267T.$$

The plot of Gibbs free energy versus concentration of Na of the alloy at temperature 713 K is shown in Fig. 1. As clear, the theoretically computed result is in good agreement with experimental result. This proves the validity of model and interaction parameters. Figure 2 is the Gibbs free energy of mixing at higher temperatures at three different compositions, $Na_{10}In_{90}$, $Na_{50}In_{50}$, and $Na_{90}In_{10}$ of the alloy. The figure depicts that as temperature increases the Gibbs free energy of mix-

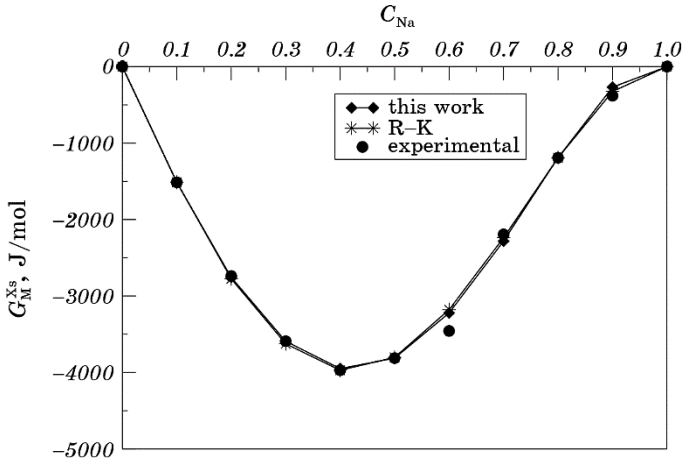

Fig. 1. Excess Gibbs energy *vs.* concentration of Na at 713 K.

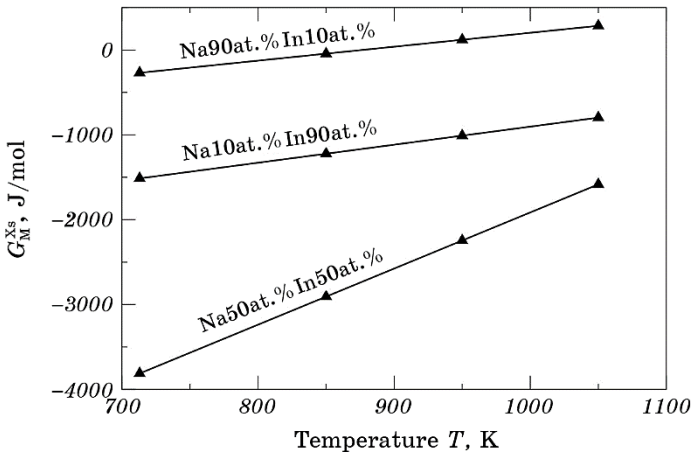

Fig. 2. Excess Gibbs energy *vs.* temperature.

ing becomes less negative indicating that interaction decreases with increase in temperature.

The temperature derivatives of interaction energy parameters are also acquired by successive approximation method by using Eq. (6) and experimental result [15] within concentration range 0.1 to 0.9. The values of such parameters at temperature 713 K are $\partial\omega/\partial T = 0.485R$, $\partial\omega_{XY}/\partial T = 3.198R$, and $\partial\omega_{XX}/\partial T = -10.154R$. However, for small change in temperature the temperature derivatives of such parameters are considered constant. Figure 3 is the computed enthalpy of mixing of alloy at 713 K, which nearly agrees with experimental results. The computed enthalpy of mixing of alloy at higher temperature and at

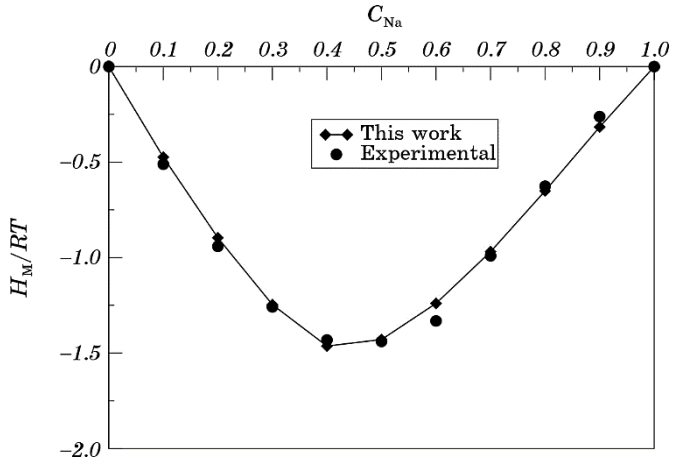

Fig. 3. Enthalpy of mixing *vs.* concentration of Na at 713 K.

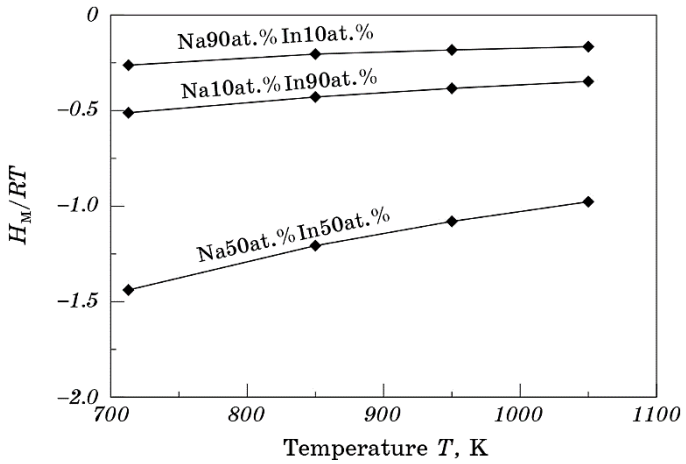

Fig. 4. Enthalpy *vs.* temperature.

$Na_{10}In_{90}$, $Na_{50}In_{50}$, and $Na_{90}In_{10}$ compositions of the alloy is shown in the Fig. 4.The less negative values of enthalpy of mixing at higher temperatures indicates that the alloy shows less interacting behaviour with increase in temperatures.

Chemical activity of constituent of the alloy is considered another important thermodynamic property of the alloy. It mainly gives the idea about the deviation of constituent element from the ideal behaviour. According to Porter and Easterling [30], the activity informs the tendency of constituents of the alloy whether they are willing to leave the mixture or not. If the activity is high, the atoms show high tenden-

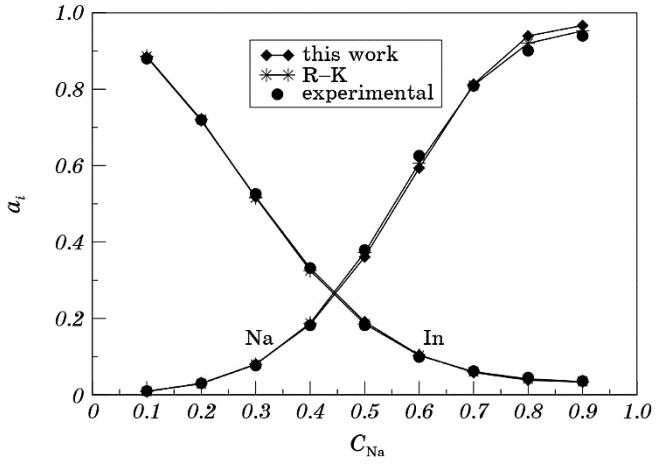

Fig. 5. Activity *vs.* concentration of Na at 713 K.

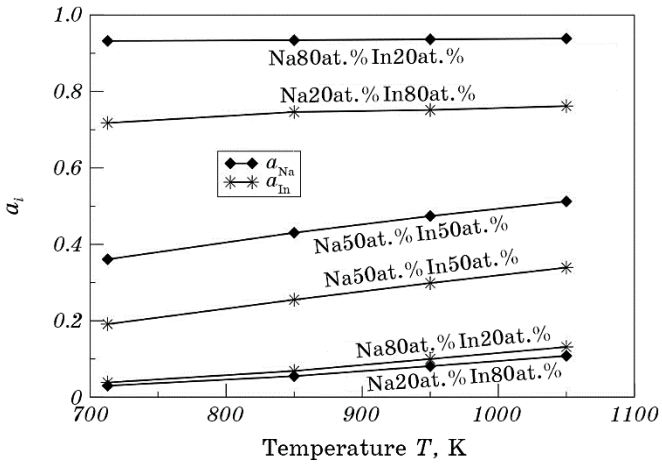

Fig. 6. Activity *vs.* temperature.

cy to leave the mixture and *vice-versa*. Equation (7) is used to calculate the chemical activity of components of alloy NaIn. Figure 5 is the result of experimental, theoretical and R–K equation of the chemical activity of the alloy at 713 K which shows a good agreement between the experimental and theoretical results. It suggests that at lower concentrations of Na, there is probability of pairing of unlike atoms. However, as temperature increases, the activity of each component increases as shown in Fig. 6 indicating that the atoms of constituent elements have less tendency to mix together when temperature of the alloy's increases.

For the theoretical analysis of internal adjustment of atoms in the binary alloy, the concentration fluctuations in the long-wavelength limit $S_{CC}(0)$ and Warren–Cowley short-range order parameter α_1 are considered important tools. The concept of $S_{CC}(0)$ removes difficulties on diffraction experiments [21].

The $S_{CC}(0)$ provides the qualitative information whereas the α_1 provides quantitative information of local arrangement of atoms. For given concentration and temperature, if $S_{CC}(0) < S_{CC}^{id}(0)$, then, $\alpha_1 = -1$. In this situation the alloy is expected to have ordering nature and if $S_{CC}(0) > S_{CC}^{id}(0)$, then, $\alpha_1 = 1$ and expected nature of the alloy is segregating. The value of $S_{CC}(0)$ goes to be zero for strong interacting alloys. The graph of experimental and theoretical values of $S_{CC}(0)$ at temperature 713 K is shown in Fig. 7, which suggests that the alloy has ordering tendency up to concentration 0.7 of Na, but at above concentration 0.7, it shows segregating nature as shown in Fig. 8. Accordingly, the value of α_1 is less than zero at 0.7 and more than zero above concentration 0.7 of Na at all temperatures as in Fig. 9.

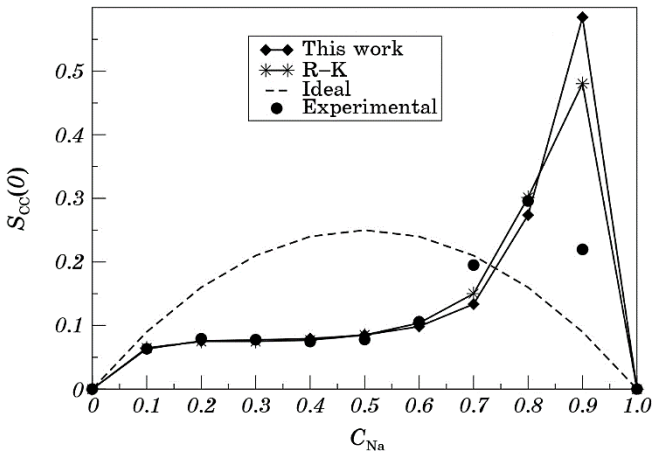

Fig. 7. Concentration fluctuation in long-wavelength limit *vs.* concentration of Na at 713 K.

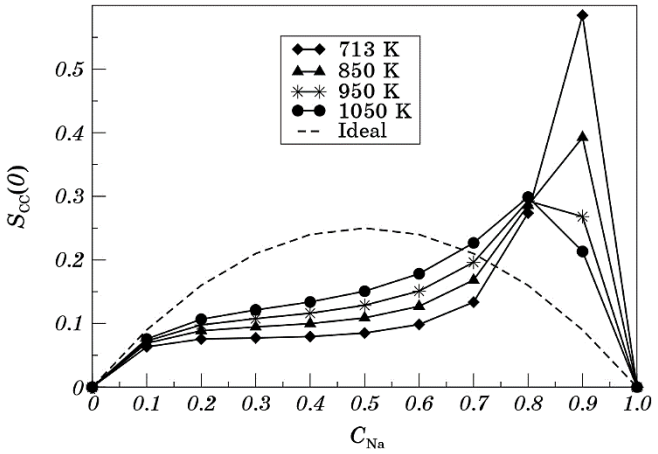

Fig. 8. Concentration fluctuation in long-wavelength limit at different temperatures.

3.2. Transport Properties

The concentration and temperature dependent viscosity at temperature 713 K–1050 K is calculated by Kaptay model as shown in Fig. 10. During the calculation, the value of V^E is taken zero due to the lack of experimental values [16, 31]. As clear, the viscosity of alloy decreases with increase in temperature which is the indication of reduction of interatomic attractive forces with rise in temperature and it is obvious.

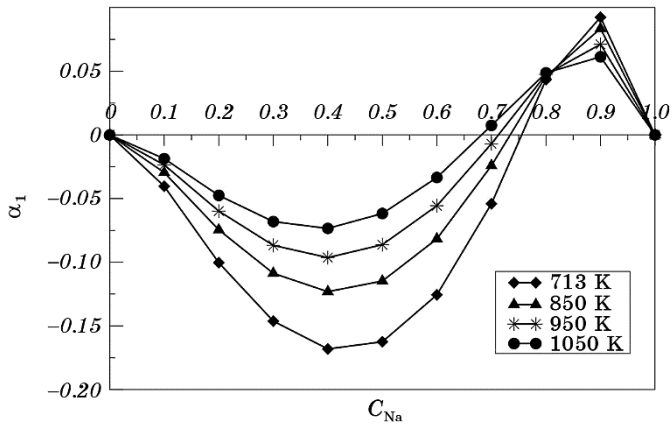

Fig. 9. Warren–Cowley short-range order parameter *vs.* concentration of Na at different temperatures.

3.3. Surface Properties

In order to calculate the surface tension of the NaIn liquid alloy, the densities and surface tension required for each metal at temperatures 713 K–1050 K are calculated using equations (19) and (20). Similarly, the partial excess free energy of Na and In at afore-mentioned temperatures are obtained by the theoretical activities obtained from equation (8).

Kaptay [17, 32] suggested that for unknown or negligible excess molar volume of the mixing, the partial molar volume of each component can be replaced by the molar volume of same component. In such situa-

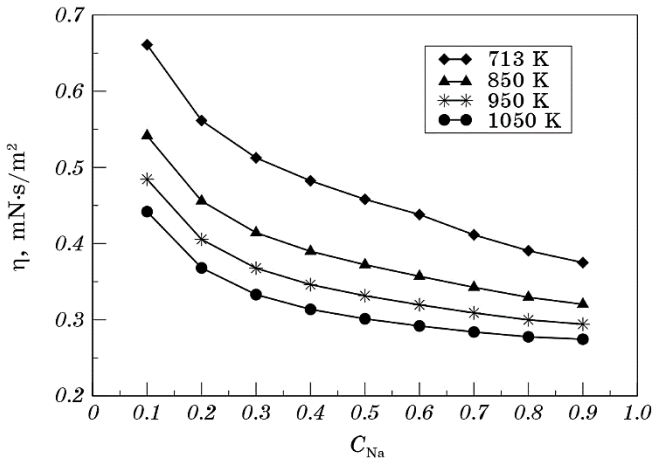

Fig. 10. Viscosity *vs.* concentration of Na at different temperatures.

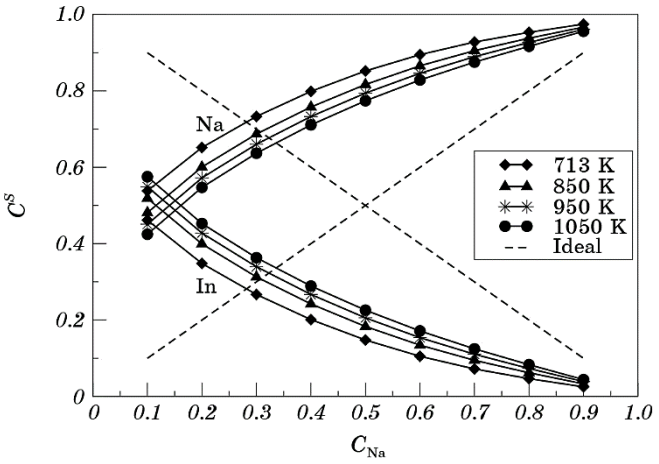

Fig. 11. Surface segregation *vs.* concentration Na at different temperatures.

tion, the surface area γ_i^0 of each component replaces the partial surface area γ_i. Now, using above-input parameters and solving Eq. (16), we find surface concentration of each component. The surface concentration of Na at afore-mentioned temperature is shown in the Fig. 11. The figure indicates that the sodium atoms prefer to stay on the surface. Similarly, at higher concentration of Na, the surface segregation of both components shifts towards the ideal value to revoke the temperature effect. Thus, it can be said that at higher concentration of Na, there appears phase separation in the alloy. Similarly, the surface segregation of Na decreases with increase in temperature. The computed values of surface tension obtained at different temperatures are shown in Fig. 12. The figure suggests that the surface tension of the alloy reduces with increase in temperature.

4. CONCLUSION

The present study is the theoretical investigation of thermodynamic, structural, transport and surface behaviours of binary liquid NaIn alloy at 713 K, 850 K, 950 K and 1050 K under the assumption of existence of Na_3In complex in the binary liquid mixture. From the thermodynamic study, we got the information that the alloy is moderately interacting and exhibits asymmetric behaviour as a function of concentration. The less negative values of thermodynamic properties at higher temperature indicate the weak tendency of compound forming alloy. The study also insights ordered tendencies of the alloy at about 0.7 concentration of Na at 713 K, but it becomes weaker with increase in temperature. As also observed, the surface segregation of sodium in-

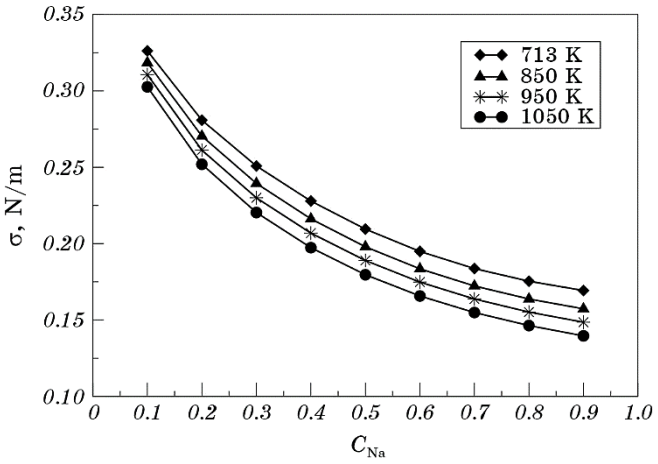

Fig. 12. Surface tension *vs.* concentration Na at different temperatures.

creases and that of indium decreases with increase in concentration of Na, which is the proof of segregating nature of alloy beyond 0.7 concentration of sodium. The thermophysical properties, viscosity and surface tension both decrease with rise in temperature.

This contribution was created under the support of University Grants Commission, Nepal.

REFERENCES

1. J. A. V. Butler, *Proc. Royal Society of London. Series A*, **135**, Iss. 827: 248 (1932).
2. O. Redlich and A. T. Kister, *Ind. Eng. Chem.*, **40**, No. 2: 345 (1948).
3. A. B. Bhatia and N. H. March, *J. Phys. F: Metal Phys.*, **5**: 1100 (1975).
4. A. B. Bhatia and R. N. Singh, *Phys. Chem. Liquids*, **11**, Iss. 4: 343 (1982).
5. A. B. Bhatia and R. N. Singh, *Phys. Chem. Liquids*, **13**, Iss. 3: 177 (1984).
6. R. N. Singh and I. K. Mishra, *Phys. Chem. Liquids*, **18**, Iss. 4: 303 (1988).
7. L. C. Prasad and R. N. Singh, *Phys. Chem. Liquids*, **22**, Iss. 1–2: 1 (1990).
8. A. G. Morachevskii, *Russian J. Applied Chem.*, **87**, No. 7: 837 (2014).
9. N. Panthi, I. B. Bhandari, and I. Koirala, *J. Phys. Commun.*, **5**: 085005 (2021).
10. N. Panthi, I. B. Bhandari, R. K. Rai, and I. Koirala, *Adv. Studies Theoretical Phys.*, **15**, No. 4: 153 (2021).
11. C. Hoch and A. Simon, *Angewandte Chemie*, **51**, Iss. 13: 3262 (2012).
12. L. Wang, Y. Liu, and J. Liu, *J. Phase Equilibria Diffusion*, **34**: 447 (2013).
13. S. Larose and A. D. Pelton, *J. Phase Equilibria*, **12**, No. 3: 371 (1991).
14. H. E. Bartlett, A. J. Neethling, and P. Crowther, *J. Chem. Thermodynamics*, **2**, Iss. 4: 523 (1970).
15. R. Hultgren, P. D. Desai, D. T. Hawkins, M. Gleiser, and K. K. Kelley, *Selected Values of the Thermodynamic Properties of Binary Alloys* (Metal Park, Ohio:

1973).
16. I. Budai, M. Z., Benko, and G. Kaptay, *Materials Science Forum*, **537–538**: 489 (2007).
17. G. Kaptay, *Langmuir*, **35**, No. 33: 10987 (2019).
18. R. N. Singh, *Canadian J. Phys.*, **65**, No. 3: 309 (1987).
19. H. Li, X. Sun, and S. Zhang, *Mater. Trans.*, **55**, No. 12: 1816 (2014).
20. S. K. Yadav, M. Gautam, and D. Adhikari, *AIP Adv.*, **10**, Iss. 12: 125320 (2020).
21. A. B. Bhatia and D. E. Thornton, *Phys. Rev. B*, **2**, No. 8: 3004 (1970).
22. J. M. Cowley, *Phys. Rev.*, **77**, No. 5: 669 (1950).
23. B. E. Warren, *X-Ray Diffraction* (Addison-Wesley: 1969).
24. E. A. Guggenheim, *Mixtures* (Oxford: Oxford University Press: 1952).
25. R. Novakovic, E. Ricci, M. L. Muolo, D. Giuranno, and A. Passerone, *Intermetallics*, **11**, No. 11–12: 1301 (2003).
26. G. Kaptay, *Z. Metallkd*, **96**, No. 1: 24(2005).
27. E. A. Brandes and G. B. Brook, *Smithells Metals Reference Book* (Elsevier: 2013).
28. G. Kaptay, *Calphad*, **29**, No. 1: 56 (2005).
29. R. K. Gohivar, S. K. Yadav, R. P. Koirala, and D. Adhikari, *Phys. Chem. Liquids*, **59**, Iss. 5: 679 (2021).
30. D. A. Porter and K. E. Easterling, *Phase Transformations in Metals and Alloys* (Boca Raton: CRC press: 2009).
31 I. S. Jha, R. Khadka, R. P. Koirala, B. P. Singh, and D. Adhikari, *Phil. Mag.*, **96**, No. 16: 1664 (2016).
32. G. Kaptay, *Adv. Colloid Interface Sci.*, **283**: 102212 (2020).

Volume 8, December 2019 ISSN 2542-2545

The HIMALAYAN PHYSICS

A peer-reviewed Journal of Physics

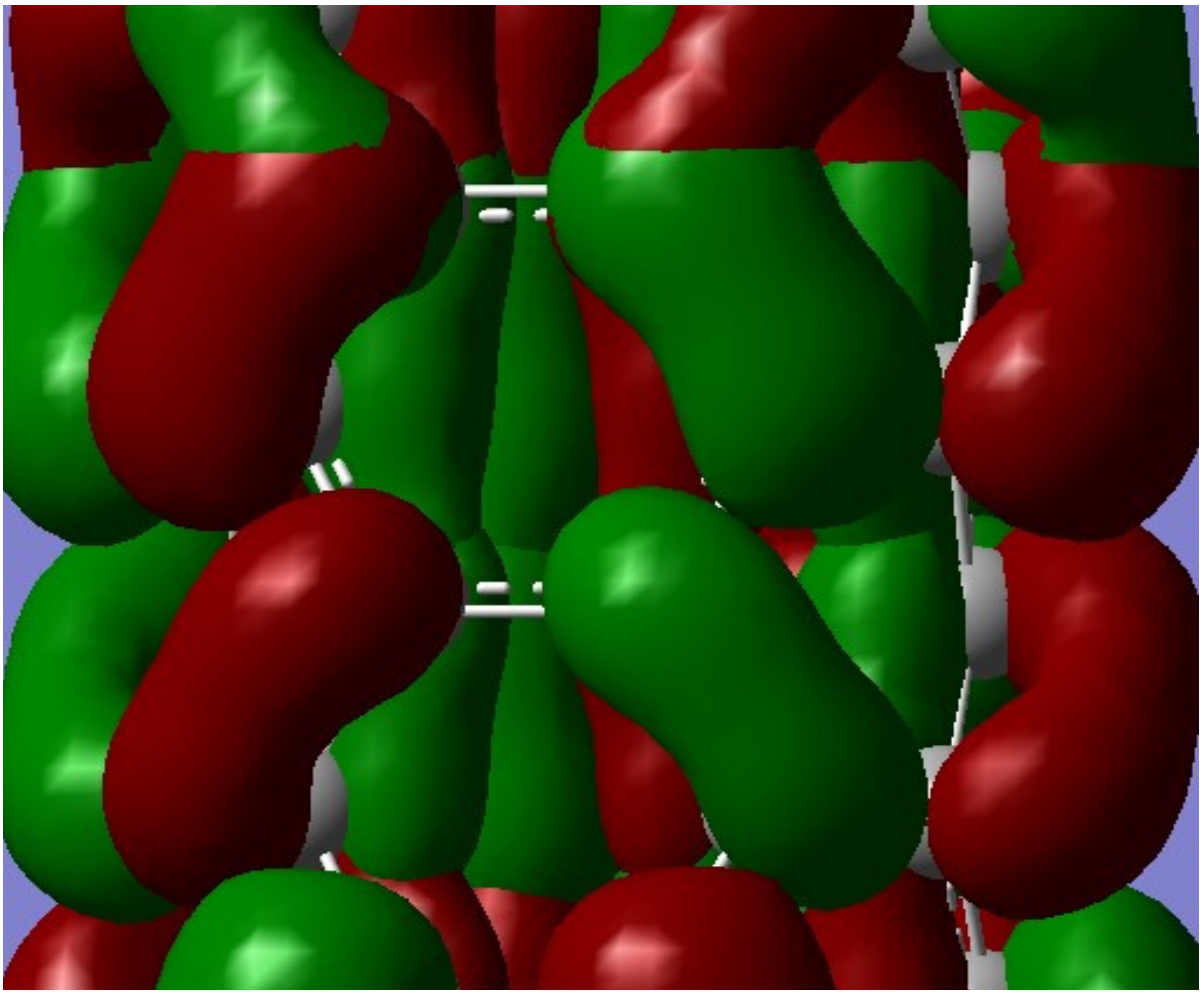

Department of Physics, Prithvi Narayan Campus, Pokhara
Nepal Physical Society, Western Chapter, Pokhara

Him. Phys. **8** 33-38, (2019)

Himalayan Physics

Thermodynamics of liquid Gallium-Zinc alloy

Research Article

I. B. Bhandari[1,2], N. Panthi[1,3], I. Koirala[1*]

1 Central Department of Physics, Tribhuvan University, Kathmandu, Nepal

2 Department of Applied Sciences, Institute of Engineering, Tribhuvan University, Kathmandu, Nepal

3 Department of Physics, Patan Multiple Campus, Tribhuvan University, Kathmandu, Nepal

Abstract: This research explores mixing behavior of Ga-Zn system throughComplex Formation Model. The variables affecting to temperature are the interaction energy parameters in which the properties under investigation are projected. The study has inspected through different thermodynamic properties such as free energy of mixing, heat of mixing and entropy of mixing. Theoretical results are in a good acceptance with the corresponding literaturedata and support a homocoordinating tendency in Ga-Zn liquid alloys.

Keywords: Thermodynamic properties • Complex formation model • Segregation

1. Introduction

Gallium lies on group IIIB in the periodic table. It is proficiently applicable as a thermometric liquid and in doping semi-conductors and production of solid-state devices like transistors. Huge amounts of zinc are used to produce die castings. These applications of the components of liquid alloys studied make them good candidates for the current kind of study. In manufacturing semiconductor devices, Gallium alloys play the pivotal role. And it is promising materials for lead free solders, because they have the traits of low melting point, good wetting properties, adhesion and oxidation resistance [1–3].Ga-Zn alloy possesses the constituents of different Gallium based multi component alloys i.e. applied in semiconducting industry. This research is significant for the study of the energetics of ternary systems such as Ga-Sn-Zn, Al-Ga-Zn, etc. It is specified that, this system is intensified low melting eutectic which is mentioned in literature [4–6].

The Ga-Zn system is analyzed through positive interaction energy, amplifying the formation of two phase structure, as presented by its simple eutectic phase diagram. The preliminary research of the empirical factors such as electronegativity difference (= 0) and size ratio $\Omega_{Ga}/\Omega_{Zn} \approx 1.19$ (Ω is atomic volume) [7, 8]. Ga-Zn system presents the values which are the characteristics for segregating alloys. However, the determining role is ascribed to the size ratio values. It purposes a limited solubility in the solid state and hence the presence of an eutectic reaction.

* *Corresponding Author: ikphysicstu@gmail.com*

Thermodynamics of Ga-Zn system is examined through various experimental methods. There are numerous findings obtained applying EMF measurements. Besides this, there are some other results derived by thermodynamic calculation based on various theoretical models [9]. Numerous investigations have been performed for different system through various approaches [10–14]. This paper presents the results of thermodynamic analysis of Ga-Zn alloys according to Conformal Solution Model. The outcomes are analyzed and compared with literature data to explicate the accuracy of this method in thermodynamic description of the presented binary system.

2. Modelling

If c is the atomic concentration of A atoms then (1-c) is atomic concentration for B atoms and such that $uA + vB = A_uB_v$ (u and v are small integer) then, number of A atoms, N_A = c. Number of B atoms, N_B = (1-c) , so that total number of atoms, $N = N_A + N_B$. When components A and B are blended together to form a binary $A - B$ solution, thermodynamic properties are changed. The liquid alloy is assumed to be composed of three species; A atom, B atom and chemical complex A_uB_v, ternary mixture also called conformal solution. The number of free atoms will be reduced due to compound formation in the melt. Now for n_1 gm atoms of A, n_2 gm atoms of B and n_3 gm atoms of A_uB_v,

$$n_1 = c - un_3 \; and \; n_2 = (1 - c) - vn_3 \tag{1}$$

The total number of atoms after mixing,

$$n = n_1 + n_2 + n_3 \tag{2}$$

$$= 1 - (u + v - 1)n_3 \tag{3}$$

The free energy of mixing of the binary A-B mixture can be written as,

$$G_M = -n_3g + G' \tag{4}$$

Here, $-n_3g$ represents lowering of free energy due to compound formation, g is the formation energy of complex. G' is the free energy of mixing of the ternary mixture of A, B and A_uB_v. If the ternary mixture is an ideal solution,

$$G' = RT \sum n_i ln \left(\frac{n_i}{n}\right) \tag{5}$$

If the effects of differences in sizes of the various constituents in the mixture cannot be ignored and the interaction ω_{ij} are small but not zero, the theory of regular solutions in the zeroth approximation [15] or the conformal solution approximation [16] is valid. For regular solution

$$G' = RT \sum n_i ln \left(\frac{n_i}{n}\right) + \sum \omega_{ij} \left(\frac{n_i n_j}{n}\right) \tag{6}$$

This equation is also referred to as conformal solution approximation. where $\omega_{ij} = 0(fori = j)$ are termed as the interaction energies and by definition are independent of concentration, although they depend upon temperature and pressure. Now the expression for free energy of mixing G_M for the compound forming binary alloy is

$$G_M = -n_3 g + RT \sum_{i=1}^{3} n_i ln\left(\frac{n_i}{n}\right) + \sum\sum_{i<j}\left(\frac{n_i n_i}{n}\right)\omega_{ij} \tag{7}$$

The expression for heat of mixing HMis given by [17],

$$H_M = G_M - T\left(\frac{\partial G_M}{\partial T}\right)_P \tag{8}$$

$$H_M = -n_3 g + RT\sum_{1}^{3} n_i ln\left(\frac{n_i}{n}\right) + \sum_{i<j}\sum\left(\frac{n_i n_j}{n}\right)\omega_{ij} - T\frac{\partial}{\partial T}\left[-n_3 g + RT\sum_{i=1}^{3} n_i ln\left(\frac{n_i}{n}\right) + \sum_{i<j}\sum\left(\frac{n_i n_j}{n}\right)\omega_{ij}\right] \tag{9}$$

$$= -n_3\left[g - T\left(\frac{\partial g}{\partial T}\right)_P\right] + \sum_{i<j}\sum\left(\frac{n_i n_j}{n}\right)\left[\omega_{ij} - T\left(\frac{\partial \omega_{ij}}{\partial T}\right)_P\right] \tag{10}$$

The expression for entropy of mixing SM can be obtained as [17],

$$S_M = n_3\frac{\partial g}{\partial T} - R\sum_{i=1}^{3} n_i ln\frac{n_i}{n} - \sum_{i<j}\sum\frac{n_i n_j}{n}\frac{\partial \omega_{ij}}{\partial T} \tag{11}$$

The equilibrium value of n_3 at a given pressure and temperature is given by

$$\left(\frac{\partial G_M}{\partial n_3}\right)_{T,P,N,C} = 0 \tag{12}$$

Substituting the value of GM from Eq. 7 and after some algebraic calculation

$$ln\left(n_3 n^{u+v-1} n_1^{-u} n_2^{-v}\right) + Y = \frac{g}{RT} \tag{13}$$

which is the equilibrium equation, where

$$Y = \left[\frac{n_1 n_2}{n^2}(u+v-1) - u\frac{n_2}{n} - v\frac{n_1}{n}\right]\frac{\omega_{12}}{RT} + \left[\frac{n_2 n_3}{n^2}(u+v-1) - v\frac{n_3}{n} + \frac{n_2}{n}\right]\frac{\omega_{23}}{RT} + \left[\frac{n_1 n_3}{n^2}(u+v-1) - u\frac{n_3}{n} + \frac{n_1}{n}\right]\frac{\omega_{13}}{RT}$$

3. Results and Discussion

Ga-Zn system has a eutectic point at 3.7 wt% Zn and at temperature of 25°C. The hexagonal (Zn) terminal solid solution has a maximum solubility of 2.36 wt% Ga at 260°C, while the orthorhombic (Ga) solid solution has a maximum solubility of 0.8 wt% Zn at 20°C [9]. Available experimental data [18] on the thermodynamic

properties as well as phase diagram information [18] have been used for the calculation of the order energy parameters for the Ga-Zn liquid phase by the CFM in a weak approximation. For the given temperatures the Gibbs free energy are negative and exhibit a flat minimum of -0.567 at the composition, $c = 0.45$.]. Accordingly, the Ga-Zn compound was postulated as energetically less favored and the preferential arrangements of Ga and Zn constituent atoms does not so favor the formation of Ga-Zn complexes ($\mu = 1, \upsilon = 1$) in the liquid alloys. Keeping in mind the Ga-Zn phase diagram and the applications related to the different melting intervals of Ga-Zn alloys, all calculations have been done at T = 750 K. The optimized data set of the Gibbs energy of mixing of liquid Ga-Zn alloys together with the enthalpy of mixing and Ga and Zn activity data [18] have been used to calculate the interaction energy parameters at T =750 K. The calculated interaction energy parameters for liquid Ga-Zn alloy, expressed in RT units at T = 750 K are; $g = 0.721$, ω_{12} = -6.091, $\omega_{13} = 1.942$, $\omega_{23} = 1.808$

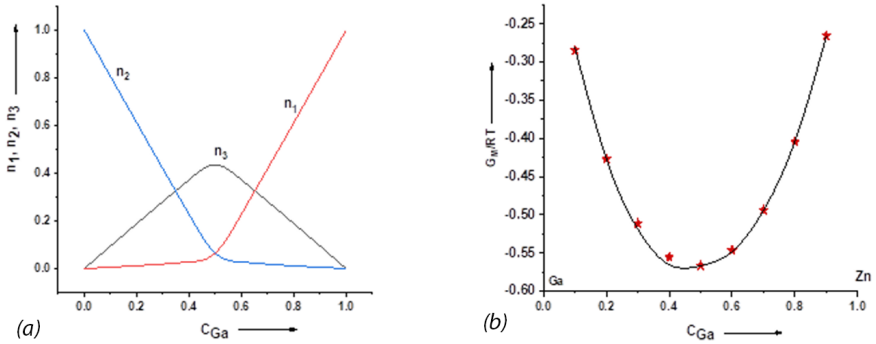

Figure 1. (a) Number of complexes (n_1, n_2, n_3) Vs concentration (c_{Ga}) of liquid Ga-Zn alloy at 750 K, (b) Free energy of mixing (GM/RT) Vs concentration (c_{Ga}) of liquid Ga-Zn alloy at 750 K [Theoretical(–) and experimental($\star$) values [18]].

Equilibrium relation Eq. 13 along with Eqs. 1 and 3 are used to compute the number of complexes, n_3, as a function of concentration. The values of interaction energy parameters are adjusted to give the concentration dependence of G_M which fits well with the corresponding thermodynamic data. The curves describing the Gibbs free energy of mixing of the Ga-Zn liquid phase are almost not symmetric with respect to the equiatomic composition. The concentration dependence of the equilibrium values of chemical complexes, n_3, at $T = 750K$ exhibits the symmetry at the same composition, $c = 0.5$, with the maximum value of about 0.4365 (Fig. 1). With an increase in temperature, the inter-atomic forces become weaker, and the corresponding maximum value of n_3 decreases. Using the order energy parameters calculated at $T = 750K$, the enthalpy of mixing, H_M and the entropy of mixing SM have been evaluated by Eqs. 10 and 11, respectively. The experimental data on the enthalpy of mixing measured at temperatures $T = 750K$ [18] have been used to calculate the variation in order energy parameters with temperature. The computed values of the derivatives are

$$\frac{1}{R}\frac{\partial g}{\partial t} = 1.224, \quad \frac{1}{R}\frac{\partial \omega_{12}}{\partial t} = 7.159, \quad \frac{1}{R}\frac{\partial \omega_{13}}{\partial t} = 0.444, \quad \frac{1}{R}\frac{\partial \omega_{23}}{\partial t} = 0.662 \tag{14}$$

A comparison between the calculated values of H_M and S_M by the CFM with the literature data [18] of liquid Ga-Zn alloy displays a good agreement between the two types of data (Fig. 2(a) and Fig. 2(b)).

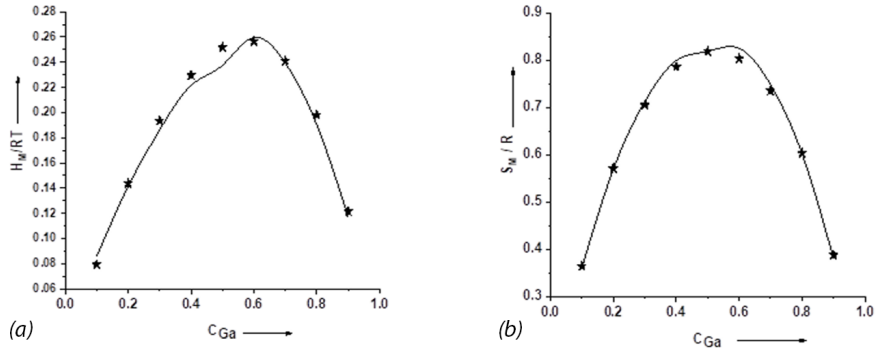

Figure 2. (a) Heat of mixing (H_M/RT), (b) Entropy of mixing (S_M/R) Vs concentration (c_{Ga}) of liquid Ga-Zn alloy at 750 K. [Theoretical(–) and experimental($\star$) values [18]]

4. Conclusions

Thermodynamic properties of Ga-Zn liquid alloy have been theoretically investigated by the CFM in a weak approximation. The thermodynamic data on mixing are used to obtain the interaction energy parameters, which are speculated to be invariant in all calculations. With the use same interaction parameters, the investigation of surface, transport and structural properties can be done further [14, 19–24]. The results obtained in the present work assure the applicability of this approach for a complete description of the thermodynamic of binary system which exhibit similar mixing properties. Moreover, it is found to be a useful tool in the interpretation of experimental results as well as in experimental planning.

References

[1] Xu Q, Oudalov N, Guo Q, Jaeger HM, Brown E. Effect of oxidation on the mechanical properties of liquid gallium and eutectic gallium-indium. Physics of fluids. 2012;24(6):063101.

[2] Wang H, Fang J, Xu Z, Zhang X. Improvement of Ga and Zn alloyed Sn–0.7 Cu solder alloys and joints. Journal of Materials Science: Materials in Electronics. 2015;26(6):3589–3595.

[3] Liu NS, Lin KL. The effect of Ga content on the wetting reaction and interfacial morphology formed between Sn–8.55 Zn–0.5 Ag–0.1 Al–xGa solders and Cu. Scripta Materialia. 2006;54(2):219–224.

[4] Dutkiewicz J, Moser Z, Zabdyr L, Gohil DD, Chart TG, Ansara I, et al. The Ga-Zn (Gallium-Zinc) system. Bulletin of Alloy Phase Diagrams. 1990;11(1):77–82.

[5] Genta V, Fiorani M, Valenti V. Thermodynamic Investigations of Metallic Systems, Note II: GaZn Liquid System. Gazz Chim Ital. 1955;85:103–110.

[6] Predel B, Frebel M, Gust W. Untersuchung der thermodynamischen Eigenschaften flüssiger gallium-zinn- und gallium-wismut-Legierungen. Journal of the Less Common Metals. 1969;17(4):391–402.

[7] Singh RN, Sommer F. Segregation and immiscibility in liquid binary alloys. Reports on Progress in Physics.

1997;60(1):57–150.

[8] Iida T. Physical Properties of Liquid Metals. (II). Structure of Liquid Metals and Their (Number) Density. Journal of the Japan Welding Society. 1993;62(8):590–594.

[9] Novakovic R, Zivkovic D. Thermodynamics and surface properties of liquid Ga-X (X = Sn, Zn) alloys. Journal of Materials Science. 2005 may;40(9-10):2251–2257.

[10] Novakovic R, Ricci E, Gnecco F, Giuranno D, Borzone G. Surface and transport properties of Au–Sn liquid alloys. Surface Science. 2005;599(1-3):230–247.

[11] Novakovic R, Ricci E, Giuranno D, Gnecco F. Surface properties of Bi–Pb liquid alloys. Surface Science. 2002;515(2-3):377–389.

[12] Prasad LC, Singh RN, Singh VN, Chatterjee SK. Compound formation in Sn-based liquid alloys. Physica B: Condensed Matter. 1995;215(2-3):225–232.

[13] Sharma N, Thakur A, Ahluwalia PK. Thermodynamic, surface and transport properties of liquid Hg–Pb and Hg–In amalgams. Journal of Molecular Liquids. 2013;188:104–112.

[14] Awe OE, Akinlade O, Hussain LA. Thermodynamic properties of liquid Te–Ga and Te–Tl alloys. Journal of Alloys and Compounds. 2003;361(1-2):227–233.

[15] Guggenheim EA. Statistical thermodynamics of mixtures with zero energies of mixing. Proceedings of the Royal Society of London Series A Mathematical and Physical Sciences. 1944;183(993):203–212.

[16] Longuet-Higgins H. The statistical thermodynamics of multicomponent systems. Proceedings of the Royal Society of London Series A Mathematical and Physical Sciences. 1951;205(1081):247–269.

[17] Lele S, Ramachandrarao P. Estimation of complex concentration in a regular associated solution. Metallurgical Transactions B. 1981;12(4):659–666.

[18] Hultgren RK, Desai PD, Hawkins DT, Gleiser M, Kelley K. Selected values of the thermodynamic properties of binary alloys. 1st ed. American Society for Metals; 1993.

[19] Bhatia AB, Hargrove WH. Concentration fluctuations and thermodynamic properties of some compound forming binary molten systems. Physical Review B. 1974;10(8):3186–3196.

[20] Bhatia AB, Hargrove WH, Thornton DE. Concentration fluctuations and partial structure factors of compound-forming binary molten alloys. Physical Review B. 1974;9(2):435–444.

[21] Koirala I, Singh BP, Jha IS. Theoretical assessment on segregating nature of liquid In–Tl alloys. Journal of Non-Crystalline Solids. 2014;398-399:26–31.

[22] Jha IS, Singh RN, Srivastava PL, Mitra NR. Stability of HgNa and HgK liquid alloys. Philosophical Magazine B. 1990;61(1):15–24.

[23] Jha IS, Koirala I, Singh BP, Adhikari D. Concentration dependence of thermodynamic, transport and surface properties in Ag–Cu liquid alloys. Applied Physics A. 2014;116(3):1517–1523.

[24] Singh BP, Koirala I, Jha IS, Adhikari D. The segregating nature of Cd–Pb liquid binary alloys. Physics and Chemistry of Liquids. 2014;52(4):457–470.

Himalayan Journal of Science and Technology, Vol. 3-4 (2020), 68-73

Himalayan Journal of Science and Technology

Original Article

Theoretical assessment on hetero-coordination of Alloys Silver-Antimony at Molten State

[a,b]*Narayan Panthi*,,[a,c]*Indra Bahadur Bhandari*, [a]*Ishwar Koirala**

[a] Central Department of Physics, Tribhuvan University, Kirtipur, Nepal
[b]Department of Physics, Patan Multiple Campus, Tribhuvan University, Nepal
[c]Department of Applied Sciences, Institute of Engineering,Tribhuvan University, Nepal

*Corresponding email: iswar.koirala@cdp.tu.edu.np

Abstract

The thermodynamic and structural properties of binary alloy Ag- Sb at temperature 1250K have been reported theoretically using quasi lattice model. The interchange energy has been considered a function of a temperature and thus various thermodynamic quantities are calculated at elevated temperature. The theoretical values of free energy of mixing, heat of mixing, entropy of mixing and chemical activity are reasonable agreement with experimental values in all concentrations of antimony from 0.1 to 0.9. The theoretical analysis tells that the alloy shows both ordering nature in Ag rich end and segregating nature in Sb rich end .The study reveals that the properties of alloy are asymmetric around equi-atomic composition. The Ag_3 Sn complexes are most likely to exist in the liquid state and are moderately interacting.

Article Info

Article history:

Received date: 07 November 2019
Accepted date: 04 May 2020

Keywords:

Thermodynamic properties
Quasi-Lattic model 2
Segregation

1. Introduction

The study of alloying behaviour is an important field in metallurgical science. The alloys may be of binary, ternary, quaternary and so on. Here our concern is only on the binary alloy. The binary alloy is a type of product formed by combination of two elements (at least one metal) in liquid state. Different properties of binary alloys are directly concerned with concentration of constituent elements .The alloys show symmetric or asymmetric behaviour in thermodynamic and structural properties with respect to concentration (Hultgren et al., 1973). Most of the used industrial and commercial materials are solid alloys. So they have deep utilization in solid state. The properties of initial melt play important role in the formation of alloys. Thus determination of different properties of the alloys in the liquid state are important to study the alloying behaviour in metallurgical science as well as knowledge of various properties of alloys at liquid state is important for the production of new materials required for high temperature application. Demand of different and new alloys in metallurgical science is increasing day by day and hence scientists are trying to find different alloys by mixing different elements at different compositions.

Silver is very soft, ductile and malleable metal. The combination of silver with different elements helps to improve hardness and wear-resistance of deposits and higher stability tarnishing antifriction characteristics. There has been growing tendency in calculating the properties of silver–antimony alloys. It has been used as electroplating deposition due to its increased hardness and wear-resistance which, finally aims to the use of smaller plate thickness and consequent saving of expensive materials (Singh et al., 2010).

Different theoreticians are working with various theoretical models to understand the alloying behaviour of compound forming binary alloys. In the present work, one of the Silver alloys Ag-Sb is studied theoretically to determine certain properties at 1250 K assuming Ag_xSb_y (x=3, y=1) complex in melt by using Quasi lattice model. Thermodynamic properties such as free energy of mixing, heat of mixing and entropy of mixing , chemical activity provide the knowledge on the interaction, stability and bonding strength among the constituent atoms whereas information on the

structural ordering of atoms in binary alloys in the liquid state is provided by the quantitative analysis of microscopic functions, the concentration fluctuations in the long wavelength limit (Scc(0)), short-range order parameter (α1)and diffusivity(D_M/D_{id})(Koirala et al., 2014; Jha et al., 2015; Koirala et al., 2018). Scc(0) represents the nature of ordering of the atoms ,α1 quantifies the degree of ordering and diffusion coefficient ratio (D_M/D_{id}) gives the structural behaviour of the alloy .

The organization of this paper is as follows. In Section 2, the expressions required for the calculation are presented. In Section 3, result and general discussion of the alloy Ag-Sb are presented. Finally the conclusions are given in Section 4.

2. Theoretical formulation

Let a binary alloy contains in all *N* atoms with N_A and N_B atoms of A and B elements respectively, k_B is Boltzmann constant, *T* is absolute temperature. Then the model considers the existence of chemical complexes A_xB_y where, A and B are the constituent species of the alloy and *x* and y are the small integers.

$$xA + yB = A_xB_y$$

With this consideration, grand partition function (Guggenheim, 1952) in terms of configurational energy 'E' is expressed as

$$\Xi = \sum_E q_A^{N_A}(T) q_B^{N_B}(T) \exp[(\mu_A N_A + \mu_B N_B - E)/k_B T] \quad (1)$$

Where $q_i(T)$ and μ_i are atomic partition function and chemical potential of the i^{th}(i =A, B) species. By using above relation we find following expressions for the determination of different properties. With this consideration the excess free energy of mixing becomes

$$G_M^{XS} = NK_B T \int_0^c \gamma dc \quad (2)$$

Where γ is ratio of the activity coefficient of atom A to B; C is the concentration of atom A

The solution of eq^n. (2) leads to

$$G_M^{XS} = N[\phi\omega + \phi_{AB}\omega_{AB} + \phi_{AA}\omega_{AA} + \phi_{BB}\omega_{BB}] \quad (3)$$

Where ω's are the ordering energies; and Φ = c (1-c) and Φij's (i,j= A,B) are the simple polynomials in c depending on the values of *x* and *y*.

For A= Ag, B=Sb, *x*=3 and y=1, the values of Φ_{ij}'s (Bhatia & Singh, 1982) are found to be

$$\Phi_{AB}(c) = \frac{1}{5}c + \frac{2}{3}c^3 - c^4 - \frac{1}{5}c^5 + \frac{1}{3}c^6$$

$$\Phi_{AA}(c) = -\frac{3}{20}c + \frac{2}{3}c^3 - \frac{3}{4}c^4 + \frac{2c^5}{5} - \frac{1}{6}c^6$$

$$\Phi_{BB}(c) = 0$$

The Free energy of mixing for complex forming

$$G_M = G_M^{XS} + Nk_B T[c\ln c + (1-c)\ln(1-c)]$$
$$= RT\left[\Phi\frac{\omega}{k_B T} + \Phi_{AB}\frac{\Delta\omega_{AB}}{k_B T} + \Phi_{AA}\frac{\Delta\omega_{AA}}{k_B T} + \Phi_{BB}\frac{\Delta\omega_{BB}}{k_B T} + c\ln c + (1-c)\ln(1-c)\right] \quad (4)$$

The heat of mixing is found out by using standard thermodynamic relation:

$$\frac{H_M}{RT} = \frac{G_M}{RT} - \left[\frac{1}{R}\frac{dG_M}{dT}\right]_{c,N,P}$$
$$= \Phi\left[\frac{\omega}{k_B T} - \frac{1}{k_B}\frac{d\omega}{dT}\right] + \Phi_{AB}\left[\frac{\Delta\omega_{AB}}{k_B T} - \frac{1}{k_B}\frac{d\Delta\omega_{AB}}{dT}\right] + \Phi_{AA}\left[\frac{\Delta\omega_{AA}}{k_B T} - \frac{1}{k_B}\frac{d\Delta\omega_{AA}}{dT}\right] + \Phi_{BB}\left[\frac{\Delta\omega_{BB}}{k_B T} - \frac{1}{k_B}\frac{d\Delta\omega_{BB}}{dT}\right] \quad (5)$$

The standard thermodynamic relation for entropy of mixing is

$$\frac{S_M}{R} = \frac{H_M}{RT} - \frac{G_M}{RT} \quad (6)$$

The activity of the constituent elements in the alloys is determined from standard thermodynamic relation

$$RT\ln a_i(i = A, B) = G_M + (1 - c_i)\left[\frac{\partial G_M}{\partial c_i}\right]_{T,P,N} \quad (7)$$

By solving eq^{ns}(4) and (7), the theoretical values activities of each component are given as follows.

$$\ln a_A = \frac{G_M}{RT} + \frac{1-C}{K_B T}[(1-2c)\,\omega + \Phi'_{AB}\,\Delta\omega_{AB} + \Phi'_{AA}\,\Delta\omega_{AA} + \Phi'_{BB}\,\Delta\omega_{BB} + \ln\frac{C}{1-C})] \quad (8)$$

$$\ln a_B = \frac{G_M}{RT} + \frac{C}{K_B T}[(1-2c)\,\omega + \Phi'_{AB}\,\Delta\omega_{AB} + \Phi'_{AA}\,\Delta\omega_{AA} + \Phi'_{BB}\,\Delta\omega_{BB} + \ln(\frac{C}{1-C})] \quad (9)$$

Where, Φ'_{AB} , Φ'_{AA} and Φ'_{BB} are concentration derivatives of Φ_{AB} ,Φ_{AA} and Φ_{BB} respectively.

The concentration fluctuation in long wavelength limit (Bhatia & Thornton,1970) for alloy is derived from standard relation

$$S_{cc}(0) = RT\left[\frac{\partial^2 G_M}{\partial c^2}\right]^{-1}_{T,P,N} \quad 10(a)$$

$$= c_2 a_1\left[\frac{\partial a_1}{\partial c_1}\right]^{-1}_{T,P,} = c_2 a_2\left[\frac{\partial a_2}{\partial c_2}\right]^{-1}_{T,P,} \quad 10(b)$$

Where c_1 (= c) and c_2(=1-c) are concentrations and $a_1$and $a_2$are observed activities of elements A and B respectively.

Solving eq[ns] (4) and 10(a), the theoretical value of Scc(0) is found as follows,

$$Scc(0) = \frac{c(1-c)}{1+c(1-c)\{-2\frac{\omega}{k_B T} + \phi''_{AB}\frac{\Delta\omega_{AB}}{k_B T} + \phi''_{AA}\frac{\Delta\omega_{AA}}{k_B T} + \phi''_{BB}\frac{\Delta\omega_{BB}}{k_B T}\}} \quad (11)$$

Where $\phi''_{i,j} = \frac{\partial^2 \phi_{i,j}}{\partial c^2}$ (i, j = A, B)

The Warren-Cowley short order parameter (Warren, 1969; Cowle, 1950) is related with concentration fluctuation in long wavelength limit as

$$\alpha 1 = \frac{S-1}{S(Z-1)+1}, \text{ where } S = \frac{S_{cc(0)}}{S^{id}_{cc\,(0)}} \quad (12)$$

$$S^{id}_{cc}(0) = c\,(1-c) \quad (13)$$

The mixing behavior of the alloy forming molten can also be studied at the microscopic level in terms of diffusion coefficient ratio which is related to concentration fluctuation in long wave length limit as,

$$\frac{D_M}{D_{id}} = \frac{S^{id}_{cc(0)}}{S_{cc(o)}} \quad (14)$$

Where D_{id} is the intrinsic diffusion coefficient for an ideal mixture and D_M is chemical or mutual diffusion coefficient.

D_M is given as (Darken & Gurrey, 1953; Singh et al., 2014)

$$D_M = D_{id} C_i \frac{d\ln a_i}{dc_i} \quad (15)$$

3. Result and Discussion

3.1 Thermodynamic Properties

Free Energy of Mixing

The energy parameters used for free energy of mixing for Ag-Sb liquid alloy is determined by successive approximation method. The parameters are determined by using Eqn. (4) with experimental value of G_M in the concentration range from 0.1 to 0.9 (Hultgren et al.,1973). The best fit values of the parameters are

$$\frac{\omega}{k_B T} = -3.97, \frac{\Delta\omega_{AB}}{k_B T} = 4.38\ ,\ \frac{\Delta\omega_{AA}}{k_B T} = -2.68 \quad (16)$$

Eqn. (4) is used to compute the free energy of mixing (G_M /RT) for Ag-Sb liquid alloy. The plot of free energy of mixing verses concentration of antimony is shown in Fig. 1. The computed and experimental values of G_M /RT are in good agreement. The theoretical value of free energy of mixing is minimum i.e. -1.2RT at C_{Sb} =0.4. The theoretical calculation of free energy of mixing shows that at liquid state, the alloy Ag-Sb is moderately interacting and hence the tendency of compound formation is not so strong.

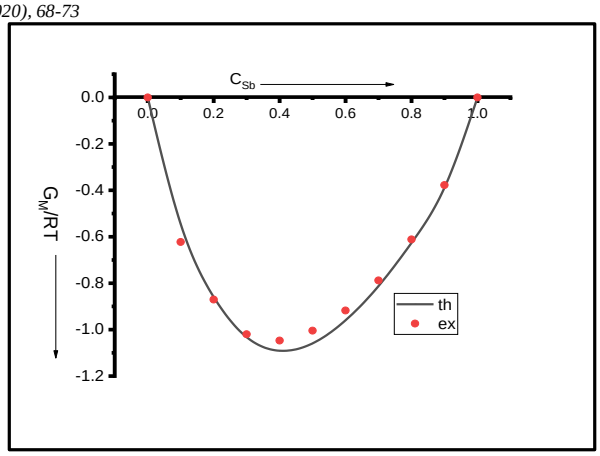

Fig. 1: Free energy of mixing (G_M/RT) vs concentration of antimony (C_{Sb}) in liquid alloy at 1250K

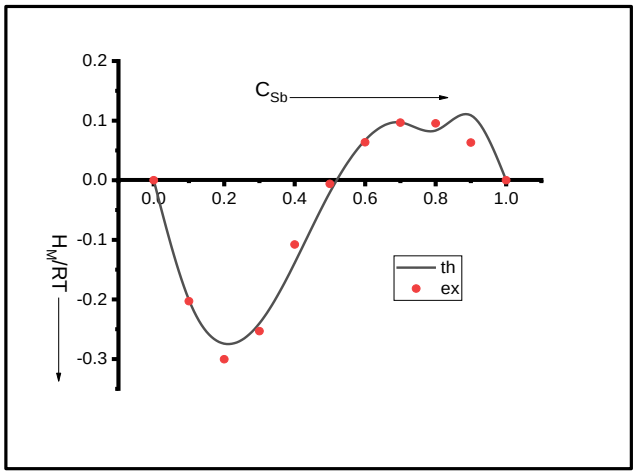

Fig. 2: Heat of mixing (H_M/RT) vs concentration of antimony (C_{Sb}) in liquid alloy at 1250K

Heat of Mixing

For the theoretical determination of heat of mixing temperature derivatives of interaction parameters are done. The observed values of H_M (Hultgren et al., 1973) are used by successive approximation method. The best fit values of parameters are

$$\frac{1}{k_B}\frac{d\omega}{dT} = 2.28, \frac{1}{k_B}\frac{d\Delta\omega_{AB}}{dT} = -7.89, \frac{1}{k_B}\frac{d\Delta\omega_{AA}}{dT} = -4.32 \quad (17)$$

Eqn. (5) is used to compute the heat of mixing (H_M/RT) for Ag-Sb alloy. The plot of heat of mixing verses concentration of antimony is shown in Fig. 2. It is found from the analysis that the heat of mixing is negative in antimony rich region whereas it is positive in the silver rich region. The observed S-shaped nature of heat of mixing verses concentration curve is well explained by the theory. The computed and experimental values of H_M/RT are in reasonable agreement with some discrepancies.

Entropy of Mixing

Using equation (6) along with equations (4) and (5), the entropy of mixing (S_M) is computed. For theoretical

calculation same energy parameters eq^{n} (17) are used.

The plot of entropy of mixing(S_M/R) verses concentration of antimony is shown in Fig. 3 for the both theoretical and observed values. From figure, it is observed that theoretical values are in good agreement with observed values.

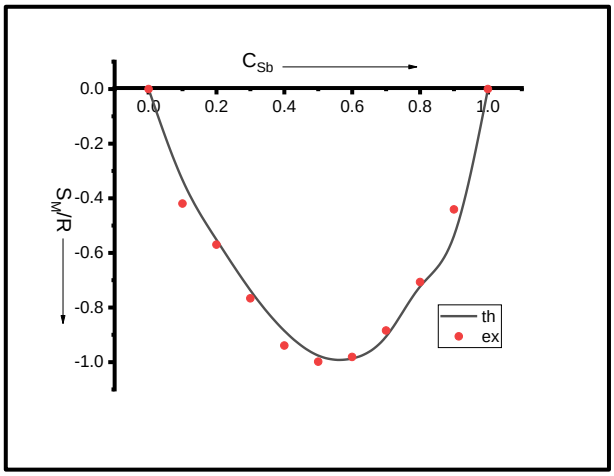

Fig. 3: Entropy of mixing(S_M/R) vs concentration of antimony(C_{Sb}) in liquid alloy at 1250K

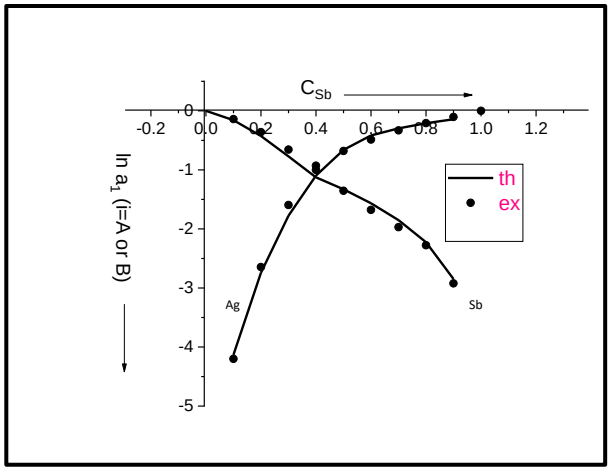

Fig. 4: Chemical activity vs concentration of antimony (C_{Sb}) in liquid alloy at 1250K

3.1.4. Chemical activity

The deviation from ideal behavior of alloys can be explained by chemical activitities. The eq^{ns} (8) and (9) are used for theoretical calculation of chemical activity of constituent elements of alloy Ag-Sb. Fig. 4 shows the observed and theoretical values of chemical activity of the alloy.There is good aggrement between experimental and thheoretical values of activity of Ag and Sb in Ag-Sb alloys at 1250K at all concentrations of Sb.

3.2 Structural Properties

Concentration fluctuation in long wave length limit

One of the important function for the study of nature of atomic order of the binary liquid is considered as the Concentration fluctuations in the long-wavelength limit(Scc(0)) because it removes difficulties in diffraction experiment(Bhatia & Thornton, 1970). For given concentration if Scc(0) > S^{id}cc(0), the alloy is expected to have tendency of segregating while if Scc(0) < S^{id}cc(0), the expected nature is complex formation .The experimental and theoretical values of Scc(0) at different concentrations of element antimony are obtained from eq^{ns} (10) and (11) respectively. The plot of experimental and theoretical along with ideal values of Scc(0) verses concentration is shown in Fig. 5.

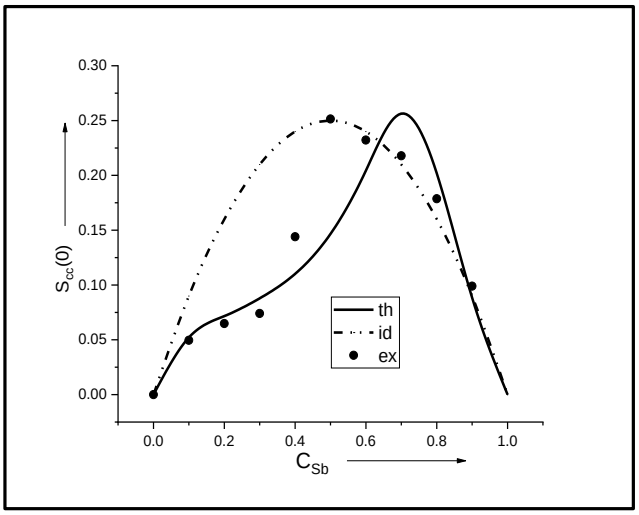

Fig. 5: Concentration fluctuation in long wavelength limit($S_{cc}(0)$) vs concentration of antimony (C_{Sb}) in liquid alloy at 1250K

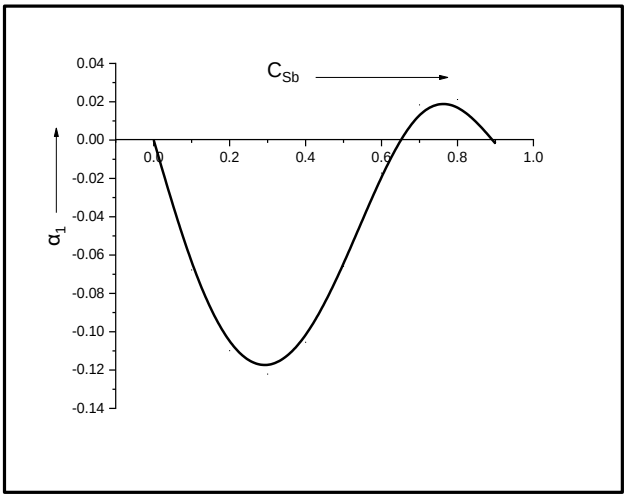

Fig. 6: Waren-Cowley short range order parameter vs concentration of antimony (C_{Sb}) in liquid alloy at 1250K

Warren- Cowley short range order parameter

The Warren-Cowley short-range orderparameter (α_1) is one of the useful parameter to quantify thedegree of chemical order in the alloy melt. It provides information of the local arrangement of the atoms in the molten alloys. For the equi-atomic composition, the

Warren-Cowley short range orderparameter is found to be $-1 \leq \alpha_1 \leq 1$. Negative values of α_1 indicate ordering nature in the melt, which is complete if $\alpha_1 = -1$. On the other hand, positive values of α_1 indicate segregating nature, which is completeonly if $\alpha_1 = 1$. But $\alpha_1 = 0$, indicates the random distribution of the atoms in the mixture. The Scc(0) and α_1 have been computed as a function of concentration of Sb using Eqns. (12) and (13) respectively. The plot of theoretical value of α_1 verses concentration of Sb is shown in Fig. 6.

The Fig. 6 also shows that α_1 is between concentrations 0 to 0.62 of Sb which is the indication of unlike atoms pairing between constituent atoms.

3.3 ***Diffusivity***

In terms of diffusion coefficient ratio, mixing behavior of liquid alloys can also be explained at the microscopic level. The relationship between Scc(0) and the diffusivity is expressed by the ratio of the mutual and self-diffusion coefficients (D_M/D_{id}) which indicates the mixing behavior of the alloys, i.e., the tendency for heterocoordination ($D_M/D_{id} > 1$) or homocoordination nature ofatoms ($D_M/D_{id} < 1$) or ideal mixing($D_M/D_{id} = 1$).

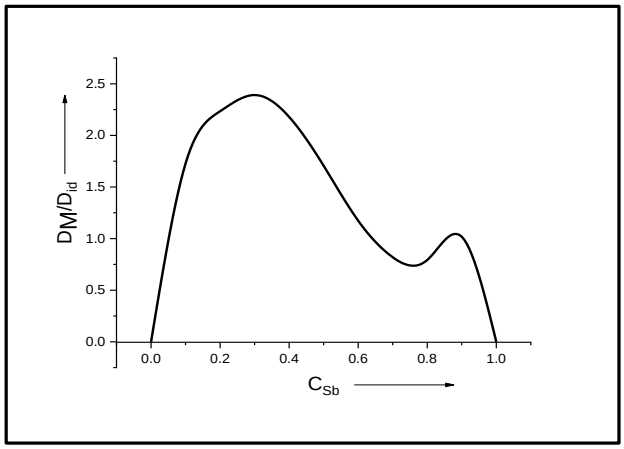

Fig. 7: Diffusion coefficient ratio vs concentration of antimony (C_{Sb}) in liquid alloy at 1250K

The calculated values of Scc(0) are used in eq^n. (15) to determine the ratio of the mutual and intrinsic-diffusion coefficients(D_M/D_{id}). Fig. 7 shows the plot of D_M/D_{id} against the concentration of antimony. In the figure, the value of D_M/D_{id} is found to be less than 1 in the range of concentration, which is indicative of the phase separarion in the mixture. A maximum value of $D_M/Di_d = 2.39$ for concentration of Sb = 0.3 confirms tendency for chemical ordering, observed by the Scc(0) and chemical short range orded parameter.

4. Conclusions

The thermodynamic properties of Ag-Sb alloy at melting temperature 1250K are examined on the basis of Quasi- lattice model. The model successively explains concentration dependent nature of the alloys by assuming Ag_3Sb complex in melt. From analysis it is justified that the alloy is moderately interacting in nature and hence it doesn't have strong tendency of compound formation. The energy parameters depend on temperature.

Acknowledgment

The authors are grateful to Dr. N.P. Adhikari, Professor, Department of Physics, Tribhuvan University, Kathmandu and R. K. Bachchan, Lecturer, Patan Multiple Campus, T.U. for helpful discussions on this work.

Conflicts of Interest

We wish to confirm that there are no known conflicts of interest associated with this publication and there has been no significant financial support for this work that could have influenced its outcome.

Funding

This research received no external funding.

References

Bhatia, A. B., & Singh, R. N. (1982). Thermodynamic properties of compound forming molten Alloys in a weak interaction approximation. Physics and Chemistry of Liquids an International Journal, 11(4), 343-351.

Bhatia, A. B., & Thornton, D. E. (1970). Structural aspects of the electrical resistivity of binary alloys. Physical Review B, 2(8), 3004.

Cowley, J. M. F. (1950). An approximate theory of order in alloys. Physical Review, 77(5),669.

Darken, L. S., & Gurry, R. W. (1953). Physical Chemistry of Metals. Mc Granw-Hill Book Company. Inc. New York Toronto London, 582.

Guggenheim, E. A. (1952). Mixture. Oxford University press. London

Hultgren, R., Desai, P. D., Hawkins, D. T., Gleiser, M., & Kelley, K. K., (1973). Selected Values of

Thermodynamic Properties of Binary Alloys. American Society for Metals, Metals Park.

Jha, I. S., Koirala, I., Singh, B. P., & Adhikari. D. (2014). Concentration dependence thermodynamic, transport and surface properties in Ag-Cu liquid alloys. Applied Physics A, 116(3)**,** 1517-1523.

Koirala, R. P., Koirala, I., & Adhikari, D. (2018). Energetics of mixing and transport phenomena in Cd-X (X=Pb, Sn) melts. Bibechana, 15, 113-120.

Koirala, I., Singh, B. P., & Jha, I. S. (2015). Theoretical Investigation of Mixing Behavior of Al-Fe Alloys in Molten Stage. African review of physics, 10, 329-335.

Singh, B. P., Adhikari, D., & Jha, I. S. (2010). Concentration dependence of the structure and thermodynamic properties of silver–antimony alloys. Journal of Non-Crystalline Solids, 356(33-34), 1730-1734.

Singh, B. P., Koirala, I., Jha, I. S., & Adhikari, D. (2014). The segregating nature of Cd-Pb liquid binary alloys. Physics and Chemistry of liquids, 52(4), 457-470.

Warren, B. E. (1969). X-ray Diffraction, Reading MA, Addison-Wesley.

How to cite: Panthi, N., Bhandari, I. B., & Koirala, I. (2020). Theoretical assessment on hetero-coordination of Alloys Silver-Antimony at Molten State. Himalayan Journal of Science and Technology, 3-4, 68-73.

BIBECHANA
ISSN 2091-0762 (Print), 2382-5340 (Online)
Journal homepage: http://nepjol.info/index.php/BIBECHANA
Publisher: Department of Physics, Mahendra Morang A.M. Campus, TU, Biratnagar, Nepal

Investigation on thermo-physical properties of liquid In-Tl alloy

I. B. Bhandari[1,2], N. Panthi[1,3] , I. Koirala[1*]
[1]Central Department of Physics, Tribhuvan University, Kirtipur, Nepal
[2]Department of Applied Sciences, Purwanchal Campus, Tribhuvan University, Dharan, Nepal
[3]Department of Physics, Patan Multiple Campus, Tribhuvan University, Lalitpur, Nepal
*E-mail**:** ikphysicstu@gmail.com

Article Information:
Received: June 29, 2020
Accepted: August 8, 2020

Keywords:
Mixing properties
Ordering energy
Complex formation model
Segregation

ABSTRACT
This research explores mixing behaviour of liquid In – Tl system through thermodynamic and the structural properties on the basis of Complex Formation Model. The properties like surface tension and viscosity have been analyzed through simple statistical model and Moelwyn – Hughes equation. The interaction parameters are found to be positive, concentration independent and temperature dependent. Theoretical results are in a good agreement with the corresponding literature data which support homo-coordinating tendency in the liquid In-Tl alloy.

DOI**:** https://doi.org/10.3126/bibechana.v18i1.29531

1. Introduction

Indium is a substance which is used in solder alloys which are applied in electronics for assembling semiconductor chips to a base and hybrid integrated circuits and to seal glass to metal in vacuum tubes. Fusible indium alloys are used to bend thin walled tubes without wrinkling the wall or changing the original cross-section. These alloys are not only used in fire control system, restraining links that hold alarm, water valve and door operating mechanism but also used as temperature indicators in situations where other methods of temperature measurements are impracticable and infeasible [1]. Indium is also used in nuclear reactor control rod alloys, low pressure sodium lamps and alkaline batteries. Additions of indium to lead–tin bearings are utilized in piston type aircraft engines, high performance automobile engines and in turbo–diesel truck engines. The addition of indium to gold dental alloys recuperates their mechanical properties and increases resistance to discoloring. Small amount of indium is used to improve the machinability of gold alloys for jewelry [1].The indium–thallium alloy is a classic type of shape memory alloy with a low melting temperature. It has wide range of practical applications in the field of metallurgy which includes the use in

thermostats, hydraulic lines and electrical circuits [2]. Thallium alone is improper for direct use because of its properties of toxicity, unfavorable mechanical properties and significant tendency to oxidize. Thallium contains the most constant atomic vibration so far experimented. This property of Tl preceded it to be used in atomic clocks. Thallium immediately forms alloys with most other metals. There is incomplete mutual insolubility with iron and limited solubility in the liquid state with copper, aluminum, zinc, arsenic, manganese and nickel. Gold, silver, cadmium and tin formulate simple eutectic point with thallium. Thallium also forms binary alloys with antimony, barium, calcium, cerium, cobalt, germanium, lanthanum, lithium, magnesium, strontium, tellurium, bismuth and indium. The ternary alloys of thallium Tl–Pb–Bi, Tl–Al–Ag, In–Hg–Tl, Sn–Cd–Tl, Bi–Sn–Tl and Bi–Cd–Tl are used as semiconductors in ceramic compounds. Thallium has good wear resistance when it is used in bearing shafts. Thallium containing alloys are frequently recommended for bearings, electronics industry such as in solid state rectifiers, electrical fuses and soldering materials [1]. The study of In-Tl alloy is also useful to investigate the corresponding higher order alloy through different approaches [3]. There is difficulty in studying the properties of alloys in liquid state due to lack of long range atomic order. Therefore, theoreticians have exercised different models to understand the properties of various binary liquid alloys [4–22]. The different properties were studied at fixed temperature of 723 K through different models. In present work, we have explored the energetic of In – Tl alloy at a temperature of 723K using complex formation model [23]. The outcomes are analyzed and compared with literature data [24] to explicate the accuracy of this method in thermodynamic and structural description of the presented binary system.

2. Theory

Thermodynamic properties

If a binary alloy contains N_A = x number of A atoms and N_B = (1-x) number of B atoms, so that total number of atoms is N = N_A + N_B. When components A and B are amalgamated together to form a binary A-B solution, thermodynamic properties are changed. The liquid alloy is considered to be ternary mixture of three species; A atom, B atom and chemical complex A_uB_v, is also called conformal solution. The number of free atoms will be reduced due to compound formation in the melt. Now for n_1g atoms of A, n_2g atoms of B and n_3g atoms of A_uB_v,

$$n_1 = x - un_3 \text{ and } n_2 = (1-x) - vn_3 \quad (1)$$

The total number of atoms after mixing can be given as

$$n = n_1 + n_2 + n_3 = 1 - (u + v - 1)n_3 \quad (2)$$

The free energy of mixing of the binary A-B mixture can be written as [23],

$$G_M = -n_3 g + G' \quad (3)$$

Here,$-n_3 g$ stands for lowering of free energy due to compound formation, g is the formation energy of complex. G' is the free energy of mixing of the ternary mixture of A, B and A_uB_v. If the ternary mixture is an ideal solution,

$$G' = RT \sum n_i ln\left(\frac{n_i}{n}\right) \quad (4)$$

If the effects of differences in sizes of the various constituents in the mixture cannot be ignored and the interaction ω_{ij} are small but not zero, the theory of regular solutions in the zeroth approximation [25] or the conformal solution approximation [26] is valid. For regular solution

$$G' = RT \sum n_i ln\left(\frac{n_i}{n}\right) + \sum \omega_{ij}\left(\frac{n_i n_j}{n}\right) \quad (5)$$

This equation is concerned to conformal solution approximation. Where ω_{ij}= 0 (for i = j) are termed as the interaction energies and by definition are independent of concentration, although they are depended upon temperature and pressure.

Now the expression for free energy of mixing G_M for the compound forming binary alloy is

$$G_M = -n_3 g + RT \sum_{i=1}^{3} n_i ln\left(\frac{n_i}{n}\right) + \sum\sum_{i<j}\left(\frac{n_i n_i}{n}\right)\omega_{ij} \quad (6)$$

The expression for heat of mixing H_M is given by[23]

$$H_M = G_M - T\left(\frac{\partial G_M}{\partial T}\right)_P \quad (7)$$

Substituting for G_M,

$$H_M = -n_3 g + RT\sum_{1}^{3} n_i ln\left(\frac{n_i}{n}\right) + \sum_{i<j}^{1}\sum\left(\frac{n_i n_j}{n}\right)\omega_{ij} - T\frac{\partial}{\partial T}\left[-n_3 g + RT\sum_{i=1}^{3} n_i\, ln\left(\frac{n_i}{n}\right) + \sum_{i<j}\sum\left(\frac{n_i n_j}{n}\right)\omega_{ij}\right]$$

$$H_M = -n_3\left[g - T\left(\frac{\partial g}{\partial T}\right)_P\right] + \frac{1}{n}\sum_{i<j}\sum\left(n_i n_j\right)\left[\omega_{ij} - T\left(\frac{\partial \omega_{ij}}{\partial T}\right)_P\right] \quad (8)$$

The expression for entropy of mixing S_M can be obtained as [23]

$$S_M = n_3\frac{\partial g}{\partial T} - R\sum_{i=1}^{3} n_i ln\frac{n_i}{n} - \sum_{i<j}\sum\frac{n_i n_j}{n}\frac{\partial \omega_{ij}}{\partial T} \quad (9)$$

The equilibrium value of n_3 at a given pressure and temperature is given by[23]

$$\left(\frac{\partial G_M}{\partial n_3}\right)_{T,P,N,C} = 0 \quad (10)$$

Substituting the value of G_M from Equation (6) and after some algebraic calculation

$$ln(n_3 n^{u+v-1} n_1^{-u} n_2^{-v}) + Y = \frac{g}{RT} \quad (11)$$

The Equation (11) is called equilibrium equation, where

$$Y = \left[\frac{n_1 n_2}{n^2}(u+v-1) - u\frac{n_2}{n} - v\frac{n_1}{n}\right]\frac{\omega_{12}}{RT} + \left[\frac{n_2 n_3}{n^2}(u+v-1) - v\frac{n_3}{n} + \frac{n_2}{n}\right]\frac{\omega_{23}}{RT} + \left[\frac{n_1 n_3}{n^2}(u+v-1) - u\frac{n_3}{n} + \frac{n_1}{n}\right]\frac{\omega_{13}}{RT} \quad (12)$$

Structural Properties

The concentration fluctuation at long wavelength limit is of good interest because any deviation from ideal value $S_{cc}^{id}(0)$ is significant in describing the nature of ordering and phase segregation in molten alloys. This has been used to investigate the nature of atomic order. The concentration fluctuation at long wavelength limit is related with free energy of mixing by the expression [27],

$$S_{cc}(0) = \frac{RT}{\frac{\partial^2 G_M}{\partial c^2}} \quad (13)$$

$$S_{cc}(0) = \frac{RT}{RT\sum_{i=1}^{3}\left(\frac{\left(n_i'\right)^2}{n_i} - \frac{\left(n'\right)^2}{n}\right) + 2n\sum_{i<j}\sum\omega_{ij}\left(\frac{n_i}{n}\right)'\left(\frac{n_j}{n}\right)'} \quad (14)$$

Theoretically computed values of $S_{cc}(0)$ can be compared with the observed values computed from activity data by the expression,

$$S_{cc}(0) = (1-x)a_A\left(\frac{\partial a_A}{\partial c}\right)^{-1}_{T,P,N} = xa_B\left(\frac{\partial a_B}{\partial c}\right)^{-1}_{T,P,N} \quad (15)$$

The ideal value of $S_{cc}(0)$ can be expressed as,

$$S_{cc}^{id}(0) = x(1-x) \quad (16)$$

The Warren–Cowley short range order parameter quantify the degree of local order in the binary alloy [28,29]. The theoretical values of this parameter can be calculated as

$$\alpha_1 = \frac{(s-1)}{s(z-1)+1}, S = \frac{S_{cc}(0)}{S_{cc}^{id}(0)} \quad (17)$$

where z is coordination number, which is taken as 10 for our calculation.

Transport Properties

The mixing behaviour of the alloys forming molten alloy can also be studied at the microscopic level in terms of coefficient of diffusion. The mutual diffusion coefficient (D_M) of binary liquid alloys can be expressed in terms of activity (a_i) and self-diffusion coefficient (D_{id}) of pure component with the help of Darken's equation [30]

$$D_M = D_{id}x\frac{dlna_i}{dx} \quad (18)$$

with $D_M = c_A D_B + c_B D_A$

where D_A and D_B are the self – diffusion coefficients of pure components A and B respectively,

The expression for D_M in terms of $S_{cc}(0)$ can be given as

$$\frac{D_M}{D_{id}} = \frac{S_{cc}^{id}(0)}{S_{cc}(0)} \quad (19)$$

The mixing behaviour of liquid alloys at microscopic level can also be understood in terms of viscosity. The Moelwyn – Hughes equation for viscosity of liquid alloy [31] is

$$\eta = \eta_{id}\left[1 - x_A x_B\left(\frac{2g}{RT}\right)\right] \quad (20)$$

with

$\eta_{id} = x\eta_A + (1-x)\eta_B$

where η_i is the viscosity of pure component i. At temperature T, it is given by [32]

$$\eta_i = \eta_{i0}\exp\left(\frac{E}{RT}\right) \quad (21)$$

Here η_{i0} a constant in the unit of viscosity and E is the activation energy.

Surface Properties

The surface properties of the liquid mixture give insight into the metallurgical phenomenon, such as crystal growth, wielding, gas absorption and nucleation of gas bubbles [33]. The expressions for surface tension proposed by Prasad et al., [34,35], has been reduced in the simple form using zeroth approximation as

$$\tau = \tau_A + \frac{k_B T}{\xi} ln\frac{x^s}{x} + \frac{g}{\xi}[p(1-x^s)^2 + (q-1)(1-x)^2] \quad (22)$$

$$\tau = \tau_B + \frac{k_B T}{\xi} ln\frac{(1-x^s)}{(1-x)} + \frac{g}{\xi}[p(x^s)^2 + (q-1)(x)^2] \quad (23)$$

where τ_A and τ_B are the surface tensions of pure components A and B respectively, x and x^s are the bulk and surface concentration of the components of alloy, p and q are called coordination fractions, which are defined as the fraction of the total number of nearest neighbors made by atom within its own layer and that in the adjoining layer. The coordination fractions p and q are related to each other by the relation

$p + 2q = 1$, for closed packed structure, $p = 0.5$ and $q = 0.25$

The expression for the mean atomic surface area ξ is

$$\xi = \sum c_i \xi_i \quad (24)$$

The atomic surface are for each component is

$$\xi_i = 1.102\left(\frac{\Omega_i}{N_A}\right)^{2/3} \quad (25)$$

where $\Omega_i$is the molar volume of the component i and $N_A$represents Avogadro number. Equating equations (22) and (23), we can solve it for x^s as the function of x and hence compositional dependence of surface tension can be evaluated.

where τ_A and τ_B are the surface tensions of pure components A and B respectively, x and x^s are the bulk and surface concentration of the components of alloy, p and q are called coordination fractions, which are defined as the fraction of the total number of nearest neighbors made by atom within its own layer and that in the adjoining layer. The coordination fractions p and q are related to each other by the relation

$p + 2q = 1$, for closed packed structure, $p = 0.5$ and $q = 0.25$

The expression for the mean atomic surface area ξ is

$$\xi = \sum c_i \xi_i \quad (24)$$

The atomic surface are for each component is

$$\xi_i = 1.102\left(\frac{\Omega_i}{N_A}\right)^{2/3} \quad (25)$$

where $\Omega_i$is the molar volume of the component i and $N_A$represents Avogadro number. Equating equations (22) and (23), we can solve it for x^s as the function of x and hence compositional dependence of surface tension can be evaluated.

3. Results and Discussion

Thermodynamic properties

The experimental data on the thermodynamic properties as well as phase diagram information [24] have been used for the calculation of order energy parameters for liquid phase In–Tl system. The data set of the Gibbs energy of mixing (G_M) were taken as input data to calculate by the CFM the interaction energy parameters, i.e. g, ω_{12}, ω_{13}, ω_{23}. The starting values of g/RT and ω_{ij}/RT were obtained as suggested in ref. [23]. Equilibrium Equation (11) along with Equations (1) and (2) were applied to compute the number of complexes,

n_3, as a function of concentration. The values of interaction energy parameters were adjusted to give the concentration dependence of free energy of mixing which fits well with the corresponding thermodynamic data. From the phase diagram [24] In-Tl alloy is expected to aggregate with stoichiometry In-Tl (u = 1, v = 1).The calculations were done at temperature of 723 K. The interaction energy parameters for In–Tl liquid alloys are found to be g = 0.755 RT, ω_{12} =0.476 RT, ω_{13}=1.610 RT and ω_{23}= 1.481 RT. The positive interaction energies imply the repulsion between the corresponding species.

The concentration dependence of the equilibrium values of chemical complexes, n_3, (Fig. 1) displays the symmetry with the maximum value of 0.4178 at equiatomic composition. The curve describing the Gibbs free energy of mixing of the In–Tl liquid phase is symmetric with respect to the equiatomic composition (Fig. 2). Theoretical calculation of free energy of mixing for In-Tl liquid alloy shows that In - Tl alloy in liquid state is weakly interacting or homo-coordinating system. There is an excellent agreement between the experimental and calculated integral free energies. Very poor agreement of calculated values of H_M and S_M with experimental simply indicates the importance of the dependence of interaction energies on temperature. To account this, we have used Equations (8) and (9) to determine the variation in energy parameters with respect to temperature from experimental values of H_M and S_M [24]. The temperature dependent interaction energies at T=723K are found to be

$$\frac{1}{R}\frac{\partial g}{\partial t} = 0.845, \quad \frac{1}{R}\frac{\partial \omega_{12}}{\partial t} = 0.383,$$

$$\frac{1}{R}\frac{\partial \omega_{13}}{\partial t} = 1.493,$$

$$\frac{1}{R}\frac{\partial \omega_{23}}{\partial t} = 1.430$$

It is found from the present analysis that the heat of mixing and entropy of mixing both are positive at all concentrations. Our theoretical calculation shows that the maximum value of the heat of mixing is 0.0512 RT at x_{In} = 0.6 (Fig.3) and the maximum value of entropy of mixing is 0.6107 at x_{In} = 0.5 (Fig.4). There is excellent agreement between experimental and calculated values of H_M. The calculated values of S_M deviates from experimental values by maximum percentage of 8.31 at x_{In} = 0.8 and by minimum percentage of 5.56 at x_{In} = 0.4. This deviation is because of the propagation of error from previous calculation.

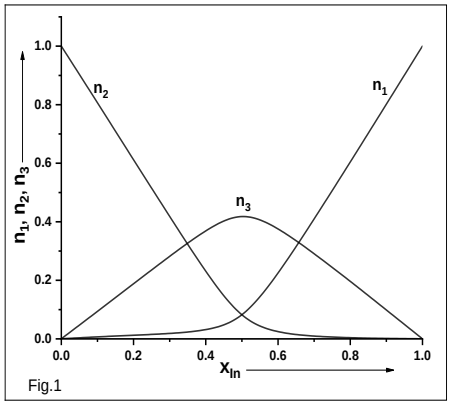

Fig.1: Number of complexes (n_1, n_2, n_3) vs. concentration x_{In} of liquid In - Tl alloy at 723K.

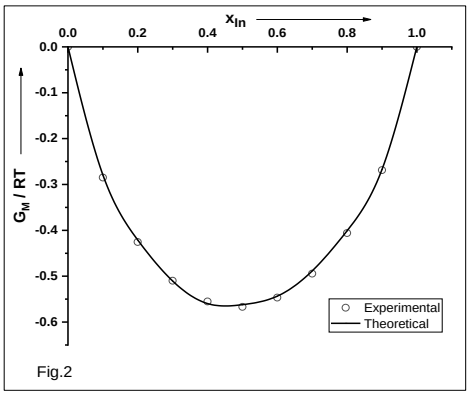

Fig. 2: Free energy of mixing (G_M/RT) vs. concentration (x_{In}) of liquid In - Tl alloy at 723K.

Structural Properties

It has been reported that when $S_{cc}(0) < S_{cc}^{id}(0)$, the existence of chemical ordering leading to complex

formation is expected while $S_{cc}(0) > S_{cc}^{id}(0)$, is an indication of segregation. The same interaction parameters used in the calculation of the thermodynamic properties were employed in the calculations of $S_{cc}(0)$ using Equation (14) while the experimental values of $S_{cc}(0)$ were obtained from Equation (15) using the experimental activity data. The results obtained from the above computations are plotted in Fig. (5). It is found that $S_{cc}(0) > S_{cc}^{id}(0)$ throughout the entire concentration range, this also confirms the presence of chemical segregation or a preference for like atoms to pair. The value of short range order parameter is positive through the whole concentration range which indicates that the alloy is segregating at all compositions. The value of short range order parameter has been found maximum (= 0.02438) at x_{In} = 0.5 at 723 K (Fig. (6)).

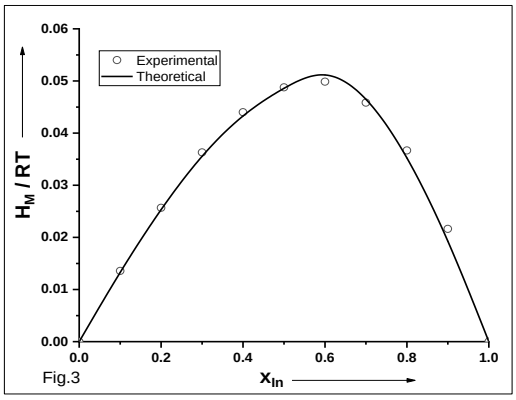

Fig. 3: Heat of mixing (H_M) vs. concentration of indium (x_{In}) in the liquid In - Tl alloy at 723K.

Transport Properties

The calculated values of $S_{cc}(0)$) by Equation (17) can be applied to evaluate the ratio of the mutual and intrinsic-diffusion coefficients (D_M/D_{id}) using Equation (19), against the concentration of indium. We note that the ratio of diffusivities can also be used to indicate levels of order in the liquid binary alloys. The presence of chemical order is indicated by $D_M/D_{id}>1$. Similarly, $D_M/D_{id}<1$ suggests the tendency for segregation. Fig. (7) shows the plots D_M/D_{id} against concentration of indium. It can be observed that the ratio D_M/D_{id} is less than 1 throughout the whole concentration range. This indicates the homo – coordinating tendency in In–Tl alloys at the temperature of investigation. It is also noticed that D_M/D_{id} exhibits maximum peak at around the equi-atomic composition. The result predicted by D_M/D_{id} is in agreement with the results obtained from the free energy of mixing, concentration fluctuations and CSRO parameter.

The viscosity of the In–Tl liquid alloy has been calculated numerically using Equation (20). From the plot of η verses bulk concentration of indium (Fig. 8) small negative deviation from the linear law (Raoult's law) in viscosity isotherms η(x) has been inspected.

Surface Properties

The surface concentrations and surface tension of In–Tl alloy have been computed numerically using Equations (22) and (23). The values of densities and surface tension at melting temperature (T^0) of pure atoms are taken from ref. [32]. These values have been optimized at required temperature (T) by using the expressions

$$\rho_i(T) = \rho_i^0 + (T - T_i^0)\, d\rho_i/dt \quad (26)$$

$$\tau_i(T) = \tau_i^0 + (T - T_i^0)\, d\tau_i/dt \quad (27)$$

where $d\rho_i/dt$ and $d\tau_i/dt$ represent temperature coefficients of density and surface tension respectively for the components of the metal alloys. The computed values of surface concentration for molten In–Tl alloys at 723 K are depicted in Fig. (9). Surface concentration of indium in In–Tl alloys is found to increase with the increase of bulk concentration of In. The computed surface tension for In–Tl alloys at 723 K is less than ideal values at all concentrations of indium; i.e., there is negative departure of surface tension from ideality ($\tau = \tau_A x + \tau_B(1-x)$) throughout the bulk concentrations of indium in In–Tl alloys (Fig. 10). For the In-Tl melt, the surface tension of Tl is smaller than that of In atom. Therefore, Tl atoms having lower surface tension segregates on the surface phase but In

atoms remains in the bulk phase throughout the entire composition.

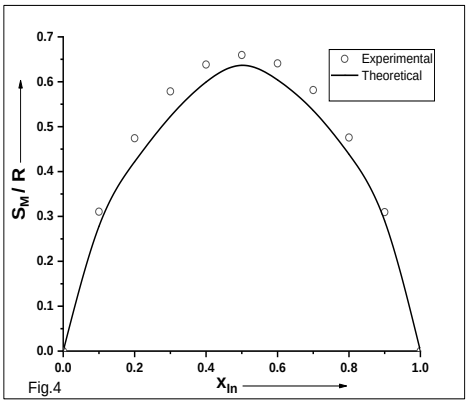

Fig. 4: Entropy of mixing (S_M) vs. concentration of indium (x_{In}) in the liquid In - Tl alloy at 723K.

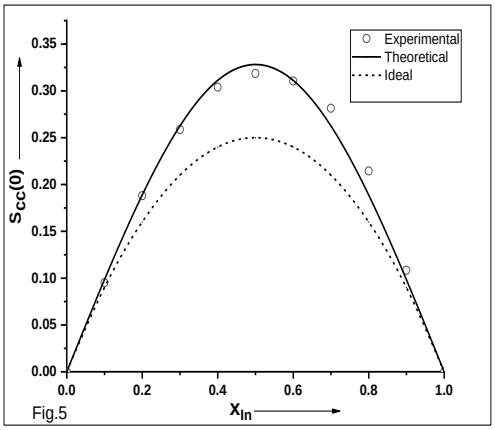

Fig. 5: Concentration fluctuation at long wavelength limit ($S_{cc}(0)$) vs. concentration of indium (x_{In}) in the liquid In - Tl alloy at 723K.

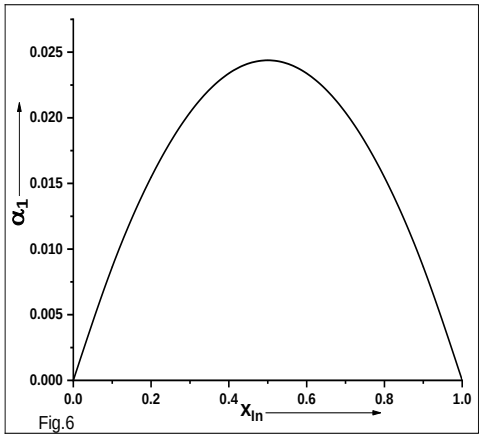

Fig. 6: Chemical short range order (α_1) vs. concentration of indium (x_{In}) in the liquid In - Tl alloy at 723K.

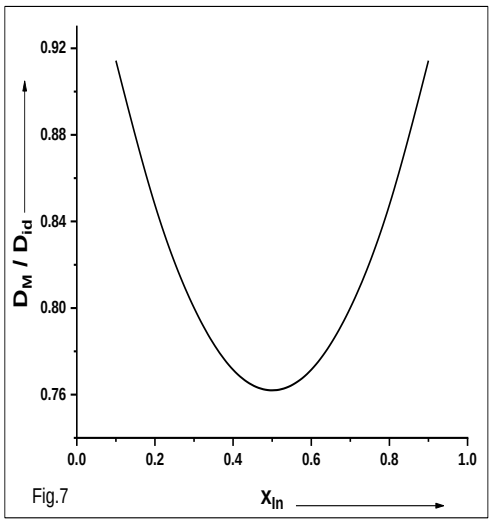

Fig. 7: Ratio of mutual and intrinsic diffusion coefficients (D_M/D_{id}) vs. concentration of indium (x_{In}) in the liquid In - Tl alloy at 723K.

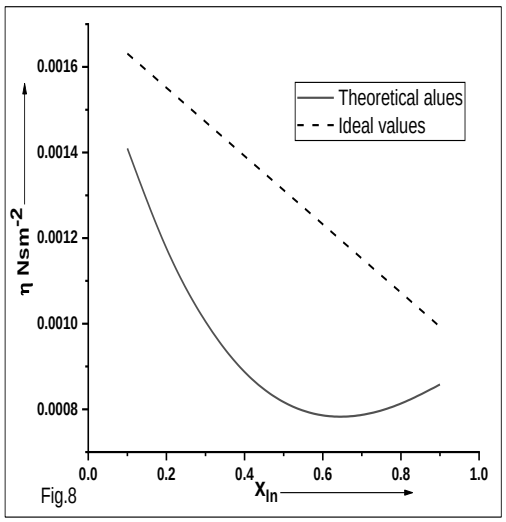

Fig. 8: Viscosity (η) vs. concentration of indium (x_{In}) in the liquid In - Tl alloy at 723K.

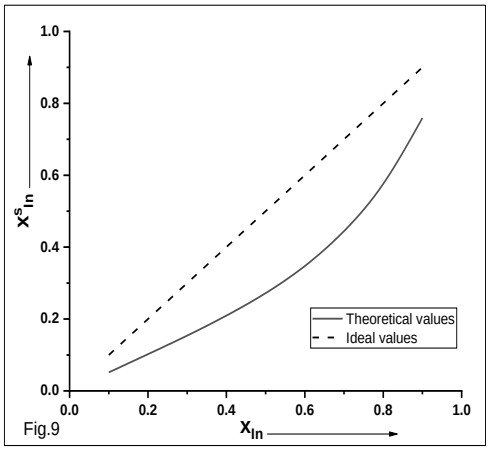

Fig. 9: Surface concentration of indium (x^s_{In}) vs. bulk concentration of indium (x_{In}) in the liquid In - Tl alloy at 723K.

4. Conclusions

The theoretical analysis of the thermodynamic properties reveals that there is a tendency of like atom pairing in the liquid In–Tl alloys at all concentrations. The ordering energy is found to be positive and temperature dependent. The study of concentration fluctuation in long wavelength limit and CSRO show that there is tendency of phase separation in In –Tl liquid alloy. Negative deviation of viscosity isotherms from Raoult law is observed. Viscosity of the alloys decreases with increase in the concentrations of indium. The ratio of diffusion coefficients (D_M/D_{id}) is found to be greater than one at all compositions which also indicates segregating tendency of the system. At the temperature of investigation, the surface tension increases with the increase in the bulk concentration of In. The surface tension of the liquid In–Tl alloy is found to be smaller than ideal values.

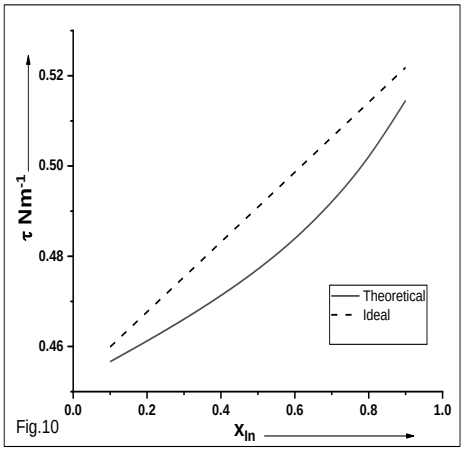

Fig. 10: Surface tension (τ) vs. bulk concentration of indium (x_{In}) in the liquid In - Tl alloy at 723K.

References

[1] F. Habashi, ed., Alloys Preparation, Properties, Applications, First, Wiley-VCH (1998).

[2] Z.P. Luo, An Overview on the Indium-Thallium (In-Tl) Shape Memory Alloy Nanowires, Metallogr. Microstruct. Anal. 1 (2012) 320. https://doi.org/10.1007/s13632-012-0046-4

[3] U. Mehta, S.K. Yadav, I. Koirala, D. Adhikari, Thermo-physical properties of ternary Al–Cu–Fe alloy in liquid state, Philos. Mag. 0 (2020) 1. https://doi.org/10.1080/14786435.2020.1775907

[4] D. Adhikari, A Theoretical study of thermodynamic properties of Cd-Bi liquid alloy, BIBECHANA 8 (2012) 90.

https://doi.org/10.3126/bibechana.v8i0.5693

[5] D. Adhikari, I.S. Jha, B.P. Singh, J. Kumar, Thermodynamic and structural investigations of liquid magnesium – thallium alloys, J. Mol. Struct. 985 (2011) 91. https://doi.org/10.1016/j.molstruc.2010.10.026

[6] S. Lele, P. Ramachandrarao, Estimation of complex concentration in a regular associated solution, Metall. Trans. B 12 (1981) 659. https://doi.org/10.1007/BF02654134

[7] R. Novakovic, Thermodynamics , surface properties and microscopic functions of liquid Al – Nb and Nb – Ti alloys, J. Non. Cryst. Solids. 356 (2010)1593. https://doi.org/10.1016/j.jnoncrysol.2010.05.055

[8] R. Novakovic, D. Giuranno, E. Ricci, T. Lanata, Surface and transport properties of In – Sn liquid alloys, Surf. Sci. 602 (2008) 1957. https://doi.org/10.1016/j.susc.2008.03.033

[9] Y.A. Odusote, Bulk and dynamic properties in Al – Zn and Bi – In liquid alloys using a theoretical model, J. Non. Cryst. Solids. 353 (2007) 1167. https://doi.org/10.1016/j.jnoncrysol.2006.12.023

[10] L.C. Prasad, R.N. Singh, A quasi-lattice model for the thermodynamic properties of au-zn liquid alloys, Phys. Chem. Liq. 22 (1990) 1. https://doi.org/10.1080/00319109008036406

[11] L.C. Prasad, R.N. Singh, V.N. Singh, S.K. Chatterjee, Compound formation in Sn-based liquid alloys, Phys. B Phys. Condens. Matter. 215 (1995) 225. https://doi.org/10.1016/0921-4526(95)00393-N

[12] R.N. Singh, A.B. Bhatia, Flory ' s formula for the entropy of mixing of NaCs alloy, J. Phys. F: Met. Phys. 14 (1984) 2309. https://doi.org/10.1088/0305-4608/14/10/009

[13] S.K. Yadav, S. Lamichhane, L.N. Jha, N.P. Adhikari, D. Adhikari, Mixing behaviour of Ni–Al melt at 1873 K, Phys. Chem. Liq. 54 (2016) 370. https://doi.org/10.1080/00319104.2015.1095640

[14] S.K. Yadav, U. Mehta, R.K. Gohivar, A. Dhungana, R.P. Koirala, D. Adhikari, Reassessments of thermo-physical properties of Si-Ti melt at different temperatures, BIBECHANA 17 (2020) 146. https://doi.org/10.3126/bibechana.v17i0.26877

[15] O. Akinlade, R.N. Singh, Bulk and surface properties of liquid In-Cu alloys, J. Alloys Compd. 333 (2002) 84. https://doi.org/10.1016/S0925-8388(01)01733-9

[16] B.C. Anusionwu, G.A. Adebayo, Quasi-chemical studies of ordering in the Cu–Zr and Cu–Si melts, J. Alloy. Compd. 329 (2001) 162. https://doi.org/10.1016/S0925-8388(01)01572-9

[17] O.E. Awe, Thermodynamic investigation of thermophysical properties of thallium-based liquid alloys, Phys. Chem. Liq. 57 (2019) 296. https://doi.org/10.1080/00319104.2018.1443453

[18] O.E. Awe, O. Akinlade, L.A. Hussain, Thermodynamic properties of liquid Te–Ga and Te–Tl alloys, J. Alloys Compd. 361 (2003) 227. https://doi.org/10.1016/S0925-8388(03)00451-1

[19] A.B. Bhatia, W.H. Hargrove, D.E. Thornton, Concentration fluctuations and partial structure factors of compound-forming binary molten alloys, Phys. Rev. B 9 (1974) 435. https://doi.org/10.1103/PhysRevB.9.435

[20] A.B. Bhatia, R.N. Singh, A Quasi-lattice Theory for Compound Forming Molten Alloys, Phys. Chem. Liq. 13 (1984) 177. https://doi.org/10.1080/00319108608078511

[21] I. Koirala, I.S. Jha, B.P. Singh, Theoretical investigation on ordering nature of Cd-Bi alloys in the molten dtatemolten state, BIBECHANA. 11 (2014) 70. https://doi.org/10.3126/bibechana.v11i0.10382

[22] I. Koirala, B.P. Singh, I.S. Jha, Theoretical assessment on segregating nature of liquid In–Tl alloys, J. Non. Cryst. Solids 398 (2014) 26. https://doi.org/10.1016/j.jnoncrysol.2014.04.018

[23] A.B. Bhatia, W.H. Hargrove, Concentration fluctuations and thermodynamic properties of some compound forming binary molten systems, Phys. Rev. B 10 (1974) 3186. https://doi.org/10.1103/PhysRevB.10.3186

[24] R. Hultgren, P.D. Desai, D.T. Hawkins, M. Gleiser, K.K. Kelley, Selected Values of the Thermodynamic Properties of Binary Alloys., American Society for Metals, Metal Park, Ohio, (1973).

[25] E.A. Guggenheim, Mixtures, Oxford University Press, London (1952).

[26] H.C. Longuet-Higgins, The statistical thermodynamics of multicomponent systems, Proc. R. Soc. London. Ser. A. Math. Phys. Sci. 205 (1951) 247. https://doi.org/10.1098/rspa.1951.0028

[27] A.B. Bhatia, D.E. Thornton, Structural aspects of the electrical resistivity of binary alloys, Phys. Rev. B 2 (1970) 3004.

https://doi.org/10.1103/PhysRevB.2.3004

[28] B.E. Warren, X-ray Diffraction, Dover Publication, New York, 1990.

[29] J.M. Cowley, An approximate theory of order in alloys, Phys. Rev. 77 (1950) 669. https://doi.org/10.1103/PhysRev.77.669

[30] L.S. Darken, R.W. Gurry, Physical Chemistry of Metals, McGraw Hill, New York (1953).

[31] E.A. Moelwyn-Hughes, Physical Chemistry, Second, Pergamon, Oxford (1964).

[32] E.A. Brandes, G.B. Brook, Smithells Metals Reference Book, Seventh, Butterw orth-Heinemann Linacre House, Jordan Hill, Oxford, 1992. https://doi.org/10.1016/B978-075067509-3/50014-2

[33] J.A.V. Butler, The Thermodynamics of the Surfaces of Solutions, R. Soc. A. (1932) 348. https://doi.org/10.1098/rspa.1983.0054

[34] L.C. Prasad, R.N. Singh, V.N. Singh, G.P. Singh, Correlation between Bulk and Surface Properties of AgSn Liquid Alloys, J. Phys. Chem. B 102 (1998) 921. https://doi.org/10.1021/jp971042l

[35] L.C. Prasad, R.N. Singh, Surface segrgation and concentration fluctuation at the liquid-vapor interface of molten Cu-Ni alloys, Phys. Rev. B 44 (1991) 768. https://doi.org/10.1103/PhysRevB.44.13768

Journal of Institute of Science and Technology, 26(1), 51-56 (2021)
ISSN: 2469-9062 (print), 2467-9240 (e)
https://doi.org/10.3126/jist.v26i1.37818

Research Article

COMPARISON OF THERMOPHYSICAL PROPERTIES OF Mg-Ga AND Mg-Pb ALLOYS AT 1000 K

N. Panthi[1, 2], **I. B. Bhandari**[1,3], **R. C. Pangeni**[1,2], **I. Koirala**[1*]

[1]*Central Department of Physics, Tribhuvan University, Kirtipur, Nepal*
[2]*Department of Physics, Patan Multiple Campus, Tribhuvan University, Lalitpur, Nepal*
[3]*Department of Applied Sciences, Pulchowk Campus, Tribhuvan University, Lalitpur, Nepal*
[*]*Corresponding author: iswar.koirala@cdp.tu.edu.np*

(***Received**: January 29, 2021; **Revised**: May 05, 2021; **Re-revised**: May 08, 2021; **Accepted**: June 04, 2021)*

ABSTRACT

Concentration-dependent thermophysical properties of molten Mg-Pb and Mg-Ga alloys at 1000 K was compared using the Redlich Kister equation by optimizing exponential interaction energy parameters based on the R-K polynomials framework. The mixing behavior was investigated by giving more emphasis to the role of temperature-dependent interaction energy parameters. Our study shows that the magnesium gallium alloy is slightly interacting than the magnesium lead alloy. The surface tension and viscosity of both alloys was compared using the Butler equation as improved by Kaptay and KRP (Kozlov-Ronanov-Petrov) approach respectively. The surface tension of Mg-Pb liquid alloy increases but decreases in Mg-Ga alloy with an increase in the concentration of Mg. The viscosity has a nonlinear variation for both alloys with the increase in the concentration of magnesium.

Keywords: Artificial miscibility gap, Energy parameters, Polynomials, Surface tension, Viscosity.

INTRODUCTION

Due to the dramatic change in the behavior of various useful properties of alloys than constituent elements, the alloys have wide application in industries. But it is tedious and time-consuming to study all properties experimentally. Different theoretical models have been developed to explore the thermodynamic behaviors of the binary molten alloys (Bhatia & March, 1975; Bhatia & Singh, 1984; Singh & Mishra, 1988). The limitation of such models is that they can predict the behavior of alloys nearly at melting temperature.

The alloys in the molten state are studied in metallurgy and industry for high-temperature application as well. Hence the mixing behavior of elements of the alloys at high temperatures was considered a prime concern to all metal physicists, metallurgists, and chemists (Shrestha *et al.*, 2017). The Redlich-Kister (R-K) equation (Redlich & Kister, 1948) is considered an important tool to understand the thermodynamic property like excess Gibbs free energy of binary molten alloy at high temperatures. The equation was formulated using linear temperature-dependent energy interaction parameters called R-K polynomials.

But there arises an artificial miscibility gap or artifact in some binary alloys using such linear interaction parameters for the high-temperature study of the alloys (Mehta *et al.*, 2020; Gohivar *et al.*, 2020). To avoid the problem raised by artifact, theoretician Kaptay (2017) suggested modifying the temperature-dependent linear interaction parameter to exponential parameter in the R-K polynomials framework where the parameters are exponentially dependent on temperature.

The present work aims to compare the concentration dependence of different properties of molten alloys Mg-Pb and Mg-Ga at temperature 1000 K by optimizing exponential temperature-dependent interaction parameters of both the alloys in the R-K polynomials framework as suggested by Kaptay (2004). Magnesium and its alloys when used in the automobile industry contribute remarkably to the fuel economy as well as the conservation of the environment. The latest technology in the coating as well as alloying of magnesium has reduced the creep and corrosion resistance behavior of the alloys at elevated temperature and corrosive environments (Kulekci, 2008). The properties of the alloys under the investigation include excess Gibb's free energy, enthalpy, entropy, chemical activity, concentration fluctuation in long-wavelength limit, surface tension, and viscosity. These studies provide knowledge of the interaction, bond strength, and stability of phases (Panthi *et al.*, 2021).

On the other hand, the knowledge of the structural adjustment of constituent atoms in the molten alloys is pictured out by the qualitative study of microscopic function; the concentration fluctuation in the long-wavelength limit ($S_{cc}(o)$). Similarly, the information of surface, as well as transport nature of alloys are provided by surface tension and viscosity (Koirala, 2018; Koirala *et al.*, 2014; Singh & Koirala, 2015). Here, it tried to study the surface tension and viscosity of the alloys using the Butler equation as improved by Kaptay (2019) and Kozlov *et al.* (1983) approaches.

THEORETICAL MODEL AND DATA

The excess Gibbs free energy (ΔG^{xs}), enthalpy (ΔH), and the excess entropy (ΔS^{xs}) of a binary alloy are related by the standard relation as;

$$\Delta G^{XS} = T\left(\frac{\Delta H}{T} - \Delta S^{xs}\right) \quad (1)$$

Similarly, the excess Gibbs free energy of an alloy is given by the R-K equation (Redlich & Kister, 1948) as;

$$\Delta G^{XS} = c_1 c_2 \sum_{i=0}^{n} L_i (c_1 - c_2)^i \quad (2)$$

Where c_1 and c_2 are the concentration of the constituent elements of the alloy and L_i is the linear temperature-dependent interaction parameter between the components of an alloy known as R-K polynomial. It is related to temperature (T), enthalpy like semi-empirical coefficient (a_i) and entropy like semi-empirical coefficient (b_i) of R-K Polynomials as;

$$L_i = T\left(\frac{a_i}{T} - b_i\right) \quad (3)$$

The total Gibbs free energy of an alloy is related to the excess Gibbs free energy and ideal Gibbs energy of the alloy as;

$$\Delta G = \Delta G^{XS} + \Delta G^{id} = \Delta G^{XS} + RT(c_1 \ln c_1 + c_2 \ln c_2) \quad (4)$$

From equations (2) and (3)

$$\Delta G^{XS} = c_1 c_2 \sum_{i=0}^{n} T\left(\frac{a_i}{T} - b_i\right)(c_1 - c_2)^i \quad (5)$$

From equations (1) and (5), we get

$$\Delta H = c_1 c_2 \sum_{i=0}^{n} a_i (c_1 - c_2)^i \quad (6)$$

$$\Delta S^{xs} = c_1 c_2 \sum_{i=0}^{n} b_i (c_1 - c_2)^i \quad (7)$$

According to Kaptay (2004), the exponential temperature-dependent interaction parameters of a binary alloy can be written as;

$$K_i = h_i \exp\left(-\frac{T}{t_i}\right) \quad (8)$$

Where, h_i(j/mol) and t_i (K) are semi-empirical parameters.

From equations (1), (5), (6), and (7), the derivations for enthalpy and excess entropy of a binary liquid alloy are obtained as shown below.

$$\Delta H = c_1 c_2 \sum_{i=0}^{n} \left(1 + \frac{T}{t_i}\right) h_i \exp\left(-\frac{T}{t_i}\right)(c_1 - c_2)^i \quad (9)$$

$$\Delta S^{xs} = c_1 c_2 \sum_{i=0}^{n} \frac{h_i}{t_i} \exp\left(-\frac{T}{t_i}\right)(c_1 - c_2)^i \quad (10)$$

The entropy of mixing is given by the standard formula as

$$\Delta S = \left(\frac{\Delta H}{T} - \frac{\Delta G}{T}\right) \quad (11)$$

The structural arrangement of the atoms of an alloy in terms of concentration fluctuation in the long-wavelength limit (S_{cc}(o) is calculated from the standard relation as;

$$S_{CC}(0) = RT\left[\frac{\partial^2 \Delta G}{\partial C^2}\right]^{-1}_{T,P,N} \quad (12)$$

From equations (1), (4), (9), (10) and (12)), we get.

$$S_{cc}(0) = RT[\frac{RT}{c_1 c_2} - 2K_0 + (-12c_1 + 6)K_1 + (-48c_1^2 + 48c_1 - 10)K_2 + (-160\,c_1^3 + 240c_1^2 - 108c_1 + 14)K_3]^{-1} \quad (13)$$

In liquid, the viscous flow depends on the cohesive interaction, and this interaction results from the grouping of geometric and electronic shell effects (Starace *et al.*, 2008). The KRP equation for liquid alloy was developed to consider the cohesion interaction in terms of the enthalpic effect to incorporate the viscous flow in the liquid alloy. The equation at temperature T is expressed as;

$$\ln \eta = c_1 \ln \eta_1 + c_2 \ln \eta_2 - \frac{\Delta H_M}{3RT} \quad (14)$$

Where, η and η_i (i=1,2), are the viscosity of the alloy and viscosity of individual components respectively. The change in viscosity with temperature for the metals is given as (Brandes & Brook, 2013);

$$\eta_i = \eta_0 exp\left(\frac{E}{RT}\right) \quad (15)$$

Where, η_o and E for metal are constants and their units are similar to the unit of viscosity and energy per mole, respectively.

The surface tension of an alloy by the Butler equation as improved by Kaptay at temperature (T) is

$$\sigma = \frac{S_i^0}{S_i}\sigma_i^0 + \frac{RT}{S_i}\ln\frac{C_i^S}{C_i^b} + \frac{G_i^{S,XS} - G_i^{b,XS}}{S_i} \#\#(16)$$

Where, σ_i^0 and S_i^0 are surface tension and molar surface area of pure liquid metal, s_i is the partial molar surface area of component i respectively. $G_i^{S,XS}$, and $G_i^{b,XS}$ are the partial excess free energy of mixing in the surface and bulk of constituent components of the alloy, respectively.

The partial excess Gibbs energy of i^{th} a component of an alloy is related to the excess Gibbs energy by the relation given below (Egry *et al.*, 2010).

$$G_i^{xs} = \Delta G^{XS} + \sum_{j=1}^{2}(\delta_{ij} - c_j)\frac{\partial(\Delta G^{XS})}{\partial c_j} \quad (17)$$

Where, δ_{ij} is the Kronecker delta function.

The molar surface area of each metal is expressed as (Kaptay, 2008);

$$S_i^0 = \chi\left(\frac{M_i^0}{\rho_i^0}\right)^{2/3} N^{1/3} \quad (18)$$

Where, M_i^0, ρ_i^0, χ, and N is molar mass, the density of each pure metal at its melting temperature, geometrical constant, and Avogadro's number, respectively. The expression of the geometrical constant is given as;

$$\chi = \left(\frac{3f_V}{4}\right)^{\frac{2}{3}}\frac{\pi^{\frac{1}{3}}}{f_S} \quad (19)$$

Where, f_V and f_S are volume and surface packing fractions, respectively. The values of these packing fractions depend on the type of crystal structure of every pure component of alloys. The surface tension (σ_i^0) and density (ρ_i^0) of metal at temperature T are expressed as (Brandes & Brook, 2013);

$$\sigma_i^0 = \sigma_i + \frac{\partial\sigma}{\partial T}(T - T_0) \quad (20)$$

$$\rho_i^0 = \rho_i + \frac{\partial\rho}{\partial T}(T - T_0) \quad (21)$$

Where, σ_i and ρ_i are surface tension and density of the metal at its melting temperature (T_0), respectively. The terms $\frac{\partial\sigma}{\partial T}$ and $\frac{\partial\rho}{\partial T}$ are temperature derivatives of surface tension and density, respectively.

RESULTS AND DISCUSSION

The exponential temperature-dependent interaction parameters for the alloys Mg-Pb and Mg-Ga were optimized using equation (8). The parameters for both alloys are given in Table 1.

Table1. The exponential temperature-dependent interaction parameters of molten Mg-Pb and Mg-Ga alloys

Mg-Pb	Mg-Ga
K_0= -37785.91exp(-7.16783x10^{-5}T)	K_0= -40495.1exp(-5.9256x10^{-5}T)
K_1= 22239.43exp(-1.8401x10^{-4}T)	K_1= -12829.43exp(-2.4428x10^{-4}T)
K_2= 505013.86exp(-8.7964x10^{-3}T)	K_2= 31004.45exp(-8.9101x10^{-3}T)
K_3= -60866.13exp(-3.5504x10^{-3}T)	

K_0, K_1, K_2, and K_3 are zeroth, first, second and third-order of exponential temperature-dependent interaction parameters, respectively

The parameters thus optimized were used to compare different properties of binary alloys Mg-Pb, and Mg-Ga at temperature 1000 K. During the calculation of parameters, it did not apply statistical method like mean square deviation or others for the best fit, and hence the parameters used here are considered as appropriate for the study.

Thermodynamic properties

For the theoretical analysis of the thermodynamic property, we considered equations (5), (9), and (11) as mentioned above. The excess Gibbs free energy of the molten alloys was computed by the R-K polynomials framework. The computed excess free energy of mixing for both alloys is shown in Fig. 1.

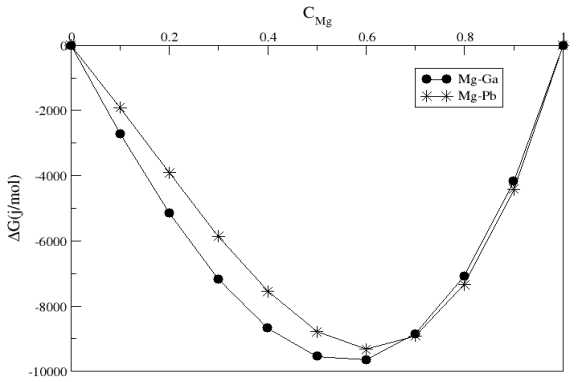

Fig. 1. Excess Gibbs free energy of mixing vs. concentration of Mg

It was observed that below 0.7 concentration of Mg, the alloy Ga-Mg seemed to be more interacting but above the 0.7 concentration of Mg, it was slightly less interacting than the alloy Mg-Pb. Similarly, the computed values of enthalpy of mixing for both the alloys are shown in Fig. 2 which tells that the enthalpy of mixing of Mg-Ga is more negative up to 0.7 concentration of Mg than the alloy Mg-Pb. Thus from both Figs. 1 and 2, it can be said that the binary liquid alloy Mg-Ga seems to be more interacting at a lower concentration of Mg, whereas it is nearly equally interacting with Mg-Pb at a higher concentration of Mg for both the alloys.

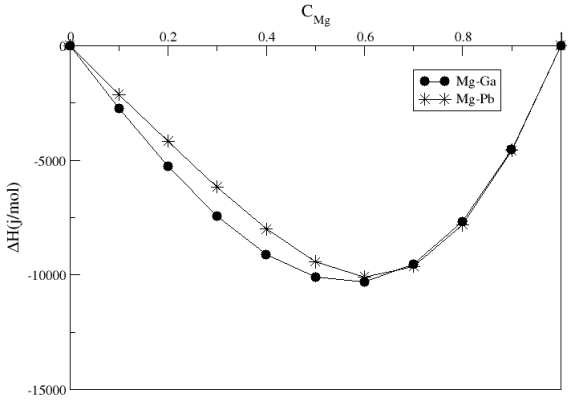

Fig. 2. Enthalpy of mixing vs. concentration of Mg

The computed values of entropy of mixing which mainly provide knowledge of constitutive molecular properties or specific molecular effects in the mixture, for both the alloys are shown in Fig. 3. It is clear from the figure that the entropy change of mixing for both the alloys remains nearly the same.

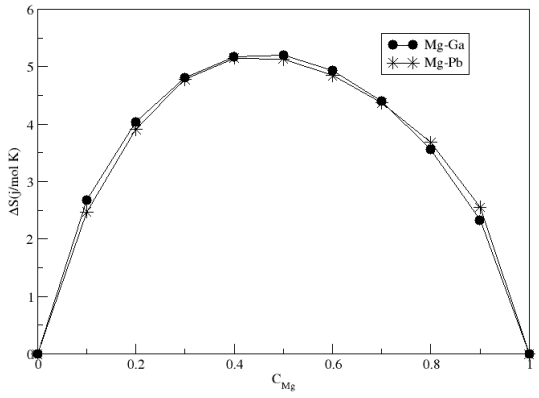

Fig. 3. The entropy of mixing vs. concentration of Mg

Structural properties

There is no direct way to distinguish the grouping of constituent atoms of the mixture. Thus, the identification of the arrangement of atoms in an alloy is very difficult. However, experimentally the local arrangement of atoms of a constituent of the mixture can be studied by diffraction method, but it is a difficult task too. To overcome this problem and to study the arrangement of constituent atoms theoretically, the determination of Concentration fluctuations in long-wavelength limit S_{cc} (0) was considered an important tool (Bhatia & Thornton, 1970). At a given concentration, the alloy is said to have the complex tendency if $S_{cc}(0) < S_{cc}^{id}(0)$, whereas it has the segregating tendency if $S_{cc}(0) > S_{cc}^{id}(0)$.

The computed values of (S_{cc}(0) at various concentrations of magnesium for both alloys are given in Fig. 4. Figure cleared that at about 0.15 concentration of Mg, the alloy Pb-Mg has segregating tendency but above this concentration of Mg, it showed an ordering nature. The alloy Mg-Ga has an ordering nature within the entire concentration of Mg.

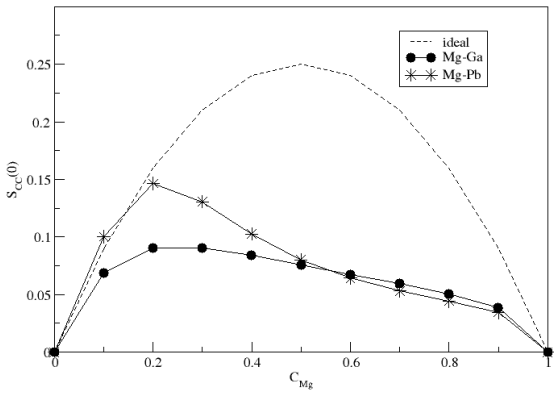

Fig. 4. Concentration fluctuation in long-wavelength limit vs. concentration of Mg

Viscosity

Viscosity is considered an important atomic transport property of liquid alloys. We used the KRP equation for the comparison of the atomic transport behavior of Mg-Pb and Mg-Ga alloys at 1000 K as a function of concentration. The viscosity of the alloys thus computed is compared in Fig. 5. The viscosity of Mg-Pb alloy was found to be more than Mg-Ga alloy with the increase in the concentration of Mg. But for both the alloys the viscosity increased up to 0.6 concentration of Mg and then it decreased beyond that concentration of Mg.

Surface tension

To calculate the surface tension by the improved derivation of the Butler equation, the densities, partial excess Gibbs free energies, and surface tensions, and the component metals at the temperature of the investigation are required. Surface tensions and densities of constituent metals at 1000 K were calculated from their values at

respective melting temperatures by using equations (20) and (21), respectively. For the unknown or negligible excess molar volume of the alloy, the partial molar volume was replaced by the molar volume of the pure component and hence the partial surface area (S_i) of each component was replaced by surface area (S_i^o) of the same pure component (Kaptay, 2020, 2019).

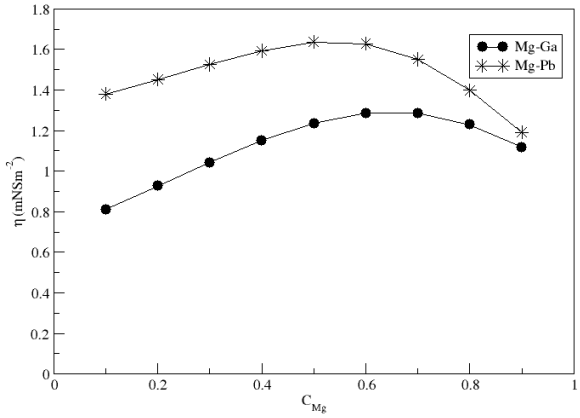

Fig. 5. Viscosity vs. concentration of Mg

Figure 6 is the graph of computed values of surface tension of binary liquid Mg-Pb and Mg-Ga alloys. In the case of alloy Mg-Ga, the surface tension decreased whereas it increased for the alloy Mg-Pb alloy with the increase in the concentration of Mg indicating that the Mg atoms tend to remain on the surface in the case of Mg-Ga alloy whereas the lead atoms show the tendency to remain on the surface of Mg-Pb alloy.

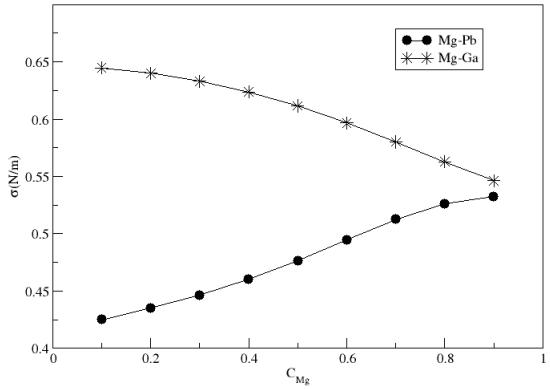

Fig. 6. Surface tension vs. concentration of Mg

CONCLUSION

The comparison of the thermodynamic, structural, and microscopic behavior of binary liquid magnesium lead and magnesium gallium alloys at 1000 K alloy under the assumption of exponential temperature-dependent interaction parameters explains that the magnesium gallium is somewhat interacting than magnesium lead alloy. The theoretical study shows that the magnesium gallium alloy has more ordering nature within the whole range of concentration. The surface tension of the Mg-Ga alloy decreases but it increases in the case of Mg-Pb alloy but viscosity at first increases and then decreases with an increase in the concentration of magnesium.

REFERENCES

Bhatia, A.B., & March, N. (1975). Size effects, peaks in concentration fluctuations, and liquidus curves of Na-Cs. *Journal of Physics F: Metal Physics*, *5*(6), 1100. https://doi.org/10.1088/0305-4608/5/6/011

Bhatia, A. B., & Singh, R. N. (1984). A quasi-lattice theory for compound forming molten alloys Physics *and Chemistry of Liquids an International Journal*, *13*(3), 177-190.

Bhatia, A., & Thornton, D. E. (1970). Structural aspects of the electrical resistivity of binary alloys. *Physical Review B*, *2*(8), 3004. https://doi.org/10.1103/PhysRevB.2.3004

Brandes, E. A., & Brook, G. (2013). *Smithells metals reference book*. Elsevier.

Egry, I., Holland-Moritz, D., Novakovic, R., Ricci, E., Wunderlich, R., & Sobczak, N. (2010). Thermophysical properties of liquid AlTi-based alloys. *International Journal of Thermophysics*, *31*(4-5), 949-965.

Gohivar, R. K., Yadav, S. K., Koirala, R. P., & Adhikari, D. (2020). Assessment of thermo-structural properties of Al-Fe and Fe-Si alloys at high temperatures. *Physics and Chemistry of Liquids*, 1-11. https://doi.org/10.1080/00319104.2020.1793985

Kaptay, G. (2004). A new equation for the temperature dependence of the excess Gibbs energy of solution phases. *Calphad*, *28*(2), 115-124.

Kaptay, G. (2020). A coherent set of model equations for various surface and interface energies in systems with liquid and solid metals and alloys. *Advances in Colloid and Interface Science*, 102212. https://doi.org/10.1016/j.cis.2020.102212

Kaptay, G. (2008). A unified model for the cohesive enthalpy, critical temperature, surface tension, and volume thermal expansion coefficient of liquid metals of bcc, fcc, and hcp crystals. *Materials Science and Engineering: A*, *495*(1- 2), 19-26.

Kaptay, G. (2019). Improved derivation of the Butler equations for surface tension of solutions. *Langmuir*, *35*(33), 10987-10992.

Kaptay, G. (2017). The exponential excess Gibbs energy model revisited. *Calphad*, *56*, 169-184.

Koirala, I. (2018). Chemical ordering of Ag-Au alloys in the molten state. *Journal of Institute of Science and Technology*, *22*(2), 191-201.

Koirala, I., Singh, B., & Jha, I. (2014). Transport and surface properties of molten Cd-Zn alloys. *Journal of Institute of Science and Technology*, *19*(1), 14-18.

Kozlov, L. Y., Romanov, L., & Petrov, N. (1983). Predicting the viscosity of multicomponent metallic melts. *Izv Vuzov Chernaya Metal.*, *3*, 7-11.

Kulekci, M. K. (2008). Magnesium and its alloys applications in automotive industry. *The International Journal of Advanced Manufacturing Technology*, *39*(9-10), 851-865.

Mehta, U., Yadav, S., Koirala, I., & Adhikari, D. (2020). Thermo-physical properties of ternary Al–Cu–Fe alloy in liquid state. *Philosophical Magazine*, *100*(19), 2417-2435.

Panthi, N., Bhandari, I.B., Jha, I, S., & Koirala, I. (2021). Complex formation behavior of copper-tin alloys at its molten state. *Advanced Material Letters*, *12*(1), 21011595. https://doi.org/10.5185/amlett.2021.011595

Redlich, O., & Kister, A. (1948). Algebraic representation of thermodynamic properties and the classification of solutions. *Industrial & Engineering Chemistry*, *40*(2), 345-348.

Shrestha, G. K., Singh, B. K., Jha, I. S., & Koirala, I. (2017). Theoretical study of thermodynamic properties of Cu-Pb liquid alloys at different temperatures by optimization method. *Journal of Institute of Science and Technology*, *22*(1), 25-33.

Singh, R. N., & Mishra, I. K. (1988). Conditional probabilities and thermodynamics of binary molten alloys. *Physics and Chemistry of Liquids*, *18*(4), 303-319.

Singh, B. P., & Koirala, I. (2015). Size sensitive transport behavior of liquid metallic mixtures. *Journal of Institute of Science and Technology*, *20*(2), 140-144.

Starace, A. K., Neal, C. M., Cao, B., Jarrold, M. F., Aguado, A., & López, J. M. (2008). Correlation between the latent heat and cohesive energies of metal clusters. *The Journal of Chemical Physics*, *129*(14), 144703. https://doi.org/10.1063/1.2987720

WORKSHOP ON RESEARCH WRITING AND PUBLISHING

8th-11th May, 2019

Certificate

This is to Certify that Mr./Mrs. Narayan Panthi

of Patan Multiple Campus, Lalitpur participated in the Workshop on Research Writting & Publishing organized by Research Management cell, Mahendra Morang Adarsh Multiple Campus, Biratnagar & supported by University Grants Commission, Nepal held at Biratnagar from 8th-11th May, 2019.

Prof. Dr. Devendra Adhikari	Mr. Baburam Timalsena	Dr. Tilak Prasad Gautam
(Facilitator)	(Campus Chief)	(Co-ordinator)
	M.M.A.M. Campus, Biratnagar	Workshop Organizing Committee,
		Reaserch Management Cell,
		M.M.A.M. Campus, Biratnagar

St. Xavier's College

Maitighar, Kathmandu, Nepal

Department of Physics

This e-certificate of appreciation is awarded to **Mr. Narayan Panthi,**

of

Central Department of Physics, Kritipur, Nepal

for poster presentation On the title "**Comparison of thermophysical properties of Mg-Ga and Mg-Pb alloys at 1000 K**"

in the

"International Conference on Material Science and Characterization Technology (ICMSCT)"

held on **September 26-28, 2021**

Mr. Drabindra Pandit Head, Department of Physics	Fr. Dr. Augustine Thomas, S.J. Principal St. Xavier's College	Prof. Dr. Bhim Prasad Subedi Chairperson, University Grants Commission Nepal

Nepal Physical Society

Ghantaghar, Kathmandu, Nepal

International Conference on Frontiers of Physics -2022

(ICFP-2022)

This Certificate of appreciation is awarded to

Narayan Panthi

from Patan M. Campus, Nepal for his oral presentation on the

"High Temperature study of complex Lead Magnesium Alloy" in the

International Conference on Frontiers of Physics -2022

held on January 22-24, 2022 via virtual platform.

Prof. Dr. Narayan P. Chapagain

Conference Chair, ICFP-2022

President, Nepal Physical Society

February 1, 2022

Certificate of Attendance

American Physical Society
March Meeting 2022
March 14–18, 2022 | Chicago & Online

THIS IS TO CERTIFY THAT

Narayan Panthi

attended the American Physical Society's March Meeting.
Pre-meeting tutorials and short courses were held on March 12 and 13.

APS physics MARCH MEETING 2022

Don Wise, Senior Meetings Registrar
March 18, 2022

Fourth International Conference on

Materials Science and Manufacturing Technology 2022 (ICMSMT 2022)

08 - 09, April 2022 | Coimbatore, India | www.icmsmt.com

CERTIFICATE

MS 2032

Peer Reviewed

This certificate is presented to

Narayan Panthi
Patan Multiple Campus,
Patandhoka, Lalitpur.

for presenting the research paper entitled "**Themo-physical Stability of K-Pb liquid alloy at different temperatures**" in the Fourth International Conference on Materials Science and Manufacturing Technology 2022 (ICMSMT 2022) held at Hotel Aloft, Coimbatore, Tamil Nadu, India during 08 - 09, April 2022. The conference has been jointly organized by the Akshaya College of Engineering and Technology (Academic Partner), Coimbatore, Tamil Nadu India and Diligentec Solutions (Industry Partner), Coimbatore, Tamil Nadu, India.

Dr. Ramya Muthusamy
Chair - TPC & Editor

Industry Partner: DILIGENTEC SOLUTIONS

Publication Partners: IOPscience, Scientific.Net

Academic Partner: Akshaya College of Engineering and Technology, Coimbatore

Fourth Edition